# THE EFFECT OF HISTONE H3 AND H4 MUTANTS ON THE CHRONOLOGICAL LIFESPAN OF *SACCHAROMYCES CEREVISIAE*

**Mzwanele Ngubo**

SUBMITTED IN ACCORDANCE WITH THE REQUIREMENTS FOR THE DEGREE

**Philosophiae Doctor**

IN THE FACULTY OF AGRICULTURE AND NATURAL SCIENCES DEPARTMENT OF BIOTECHNOLOGY UNIVERSITY OF THE FREE STATE

**2015**

**Prof. Hugh-George Patterton**

## Indexes

**Acknowledgements**

I would like to thank the living God for the grace, wisdom and sanity He has given me throughout the duration of this study.For He made my declarations not to come back to me void.

To my parents for their unconditional love, support, understanding, and providing me this opportunity – I am forever grateful.

I would also like to express my gratitude to my supervisor, Prof. H-G. Patterton, for the support, and guidance.

To all my friends, and members of the Lab of Epigenomics and DNA Function, thank you for your support, kindness and sometimes counsel. I really appreciate it.

This research was supported by the NRF (National Research Foundation, South Africa) and ABRC (Advance Biomolecular Research Cluster, University of the Free State).

## Table of Contents

# CHAPTER 1

## The Role of Epigenetics in the Lifespan of *Saccharomyces cerevisiae*

### 1.1. Introduction

Humans develop a variety of “diseases of aging”, including cancer,Alzheimer’s disease, which is characterised by loss of neurons and synapses, aggregation of amyloid fibrils and induce programmed cell death (PCD);Parkinson’s disease, which is characterized by brain cell death that show apoptotic makers,and dementia (Blasco, 2005; Coria *et al.,* 1993). Therefore our understanding of the process of aging is an essential health focus.

Two major approaches have been used to determine aging in yeast. The first classical approach measures the mother cell’s replicative lifespan by monitoring the number of cell divisions over time in culture (Mortimer and Johnston, 1959).A method to determine the replicative lifespan of *Saccharomyces cerevisiae*was established five decades ago and extensively employed from the nineties (Kennedy, 1994; Smeal *et al.,* 1996). In replicative lifespan, the division potential of the individual mother cells is determined by counting the total number of daughter cells before asymmetrical cell division stops. The mother cell is characterised based on its mean and maximum replicative lifespan estimated by measuring the number of total buds produced. Replicative aging can be caused by accumulation of extrachromosomal ribosomal DNA circles (ERCs) (Sinclair and Guarente, 1997).ERCs are self-replicating units which divide asymmetrically in the mother cell during cell division and are produced in the nucleolus by rDNA homologous recombination. The silent information regulator proteins Sir2, Sir3, and Sir4, which

regulate silenced chromatin at different DNA sites, were described to regulate ERCs accumulation and aging (Kaeberlein *et al.,* 1999). Notably, the NAD-dependent deacetylase Sir2 inhibits rDNA recombination and ERCs accumulation. Increasing the levels Sir2 extended replicative lifespan, whereas the deletion of *SIR2*decreased replicative lifespan (Kaeberlein *et al.,* 1999). In addition, overexpression of the homologue of *SIR2* extended longevity in *Caenorhabditis elagans*, suggesting that this conserved gene may affect both chronological aging and replicative aging in other eukaryotes (Tissenbaum and Guarente, 2001). Approximately 100 yeast replicative aging genes have been identified where deletion results in enhanced longevity (Kaeberlein et al 2005).*LAG1* and *LAG2* genes are also implicated in the control of replicative lifespan. The deletion of each of these genes decreased lifespan by 40% and 50%, respectively. Conversely, their overexpression increased bud formation by mother cells (D'mello *et al.,* 1994).

The second approach measures chronological lifespan, typically in stationary phase by monitoring the mean and maximum survival times of populations of post-mitotic cells. The post-diauxic phase is the period that begins approximately 24 hours after initial inoculation when cells exhaust glucose, drastically reduce growth and switch to a mitochondrial respiratory mode of metabolism dependent on the ethanol generated during fermentation (Werner-Wasburne *et al*., 1996). Stationary phase starts at the end of the post-diauxic phase between day 2 and 7, and is characterized by lower metabolic rates and up-regulation of stress resistance pathways(Werner-Wasburne *et al*., 1996). The yeast chronological lifespan assay was developed to provide an aging model for non-dividing cells of higher organisms (Fabrizio and Longo 2007; Longo, 1997).The important genes and pathways regulating yeast chronological lifespan showed significant similarities to those in

worms, flies, and mammals (Longo *et al*., 2012).Chronological lifespan was introduced in 1996 and since then has become more widely studied (Longo *et al.,* 1996). Yeast and other microorganisms have evolved to survive under adverse conditions, such as starvation. In fact, most microorganisms are likely to survive in a low metabolism stationary phase under nutrient depleted conditions (Werner-Washburne *et al.,* 1996). Yeast grown and incubated in nutrient rich medium YPD, survives for months in a low metabolism,stationary phase.

In yeast aging research, the genes and parts of pathways that affect replicative lifespan and chronological lifespan, as well as many downstream factors affecting stress-dependent transcription and translation have conserved orthologs or analogs in higher eukaryotes (Longo *et al*., 2012).

Aging and longevity are influenced by many complex interacting factors. Epigenetics has previously emerged as another possible regulator of aging(Calvanese *et al.,* 2009). Since epigenetic alterations are more readily reversible than genetic alterations, interventions aimed to reverse epigenetic changes may have a great potential to treat age-associated “diseases of aging”.

### 1.2. The Nucleosome

The central region of all four core histone proteins share a similar structural motif,constructed from three α-helices connected by two loops, L1 and L2, and is denoted as α1-L1-α2-L2-α3. This “histone-fold” motif is highly conserved, as was seen in structures obtained from organisms as diverse as archaea (Starich *et al.,* 1996), insects (Xie *et al.,* 1996), birds (Arents *et al.,* 1991) and amphibians (Luger *et al.,* 1997), presumably because of its unique dimerisation and DNA binding properties. The histones form crescent-shaped (“hand-shake”) heterodimers [H3-H4

and H2A-H2B] that bind 1.7 turns of DNA double helix, which arcs over each dimer of the histone pair to generate a 140 base-pair bend. As the contact surfaces of the heterodimers offset towards the N terminus by one helical turn, the C-terminus of each α2 helix extends further along the long axis than the adjacent N terminus of the paired histone. The full N-terminal tails do not have a distinct structure in the crystal (Luger *et al.,* 1997), suggesting that they are highly flexible. The X-ray crystal structures did, however, show that the H3 and H2B amino-terminal tails passed over and between the gyres of the DNA superhelix in the nucleosome. These tails may contact neighbouring nucleosomes (Davey *et al.,* 2002; Luger *et al.,* 1997).

Eukaryotic DNA is organized in subunits called nucleosomes, the basic repeating structural element of chromatin. These subunits are formed by the association of about 146 bp of duplex DNA with two copies of each of the core histones H2A, H2B, H3 and H4 (Kornberg, 1974). DNA is bound to the histones through electrostatic forces between the negatively charged phosphate groups on the DNA backbone and positively charged amino acids (e.g., lysine and arginine) in the histone proteins (Wolfe and Grimes, 1993). As the DNA double helix spools around the histone octamer to create a nucleosome core, it contacts the histone surface at 14 sites with clusters of hydrogen bonds and salt links (Luger and Richmond, 1998). Communally, these weak interactions render the nucleosome a stable particle.

Previous work has shown that chromatin assembly is a step-wise process involving the association of a tetramer of histone H3-H4 with the DNA followed by the incorporation of H2A-H2B dimers to form the nucleosome (Van Holde, 1988). Additionally, linker histone H1 binds to approximately 20bp of DNA in between nucleosomes augmenting the compaction of the chromatin polymer (Garcia *et*

*al.,*2007). Linker histone H1abundance is roughly half as much as the other core histones. X-ray diffraction pattern showed that the reconstitution of the nucleosome did not require linker histone H1, suggesting that H1 is bound on the outside of the nucleosome (Kornberg, 1974). Through an ill-defined hierarchical series of compaction steps involving histone tails, nucleosome-nucleosome interactions are formed both within and between individual nucleosomal arrays. This results in the formation of the 30 nm chromatin fibre. The nucleosome, in its role as the principal packaging element of DNA within the nucleus, is the primary determinant of DNA accessibility (Belmont and Bruce, 1994).

Nucleosomes are arranged into regularly spaced arrays, with the length of linker region between nucleosomes varying among species and cell types. Although initially nucleosomes were believed to provide universal, nonspecific spools for genomic DNA, it was known that nucleosomes occupy favoured positions throughout the genome. High resolution, genome-wide analysis showed a common pattern with depleted nucleosomes at many enhancer, promoter and terminator regions, and they mostly occupy preferred positions in genes and non-gene regions (Yuan *et al.,* 2005). In yeast, the -1 and +1 nucleosomes flanking the promoter are located at highly preferred positions, and the extent of preferred nucleosome positioning gradually decreases from the 5'-3' end of the coding region (Mavrich *et al.,* 2008). It was suggested that a number of factors, including the DNA sequence, DNA binding factors, chromatin remodelers, and the transcription machinery, in consort, regulate nucleosome positioning (Hughes *et al.,* 2012).

## 1.3. Enzymes Involved in Histone Modifications and their Physiological Roles

The post-translational modifications of the core histone tails are catalysed by numerous different enzymes, such as kinases, histone methyltransferases (HMTases), protein R methyltransferase (PMRT) and histone acetyltransferases (HATs) (McManus and Hendzel, 2006). Until recently, there were at least 35 different residues within the tails that serve as substrates for at least 31 post-translational modifications (Bonaldi *et al.,* 2004; Zhang *et al.,* 2003). The chemical modifications may function by two characterized mechanisms: the first is the disruption of the interactions between nucleosomes in order to “unravel” chromatin, and the second is the provision of molecular surfaces recognized by other proteins, thereby recruiting non-histone proteins. A large number of papers have suggested that numerous proteins, thus far considered to be transcriptional activators, co-activators, or repressors, were actually enzymes that covalently modified the histone N-termini (Pazin and Kadonaga, 1997; Wade and Wolffe, 1997). It was also shown that a number of transcriptional regulators had high homology to the subunits of both HATs and HDACs (Brownell *et al.,* 1996). To date, the most studied modifications of histones are acetylation, ubiquitination, methylation, phosphorylation, sumoylation and ADP-ribosylation.

### *1.3.1. Lysine Acetylation*

A number of acetylation sites in yeast histones have been identified by mass spectrometry and the use of specific antibodies against specific sites of acetylation (Kouzarides, 2007; Suka *et al.,* 2001). In euchromatin H4K5, 8 and 12 were shown to be predominantly bound by a bromodomain of a transcriptional activation factor. This has strengthened the long held belief that acetylation enhances transcription

(Johnson, 1998). Acetylation of histone H4K16 was found to regulate both chromatin structure and the physiological cooperation between recruited non-histone proteins and the chromatin fibre (Shogren-Knaak *et al.,* 2006). Histone acetylation is catalysed by a class of enzymes known as histone acetyltransferases (HATs), which use acetyl-CoA as a substrate to acetylate specific lysine residues within histones. Numerous multi-protein complexes have been identified that possess HAT activity. These complexes generally consist of one protein that serves as the catalytic subunit, and supporting proteins that serve to potentiate, regulate, or target the HAT activity to specific locations within the genome. In *Saccharomyces cerevisiae*the typical example is the 1.8-MDa SAGA complex which has a Gcn5-dependent HAT activity, and contains at least three distinct groups of gene products (Grant *et al.,* 1997). The first of these are the Ada proteins isolated as proteins that interact functionally with the transcription factor Gcn4 and the activation domain. The second group comprises all members of the TBP related set of Spt proteins, except Spt15. The third group within SAGA complex includes a subset of TBP-associated factors (Grant *et al.,* 1998). Nuclear HATs (Brown*et al.,* 2000; Marmorstein and Roth, 2001), generally function to regulate chromatin structure and gene transcription by neutralizing the positive charge associated with lysine residues at physiological pH.The reverse reaction of acetylation is carried out by histone deacetylases (HDACs), which mediate transcriptional repression (Kouzarides, 2002). Moreover, acetylation in a specific manner can also regulate DNA replication, histone deposition, and DNA repair by recruiting proteins that have an acetyl-lysine binding module, the bromodomain (Khorasanizadeh, 2004). Studies in animal cells have shown that equilibrium between acetylation and deacetylation can tilt rapidly in response to stimuli that switches genes off or on (Imai*et al.,* 2000). Acetyl groups are

repeatedly introduced and taken off histones, with turnover half-lives ranging in the order of minutes to hours when different chromatin fractions are studied by radioactive acetate incorporation in cultured cells (Hendzel and Davie, 1991). It has been demonstrated that histone acetylation mediate intracellular pH. Histones are deacetylated by HDACs on a genome-wide scale as the intracellular pH decreases(McBrian *et al*., 2013).

### *1.3.2. Lysine and Arginine Methylation*

Previous studies have demonstrated that several lysine residues, including H3K4, 9, 27, and 36, and H4K20, are predominant sites of methylation (van Holde, 1988; Strahl *et al.,* 1999). Different histone methylation states are associated with different chromatin functions, and early experiments proposed that H3K4 methylation was linked to active genes, whereas H3K9 methylation was linked to inactive genes (Lachner and Jenuwein, 2002). However, in budding yeast, Set1-mediated methylation of H3K4 is involved in rDNA silencing and H3K4 methylation is enriched in silenced regions (Briggs *et al.,* 2001; Bryk *et al.,* 2002). The SET domain contains the enzymatic activity responsible for lysine methylation of histone tails, and was shown to be responsible for methyl transfer from *S*-adenosylmethionine (AdoMet) to the histone lysine side-chain nitrogen (ε-NH2) (Rea *et al.,* 2000). Histone methylation has important roles in regulating gene expression and forms part of the epigenetic memory system that regulates cell fate and identity. Lysine methylation is directly implicated in epigenetic inheritance. Histone H3K36 methylation was showed to facilitate targeting of a chromatin-remodelling complex, Isw1b, to the nucleosome.Similar to H3K36 methylation, Isw1b was found at the mid- and 3′ regions of expressed genes genome wide, and its presence at active genes was dependent on H3K36 methylation(Maltby *et al*., 2012). Methylation of specific

arginines in histones H3 and H4 correlate with the active state of transcription (Zhang and Reinberg, 2001). The catalytic module that methylates specific arginines is known as a protein R methyltransferase (PRMT) domain, and was linked to transcriptional activation. Methylation of histone H4 arginine residue 3 by PMRT1 allowed subsequent acetylation of histone tails p300 (Wang *et al.,* 2001). In another publication, Rice and colleagues showed that monomethylation (me1) and di-methylation (me2) at histone H3K9 (H3K9me1 and H3K9me2) were localized to silenced euchromatin, whereas tri-methylation (H3K9me3) was predominantly found at pericentric heterochromatin. Although, the functional importance of mono-, di-, and tri-methylation of lysine residues is poorly understood, it is tempting to speculate that the elevated levels of H3K9 methylation may function to stabilize the silenced regions of heterochromatin (Rice *et al.,* 2003).

The opposing activity to histone methylation was earlier described by Shi and colleagues. They showed that LSD1, a nuclear homolog of amine oxidases, acts as a histone demethylase and transcriptional corepressor, and that RNAi inhibition of LSD1 causes an increase in H3K4 methylation resulting in derepression of target genes(Shi *et al*., 2004). It was also described that overexpression of JHDM1, a JmjC domain-containing histone demethylase 1, reduced the level of H3K36 dimethylation *in vivo*(Tsukada *et al*., 2006). In yeast, JmjC domain–containing H3K4 demethylase, Jhd2p, was identifiedto antagonize the trimethylation modification state and was linked to regulation of telomeric silencing(Liang *et al*., 2007). It was demonstrated that the histone demethylase activity of Jhd2 regulates mitotic rDNA condensation and that*JHD2*deficient cells contain highly condensed rDNA (Ryu and Ahn, 2014)

### *1.3.3. Serine and Threonine Phosphorylation*

The proper segregation of chromosomes is an essential step in the accurate execution of each cell cycle and requires the precise coordination of a large number of events governing chromosome and microtubule dynamics (Nurse, 2000). One of these events is the ordered inter-conversion between extended interphase chromatin and highly compacted mitotic chromosomes. Phosphorylation of histone H3 and linker histone H1 has long been known to correlate with chromosome condensation during mitosis (Bradbury *et al.,* 1973; Gurley, 1974). In fact, mutational studies have shown that the phosphorylation of histone H3S10 and 28 correlated with mitosis and chromosome condensation (Hsu *et al.,* 2000). Recent data even suggest that one of the mechanisms by which H3S10 phosphorylation may function is via the displacement of HP1, which recognizes H3K9methylation, which is normally associated with condensed chromatin (Fischle *et al.,* 2003). Other serine phosphorylation sites were also identified on histones H4, H2A, and H2B (Cheung *et al.,* 2000). Serine 10 phosphorylation on histone H3 is also linked to the activation of transcription. When mammalian cells were exposed to a mitogen or stress, the time course of this phosphorylation corresponded to the transient expression of activated “immediate-early” genes (Thomson *et al.,* 1999). The kinases that phosphorylate H3 are Aurora-B/Ipl1, PKA, Rsk-2, and Msk1, which tend to add a phosphate group to the targeted Ser/Thr sites that are surrounded by basic residues (Hsu *et al.,* 2000). Phosphorylation is reversed by the protein phosphatase 1 (PP1) family of enzymes (Hsu *et al.,* 2000).Yeast histone H3T45, a residue located within the H3 alphaN helix, wasreported to be phosphorylated. In addition, H3T45 phosphorylation increases during DNA replication, and is regulated by the S phase kinase Cdc7-Dbf4 as part of a multiprotein complex (Baker *et al*., 2010).

### *1.3.4. Lysine Ubiquitination*

The linking of ubiquitin or a small ubiquitin-related modifier, sumo, to a specific lysine residue in histones plays an important role in regulating transcription either through proteasome dependent degradation of transcription factors or other mechanisms related to the recruitment of modification complexes. While histone ubiquitination has typically been attributed to the positive control of transcription (Bonaldi *et al.,* 2004), recent studies indicated that sumoylation of histone H4 was important for transcriptional repression (Shiio and Eisenman, 2003). The ubiquitin attachment is a three step process involving E1 activating, E2 conjugating and an E3 ligase enzyme. In general, ubiquitination is initiated when ubiquitin-activating enzyme E1 first activates ubiquitin. Activated ubiquitin is then transferred to a cysteine residue of the 10 ubiquitin-conjugating enzymes (E2). In the last step, an iso-peptide bond is formed between ubiquitin and a lysyl ε-amino group within a substrate protein. This step can be catalysed either directly by the E2, or is facilitated by a third enzyme called the ubiquitin-protein ligase (E3). Proteins targeted for poly-ubiquitination commonly contain a degradation motif termed a degron, which is recognized by the E3 (Caron *et al.,* 2005). Poly-ubiquitinated protein targets are recognized and degraded by the 26S proteasome. Additionally, H2B ubiquitination has been illustrated through mutational studies to be important for methylation of histone H3K4 and 79(Sun and Allis, 2002). H2B ubiquitination is present in chromatin around origins of DNA replication in yeast, and as DNA is replicated its levels are maintained on daughter strands by the Bre1 ubiquitin ligase(Trujillo and Osley, 2012). Genome-wide analysis showed that inhibition of H2B ubiquitination impairs splicing in budding yeast, and thatH2B ubiquitination stimulates recruitment

of the early splicing factors, such as U1 and U2 snRNPs, onto nascent RNAs(Hérissant *et al*., 2014).

### *1.3.5. ADP Ribosylation*

The functional role of the ADP ribosylation of histones is not well understood. Proteins can be singly (mono) or multiply (poly) ADP ribosylated. Enzymes that mediate the modification are Mono-ADP ribosyltransferases (MARTs) and poly-ADP-ribose polymerases (PARPs) (Hassa *et al.,* 2006). Poly-ADP-ribosylation of histones and several other nuclear proteins seem to participate in nuclear processes involving the repair of DNA strand breaks, replication or recombination. PARPs, for instance, are activated by DNA strand breaks. It was also proposed that the PARP-associated polymers may recruit proteins that act as molecular "flags" to sites of DNA breaks. In addition, the Sir family of NAD-dependent histone deacetylases was shown to have low levels of ADP ribosyltransferase activity. There are many reports of ADP ribosylation of histones, but only one site was definitively mapped: H2B ADP ribosylation at Glu2 (Ogata *et al.,* 1980). Experimental evidence that may link ADP-ribosyltransferase catalytic activity to transcription is sparse. Nonetheless, recently a role for PARP-1 activity in transcription was demonstrated under conditions where DNA repair was induced (Kraus and Lis, 2003).

## 1.4. Histone Core Domain Modifications

The use of mass spectrometry to scrutinize histone post-translational modifications (PTMs) identified H3K79 methylation and numerous other modifications in the core (histone fold) domains (Cocklin and Wang, 2003; Zhang *et al.,* 2003). Mapping of the positions of these core modifications onto the nucleosome crystal structure showed that these modifications fell into groups that could be

organized into three distinct classes: (i) the solute accessible face, (ii) the nucleosome lateral surface and (iii) the histone–histone contact sites (Cosgrove *et al.,* 2004; Freitas *et al.,* 2004). It is likely that modifications in these classes will have unique effects on chromatin structure and act through mechanisms that are distinct from those observed with tail domain modifications. The locations and the evolutionary conservation of the residues involved in these modifications predict that they may be of great physiological relevance. The limited data available concerning these modifications support this idea and suggest that histone core domain modifications may turn out to play as significant a role as modifications of the histone tails. The different classes of core domain modifications are discussed below.

### *1.4.1. Solute Accessible Face*

Similar to the situation observed with histone tail modifications, modifications located on the solute accessible face of the nucleosome have the ability to alter higher-order chromatin structure and chromatin–protein interactions (Mersfelder and Parthun, 2006). Histone lateral surface modifications are uniquely capable of affecting histone-DNA interaction, and modifications on the histone–histone interface have the exclusive ability to disrupt intranucleosomal, interactions thereby altering nucleosome stability. Mutations that alter sites of histone tail modifications have been shown to affect processes such as transcription, heterochromatic silencing and DNA damage repair; however, the effects in many cases were minor (Ma *et al.,* 1998). Single amino acid substitutions of modifiable residues within the histone core have been shown to dramatically affect transcription, DNA damage repair, chromatin structure, chromatin assembly and heterochromatic gene silencing (van Leeuwen *et al.,* 2002; Masumoto *et al.,* 2005). Specific regions of the nucleosome surface are critical for the assembly of a silent chromatin structure in yeast, and contacts

between surface residues of histones H2A and H2B may mediate the inter-nucleosome interactions involved in the formation of higher order chromatin structures (Park and Szostak, 1990; Schalch *et al.,* 2005). Therefore, modifications to this surface may function through a number of mechanisms to regulate chromatin structure. First, they may function similarly to N-terminal tail modifications by controlling the ability of non-histone proteins to bind to the nucleosome. Additionally, modifications to the nucleosome face may have more direct structural effects by influencing nucleosome–nucleosome interactions that are thought to occur during the formation of the 30 nm chromatin fibre. Histone H3K79 methylation is the well-characterized modification of the nucleosome face. This modification was observed in a number of organisms including yeast, calf thymus, human and chicken (van Leeuwen *et al.,* 2002). This evolutionary conservation in such a wide variety of eukaryotes is a strong indication that it played a fundamental role in the regulation of chromatin structure (Mersfelder and Parthun, 2006).

### *1.4.2. Histone Lateral Surface*

Several of the newly identified core modifications were mapped to residues that are involved in direct contacts with the DNA molecule, while others were positioned in close proximity to the DNA. The position of modifications on the lateral surface of the nucleosome immediately suggested that their primary function would be through the regulation of histone–DNA interactions (Freitas *et al.,* 2004). A chromatin remodelling activity (either an ATP-dependent chromatin remodeler or nucleosome assembly/disassembly activity) acts on a nucleosome to alter histone–DNA contacts such that sites of modification on the lateral surface are exposed. The exposed sites can then be acted on by histone modifying activities to either add or remove post-translational modifications which, in turn, lead to nucleosomes with

altered mobility, similar to a spool slipping more easily along a rope wound around it. This altered mobility can then lead to changes in the accessibility of specific sequences of DNA or changes in higher order chromatin structure. Lysine 56 within the core domain of H3 has recently been found to be acetylated (Xu *et al.,* 2005). The lysine 56 residue is facing toward the major groove of the DNA within the nucleosome, so it is in a particularly good position to affect histone-DNA interactions when acetylated. Histone H3K122, a residue located on the lateral surface of the histone octamer, when acetylated was demonstrated to stimulate transcription. Likewise,its mutation impedes transcriptional activation, which waslinked to a direct effect of H3K122acetylation on histone-DNA binding(Tropberger *et al*., 2013).

### *1.4.3. Histone-Histone Interfaces*

At a very basic level, chromatin structure is dependent upon specific histone–histone interactions that lead to the formation of the histone octamer. These histone–histone interactions include those that mediate the formation of the H3/H4 and H2A/H2B histone fold pairs, those that allow the formation of the H3/H4 tetramer, and those between tetramers and H2A/H2B dimers that result in formation of the histone octamer. In this model, the modification of residues at points of histone–histone contact would influence chromatin structure by directly impacting the structure of the histone octamer. The best example of a PTM that functions through structural effects on the histone octamer is the acetylation of histone H4K91 which was first identified by mass spectrometric analysis of bovine histones (Zhang and Freitas, 2004). Lysine 91 is in the region of histone H4 that interacts with histone H2B and helps to stabilize the tetramer–dimer interaction necessary for the formation of the histone octamer (Santisteban *et al.,* 1997). This PTM seems highly conserved, because it was also identified in yeast (Ye *et al.,* 2005). The association of histone

H4 acetylated on lysine 91 with proteins involved in histone deposition suggested that this modification occurred prior to chromatin assembly (Ye *et al.,* 2005).

### 1.5. Histone Code

The histone code hypothesis proposes that the combinatorial pattern of N-terminal modifications of histones provides an identity to each nucleosome that the cell interprets as a code from the genome to regulate various cellular processes (Nowak and Corces, 2004). These modifications occur on multiple and specific residues, and the combinatorial modification profiles of histones suggest that the modification sites can act as binding surfaces for specific proteins that recognize these particular marks, leading to active or silenced genomic regions (Jenuwein and Allis, 2001). The hypothesis predicts that distinct modifications of the histone tails will change the affinities of non-histone proteins for chromatin, and modifications on the same or different histone tails may be complementary and generate various combinations on any one nucleosome. However, there is growing evidence that suggest that chromatin modifications function in a combinatorial code that extends across several neighbouring nucleosomes (Rando, 2012). The enzymes that recognise and act upon these histone tail modifications are highly specific for particular amino acid positions (Strahl and Allis, 2000; Turner, 2000), thereby extending the information content of the genome beyond simply the sequence of nucleotides in the genome. This additional level of information associated with chromatin is known as epigenetics, and includes chemical modifications of the DNA molecule such as methylation of cytosines as well.

Mechanical communication between modifications may occur at several different levels. For example, the histone H3 N-terminus appears to exist in two

distinct modification states that are likely to be regulated by a “switch” between H3K9 methylation and H3S10 phosphorylation. Histone H3S10 phosphorylation inhibits H3K9 methylation (Rea *et al.,* 2000) but is synergistically coupled with H3K9 and/or H3K14 acetylation during mitogenic and hormonal stimulation in mammalian cells (Cheung *et al.,* 2000; Clayton *et al.,* 2000). The histone code hypothesis infers that the histone modification marks provide recognition sites for effector proteins. Consistent with this view, the bromodomain has been the first protein module to be described to selectively associate with a chemical covalent mark, acetylated lysine in the N-terminal tail (Dhalluin *et al.,* 1999; Owen *et al.,* 2000; Winston and Allis, 1999). Structural studies and binding affinities of other bromodomains infers an important notion that bromodomain proteins can interact with other proteins in an acetylation-dependent manner (Hudson *et al.,* 2000; Jacobson, 2000; Owen et al, 2000). Roles of bromodomains in at least four functions have been described. Firstly, bromodomains are important for chromatin acetylation by HATs. Gcn5 is a catalytic subunit of multiple HAT complexes, and Spt7 is a subunit of two such complexes that couple the acetyltransferase activity to the acetyllysine binding ability (Sterner and Berger, 2000). Secondly, bromodomains play a role in acetylation-dependent nucleosome assembly and remodelling. The subunit of SWI/SNF chromatin remodelling complex, ATPase, contains one bromodomain (Fry and Peterson, 2001). The presence of a bromodomain in these complexes makes a putative link between histone acetylation and ATP-dependent chromatin assembly and remodelling. Thirdly, bromodomains play a role in organising chromosome or chromatin domains. Bromodomain factor 1(Bdf1), was described to bind acetylated histone H4 and impose a physical barrier between euchromatin and heterochromatin (Ladurner *et al.,* 2003). Fourthly, bromodomains also recognise non histone proteins. Acetylation

of p53 and c-Myb promotes association with bromodomain containing HATs (Sano and Ishii, 2001).

Stable and heritable inactivation of transcription is sustained at the level of higher order chromatin structure. Several proteins linked with gene silencing were found to share a similar structure motif, the chromodomain (Paro and Hogness, 1991). The chromodomain (chromatin organising modifier) was originally defined as a 37 amino acid residue region of homology shared by two Drosophila poly peptides HP1 (Heterochromatin protein) and Pc (Polycomb). Chromodomain modules seem to be targeting chemical covalent methylation marks. It is suggested that chromodomain proteins may be involved in compartmentalising the nuclear environment (Jones *et al.,* 2000).

### 1.6. Apoptosis Pathways

Apoptosis is a highly regulated cellular suicide program which is triggered by external and internal signals essential to the development and homeostasis of multicellular organisms. Until the 1990's, apoptosis was not identified in yeast cells. Important regulators of apoptosis were not found in yeast when homology searches were done. Moreover, a self-induced cellular death program was unfathomable for an organism that consists of only one cell. Therefore, the identification of an apoptotic phenotype in *CDC48*mutant yeast strain was unforeseen (Madeo, 1997). Cdc48p is an ATPase involved in ubiquitin protein degradation. The apoptotic phenotype showed: DNA cleavage, chromatin condensation, externalisation of phosphatidylserine through the plasma membrane and cytochrome c release from mitochondria (Madeo *et al*, 1997; Ludovico *et al.,* 2002). Apoptosis has also been reported in other model, unicellular organisms such as *Schizosaccharomyces pombe*

(Ink *et al.,* 1997). It has been suggested that the reason why a unicellular organism would undergo suicide, is to save nutrient resources for the fittest individuals in times of stress (Herker *et al.,* 2004).

Apoptosis is exogenously induced in yeast by several substances, most commonly, hydrogen peroxide ($H_2O_2$) and acetic acid. Reactive oxygen species (ROS) were showed to be key regulators of yeast apoptosis by treating *S. cerevisiae*with low doses of hydrogen peroxide (Madeo, 1999). Yeast caspase *YCA1* and apoptosis-inducing factor-1 *AIF1,* are involved in apoptosis in addition to several other molecular factors (Madeo *et al.,* 2002; Wissing *et al.,* 2004). The knockout of *YCA1*or *AIF1*increased resistance to $H_2O_2$. Yca1p is required for cell death following defective DNA replication initiation, loss of ubiquitination control, and mRNA instability. The potential sources of ROS include the mitochondrial respiratory chain and endoplasmic reticulum.

Treatment of yeast cells with acetic acid results in mitochondrial cytochrome *c* release. Consistently, alteration of cytochrome *c* partly hampered acetic acid-induced cell death (Ludovico *et al.,* 2002). Further exogenous triggers that induce an apoptotic phenotype in yeast include ethanol, hypochlorous acid, high salt, UV irradiation and heat stress (Carmona-Gutierrez *et al.,* 2010). The endogenous triggers such as DNA damage and replication failure can trigger yeast cell death programs (Weinberger *et al.,* 2005). Genome instability which is linked to aging in all eukaryotes is closely associated with replication stress, which in yeast affects both chronological and replicative aging. The chronological lifespan is measured by the time post-mitotic cells remain viable in a culture with limited nutrient availability. Under the conditions of limited nutrient availability, unhealthy cells undergo

apoptosis in order to avert wasting nutrients. When the unhealthy cells die they release nutrients to benefit healthy cells (Herker *et al.,* 2004).

Yeast replicative lifespan is measured by monitoring the number of cell divisions a mother cell undergoes over time in culture. The replicative aging provides a model for proliferating cells such as asymmetrically dividing stem cells. After several division cycles the mother cell eventually undergoes cell death that is followed by essential apoptotic markers such as ROS overproduction, phosphophatidylserine externalisation and DNA fragmentation (Laun *et al.,* 2001).

Chronological and replicative aging depend on nutrient availability, which affects three nutrient-dependent kinases, *TOR1/2*, *SCH9*, and protein kinase-A (PKA) (Rockenfeller and Madeo, 2008). Hyper-activation of Ras protein Ras2p, a signalling pathway upstream from PKA activation, increases apoptosis while shortening the replicative and chronological lifespans (Longo, 2004).

Mitochondrion factors are considered to be “friends” when they are localised in the mitochondrion and are considered “foes” when they are shuttled out,as is shown in Figure 1.1. The NADH dehydrogenase Ndi1p, which catalyses oxidation of intra-mitochondrial NADH and is localised to the inner mitochondrial membrane, represents another mitochondrion-associated protein that is involved in yeast cell death (Li *et al.,* 2006). The *NDI1* mutation decreases ROS production and extends the chronological lifespan. The yeast homolog of dynamin-related protein-1, Dnm1p, regulates mitochondrial fragmentation which is essential in apoptosis (Fannjiang *et al.,* 2004).

Bir1p, is the only known inhibitor-of-apoptosis protein in yeast (Walter *et al.,* 2006). Bir1p participates in chromosome segregation events by controlling and targeting activation of Ipl1p, a spindle assembly check point kinase that

phosphorylates histone H3 at Ser10 during meiosis and mitosis. Ipl1p regulates centromere-microtubule interactions that ensure chromosome bi-orientation on the spindle (Sandall *et al.,* 2006). In the presence of oxidative stress, *BIR1* disruption results in higher cell death rates. Bir1p overexpression also impedes onset of cell death during chronological lifespan (Walter *et al.,* 2006).

Biochemical assays that were conducted showed that Tat-D is an endo/exonuclease. It has an endonuclease activity that incises double-stranded DNA and excises DNA from the 3'-5' end by its exonuclease activity. The study also showed that under mild hydrogen peroxide stress, the TAT-D knock-out mutant increased cell survival, whereas overexpression of the nuclease leads to enhanced apoptosis (Qiu *et al.,* 2005).

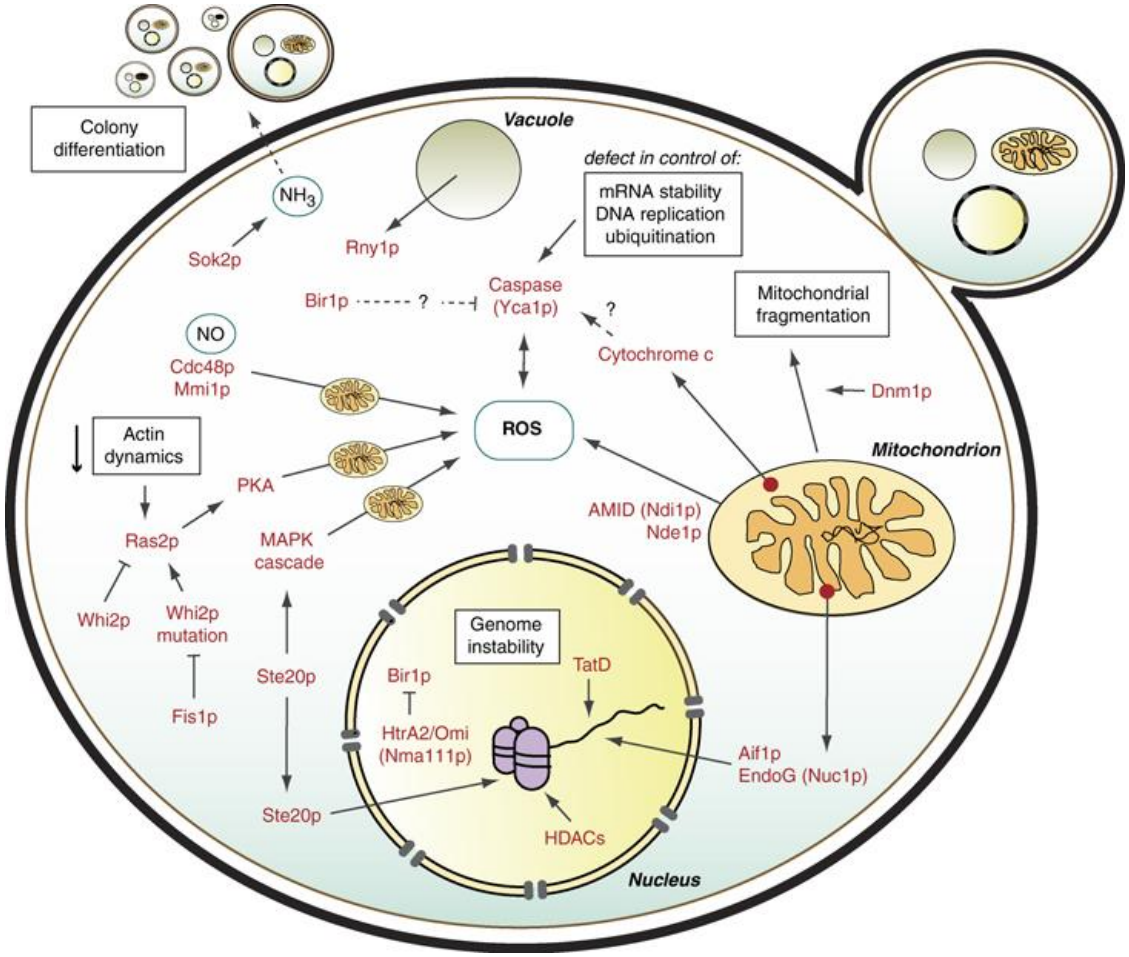


**Figure1.1. Yeast apoptosis pathways.** Crucial proteins and pathways that execute programmed cell death and its regulation. The yeast apoptosis machinery comprises of the interaction between small molecules, proteins, and pathways, which execute their functions at different locations in the cell (Adapted from Carmona-Gutierrez *et al.,* 2010).

Apoptosis inducing factor, Aif1p, undergoes mitochondrial-nuclear transportation upon apoptosis. Yeast cell death by Ai1p is dependent on cyclophilin-A and is independent of caspase. Ai1p showed DNase activity on purified yeast nuclei and plasmid DNA (Wissing *et al.,* 2004). Similarly, Nuc1p, a yeast ortholog of the proapoptotic EndoG, shuttles from the mitochondrion to the nucleus. Permeability transition pore, Kap123p, and histone H2B co-purified with FLAG-tagged Nuc1p. This immediately suggests a pathway in which mitochondrial pore opening, nuclear translocation and chromatin association are communally involved in

EndoG regulated apoptosis. *NUC1* gene deletion was illustrated to inhibit apoptosis (Büttner *et al.,* 2007).

## 1.7. Calorie restriction

Numerous advances in aging-related research stemmed from showing interventions that slow aging across evolutionary divergent species. Calorie-restriction (CR) is the most studied intervention and was showed to increase longevity from yeast to humans (Kennedy *et al.,* 2007). A similar effect is seen when nutrient-sensing pathways are impeded by mutations and chemical inhibitors. CR is simply, a limitation of food intake without malnutrition. The most typical dietary restriction protocol in yeast involves reducing the concentration of glucose in the growth medium from 2% to 0.5% or lower, which was showed to increase both replicative lifespan and chronological lifespan (Kaeberlein *et al.,* 2004; Smith *et al.,* 2007). In rodents, both CR and impeded signalling pathways can decrease aging-related loss of function and disease, including cancer, diabetes and neurodegenerative disorders (Anson *et al.,* 2003; Wang *et al.,* 2005; Weindruch and Walford, 1988). Seemingly, identification of the genetic mechanisms that regulate the protective effects of CR would have deep implications for the development of new medical interventions for diseases of aging.

### *1.7.1. TOR Signalling Pathway*

Lowered activity of two major signallingpathways can increase both chronological and replicative yeast life span. The first signalling pathway involves amino acid sensing activity, including the target of rapamycin (TOR) protein and the serine-threonine kinase Sch9(Jacinto and Hall, 2003). TOR was first identified in *S. cerevisiae* and later in mammalian cells, and is emerging as a key modulator of

eukaryotic cell growth and proliferation(Harris and Lawrence, 2003). *TOR1*and*TOR2*encode two related factors thatmodulate cell growthin response tonutrient availabilityandcellular stresses(Loewith *et al.,* 2002). TOR1andTOR2are involved in the regulation of many cellular processes includingprotein synthesis,ribosome biogenesis,autophagy,transcriptional activation,meiosis andcell cycling(Lorberg and Hall, 2004). There are two functionally distinct TOR complexes. The TOR complex 1 (TORC1) is responsible for most of the aforementioned processes and consists of eitherTor1porTor2p, together withKog1p,Lst8p, andTco89p(Loewith *et al.,*2002).TORC1 is sensitive to the drug rapamycin, which forms a complex withFpr1pthat binds to the Tor protein and inhibits complex activity(Stan *et al.,* 1994). TOR complex 2 (TORC2) is involved in regulatingactin cytoskeleton polarization during cell cycle progression,cell wall integrity, and receptorendocytosis(deHart *et al.,* 2003). TORC2 is rapamycin insensitive because the rapamycin-Fpr1p complex does not bind toTor2pwhen it is present in TORC2(Loewith *et al.,*2002).

TOR was showed to be involved insensing nutrient levels and mitogens in mammalian cells, and allowed progression from G1 to S phase (Harris & Lawrence, 2003).TOR depletion or treatment with rapamycin results in growth arrest that is linked with physiological changes, which are characteristic of stationary phase (G0) cells(Werner-Washburne *et al.,* 1993). The stationary phase characteristics include G1cell cycle arrest, repression of general transcription and mRNA translation, induction of a set of stress response genes, and synthesis of glycogen and trehalose(Werner-Washburne *et al.,* 1993; Jacinto and Hall, 2003).

Deletion of *SCH9*, which has sequence and functional similarity to the mammalian, ribosomal protein S6 kinase (S6K), causes a lifespan increase of up to

several fold in both chronological and replicative lifespan, as does deletion or inhibition of *TOR1*, probably by inactivating the downstream Sch9 (Kaeberlein *et al.,* 2005).Sch9 is phosphorylated by Tor1p and required for TORC1 complex-mediated regulation of ribosome biogenesis(Urban *et al.,* 2007).Alterations to protein synthesis are strongly implicated in extension of replicative lifespan by reduced TOR/Sch9 and may play a key role in chronological life span as well (Steffen *et al.,* 2008). Rim15 is a glucose-repressible protein kinase and it is required for transferring signals from the Sch9, Ras, and Tor pathways in response to nutrients(Swinnen *et al.,* 2006). Extension of chronological life span by reduced activity of the TOR pathway depends on the transcription factor Gis1, which activates many protective systems including *Mn-SOD*(superoxide dismutase), (Kaeberlein *et al.,* 2005).

### *1.7.2. cAMP/PKA Signalling Pathway*

The second signallingpathway includes three proteins: Ras, adenylate cyclase (AC), and protein kinase A (PKA). The yeast Ras proteins, Ras1p and Ras2p, bind directly to adenylate cyclase, and activate the production of cAMP (Field *et al.,* 1990). This, in turn, results in increased levels of PKA activity and the increased phosphorylation of proteins presumably important for cell proliferation, and other processes, such as response tonutrientsandstress, nutrient sensing,energy metabolism,carbohydrate utilisation,cell cycle progression,thermotolerance,osmotic shock tolerance,sporulation,bud site selection,pseudohyphal growth,aging, andautophagy(Broach, 1991; Norbeck and Blomberg, 2000; Estruch, 2000).cAMP activates PKA by binding to the regulatory subunit (Bcy1), which results in the release of active catalytic subunits, encoded by three genes, namely,*TPK1*, *TPK2*and*TPK3*, that then presumably phosphorylate target proteins and induce growth(Toda *et al.,* 1987).

The substrates of PKA include two transcription factors (Msn2 and Msn4) that control cellular protection systems and regulate the effect of reduced Ras-AC-PKA signalling on chronological lifespan extension, and may also regulate the extension of replicative lifespan (Fabrizio *et al.,* 2001; Medvedik *et al.,* 2007). The extension of yeast lifespan by these pathways requires the antioxidant enzyme *Mn-SOD*, which scavenges the superoxide free radicals(Wei *et al.,* 2008). Superoxide level increases during yeast aging and is reduced in long-lived mutants deficient in Ras-AC-PKA or Tor-Sch9 signalling (Fabrizio *et al.,* 2001). However, overexpression of both the antioxidant enzymes *SOD1* and *SOD2* or catalase in yeast results in a minor increase of mean survival, suggesting that many other systems, including DNA-repair genes, are important in longevity regulation (Fabrizio *et al.,* 2005).

Inyeast,depletion of either TOR or PKA causes cells to arrest growth early in G1and to enter G0 by mechanisms that are poorly understood. The protein kinase Rim15 is required for entry into G0following inactivation of TOR and/or PKA(Pedruzzi *et al.,* 2003).Rim15 is required for proper establishment of the G0phase and is hampered by PKA-mediated phosphorylation under nutrient availability (Reinders *et al.,* 1998). Figure 1.2 depicts a summary of the role of calorie restriction and the signalling pathways in yeast chronological lifespan.

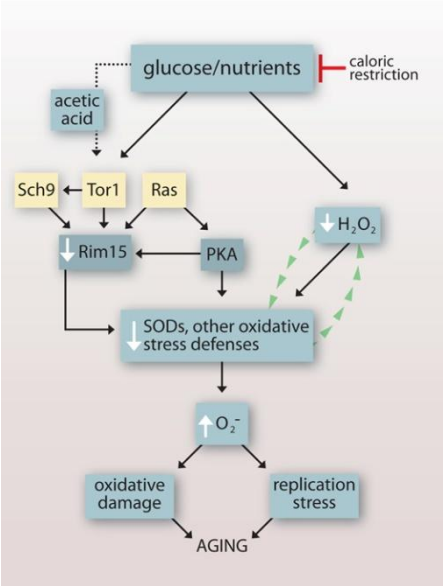


**Figure 1.2.The role of signaling pathways and calorie restriction on chronological lifespan in yeast.**Calorie restriction extends chronological lifespan by downregulating Tor1p, Ras2p and Sch9p-dependent growth signaling pathways, which results in induction of oxidative stress defences by Rim15p kinase (Adapted from Weinberger *et al.,* 2010).

### 1.8. Cellular Stress Response Pathways

Aging is a complex process associated with accumulative degeneration of physiological function and internal system of cells. Unicellular organisms require specific internal conditions for optimal growth and function, however sudden alterations in the external environment can be impeding to the internal system, disrupting normal processes. Therefore, cells must maintain their internal system despite fluctuations in the external surroundings. Internal system perturbations can hinder optimal enzyme activities, disrupt metabolic fluxes, destabilize cellular structures, and perturb chemical gradients leading to overall cell instability. Studies have identified classical signalling pathways that impact aging in different species (Kenyon, 2010). It was showed that lifespan extension depends on the ability of the organism to deal with external or internal stress. Stress is typically defined as a harmful factor (physical, chemical or biological), which activates a series of cellular

and systematic events, resulting in restoration of cellular and organismal homeostasis. Cells respond to stress in a number of ways varying from activating pathways involved in survival or initiation of cell death. Yeast cells have evolved to be very efficient at surviving sudden and often harsh changes in their external environment. Cells have developed a wide range of sophisticated stress response mechanisms, functioning at organelle-specific level, to survive conditions of stress. A number of mechanisms reduce insults and remove damaged components in normal young cells, including enzymes to remove reactive oxygen species (Landis and Tower, 2005), heat shock proteins to remove mis-folded proteins (Koga *et al.,* 2011; Kourtis and Tavernarakis, 2011), recycling of damaged organelles (Green *et al.,* 2011; Koga *et al.,* 2011), and DNA repair and check point systems to fix DNA damage prior to replication (Langerak and Russell, 2011). Like the genome-wide expression responses, activation of the environmental stress response is often transient, immediately after the shift to a new environment, the cell responds with notable changes in the expression levels of genes. However, over time the differences in expression levels usually decline, and transcript levels return to near pre-stress levels (Causton *et al.,* 2001; Gasch *et al.,* 2000). The cellular stress response system, genetic and environmental interventions often extend lifespan via enhanced stress responses (Kourtis and Tavernarakis, 2011). Efficient restriction of stress in cells is showing great potential as a strategy to alleviate age-associated diseases.

### *1.8.1. The Heat Shock Response*

Cells or tissues of various living organisms that are exposed to high temperatures specifically induce synthesis of a family of highly conserved specific proteins called heat-shock proteins (HSPs) (Ashburner and Bonner, 1979). The

expression of many genes encoding protein folding chaperones is known to be induced specifically in response to heat-denatured proteins. However, it was reported that a subset of chaperone genes is induced by different stressful conditions (Werner-Washburne *et al.,* 1989). Based on their molecular weight, HSPs are categorized into the Hsp100, Hsp90, Hsp70, Hsp60 and the small heat shock proteins (Hsp12, Hsp26, and Hsp48). Members of the Hsp70 family of chaperones include Ssa4, Sse2, andHsp78. Heat shock protein Hsp26p, was showed to protect proteins from heat-denaturation *in vitro* (Haslbeck *et al.,* 1999). However, Hsp26p and Hsp42p chaperones appear to contribute little to thermotolerance in yeast, as deletion of any of the factors does not result in cellular sensitivity to heat shock or other conditions (Gu *et al.,* 1997; Susek and Lindquist, 1989). On the contrary, inactivation of the HSP104chaperone gene does affect viability during heat shock (Lindquist and Kim, 1996). There is growing evidence that suggests Hsp104 helps disassociate aggregates of unfolded proteins to allow Hsp70 chaperones, possibly including chaperones encoded by *SSA4* and *SSE2* which are activated in environmental stress response, to bind and refold protein substrates (Glover and Lindquist, 1998; Parsell *et al.,* 1994). The heat stress response in its simplicity is viewed as repair and adaptation to damage caused by the stress rather than a preventive measure (Verghese *et al.,* 2012). Heat shock protein genes were showed to be involved in aging in the absence of other external stressors. However, the efficiency of heat shock response was observed to decline with age (Sőti and Csermely, 2000).

In yeast, the heat shock factor (HSF) protein family is the primary regulator of the heat shock stress response, Msn2 and Msn4 transcription factors are also involved in heat shock gene expression. Microarray data showed that the knockout

mutants of *HSF1*, *MSN2* and *MSN4* genes are responsible for the bulk of the heat shock stress response (Morano *et al.,* 2012).

### *1.8.2. Oxidative Stress Response*

Cell survival requires appropriate proportions of molecular oxygen and various antioxidants. Reactive products of oxygen are amongst the most damaging and constant threats encountered by cells. Cells in a human body metabolize approximately $10^{12}$oxygen molecules per day during the normal respiration process, and ~1% of the oxygen metabolized results in the formation of reactive oxygen species(Jackson and Loeb, 2001). The ROS include superoxide anion, hydrogen peroxide, singlet oxygen, hydroxyl radical, peroxyl radical, as well as the second messenger nitric oxide.Hydrogen peroxide can rapidly diffuse throughout the cell, however, its reactivity is restricted to proteins containing transition metals, including Fe-S clusters and low pKa thiols (D'Autréaux and Toledano, 2007). The transition metal-catalyzed reduction of hydrogen peroxide to hydroxyl radical is strongly reactive. Hydroxyl radical shows the widest reactivity, and non-selectively oxidizes lipids, nucleic acids, and amino acids.

ROS generated endogenously through oxidative phosphorylation and enzymatic activities or exogenously by environmental factors, can lead to a chain of oxidation reactions in the cell, which damage cellular biomolecules such as proteins, lipids and DNA, and prevent proper enzymatic activity by disrupting the internal redox potential (Radák *et al.,* 1999). Oxidative DNA damage can change purine and pyrimidine bases as well as cleave the phosphodiester DNA backbone. One of the most studied mutations caused by ROS is 8-hydroxyguanine (8-OH-Gua), which leads to GC-TA transversions unless repaired before the DNA is replicated(Olinski *et al.,* 2002).

In cells, there is equilibrium between pro-oxidant species and antioxidant defence mechanisms such as ROS-metabolizing enzymes including catalase, glutathione peroxidase, and superoxide dismutases (SODs) and other antioxidant proteins such as glutathione peroxidase (Gpx) (Trachootham *et al.,* 2008). Cytosolic superoxide dismutase Sod1p is an enzyme that detoxifies ROS by reducing superoxide. On the other hand, cytosolic catalase and Gpx detoxifies hydrogen peroxide (Figure1.3).

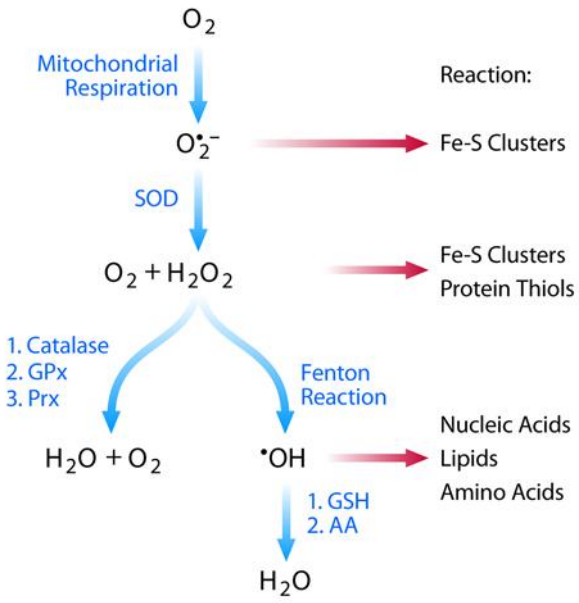


**Figure 1.3.Overview of oxidative stress response.**Majorreactive oxygen species associated with cellular respiration. ROS-metabolizing mechanisms are shown by the blue arrows, while the red arrows show reactivity for each ROS. (Adapted from Merksamer *et al.,* 2013)

A number of detoxification enzymes are induced not only by conditions that cause oxidative damage but also in response to various stressful environments. Endogenous ROS are suggested to be generated mainly by electron leakage from the oxidative phosphorylation chain in mitochondria, and thus, it is expected that this organelle has its own local ROS protection (Scandalios, 1997). Cytochrome b5 reductase and cytochrome c peroxidase both were noted to protect against oxidative

stress. Inactivation of cytochrome b5 reductase and cytochrome c peroxidase increase the sensitivity of yeast cells to drugs that induce oxidative damage (Charizanis *et al.,* 1999).

### *1.8.3. Ubiquitin-Proteasome System*

Accumulation of damaged and modified proteins is linked to aging. The accumulation of misfolded or damaged proteins is the result of a gradual deterioration of a cell's quality control mechanisms or a decline in protein degradation. The ubiquitin-proteasome system (UPS) is chiefly responsible for the proteolytic mechanisms that degrade damaged proteins and the turnover of most cytoplasmic and nuclear proteins. The process of UPS involves two steps: the linking of the protein with polyubiquitination chain and the degradation of the linked protein by the proteasome (Ciechanover, 2005). Polyubiquitination is a complex reaction involving ubiquitin, a highly conserved 76 amino acid protein, and three different enzymes (E1–E3) (Sadowski and Sarcevic, 2010).

In wild type cells, free ubiquitin levels are subject to environmentally induced fluctuations (Mimnaugh *et al.,* 1997). Very low levels of ubiquitin sensitise yeast cells to different chemical and environmental stresses, including stresses associated with heat, protein misfolding, DNA damage, exposure to heavy metals, inhibition of translation, and starvation (Chernova *et al.,* 2003; Finley *et al.,* 1987; Hanna *et al.,* 2003). Inactivation of ubiquitin-conjugating enzyme Ubc5, or ubiquitin-specific protease Ubp15was observed to render cells sensitive to different stresses (Finley *et al.,* 1987). Ubiquitination is important not only for removing misfolded proteins from the cell but also for targeting active proteins for turnover, and the induction of ubiquitin-mediated protein degradation may help the cell to rapidly alter the proteome during stress response. Mutations in a number of genes that are linked in age-

related diseases including Alzheimer's and Parkinson's disease play a major role in UPS (Jenner, 2001; Keller *et al.,* 2001). Efficient proteolytic activity of the proteasome during aging might provide protection against neuronal cell death observed in neurodegenerative diseases.

### *1.8.4. Autophagy*

Autophagy is a catabolic pathway that is highly conserved among all eukaryotes. Autophagy mediates sequestration and transportation of bulk cytoplasm, including proteins and organelle material, to thelysosomefor degradation (Budovskaya *et al.,* 2004). Organelle degradation may occur in response to organelle damage or dysfunction (Reggiori and Klionsky, 2013). When yeast cells are under unfavourable conditions such as growth on methanol or oleic acid to a preferred carbon source such as glucose they rapidly turn over the damaged organelles that are in surplus (Titorenko *et al.,* 1995). Cells form double membrane vesicles when starved for nutrients such as carbon, nitrogen, sulphur and various amino acids, or upon endoplasmic reticulum stress. The formation of double membrane vesicles is known as autophagosome (Takeshige, 1992). There are 30 autophagy-related proteins Atg, which have been identified in yeast, 17 of which are important for formation of autophagosome (Suzuki and Ohsumi, 2007). *ATG27* gene expresses a phosphatidylinositol 3-phosphate-binding transmembrane protein that, along with Atg9p is suggested to be linked to membrane delivery to pre-autophagosomal structure (Wurmser and Emr, 2002). Inactivation of most of the *ATG* genes represses induction of autophagy, and cells do not survive nutrient starvation. However, the mutants are viable in rich medium. Autophagy shares many features with the constitutive process of cytoplasm-to-vacuole targeting Cvt, which transport selective cytoplasmic proteins to the vacuole (Harding *et al.,* 1996). Unlike

autophagy, which is fundamentally a catabolic process, Cvt is a biosynthetic process(Harding *et al.,* 1996).

In higher eukaryotes, it is uncertain whether autophagy has a beneficial or harmful effect in the heart. However, there is growing evidence that points to the beneficial role of autophagy in heart under both physiological and pathological conditions (Nakai *et al.,* 2007).

### *1.8.5. TheDNA Damage Response*

Genetic control of cell-cycle transitions in response to DNA damage was first observed in the SOS DNA damage response pathway of *Escherichia coli* and in mammals in ataxia telangiectasia (AT) cells, which are defective for the ataxia telangiectasia mutated (*ATM*) gene (Painter and Young, 1980). This genetic control was later observed in yeast and the term “checkpoint” was applied to the yeast pathway (Weinert and Hartwell, 1988). DNA damage checkpoint is the mechanism that detects DNA damage and activates arrest of cells in the G1 phase of the cell-cycle. DNA damage checkpoint slows down S phase (DNA synthesis), arrests cells in the G2 phase, and induces transcription of DNA repair genes (Hartwell and Weinert, 1989). Transcriptome analysis of yeast cells exposed to genotoxic agents showed clear involvement of the Mec1 pathway in mediating environmental stress response (Gasch *et al.,* 2001). Mec1p is a protein kinase that is related to phospho-inositol kinases, and isrequired for cell cycle checkpoint function (Weinert *et al.,* 1994). Mec1p initiates a signal pathway in response to DNA damage, and replication blocks by phosphorylating other proteins(Elledge, 1996). In addition to its checkpoint function,Mec1pwas showed to preferentiallybindshortened telomeres to act as a sensor for telomere abnormalities, and is required for telomere silencing(Craven and Petes, 2000; Takata *et al.,* 2004). Mec1p signalling pathway begins with

phosphorylation of DNA damage checkpoint protein Rad9p (Naiki *et al.,* 2004). In turn Rad9p activates Mec1p phosphorylation of the effector kinases Chk1p and Rad53p (Blankley and Lydall, 2004). Phosphorylated Chk1p and Rad53p result in the arrest of cells in G1/S, S, or G2/M cell cycle phases. Additionally, phosphorylated Chk1p and Rad53p mediate transcriptional up-regulation of DNA damage repair genes, transcriptional repressionof cyclins, andstabilization of replication forks(Chen and Sanchez, 2004; Weinert and Hartwell, 1988). Yeast cells lacking the Chk1p shortens the cell cycle arrest time in response to DNA damage (Dotiwala *et al.,* 2007).*MEC1* gene mutations have multiple defects including DNA damaging agents, impeded checkpoint functions, chromosome breakage, and loss of telomeric silencing (Cha and Kleckner, 2002; Kato and Ogawa, 1994).

### 1.9. Epigenetics and Lifespan Extension Overview

In general, rapid posttranslational protein modifications allow the cell to promptly adapt to environmental changes. The transient nature of aging suggests that longevity may be controlled epigenetically by specific alterations in chromatin state. The connection between chromatin and aging has mostly focused on histone deacetylation and Sir2 family, but less is known about the role of many other histone residues and modifications in longevity.

Yeast Sir2 is a heterochromatin component that silences transcription at silent mating loci, telomeres and the ribosomal DNA (Gottschling *et al.,* 1990; Rine and Herskowitz, 1987; Smith and Boeke, 1997). Sir2 was showed to also suppress recombination in the rDNA and extend replicative lifespan in yeast (Kaeberlein *et al.,* 1999). It was showed that yeast and mouse Sir2 proteins are nicotinamide adenine dinucleotide (NAD)-dependent histone decetylases, which remove the acetyl group

from histone H3K9 and K14 and more specifically histone H4K16 (Imai *et al.,* 2000). Cells lacking Sir2 showed shortened replicative lifespan and cells with an extra copy of the *SIR2* gene had significantly longer lifespan than wild type cells (Kaeberlein *et al.,* 1999). Sir2 homologues have been identified in many organisms ranging from bacteria to humans (Brachmann *et al.,* 1995). A recent study showed that by increasing the stability of the rDNA genes, which are reportedly unstable, could extend the lifespan of *S. cerevisiae*. The separation of the effect of Sir2 on the rDNA from its other effects on genomic regions showed that Sir2's lifespan extension effect came only through stabilization of the rDNA genes (Saka *et al.,* 2013).

Modulation of histone methylation has long been linked to aging in flies (Siebold *et al.,* 2010). ASH-2 trithorax complex, which trimethylates histone H3K4 was reported as a regulator of lifespan in worms (Greer *et al*., 2010).The disruption of the subunits of ASH-2 complex, WDR-5 and the H3K4 methyltransferase SET-2, increased worm lifespan. RBR-2, a histone H3K4 demethylase is required for normal lifespan, which is in agreement with the notion that excess histone H3K4 trimethylation is detrimental for longevity(Greer *et al*., 2010).

The acetylation of histone H3K56 occurs during S phase and is involved in DNA damage repair and histone gene transcription (Masumoto *et al.,* 2005). Histone deacetylases Hst3 and Hst4 have been associated with the removal of H3K56 acetylation in yeast (Celic *et al.,* 2006). It was showed that Hst3 and Hst4 regulate replicative lifespan in yeast (Hachinohe *et al.,* 2011). *HST3* and *HST4* double knock-out mutant strain, in which H3K56 is constitutively acetylated throughout the genome, exhibited genomic instability (Hachinohe *et al.,* 2011).

Polycomb Group (PcG) and Trithorax Group (TrxG) are crucial epigenetic modulators of genome-wide transcription programs. Their opposing chromatin-

modifying activities modulate the expression of many genes and influence various biological processes. It was reported that mutations in two subunits of Polycomb Repressive Complex 2 (PRC2), the histone H3K27 methyltransferase E(Z) and its partner, histone H3 associating protein ESC, extend lifespan and decrease adult levels of H3K27 trimethylation (Siebold *et al.,* 2010). Disruption of Trithorax (TRX) increases the H3K27 trimethylation levels and shortens the expected lifespan (Siebold *et al.,* 2010). Similar to many longevity mutants, E(Z) and ESC mutants showed increased resistance to oxidative stress and starvation (Siebold *et al.,* 2010).

*BRE1* encodes an ubiquitin protein ligase that is essential for ubiquitination of histone H2BK123. Histone H2BK123 ubiquitination is implicated in gene activation and gene silencing (Hwang *et al.,* 2003). Abrogation of histone H2B ubiquitination renders X-ray sensitivity and causes defects in checkpoint activation after DNA damage (Game *et al.,* 2006). It was showed that cells lacking Bre1p, exhibited shortened lifespan during chronological aging (Walter *et al.,* 2010). Histone H2BS14 phosphorylation has been conferred as an epigenetic marker of apoptotic cells, whereas acetylation at adjacent H2BK15 is a marker of non-dying cells (Ajiro, 2000). The H2BS14 phosphorylation mark has been linked with chromatin condensation or internucleosomal DNA fragmentation (Ajiro *et al.,* 2010). Deacetylation of H2BK15 is required to allow histone H2BS14 phosphorylation (Ajiro, 2010). A similar mechanism is observed in yeast cells. Here, deacetylation of H2BK11, a mark for growing cells is required for phosphorylation of apoptotic mark H2BS10. Phosphorylation of H2BS10 is catalysed by Ste20 kinase, a yeast homologue of mammalian Mst1 kinase that translocates into the nucleus, but in a caspase-independent manner (Ahn *et al.,* 2005).

### 1.10. Chromatin and Stress Response

An expanding body of evidence suggests that combinations of epigenetic histone modifications affect the overall chromatin structure and have clear functional consequences in cellular life extension. We note with interest the known proteins that effect resistance to environmental stress by associating and interacting with chromatin.

NF-kB (Nuclear factor kappa-light-chain-enhancer of activated B cells) is found in almost all animal cell types and is involved in cellular responses to stimuli such as stress, cytokines, reactive oxygen species, ultraviolet irradiation, bacterial or viral antigens (Gilmore, 2006). It was demonstrated that in the presence of a chromatin template, the p56 subunit of NF-kB is a strong activator of HIV-1 promoter (Pazin *et al.,* 1996).

Gis1p is a stress resistant transcription factor that contains the JmjC histone demethylase domain. Gis1p regulates expression of stress resistant genes upon nutrient-limitation (Jang *et al.,* 1999). The JmjC domain was earlier shown to specifically demethylates H3K36 trimethylation primarily, and H3K36 dimethylation secondarily (Tu *et al.,* 2007).

Msn2p is a positive transcriptional factor that plays a role in stress responsive system. Msn2p recognises and binds DNA at stress response element (STRE), which is involved in the response to various forms of stress,including heat, oxidative, and osmotic.(Schmitt and McEntee, 1996).Msn4p is a transcriptional activator that is related to Msn2p (Martínez-Pastor *et al.,* 1996).

Ubp10p plays a role in telomeric and HM silencing, which is the repression of chromatin structure which leads to a stop in the transcription of nearby genes (Gardner *et al.,* 2005). It was showed that Ubp10p is an ubiquitin-specific protease

that removed ubiquitin from histone H2B. *UBP10*mutations showed changes in expression of subtelomeric genes followed by enhanced oxidative stress as well as DNA fragmentation (Orlandi *et al.,* 2004).

### 1.11. Problem Statement and Aims

Histone H4K16, H3K56 mutations and H2BK123 ubiquitination were described to affect replicative aging (Dang *et al.,* 2009; Rhie *et al.,* 2013). Histone H3K4 methylation was the only histone modification showed to affect chronological aging in yeast (Walter *et al.,* 2014). To date there are at least eleven types of post-translationalmodifications that have been described on over 60 different residues in histones(Martin and Zhang, 2007; Ruthenburg *et al.,* 2007). There are many modified residues and number of modifications, and the involvement of histone modifications in lifespan, it is possible that there are many more histone modifications and chromatin readers involved in modulating lifespan that have not been identified to date.

In this study we investigated the lifespan of approximately 400 yeast synthetic histone H3 and H4 mutants (Dai *et al.,* 2008), to gain an insight on the role of chromatin, histone modifications and possible pathwaysinvolved in regulating chronological lifespan.

## 1.11. Reference List


Ahn, S.-H., Cheung, W.L., Hsu, J.-Y., Diaz, R.L., Smith, M.M., and Allis, C.D. (2005). Sterile 20 kinase phosphorylates histone H2B at serine 10 during hydrogen peroxide-induced apoptosis in *S. cerevisiae*. Cell *120*, 25–36.

Ajiro, K. (2000). Histone H2B Phosphorylation in Mammalian Apoptotic Cells: an association with DNA fragmentation. J. Biol. Chem. *275*, 439–443.

Ajiro, K., Scoltock, A.B., Smith, L.K., Ashasima, M., and Cidlowski, J.A. (2010). Reciprocal epigenetic modification of histone H2B occurs in chromatin during apoptosis *in vitro* and *in vivo*. Cell Death Differ. *17*, 984–993.

Anson, R.M., Guo, Z., de Cabo, R., Iyun, T., Rios, M., Hagepanos, A., Ingram, D.K., Lane, M.A., and Mattson, M.P. (2003). Intermittent fasting dissociates beneficial effects of dietary restriction on glucose metabolism and neuronal resistance to injury from calorie intake. Proc. Natl. Acad. Sci. U. S. A. *100*, 6216–6220.

Arents, G., Burlingame, R.W., Wang, B.C., Love, W.E., and Moudrianakis, E.N. (1991). The nucleosomal core histone octamer at 3.1 A resolution: a tripartite protein assembly and a left-handed superhelix. Proc. Natl. Acad. Sci. *88*, 10148–10152.

Ashburner, M., and Bonner, J.J. (1979). The induction of gene activity in drosophila by heat shock. Cell *17*, 241–254.

Baker, S.P., Phillips, J., Anderson, S., Qiu, Q., Shabanowitz, J., Smith, M.M., Yates, J.R., Hunt, D.F., and Grant, P.A. (2010). Histone H3 Thr 45 phosphorylation is a replication-associated post-translational modification in *S. cerevisiae*. Nat. Cell Biol. *12*, 294–298.

Belmont, A. S and Bruce, K. (1994). Visualization of G1 chromosomes: a folded, twisted, supercoiled chromonema model of interphase chromatid structure. J. Cell Biol. *127*, 287–302.

Blankley, R.T., and Lydall, D. (2004). A domain of Rad9 specifically required for activation of Chk1 in budding yeast. J. Cell Sci. *117*, 601–608.

Blasco, M.A. (2005). Telomeres and human disease: ageing, cancer and beyond. Nat. Rev. Genet. *6*, 611–622.

Bonaldi, T., Imhof, A., and Regula, J.T. (2004). A combination of different mass spectroscopic techniques for the analysis of dynamic changes of histone modifications. Proteomics *4*, 1382–1396.

Brachmann, C.B., Sherman, J.M., Devine, S.E., Cameron, E.E., Pillus, L., and Boeke, J.D. (1995). The SIR2 gene family, conserved from bacteria to humans,

functions in silencing, cell cycle progression, and chromosome stability. Genes Dev. *9*, 2888–2902.

Bradbury, E.M., Inglis, R.J., Matthews, H.R., and Sarner, N. (1973). Phosphorylation of very-lysine-rich histone in *Physarum polycephalum*. correlation with chromosome condensation. Eur. J. Biochem. *33*, 131–139.

Briggs, S.D., Bryk, M., Strahl, B.D., Cheung, W.L., Davie, J.K., Dent, S.Y., Winston, F., and Allis, C.D. (2001). Histone H3 lysine 4 methylation is mediated by Set1 and required for cell growth and rDNA silencing in *Saccharomyces cerevisiae*. Genes Dev. *15*, 3286–3295.

Broach, J.R. (1991). RAS genes in *Saccharomyces cerevisiae*: signal transduction in search of a pathway. Trends Genet. *7*, 28–33.

Brown, C., Lechner, T., Howe, L., and Workman, J. (2000). The many HATs of transcription coactivators. Trends Biochem. Sci. *25*, 15–19.

Brownell, J.E., Zhou, J., Ranalli, T., Kobayashi, R., Edmondson, D.G., Roth, S.Y., and Allis, C.D. (1996). Tetrahymena histone acetyltransferase A: ahomolog to yeast Gcn5p linking histone acetylation to gene activation. Cell *84*, 843–851.

Bryk, M., Briggs, S.D., Strahl, B.D., Curcio, M.J., Allis, C.D., and Winston, F. (2002). Evidence that Set1, a factor required for methylation of histone H3, regulates rDNA silencing in *S. cerevisiae* by a Sir2-independent mechanism. Curr. Biol. *12*, 165–170.

Budovskaya, Y. V, Stephan, J.S., Reggiori, F., Klionsky, D.J., and Herman, P.K. (2004). The Ras/cAMP-dependent protein kinase signaling pathway regulates an early step of the autophagy process in *Saccharomyces cerevisiae*. J. Biol. Chem. *279*, 20663–20671.

Büttner, S., Eisenberg, T., Carmona-Gutierrez, D., Ruli, D., Knauer, H., Ruckenstuhl, C., Sigrist, C., Wissing, S., Kollroser, M., Fröhlich, K.-U., et al. (2007). Endonuclease G regulates budding yeast life and death. Mol. Cell *25*, 233–246.

Calvanese, V., Lara, E., Kahn, A., and Fraga, M.F. (2009). The role of epigenetics in aging and age-related diseases. Ageing Res. Rev. *8*, 268–276.

Carmona-Gutierrez, D., Eisenberg, T., Büttner, S., Meisinger, C., Kroemer, G., and Madeo, F. (2010). Apoptosis in yeast: triggers, pathways, subroutines. Cell Death Differ. *17*, 763–773.

Caron, C., Boyault, C., and Khochbin, S. (2005). Regulatory cross-talk between lysine acetylation and ubiquitination: role in the control of protein stability. Bioessays *27*, 408–415.

Causton, H.C., Ren, B., Koh, S.S., Harbison, C.T., Kanin, E., Jennings, E.G., Lee, T.I., True, H.L., Lander, E.S., and Young, R.A. (2001). Remodeling of yeast

genome expression in response to environmental changes. Mol. Biol. Cell *12*, 323–337.

Celic, I., Masumoto, H., Griffith, W.P., Meluh, P., Cotter, R.J., Boeke, J.D., and Verreault, A. (2006). The sirtuins hst3 and Hst4p preserve genome integrity by controlling histone H3 lysine 56 deacetylation. Curr. Biol. *16*, 1280–1289.

Cha, R.S., and Kleckner, N. (2002). ATR homolog Mec1 promotes fork progression, thus averting breaks in replication slow zones. Science *297*, 602–606.

Charizanis, C., Juhnke, H., Krems, B., and Entian, K.-D. (1999). The mitochondrial cytochrome c peroxidase Ccp1 of *Saccharomyces cerevisiae* is involved in conveying an oxidative stress signal to the transcription factor Pos9 (Skn7). Mol. Gen. Genet. MGG *262*, 437–447.

Chen, Y., and Sanchez, Y. (2004). Chk1 in the DNA damage response: conserved roles from yeasts to mammals. DNA Repair (Amst). *3*, 1025–1032.

Chernova, T.A., Allen, K.D., Wesoloski, L.M., Shanks, J.R., Chernoff, Y.O., and Wilkinson, K.D. (2003). Pleiotropic effects of Ubp6 loss on drug sensitivities and yeast prion are due to depletion of the free ubiquitin pool. J. Biol. Chem. *278*, 52102–52115.

Cheung, P., Tanner, K.G., Cheung, W.L., Sassone-Corsi, P., Denu, J.M., and Allis, C.D. (2000). Synergistic coupling of histone H3 phosphorylation and acetylation in response to epidermal growth factor stimulation. Mol. Cell *5*, 905–915.

Ciechanover, A. (2005). Proteolysis: from the lysosome to ubiquitin and the proteasome. Nat. Rev. Mol. Cell Biol. *6*, 79–87.

Clayton, A.L., Rose, S., Barratt, M.J., and Mahadevan, L.C. (2000). Phosphoacetylation of histone H3 on c-fos- and c-jun-associated nucleosomes upon gene activation. EMBO J. *19*, 3714–3726.

Cocklin, R.R., and Wang, M. (2003). Identification of methylation and acetylation Sites on mouse histone H3 using matrix-aassisted laser desorption/ionization time-of-flight and nanoelectrospray ionization tandem mass spectrometry. J. Protein Chem. *22*, 327–334.

Coria, F., Gomez de Caso, J.A., Minguez, L., Rodriguez-Artalejo, F., and Claveria, L.E. (1993). Prevalence of age-associated memory impairment and dementia in a rural community. J. Neurol. Neurosurg. Psychiatry *56*, 973–976.

Cosgrove, M.S., Boeke, J.D., and Wolberger, C. (2004). Regulated nucleosome mobility and the histone code. Nat. Struct. Mol. Biol. *11*, 1037–1043.

Craven, R.J., and Petes, T.D. (2000). Involvement of the checkpoint protein Mec1p in silencing of gene expression at telomeres in *Saccharomyces cerevisiae*. Mol. Cell. Biol. *20*, 2378–2384.

D’Autréaux, B., and Toledano, M.B. (2007). ROS as signalling molecules: mechanisms that generate specificity in ROS homeostasis. Nat. Rev. Mol. Cell Biol. *8*, 813–824.

D’mello, N., Childress, A., Franklin, D., Kale, S., Pinswasdi, C., and Jazwinski, S. (1994). Cloning and characterization of *LAG1*, a longevity-assurance gene in yeast. J. Biol. Chem. *269*, 15451–15459.

Dai, J., Hyland, E.M., Yuan, D.S., Huang, H., Bader, J.S., and Boeke, J.D. (2008). Probing nucleosome function: ahighly versatile library of synthetic histone H3 and H4 mutants. Cell *134*, 1066–1078.

Dang, W., Steffen, K.K., Perry, R., Dorsey, J.A., Johnson, F.B., Shilatifard, A., Kaeberlein, M., Kennedy, B.K., and Berger, S.L. (2009). Histone H4 lysine 16 acetylation regulates cellular lifespan. Nature *459*, 802–807.

Davey, C.A., Sargent, D.F., Luger, K., Maeder, A.W., and Richmond, T.J. (2002). Solvent mediated interactions in the structure of the nucleosome core particle at 1.9 a resolution. J. Mol. Biol. *319*, 1097–1113.

deHart, A.K.A., Schnell, J.D., Allen, D.A., Tsai, J.-Y., and Hicke, L. (2003). Receptor internalization in yeast requires the Tor2-Rho1 signaling pathway. Mol. Biol. Cell *14*, 4676–4684.

Dhalluin, C., Carlson, J.E., Zeng, L., He, C., Aggarwal, A.K., and Zhou, M.M. (1999). Structure and ligand of a histone acetyltransferase bromodomain. Nature *399*, 491–496.

Dotiwala, F., Haase, J., Arbel-Eden, A., Bloom, K., and Haber, J.E. (2007). The yeast DNA damage checkpoint proteins control a cytoplasmic response to DNA damage. Proc. Natl. Acad. Sci. U. S. A. *104*, 11358–11363.

Elledge, S.J. (1996). Cell cycle checkpoints: peventing an identity crisis. Science (80-. ). *274*, 1664–1672.

Estruch, F. (2000). Stress-controlled transcription factors, stress-induced genes and stress tolerance in budding yeast. FEMS Microbiol. Rev. *24*, 469–486.

Fabrizio, P., Pozza, F., Pletcher, S.D., Gendron, C.M., and Longo, V.D. (2001). Regulation of longevity and stress resistance by Sch9 in yeast. Science *292*, 288–290.

Fabrizio, P., Gattazzo, C., Battistella, L., Wei, M., Cheng, C., McGrew, K., and Longo, V.D. (2005). Sir2 blocks extreme life-span extension. Cell *123*, 655–667.

Fannjiang, Y., Cheng, W.-C., Lee, S.J., Qi, B., Pevsner, J., McCaffery, J.M., Hill, R.B., Basañez, G., and Hardwick, J.M. (2004). Mitochondrial fission proteins regulate programmed cell death in yeast. Genes Dev. *18*, 2785–2797.

Field, J., Vojtek, A., Ballester, R., Bolger, G., Colicelli, J., Ferguson, K., Gerst, J., Kataoka, T., Michaeli, T., Powers, S., et al. (1990). Cloning and characterization of CAP, the *S. cerevisiae* gene encoding the 70 kd adenylyl cyclase-associated protein. Cell *61*, 319–327.

Finley, D., Özkaynak, E., and Varshavsky, A. (1987). The yeast polyubiquitin gene is essential for resistance to high temperatures, starvation, and other stresses. Cell *48*, 1035–1046.

Fischle, W., Wang, Y., and Allis, C.D. (2003). Binary switches and modification cassettes in histone biology and beyond. Nature *425*, 475–479.

Freitas, M.A., Sklenar, A.R., and Parthun, M.R. (2004). Application of mass spectrometry to the identification and quantification of histone post-translational modifications. J. Cell. Biochem. *92*, 691–700.

Fry, C.J., and Peterson, C.L. (2001). Chromatin remodeling enzymes: who's on first? Curr. Biol. *11*, R185–R197.

Game, J.C., Williamson, M.S., Spicakova, T., and Brown, J.M. (2006). The RAD6/BRE1 histone modification pathway in *Saccharomyces* confers radiation resistance through a RAD51-dependent process that is independent of RAD18. Genetics *173*, 1951–1968.

Garcia, B.A., Shabanowitz, J., and Hunt, D.F. (2007). Characterization of histones and their post-translational modifications by mass spectrometry. Curr. Opin. Chem. Biol. *11*, 66–73.

Gardner, R.G., Nelson, Z.W., and Gottschling, D.E. (2005). Ubp10/Dot4p regulates the persistence of ubiquitinated histone H2B: distinct roles in telomeric silencing and general chromatin. Mol. Cell. Biol. *25*, 6123–6139.

Gasch, A.P., Spellman, P.T., Kao, C.M., Carmel-Harel, O., Eisen, M.B., Storz, G., Botstein, D., and Brown, P.O. (2000). Genomic expression programs in the response of yeast cells to environmental changes. Mol. Biol. Cell *11*, 4241–4257.

Gasch, A.P., Huang, M., Metzner, S., Botstein, D., Elledge, S.J., and Brown, P.O. (2001). Genomic expression responses to DNA-damaging agents and the regulatory role of the yeast aTR homolog Mec1p. Mol. Biol. Cell *12*, 2987–3003.

Gilmore, T.D. (2006). Introduction to NF-kappaB: players, pathways, perspectives. Oncogene *25*, 6680–6684.

Glover, J.R., and Lindquist, S. (1998). Hsp104, Hsp70, and Hsp40. Cell *94*, 73–82.

Gottschling, D.E., Aparicio, O.M., Billington, B.L., and Zakian, V.A. (1990). Position effect at *S. cerevisiae* telomeres: Reversible repression of Pol II transcription. Cell *63*, 751–762.

Grant, P.A., Duggan, L., Cote, J., Roberts, S.M., Brownell, J.E., Candau, R., Ohba, R., Owen-Hughes, T., Allis, C.D., Winston, F., et al. (1997). Yeast Gcn5 functions in two multisubunit complexes to acetylate nucleosomal histones: characterization of an Ada complex and the SAGA (Spt/Ada) complex. Genes Dev. *11*, 1640–1650.

Grant, P.A., Schieltz, D., Pray-Grant, M.G., Steger, D.J., Reese, J.C., Yates, J.R., and Workman, J.L. (1998). A subset of TAFIIs are integral components of the SAGA complex required for nucleosome acetylation and transcriptional stimulation. Cell *94*, 45–53.

Green, D.R., Galluzzi, L., and Kroemer, G. (2011). Mitochondria and the autophagy-inflammation-cell death axis in organismal aging. Science *333*, 1109–1112.

Greer, E.L., Maures, T.J., Hauswirth, A.G., Green, E.M., Leeman, D.S., Maro, G.S., Han, S., Banko, M.R., Gozani, O., and Brunet, A. (2010). Members of the H3K4 trimethylation complex regulate lifespan in a germline-dependent manner in *C. elegans*. Nature *466*, 383–387.

Gu, J., Emerman, M., and Sandmeyer, S. (1997). Small heat shock protein suppression of Vpr-induced cytoskeletal defects in budding yeast. Mol. Cell. Biol. *17*, 4033–4042.

Gurley, L.R. (1974). Cell cycle-spefic changes in histone phosphorylation associated with cell proliferation and chromosome condensation. J. Cell Biol. *60*, 356–364.

Hachinohe, M., Hanaoka, F., and Masumoto, H. (2011). Hst3 and Hst4 histone deacetylases regulate replicative lifespan by preventing genome instability in *Saccharomyces cerevisiae*. Genes Cells *16*, 467–477.

Hanna, J., Leggett, D.S., and Finley, D. (2003). Ubiquitin depletion as a key mediator of toxicity by translational inhibitors. Mol. Cell. Biol. *23*, 9251–9261.

Harding, T.M., Hefner-Gravink, A., Thumm, M., and Klionsky, D.J. (1996). Genetic and phenotypic overlap between autophagy and the cytoplasm to vacuole protein targeting pathway. J. Biol. Chem. *271*, 17621–17624.

Harris, T.E., and Lawrence, J.C. (2003). TOR signaling. Sci. STKE *2003*, re15.

Hartwell, L.H., and Weinert, T.A. (1989). Checkpoints: controls that ensure the order of cell cycle events. Science (80-. ). *246*, 629–634.

Haslbeck, M., Walke, S., Stromer, T., Ehrnsperger, M., White, H.E., Chen, S., Saibil, H.R., and Buchner, J. (1999). Hsp26: a temperature-regulated chaperone. EMBO J. *18*, 6744–6751.

Hassa, P.O., Haenni, S.S., Elser, M., and Hottiger, M.O. (2006). Nuclear ADP-ribosylation reactions in mammalian cells: where are we today and where are we going? Microbiol. Mol. Biol. Rev. *70*, 789–829.

Hérissant, L., Moehle, E.A., Bertaccini, D., Van Dorsselaer, A., Schaeffer-Reiss, C., Guthrie, C., and Dargemont, C. (2014). H2B ubiquitylation modulates spliceosome assembly and function in budding yeast. Biol. Cell *106*, 126–138.

Herker, E., Jungwirth, H., Lehmann, K.A., Maldener, C., Fröhlich, K.-U., Wissing, S., Büttner, S., Fehr, M., Sigrist, S., and Madeo, F. (2004). Chronological aging leads to apoptosis in yeast. J. Cell Biol. *164*, 501–507.

Van Holde, K.E. Chromatin. 1988. NY Springer-Verlag.

Hsu, J.-Y., Sun, Z.-W., Li, X., Reuben, M., Tatchell, K., Bishop, D.K., Grushcow, J.M., Brame, C.J., Caldwell, J.A., Hunt, D.F., et al. (2000). Mitotic phosphorylation of histone H3 is governed by Ipl1/aurora kinase and Glc7/PP1 phosphatase in budding yeast and nematodes. Cell *102*, 279–291.

Hudson, B.P., Martinez-Yamout, M.A., Dyson, H.J., and Wright, P.E. (2000). Solution structure and acetyl-lysine binding activity of the GCN5 bromodomain. J. Mol. Biol. *304*, 355–370.

Hughes, A.L., Jin, Y., Rando, O.J., and Struhl, K. (2012). A functional evolutionary approach to identify determinants of nucleosome positioning: a unifying model for establishing the genome-wide pattern. Mol. Cell *48*, 5–15.

Hwang, W.W., Venkatasubrahmanyam, S., Ianculescu, A.G., Tong, A., Boone, C., and Madhani, H.D. (2003). A conserved RING finger protein required for histone H2B monoubiquitination and cell size control. Mol. Cell *11*, 261–266.

Imai, S., Johnson, F.B., Marciniak, R.A., Mcvey, M., Park, P.U., and Guarente, L. (2000). Sir2: an NAD-dependent histone deacetylase that connects chromatin silencing, metabolism, and aging. Cold Spring Harb. Symp. Quant. Biol. *65*, 297–302.

Ink, B., Zornig, M., Baum, B., Hajibagheri, N., James, C., Chittenden, T., and Evan, G. (1997). Human Bak induces cell death in *Schizosaccharomyces pombe* with morphological changes similar to those with apoptosis in mammalian cells. Mol. Cell. Biol. *17*, 2468–2474.

J, H.M., and R, D.J. (1991). Dynamically acetylated histones of chicken erythrocytes are selectively methylated.

Jacinto, E., and Hall, M.N. (2003). Tor signalling in bugs, brain and brawn. Nat. Rev. Mol. Cell Biol. *4*, 117–126.

Jackson, A.L., and Loeb, L.A. (2001). The contribution of endogenous sources of DNA damage to the multiple mutations in cancer. Mutat. Res. Mol. Mech. Mutagen. *477*, 7–21.

Jacobson, R.H. (2000). Structure and function of a human TAFII250 double bromodomain module. Science (80-. ). *288*, 1422–1425.

Jang, Y.K., Wang, L., and Sancar, G.B. (1999). RPH1 and GIS1 are damage-responsive repressors of PHR1. Mol. Cell. Biol. *19*, 7630–7638.

Jenner, P. (2001). Parkinson's disease, pesticides and mitochondrial dysfunction. Trends Neurosci. *24*, 245–246.

Johnson, C. (1998). Distinctive patterns of histone H4 acetylation are associated with defined sequence elements within both heterochromatic and euchromatic regions of the human genome. Nucleic Acids Res. *26*, 994–1001.

Jones, D.O., Cowell, I.G., and Singh, P.B. (2000). Mammalian chromodomain proteins: their role in genome organisation and expression. Bioessays *22*, 124–137.

Kaeberlein, M., McVey, M., and Guarente, L. (1999). The SIR2/3/4 complex and SIR2 alone promote longevity in *Saccharomyces cerevisiae* by two different mechanisms. Genes Dev. *13*, 2570–2580.

Kaeberlein, M., Kirkland, K.T., Fields, S., and Kennedy, B.K. (2004). Sir2-independent life span extension by calorie restriction in yeast. PLoS Biol. *2*, E296.

Kaeberlein, M., Powers, R.W., Steffen, K.K., Westman, E.A., Hu, D., Dang, N., Kerr, E.O., Kirkland, K.T., Fields, S., and Kennedy, B.K. (2005). Regulation of yeast replicative life span by TOR and Sch9 in response to nutrients. Science *310*, 1193–1196.

Kato, R., and Ogawa, H. (1994). An essential gene, ESR1, is required for mitotic growth, DNA repair and meiotic recombination *Saccharomyces cerevisiae*. Nucleic Acids Res. *22*, 3104–3112.

Keller, J.N., Hanni, K.B., and Markesbery, W.R. (2001). Impaired proteasome function in Alzheimer's disease. J. Neurochem. *75*, 436–439.

Kennedy, B.K. (1994). Daughter cells of *Saccharomyces cerevisiae* from old mothers display a reduced life span. J. Cell Biol. *127*, 1985–1993.

Kennedy, B.K., Steffen, K.K., and Kaeberlein, M. (2007). Ruminations on dietary restriction and aging. Cell. Mol. Life Sci. *64*, 1323–1328.

Kenyon, C.J. (2010). The genetics of ageing. Nature *464*, 504–512.

Khorasanizadeh, S. (2004). The nucleosome from genomic organization to genomic regulation. Cell *116*, 259–272.

Koga, H., Kaushik, S., and Cuervo, A.M. (2011). Protein homeostasis and aging: The importance of exquisite quality control. Ageing Res. Rev. *10*, 205–215.

Kornberg, R.D. (1974). Chromatin structure: repeating unit of histones and DNA. Science (80-. ). *184*, 868–871.

Kourtis, N., and Tavernarakis, N. (2011). Cellular stress response pathways and ageing: intricate molecular relationships. EMBO J. *30*, 2520–2531.

Kouzarides, T. (2002). Histone methylation in transcriptional control. Curr. Opin. Genet. Dev. *12*, 198–209.

Kouzarides, T. (2007). Chromatin modifications and their function. Cell *128*, 693–705.

Kraus, W.L., and Lis, J.T. (2003). PARP goes transcription. Cell *113*, 677–683.

Lachner, M., and Jenuwein, T. (2002). The many faces of histone lysine methylation. Curr. Opin. Cell Biol. *14*, 286–298.

Ladurner, A.G., Inouye, C., Jain, R., and Tjian, R. (2003). Bromodomains mediate an acetyl-histone encoded antisilencing function at heterochromatin boundaries. Mol. Cell *11*, 365–376.

Landis, G.N., and Tower, J. (2005). Superoxide dismutase evolution and life span regulation. Mech. Ageing Dev. *126*, 365–379.

Langerak, P., and Russell, P. (2011). Regulatory networks integrating cell cycle control with DNA damage checkpoints and double-strand break repair. Philos. Trans. R. Soc. Lond. B. Biol. Sci. *366*, 3562–3571.

Laun, P., Pichova, A., Madeo, F., Fuchs, J., Ellinger, A., Kohlwein, S., Dawes, I., Fröhlich, K.-U., and Breitenbach, M. (2001). Aged mother cells of *Saccharomyces cerevisiae* show markers of oxidative stress and apoptosis. Mol. Microbiol. *39*, 1166–1173.

Van Leeuwen, F., Gafken, P.R., and Gottschling, D.E. (2002). Dot1p modulates silencing in yeast by methylation of the nucleosome core. Cell *109*, 745–756.

Li, W., Sun, L., Liang, Q., Wang, J., Mo, W., and Zhou, B. (2006). Yeast AMID homologue Ndi1p displays respiration-restricted apoptotic activity and is involved in chronological aging. Mol. Biol. Cell *17*, 1802–1811.

Liang, G., Klose, R.J., Gardner, K.E., and Zhang, Y. (2007). Yeast Jhd2p is a histone H3 Lys4 trimethyl demethylase. Nat. Struct. Mol. Biol. *14*, 243–245.

Lindquist, S., and Kim, G. (1996). Heat-shock protein 104 expression is sufficient for thermotolerance in yeast. Proc. Natl. Acad. Sci. *93*, 5301–5306.

Loewith, R., Jacinto, E., Wullschleger, S., Lorberg, A., Crespo, J.L., Bonenfant, D., Oppliger, W., Jenoe, P., and Hall, M.N. (2002). Two TOR complexes,

only one of which is rapamycin sensitive, have distinct roles in cell growth control. Mol. Cell *10*, 457–468.

Longo, V.D. (2004). Ras: the other pro-aging pathway. Sci. Aging Knowledge Environ. *2004*, pe36.

Longo, V.D., Gralla, E.B., and Valentine, J.S. (1996). Superoxide dismutase activity is essential for stationary phase survival in *Saccharomyces cerevisiae*: mitochondrial production of toxic oxygen species *in vivo*. J. Biol. Chem. *271*, 12275–12280.

Longo, V.D., Shadel, G.S., Kaeberlein, M., and Kennedy, B. (2012). Replicative and chronological aging in *Saccharomyces cerevisiae*. Cell Metab. *16*, 18–31.

Lorberg, A., and Hall, M.N. (2004). TOR: the first 10 years. Curr. Top. Microbiol. Immunol. *279*, 1–18.

Ludovico, P., Rodrigues, F., Almeida, A., Silva, M.T., Barrientos, A., and Côrte-Real, M. (2002). Cytochrome c release and mitochondria involvement in programmed cell death induced by acetic acid in *Saccharomyces cerevisiae*. Mol. Biol. Cell *13*, 2598–2606.

Luger, K., and Richmond, T.J. (1998). DNA binding within the nucleosome core. Curr. Opin. Struct. Biol. *8*, 33–40.

Luger, K., Mäder, A.W., Richmond, R.K., Sargent, D.F., and Richmond, T.J. (1997). Crystal structure of the nucleosome core particle at 2.8 A resolution. Nature *389*, 251–260.

Ma, X.-J., Wu, J., Altheim, B.A., Schultz, M.C., and Grunstein, M. (1998). Deposition-related sites K5/K12 in histone H4 are not required for nucleosome deposition in yeast. Proc. Natl. Acad. Sci. *95*, 6693–6698.

Madeo, F. (1997). A yeast mutant showing diagnostic markers of early and late apoptosis. J. Cell Biol. *139*, 729–734.

Madeo, F. (1999). Oxygen stress: aregulator of apoptosis in yeast. J. Cell Biol. *145*, 757–767.

Madeo, F., Herker, E., Maldener, C., Wissing, S., Lächelt, S., Herlan, M., Fehr, M., Lauber, K., Sigrist, S.J., Wesselborg, S., et al. (2002). A caspase-related protease regulates apoptosis in yeast. Mol. Cell *9*, 911–917.

Maltby, V.E., Martin, B.J.E., Schulze, J.M., Johnson, I., Hentrich, T., Sharma, A., Kobor, M.S., and Howe, L. (2012). Histone H3 lysine 36 methylation targets the Isw1b remodeling complex to chromatin. Mol. Cell. Biol. *32*, 3479–3485.

Marmorstein, R., and Roth, S.Y. (2001). Histone acetyltransferases: function, structure, and catalysis. Curr. Opin. Genet. Dev. *11*, 155–161.

Martin, C., and Zhang, Y. (2007). Mechanisms of epigenetic inheritance. Curr. Opin. Cell Biol. *19*, 266–272.

Martínez-Pastor, M.T., Marchler, G., Schüller, C., Marchler-Bauer, A., Ruis, H., and Estruch, F. (1996). The *Saccharomyces cerevisiae* zinc finger proteins Msn2p and Msn4p are required for transcriptional induction through the stress response element (STRE). EMBO J. *15*, 2227–2235.

Masumoto, H., Hawke, D., Kobayashi, R., and Verreault, A. (2005). A role for cell-cycle-regulated histone H3 lysine 56 acetylation in the DNA damage response. Nature *436*, 294–298.

Mavrich, T.N., Ioshikhes, I.P., Venters, B.J., Jiang, C., Tomsho, L.P., Qi, J., Schuster, S.C., Albert, I., and Pugh, B.F. (2008). A barrier nucleosome model for statistical positioning of nucleosomes throughout the yeast genome. Genome Res. *18*, 1073–1083.

McBrian, M.A., Behbahan, I.S., Ferrari, R., Su, T., Huang, T.-W., Li, K., Hong, C.S., Christofk, H.R., Vogelauer, M., Seligson, D.B., et al. (2013). Histone acetylation regulates intracellular pH. Mol. Cell *49*, 310–321.

McManus, K.J., and Hendzel, M.J. (2006). The relationship between histone H3 phosphorylation and acetylation throughout the mammalian cell cycle. Biochem. Cell Biol. *84*, 640–657.

Medvedik, O., Lamming, D.W., Kim, K.D., and Sinclair, D.A. (2007). MSN2 and MSN4 link calorie restriction and TOR to sirtuin-mediated lifespan extension in *Saccharomyces cerevisiae*. PLoS Biol. *5*, e261.

Mersfelder, E.L., and Parthun, M.R. (2006). The tale beyond the tail: histone core domain modifications and the regulation of chromatin structure. Nucleic Acids Res. *34*, 2653–2662.

Mimnaugh, E.G., Chen, H.Y., Davie, J.R., Celis, J.E., and Neckers, L. (1997). Rapid deubiquitination of nucleosomal histones in human tumor cells caused by proteasome inhibitors and stress response inducers: effects on replication, transcription, translation, and the cellular stress response. Biochemistry *36*, 14418–14429.

Morano, K.A., Grant, C.M., and Moye-Rowley, W.S. (2012). The response to heat shock and oxidative stress in *Saccharomyces cerevisiae*. Genetics *190*, 1157–1195.

Mortimer, R.K., and Johnston, J.R. (1959). Life span of individual yeast cells. Nature *183*, 1751–1752.

Naiki, T., Wakayama, T., Nakada, D., Matsumoto, K., and Sugimoto, K. (2004). Association of Rad9 with double-strand breaks through a Mec1-dependent mechanism. Mol. Cell. Biol. *24*, 3277–3285.

Nakai, A., Yamaguchi, O., Takeda, T., Higuchi, Y., Hikoso, S., Taniike, M., Omiya, S., Mizote, I., Matsumura, Y., Asahi, M., et al. (2007). The role of autophagy in cardiomyocytes in the basal state and in response to hemodynamic stress. Nat. Med. *13*, 619–624.

Norbeck, J., and Blomberg, A. (2000). The level of cAMP-dependent protein kinase A activity strongly affects osmotolerance and osmo-instigated gene expression changes in *Saccharomyces cerevisiae*. Yeast *16*, 121–137.

Nowak, S.J., and Corces, V.G. (2004). Phosphorylation of histone H3: a balancing act between chromosome condensation and transcriptional activation. Trends Genet. *20*, 214–220.

Nurse, P. (2000). A long twentieth century of the cell cycle and beyond. Cell *100*, 71–78.

Ogata, N., Ueda, K., and Hayaishi, O. (1980). ADP-ribosylation of histone H2B. Identification of glutamic acid residue 2 as the modification site. J. Biol. Chem. *255*, 7610–7615.

Olinski, R., Gackowski, D., Foksinski, M., Rozalski, R., Roszkowski, K., and Jaruga, P. (2002). Oxidative DNA damage: assessment of the role in carcinogenesis, atherosclerosis, and acquired immunodeficiency syndrome1 1This article is part of a series of reviews on “Oxidative DNA Damage and Repair.” The full list of papers may be found on the homepag. Free Radic. Biol. Med. *33*, 192–200.

Orlandi, I., Bettiga, M., Alberghina, L., and Vai, M. (2004). Transcriptional profiling of ubp10 null mutant reveals altered subtelomeric gene expression and insurgence of oxidative stress response. J. Biol. Chem. *279*, 6414–6425.

Owen, D.J., Ornaghi, P., Yang, J.C., Lowe, N., Evans, P.R., Ballario, P., Neuhaus, D., Filetici, P., and Travers, A.A. (2000). The structural basis for the recognition of acetylated histone H4 by the bromodomain of histone acetyltransferase gcn5p. EMBO J. *19*, 6141–6149.

Painter, R.B., and Young, B.R. (1980). Radiosensitivity in ataxia-telangiectasia: a new explanation. Proc. Natl. Acad. Sci. *77*, 7315–7317.

Park, E.C., and Szostak, J.W. (1990). Point mutations in the yeast histone H4 gene prevent silencing of the silent mating type locus HML. Mol. Cell. Biol. *10*, 4932–4934.

Paro, R., and Hogness, D.S. (1991). The Polycomb protein shares a homologous domain with a heterochromatin-associated protein of Drosophila. Proc. Natl. Acad. Sci. *88*, 263–267.

Parsell, D.A., Kowal, A.S., Singer, M.A., and Lindquist, S. (1994). Protein disaggregation mediated by heat-shock protein Hsp104. Nature *372*, 475–478.

Pazin, M.J., and Kadonaga, J.T. (1997). What's up and down with histone deacetylation and transcription? Cell *89*, 325–328.

Pazin, M.J., Sheridan, P.L., Cannon, K., Cao, Z., Keck, J.G., Kadonaga, J.T., and Jones, K.A. (1996). NF-kappa B-mediated chromatin reconfiguration and transcriptional activation of the HIV-1 enhancer in vitro. Genes Dev. *10*, 37–49.

Pedruzzi, I., Dubouloz, F., Cameroni, E., Wanke, V., Roosen, J., Winderickx, J., and De Virgilio, C. (2003). TOR and PKA signaling pathways converge on the protein kinase Rim15 to control entry into G0. Mol. Cell *12*, 1607–1613.

Qiu, J., Yoon, J.-H., and Shen, B. (2005). Search for apoptotic nucleases in yeast: role of Tat-D nuclease in apoptotic DNA degradation. J. Biol. Chem. *280*, 15370–15379.

Radák, Z., Kaneko, T., Tahara, S., Nakamoto, H., Ohno, H., Sasvári, M., Nyakas, C., and Goto, S. (1999). The effect of exercise training on oxidative damage of lipids, proteins, and DNA in rat skeletal muscle: evidence for beneficial outcomes. Free Radic. Biol. Med. *27*, 69–74.

Rando, O.J. (2012). Combinatorial complexity in chromatin structure and function: revisiting the histone code. Curr. Opin. Genet. Dev. *22*, 148–155.

Rea, S., Eisenhaber, F., O'Carroll, D., Strahl, B.D., Sun, Z.W., Schmid, M., Opravil, S., Mechtler, K., Ponting, C.P., Allis, C.D., et al. (2000). Regulation of chromatin structure by site-specific histone H3 methyltransferases. Nature *406*, 593–599.

Reggiori, F., and Klionsky, D.J. (2013). Autophagic processes in yeast: mechanism, machinery and regulation. Genetics *194*, 341–361.

Reinders, A., Burckert, N., Boller, T., Wiemken, A., and De Virgilio, C. (1998). *Saccharomyces cerevisiae* cAMP-dependent protein kinase controls entry into stationary phase through the Rim15p protein kinase. Genes Dev. *12*, 2943–2955.

Rhie, B.-H., Song, Y.-H., Ryu, H.-Y., and Ahn, S.H. (2013). Cellular aging is associated with increased ubiquitylation of histone H2B in yeast telomeric heterochromatin. Biochem. Biophys. Res. Commun. *439*, 570–575.

Rice, J.C., Briggs, S.D., Ueberheide, B., Barber, C.M., Shabanowitz, J., Hunt, D.F., Shinkai, Y., and Allis, C.D. (2003). Histone methyltransferases direct different degrees of methylation to define distinct chromatin domains. Mol. Cell *12*, 1591–1598.

Rine, J., and Herskowitz, I. (1987). Four genes responsible for a position effect on expression from HML and HMR in *Saccharomyces cerevisiae*. Genetics *116*, 9–22.

Rockenfeller, P., and Madeo, F. (2008). Apoptotic death of ageing yeast. Exp. Gerontol. *43*, 876–881.

Ruthenburg, A.J., Li, H., Patel, D.J., and Allis, C.D. (2007). Multivalent engagement of chromatin modifications by linked binding modules. Nat. Rev. Mol. Cell Biol. *8*, 983–994.

Ryu, H.-Y., and Ahn, S. (2014). Yeast histone H3 lysine 4 demethylase Jhd2 regulates mitotic rDNA condensation. BMC Biol. *12*, 75.

Sadowski, M., and Sarcevic, B. (2010). Mechanisms of mono- and poly-ubiquitination: Ubiquitination specificity depends on compatibility between the E2 catalytic core and amino acid residues proximal to the lysine. Cell Div. *5*, 19.

Saka, K., Ide, S., Ganley, A.R.D., and Kobayashi, T. (2013). Cellular senescence in yeast is regulated by rDNA noncoding transcription. Curr. Biol. *23*, 1794–1798.

Sandall, S., Severin, F., McLeod, I.X., Yates, J.R., Oegema, K., Hyman, A., and Desai, A. (2006). A Bir1-Sli15 complex connects centromeres to microtubules and is required to sense kinetochore tension. Cell *127*, 1179–1191.

Sano, Y., and Ishii, S. (2001). Increased affinity of c-Myb for CREB-binding protein (CBP) after CBP-induced acetylation. J. Biol. Chem. *276*, 3674–3682.

Santisteban, M.S., Arents, G., Moudrianakis, E.N., and Smith, M.M. (1997). Histone octamer function in vivo: mutations in the dimer-tetramer interfaces disrupt both gene activation and repression. EMBO J. *16*, 2493–2506.

Scandalios, J.G. (1997). Oxidative stress and the molecular biology of antioxidant defenses.

Schalch, T., Duda, S., Sargent, D.F., and Richmond, T.J. (2005). X-ray structure of a tetranucleosome and its implications for the chromatin fibre. Nature *436*, 138–141.

Schmitt, A.P., and McEntee, K. (1996). Msn2p, a zinc finger DNA-binding protein, is the transcriptional activator of the multistress response in *Saccharomyces cerevisiae*. Proc. Natl. Acad. Sci. *93*, 5777–5782.

Shi, Y., Lan, F., Matson, C., Mulligan, P., Whetstine, J.R., Cole, P.A., Casero, R.A., and Shi, Y. (2004). Histone demethylation mediated by the nuclear amine oxidase homolog LSD1. Cell *119*, 941–953.

Shiio, Y., and Eisenman, R.N. (2003). Histone sumoylation is associated with transcriptional repression. Proc. Natl. Acad. Sci. U. S. A. *100*, 13225–13230.

Shogren-Knaak, M., Ishii, H., Sun, J.-M., Pazin, M.J., Davie, J.R., and Peterson, C.L. (2006). Histone H4-K16 acetylation controls chromatin structure and protein interactions. Science *311*, 844–847.

Siebold, A.P., Banerjee, R., Tie, F., Kiss, D.L., Moskowitz, J., and Harte, P.J. (2010). Polycomb repressive complex 2 and Trithorax modulate *Drosophila* longevity and stress resistance. Proc. Natl. Acad. Sci. U. S. A. *107*, 169–174.

Sinclair, D.A., and Guarente, L. (1997). Extrachromosomal rDNA circles — acause of aging in yeast. Cell *91*, 1033–1042.

Smeal, T., Claus, J., Kennedy, B., Cole, F., and Guarente, L. (1996). Loss of Transcriptional Silencing Causes Sterility in Old Mother Cells of *S. cerevisiae*. Cell *84*, 633–642.

Smith, J.S., and Boeke, J.D. (1997). An unusual form of transcriptional silencing in yeast ribosomal DNA. Genes Dev. *11*, 241–254.

Smith, E.D., Kennedy, B.K., and Kaeberlein, M. (2007). Genome-wide identification of conserved longevity genes in yeast and worms. Mech. Ageing Dev. *128*, 106–111.

Sőti, C., and Csermely, P. (2000). Molecular chaperones and the aging process. Biogerontology *1*, 225–233.

Stan, R., McLaughlin, M.M., Cafferkey, R., Johnson, R.K., Rosenberg, M., and Livi, G.P. (1994). Interaction between FKBP12-rapamycin and TOR involves a conserved serine residue. J. Biol. Chem. *269*, 32027–32030.

Starich, M.R., Sandman, K., Reeve, J.N., and Summers, M.F. (1996). NMR structure of HMfB from the hyperthermophile, *Methanothermus fervidus*, confirms that this archaeal protein is a histone. J. Mol. Biol. *255*, 187–203.

Steffen, K.K., MacKay, V.L., Kerr, E.O., Tsuchiya, M., Hu, D., Fox, L.A., Dang, N., Johnston, E.D., Oakes, J.A., Tchao, B.N., et al. (2008). Yeast life span extension by depletion of 60s ribosomal subunits is mediated by Gcn4. Cell *133*, 292–302.

Sterner, D.E., and Berger, S.L. (2000). Acetylation of histones and transcription-related factors. Microbiol. Mol. Biol. Rev. *64*, 435–459.

Strahl, B.D., and Allis, C.D. (2000). The language of covalent histone modifications. Nature *403*, 41–45.

Suka, N., Suka, Y., Carmen, A.A., Wu, J., and Grunstein, M. (2001). Highly specific antibodies determine histone acetylation site usage in yeast heterochromatin and euchromatin. Mol. Cell *8*, 473–479.

Sun, Z.-W., and Allis, C.D. (2002). Ubiquitination of histone H2B regulates H3 methylation and gene silencing in yeast. Nature *418*, 104–108.

Susek, R.E., and Lindquist, S.L. (1989). Hsp26 of *Saccharomyces cerevisiae* is related to the superfamily of small heat shock proteins but is without a demonstrable function. Mol. Cell. Biol. *9*, 5265–5271.

Suzuki, K., and Ohsumi, Y. (2007). Molecular machinery of autophagosome formation in yeast, *Saccharomyces cerevisiae*. FEBS Lett. *581*, 2156–2161.

Swinnen, E., Wanke, V., Roosen, J., Smets, B., Dubouloz, F., Pedruzzi, I., Cameroni, E., De Virgilio, C., and Winderickx, J. (2006). Rim15 and the crossroads of nutrient signalling pathways in *Saccharomyces cerevisiae*. Cell Div. *1*, 3.

Takata, H., Kanoh, Y., Gunge, N., Shirahige, K., and Matsuura, A. (2004). Reciprocal association of the budding yeast ATM-related proteins Tel1 and Mec1 with telomeres *in vivo*. Mol. Cell *14*, 515–522.

Takeshige, K. (1992). Autophagy in yeast demonstrated with proteinase-deficient mutants and conditions for its induction. J. Cell Biol. *119*, 301–311.

Thomson, S., Clayton, A.L., Hazzalin, C.A., Rose, S., Barratt, M.J., and Mahadevan, L.C. (1999). The nucleosomal response associated with immediate-early gene induction is mediated via alternative MAP kinase cascades: MSK1 as a potential histone H3/HMG-14 kinase. EMBO J. *18*, 4779–4793.

Tissenbaum, H.A., and Guarente, L. (2001). Increased dosage of a sir-2 gene extends lifespan in *Caenorhabditis elegans*. *1252*, 1–4.

Titorenko, V., Keizer, I., Harder, W., and Veenhuis, M. (1995). Isolation and characterization of mutants impaired in the selective degradation of peroxisomes in the yeast Hansenula polymorpha. J. Bacteriol. *177*, 357–363.

Toda, T., Cameron, S., Sass, P., Zoller, M., and Wigler, M. (1987). Three different genes in *S. cerevisiae* encode the catalytic subunits of the cAMP-dependent protein kinase. Cell *50*, 277–287.

Trachootham, D., Zhang, H., Zhang, W., Feng, L., Du, M., Zhou, Y., Chen, Z., Pelicano, H., Plunkett, W., Wierda, W.G., et al. (2008). Effective elimination of fludarabine-resistant CLL cells by PEITC through a redox-mediated mechanism. Blood *112*, 1912–1922.

Tropberger, P., Pott, S., Keller, C., Kamieniarz-Gdula, K., Caron, M., Richter, F., Li, G., Mittler, G., Liu, E.T., Bühler, M., et al. (2013). Regulation of transcription through acetylation of H3K122 on the lateral surface of the histone octamer. Cell *152*, 859–872.

Trujillo, K.M., and Osley, M.A. (2012). A role for H2B ubiquitylation in DNA replication. Mol. Cell *48*, 734–746.

Tsukada, Y., Fang, J., Erdjument-Bromage, H., Warren, M.E., Borchers, C.H., Tempst, P., and Zhang, Y. (2006). Histone demethylation by a family of JmjC domain-containing proteins. Nature *439*, 811–816.

Tu, S., Bulloch, E.M.M., Yang, L., Ren, C., Huang, W.-C., Hsu, P.-H., Chen, C.-H., Liao, C.-L., Yu, H.-M., Lo, W.-S., et al. (2007). Identification of histone demethylases in *Saccharomyces cerevisiae*. J. Biol. Chem. *282*, 14262–14271.

Turner, B.M. (2000). Histone acetylation and an epigenetic code. BioEssays *22*, 836–845.

Urban, J., Soulard, A., Huber, A., Lippman, S., Mukhopadhyay, D., Deloche, O., Wanke, V., Anrather, D., Ammerer, G., Riezman, H., et al. (2007). Sch9 is a major target of TORC1 in *Saccharomyces cerevisiae*. Mol. Cell *26*, 663–674.

Verghese, J., Abrams, J., Wang, Y., and Morano, K. a (2012). Biology of the heat shock response and protein chaperones: budding yeast (*Saccharomyces cerevisiae*) as a model system. Microbiol. Mol. Biol. Rev. *76*, 115–158.

Wade, P.A., and Wolffe, A.P. (1997). Chromatin: Histone acetyltransferases in control. Curr. Biol. *7*, R82–R84.

Walter, D., Wissing, S., Madeo, F., and Fahrenkrog, B. (2006). The inhibitor-of-apoptosis protein Bir1p protects against apoptosis in *S. cerevisiae* and is a substrate for the yeast homologue of Omi/HtrA2. J. Cell Sci. *119*, 1843–1851.

Walter, D., Matter, A., and Fahrenkrog, B. (2010). Bre1p-mediated histone H2B ubiquitylation regulates apoptosis in *Saccharomyces cerevisiae*. J. Cell Sci. *123*, 1931–1939.

Walter, D., Matter, A., and Fahrenkrog, B. (2014). Loss of histone H3 methylation at lysine 4 triggers apoptosis in *Saccharomyces cerevisiae*. PLoS Genet. *10*, e1004095.

Wang, H., Huang, Z.Q., Xia, L., Feng, Q., Erdjument-Bromage, H., Strahl, B.D., Briggs, S.D., Allis, C.D., Wong, J., Tempst, P., et al. (2001). Methylation of histone H4 at arginine 3 facilitating transcriptional activation by nuclear hormone receptor. Science *293*, 853–857.

Wang, J., Ho, L., Qin, W., Rocher, A.B., Seror, I., Humala, N., Maniar, K., Dolios, G., Wang, R., Hof, P.R., et al. (2005). Caloric restriction attenuates beta-amyloid neuropathology in a mouse model of Alzheimer's disease. FASEB J. *19*, 659–661.

Wei, M., Fabrizio, P., Hu, J., Ge, H., Cheng, C., Li, L., and Longo, V.D. (2008). Life span extension by calorie restriction depends on Rim15 and transcription factors downstream of Ras/PKA, Tor, and Sch9. PLoS Genet. *4*, e13.

Weinberger, M., Ramachandran, L., Feng, L., Sharma, K., Sun, X., Marchetti, M., Huberman, J.A., and Burhans, W.C. (2005). Apoptosis in budding yeast caused by defects in initiation of DNA replication. J. Cell Sci. *118*, 3543–3553.

Weindruch, R., and Walford, R.L. (1988). retardation of aging and disease by dietary restriction.

Weinert, T., and Hartwell, L. (1988). The RAD9 gene controls the cell cycle response to DNA damage in *Saccharomyces cerevisiae*. Science (80-. ). *241*, 317–322.

Weinert, T.A., Kiser, G.L., and Hartwell, L.H. (1994). Mitotic checkpoint genes in budding yeast and the dependence of mitosis on DNA replication and repair. Genes Dev. *8*, 652–665.

Werner-Washburne, M., Becker, J., Kosic-Smithers, J., and Craig, E.A. (1989). Yeast Hsp70 RNA levels vary in response to the physiological status of the cell. J. Bacteriol. *171*, 2680–2688.

Werner-Washburne, M., Braun, E., Johnston, G.C., and Singer, R.A. (1993). Stationary phase in the yeast *Saccharomyces cerevisiae*. Microbiol. Mol. Biol. Rev. *57*, 383–401.

Werner-Washburne, M., Braun, E.L., Crawford, M.E., and Peck, V.M. (1996). Stationary phase in *Saccharomyces cerevisiae*. Mol. Microbiol. *19*, 1159–1166.

Winston, F., and Allis, C.D. (1999). The bromodomain: a chromatin-targeting module? Nat. Struct. Biol. *6*, 601–604.

Wissing, S., Ludovico, P., Herker, E., Büttner, S., Engelhardt, S.M., Decker, T., Link, A., Proksch, A., Rodrigues, F., Corte-Real, M., et al. (2004). An AIF orthologue regulates apoptosis in yeast. J. Cell Biol. *166*, 969–974.

Wolfe, S.A., and Grimes, S.R. (1993). Histone H1t: a tissue-specific model used to study transcriptional control and nuclear function during cellular differentiation. J. Cell. Biochem. *53*, 156–160.

Wurmser, A.E., and Emr, S.D. (2002). Novel PtdIns(3)P-binding protein Etf1 functions as an effector of the Vps34 PtdIns 3-kinase in autophagy. J. Cell Biol. *158*, 761–772.

Xie, X., Kokubo, T., Cohen, S.L., Mirza, U.A., Hoffmann, A., Chait, B.T., Roeder, R.G., Nakatani, Y., and Burley, S.K. (1996). Structural similarity between TAFs and the heterotetrameric core of the histone octamer. Nature *380*, 316–322.

Xu, F., Zhang, K., and Grunstein, M. (2005). Acetylation in histone H3 globular domain regulates gene expression in yeast. Cell *121*, 375–385.

Ye, J., Ai, X., Eugeni, E.E., Zhang, L., Carpenter, L.R., Jelinek, M.A., Freitas, M.A., and Parthun, M.R. (2005). Histone H4 lysine 91 acetylation a core domain modification associated with chromatin assembly. Mol. Cell *18*, 123–130.

Yuan, G.-C., Liu, Y.-J., Dion, M.F., Slack, M.D., Wu, L.F., Altschuler, S.J., and Rando, O.J. (2005). Genome-scale identification of nucleosome positions in *S. cerevisiae*. Science *309*, 626–630.

Zhang, L., and Freitas, M.A. (2004). Comparison of peptide mass mapping and electron capture dissociation as assays for histone posttranslational modifications. Int. J. Mass Spectrom. *234*, 213–225.

Zhang, Y., and Reinberg, D. (2001). Transcription regulation by histone methylation: interplay between different covalent modifications of the core histone tails. Genes Dev. *15*, 2343–2360.

Zhang, L., Eugeni, E.E., Parthun, M.R., and Freitas, M.A. (2003). Identification of novel histone post-translational modifications by peptide mass fingerprinting. Chromosoma *112*, 77–86.

# CHAPTER 2

## Screening of a Histone H3 and H4 Mutant Library for Strains with Shortened or Expanded Chronological Lifespans

### 2.1. Introduction

Histone N-terminal tails provide a binding surface to many proteins that are sensitive to the post-translational modification state of specific residues, the basis of the “histone code hypothesis” (Strahl and Allis, 2000). These proteins are involved in a plethora of genetic processes, including transcription and DNA replication, repair and recombination (Jenuwein and Allis, 2001). Modifications of residues located on the solute accessible face or side surface of the nucleosome have the ability to alter higher-order chromatin structure (Robinson *et al*., 2008). Furthermore, solute accessible residues may impede chromatin–protein interactions by disrupting the ability of non-histone proteins to bind to the surface of the nucleosome (Mersfelder and Parthun, 2006). On the other hand, residues present in the histone fold regions that are not solvent exposed may mediate histone-histone contacts that stabilize interactions between constituent histones in the octamer.

Histone H4K16 and H3K56 mutations were showed to affect replicative aging through a pathway that was different from that previously identified in yeast (Dang *et al*., 2009). Low levels of histone H2BK123 ubiquitination, and methylation at both H3K4 and H4K79 at telomere-proximal regions were critical for normal replicative lifespan (Rhie *et al*., 2013). In worms, the decrease of histone H3K4me3 by disrupting the ASH-2 trithorax complex, which trimethylates H3K4, extended lifespan (Greer *et al*., 2010). To date there are at least eleven types of post-translational modifications that have been reported on over 60 different residues in histones

(Martin and Zhang, 2007; Ruthenburg *et al*., 2007). Given the wide number of modified residues and range of modifications, and the involvement of histone modifications in lifespan, it is likely that there are many more histone modifications and chromatin modifiers involved in regulating lifespan that have simply not been identified to date.

In this study we looked at the retention of cell viability during extended incubation in stationary phase as a measure of chronological lifespan. This approach has been widely used in the longevity field(Longo, 1999). We were specifically interested in the lifespan of approximately 400 yeast synthetic histone H3 and H4 mutants (Dai *et al*., 2008), to gain a better perspective on the role of chromatin and histone modifications on the regulation of chronological lifespan. Each residue in histone H3 and H4 mutant library was systemically substituted with alanine. Naturally occurring alanine residues were changed to serine. To test the role of select histone post-translational modifications, all modifiable residues were substituted with residues mimicking constitutively modified and unmodified marks. For example, lysine was changed to arginine and glutamine, in order to mimic the deacetylated and acetylated states, respectively. Substitution of threonine with aspartic acid mimicked phosphorylation.

Two unique 20 bp DNA barcodes were integrated into each of the histone mutants allowing unambiguous identification of the histone mutants. In addition, systematic histone N-terminal tail deletions were also linked with two unique 20bp DNA barcodes.

Chronological lifespan is monitored in stationary phase. Yeast cells in stationary phase are not homogenous (Allen *et al*., 2006). There are non-quiescent (NQ) cells which constitute, predominantly, mother cells that are often *en route* to

apoptosis, and there are quiescent (Q) cells, which constitute daughter cells that can re-enter the cell cycle upon replenishment of the carbon source (Allen *et al*., 2006). Since these two cell populations are likely to differ significantly in transcriptomic, proteomic and metabolomic states, it was critical to separate the two cell populations to be able to analyse gene expression and protein states in an attempt to identify biochemical pathways downstream of any histone modification that had an impact on chronological lifespan of the mutant strain.

## 2.2. Materials and Methods

### *2.2.1. Yeast Strains and Growth Media*

The histone mutant library is based on a parental strain (JDY86) where one copy of the H3 (*HHT1*) and H4 (*HHF1*) have been deleted. The second copy (*HHT2* and *HHF2*) was replaced with a histone mutant expressed from its natural promoter. The genotype of JDY86 is *MATa, his3Δ200, leu2Δ0, K2Δ0, trp1Δ63, ura3Δ0*, *met15Δ0, can1::MFA1pr-HIS3, hht1-hhf1::NatMX4, hht2-hhf2::[HHTS-HHFS]-URA3*, where *[HHTS-HHFS]* designates the mutated histone which is either H3 or H4. In some cases, where specific mutations proved lethal, the strains were maintained by expressing wild type H3 and H4 episomally in addition to the mutant, genomic copy of H3 and H4. The genome type of the latter strains is *MAT*a,*his3Δ200, leu2Δ0, K2Δ0, trp1Δ63, ura3Δ0, met15Δ0, can1::MFA1pr-HIS3 hht1-hhf1::NatMX4, hht2-hhf2::[HHTS-HHFS]-URA3,* pJP11 plasmid (*CEN K HHF1-HHT1*). The histone H3 and H4 mutant library of approximately 400 strains was constructed in the laboratory of Jeff Boeke (Dai *et al*., 2008), and the commercial version was obtained from Thermo Fisher Scientific. All chemicals were of biochemical analysis or of molecular biology purity.

Rich YPD yeast growth medium was prepared with 1% (w/v) yeast extract, 2% (w/v) peptone and 2% (w/v) glucose. Agar-YPD contained 2% (w/v) bacto-agar. All media were sterilized by autoclaving before use.

### *2.2.2. Culturing of the Pooled Histone H3 and H4 Mutant Library*

The histone H3 and H4 mutant library was replica plated onto omnitray YPD-agar plates, and selected with 200 ng/ml nourseothricin antibiotic. Colonies were grown for 2-3 days at 30°C. Slow-growing colonies were separately streaked out

from the original frozen stock, and grown for 2-3 days at 30°C. The entire contents of all the plates, including the slow-growers (equivalent volume of a normal colony) were scraped off, and pooled in a 50 ml conical centrifuge tube containing YPD liquid media with 200 ng/ml nourseothricin. The pooled culture was diluted to a final concentration of $OD_{600}$ = 50, 15% (v/v) glycerol was added, and the pooled culture aliquoted and stored frozen at -80°C.

The pooled culture was inoculated into 100ml YPD liquid media to a final concentration of $OD_{600}$ ~ 0.003. Cells were grown with rotary shaking (180 rpm) at 30°C for approximately 10 generations (~15 h). The pooled culture was then further diluted to $OD_{600}$ of 0.06 in 250 ml YPD liquid media, and maintained in batch culture for up to 40 days with continual shaking (180 rpm) at 30°C. Aliquots (10 ml) were recovered at the times indicated.

### *2.2.3. Percoll Gradient Fractionation of Stationary Phase Cells*

A 9:1 (v/v). Percoll solution of Percoll:NaCl(1.5 M) was prepared. The non-quiescent and quiescent cells were fractionated by centrifugation on the Percoll gradient as described (Allen *et al*., 2006). Briefly, to form the Percoll gradients, 8 ml of the Percoll solution was centrifuged at 19 240 x g for 20 min at 20°C in a JA 20.1 rotor (Beckman). Culture aliquots (10 ml) recovered at specific times was washed twice with 5 ml sterile water. The cells were resuspended in 1 ml 50 mM Tris-HCl pH 7.5, carefully overlaid onto the performed Percoll gradient, and centrifuged at 400 x g for 60 min at 20°C in a GH-3.8 swinging bucket rotor (Beckman). NQ and Q fractions were collected carefully by using a Pasteur pipette. The collected fractions were washed once with 30 ml of 50 mM Tris-HCl pH 7.5, and centrifuged at 650 x gfor 5 min at 20°C in a GH-3.8 swinging bucket rotor.

### *2.2.4. Genomic DNA Purification*

Genomic DNA was isolated from 1 ml NQ and Q fractions (Zymo Research Yeastar kit, Protocol I). The DNA was eluted with 60 µl of TE buffer (10 mM Tris-HCl pH 8.0, 0.1 mM Na-EDTA), and the genomic DNA pellet stored at -80°C.

### *2.2.5. PCR Amplification of 20 bp DNA Barcodes*

Two PCR reactions with final volumes of 30 µl were set up for each sample, one for the “up” barcodes and one for the “down” barcodes. The reaction mixture contained 50ng of genomic DNA, 0.3 µl of 5 U/µl FastStart Taq DNA polymerase (Roche), 0.4 µl of 100 µM “up” or “down” barcode primer pair, 0.5 µl of 10 mM dNTP, 12 µl of 25 mM $MgCl_2$, 3 µl of 10x PCR buffer without $MgCl_2$, and water to a final volume of 30 µl.The primer sequences are shown in Table 2.1. PCR amplification was performed in a Mastercycler gradient thermocycler (Eppendorf) with the following cycling settings: one cycle of 94°C for 3 min, 30 cycles of 94°C for 30 sec, 55°C for 30 sec, 72°C for 30 sec, one cycle of 72°C for 3 min, and, finally, maintained at 4°C

**Table 2.1 Primer sequences used for the amplifination of "up" and "down" barcodes in the Boeke H3 and H4 histone mutant library.**

| Primer ID | Sequence |
|---|---|
| FU (forward "up") | ATGTCCACGAGGTCTCT |
| RU(reverse "up") | CCTCGACCTGCAGCGTA |
| FD (forward "down") | CGGTGTCGGTCTCGTAG |
| RD (reverse "down") | CCCAGCTCGAATTCATC |

### *2.2.6. Freeze and squeeze DNA Purification of 54 bp barcode containing fragments*

The "up" and "down" 54 bp barcode containing fragments of each NQ or Q fraction were combined, and run on a 1.5% (w/v) agarose gels (Sigma) in 89 mM Tris-borate and 2 mM EDTA, pH 8.3 (1×TBE) at 60 V, and stained with 0.1 µg/ml ethidium bromide. The DNA bands were visualized and excised on a glass back plate to minimize exposure of DNA to UV. The DNA was purified as described(Cole *et al.*, 2012) with modifications, using a Freeze 'N Squeeze DNA Gel Extraction kit (BioRad). Briefly, the gel slices were chopped into small pieces. The gel pieces were placed into a spin column (filter cup with dolphin tube). The spin column was incubated at -20°C for 5 min, repeated three times. The gel pieces were centrifuged at 13 000 x g for 3 min at room temperature. The DNA was collected in the dolphin tube. A volume (0.1×) of 3 M sodium acetate pH 5.2 and 20 mg/ml of glycogen was added as a carrier. The DNA was precipitated with cold absolute ethanol (-80°C) at -20°C overnight, washed with 70% ethanol, air dried, and resuspended in 15 µl TE buffer.

### *2.2.7. Multiplex Single-End Sequencing with Illumina*

All samples were prepared for single-end sequencing by ligating the 54 bp DNA barcode containing fragments to Illumina single-end adapters as well as index primers (Illumina). All reactions were carried out as recommended by the manufacturer.The sequencing reactions were performed by the ARC Biotechnology Platform, University of Pretoria. The generated FASTQ format sequence files were provided to me for analysis.

#### *2.2.7.1. Data analysis*

We used the program *get_seqs_from_fastq* to quantitate the number of times that each barcode sequence was present in the FASTQ file. Only perfect matches to barcodes of 20 nt were used. The program was coded in C++ using the 64 bit GNU compiler collection (GCC) version 4.5 (gcc.gnu.org). The code was compiled on a 64 bit Windows version 7 (Microsoft). All source files and compilation instructions, allowing local recompilation of *get_seqs_from_fastq*, can be downloaded from http://cbio.ufs.ac.za/Ngubo.

#### *2.2.7.2. Bin Analysis and Data Normalization*

The total number of barcodes retrieved at each time point was normalized to the intensity of the PCR amplified band, quantitated with Quantity One (BioRad) after scanning of the stained gel on a Pharos Molecular Imager (BioRad) following gel electrophoresis. This normalization ensures that samples that were amplified with different efficiencies could be quantitatively compared. Sequenced barcodes of all mutant strains were quantitated atthe different time points in stationary phase. The normalized levels of each barcode were expressed as the $\log_2$ ratio relative to the

level in the starting mixed population. All sequence read levels were quantile-normalized within time points.

### *2.2.8. Verification of Barcode Survival Curves of Individual Strains*

To verify the results of the barcode analysis, survival curves were constructed by inoculating 100 ml YPD liquid media with selected individual mutant strains to a final concentration of $OD_{600}$ ~ 0.003, as detailed previously. Yeast cultures were grown in duplicates overnight at 30°C, diluted to $OD_{600}$ of 0.06 in 250 ml YPD liquid media, and maintained in batch culture for up to 50 days shaking at 180 rpm at 30°C. At specific times, 100 µl of cells were removed and serially diluted in YPD liquid media. Tenfold dilutions were plated onto three YPD agar plates and incubated for 2-3 days at 30°C, and the number of colonies counted to determine viability based on colony forming units per ml (CFU/ml).

## 2.3. Results

We examined the role of histone H3 and H4 in chronological lifespan in yeast. As a first step, individual strains in a histone H3 and H4 mutant library composed of about 400 strains were pooled and maintained in batch culture for up to 40 days. Fractions that were recovered at specific times were separated into quiescent and non-quiescent cell populations by centrifugation on a Percoll gradient. A typical separation of the distinct quiescent and non-quiescent cell populations are shown in Figure 2.1 after incubation for 1 and 24 days, respectively.

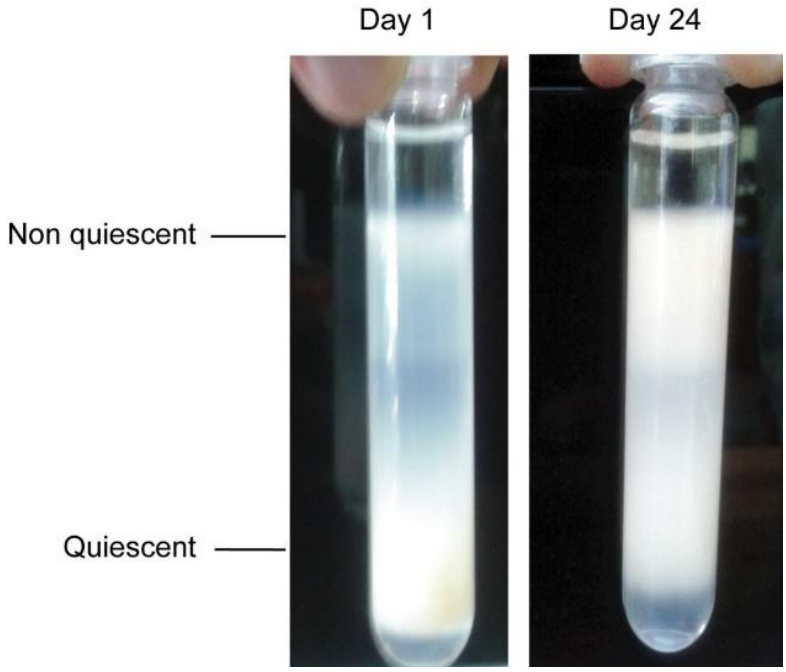


**Figure 2.1.Percoll gradient fractionation.**Percoll gradient separation of two distinct populations of cells at day 1 and 24. The fraction at the top of the gradient is the non-quiescent fraction and the fraction at the bottom of the gradient is the quiescent fraction.

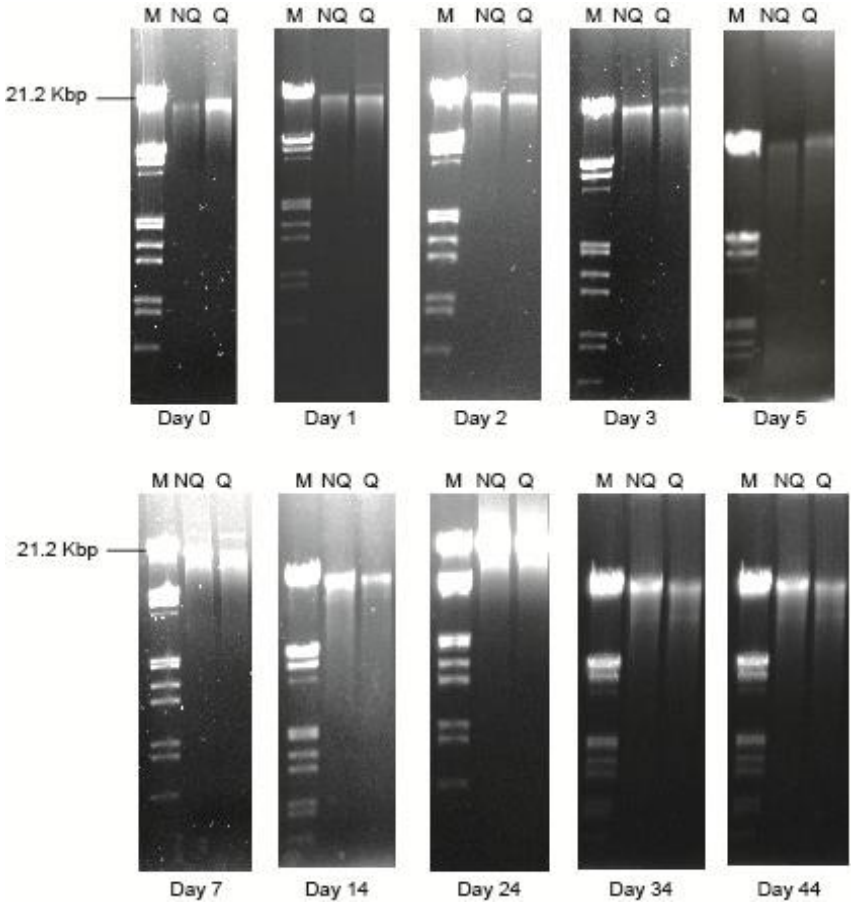


**Figure 2.2.Genomic DNA purification of the collected NQ and Q fractions.**Genomic DNA was isolated from NQ and Q fractions at different culturing periods, as is indicated for each panel. DNA size markers are shown in lane M of each panel.

To quantitate the lifespan of each histone mutant strain, genomic DNA was isolated from the non-quiescent and quiescent populations (Figure 2.2). “Up” and “down” DNA barcodes of the histone H3 and H4 mutant library were amplified at indicated times. The fragments recovered after PCR amplification using the genomic DNA as template are shown in Figure 2.3. The resulting 54 bp DNA barcode containing fragments were isolated from the gel and purified.

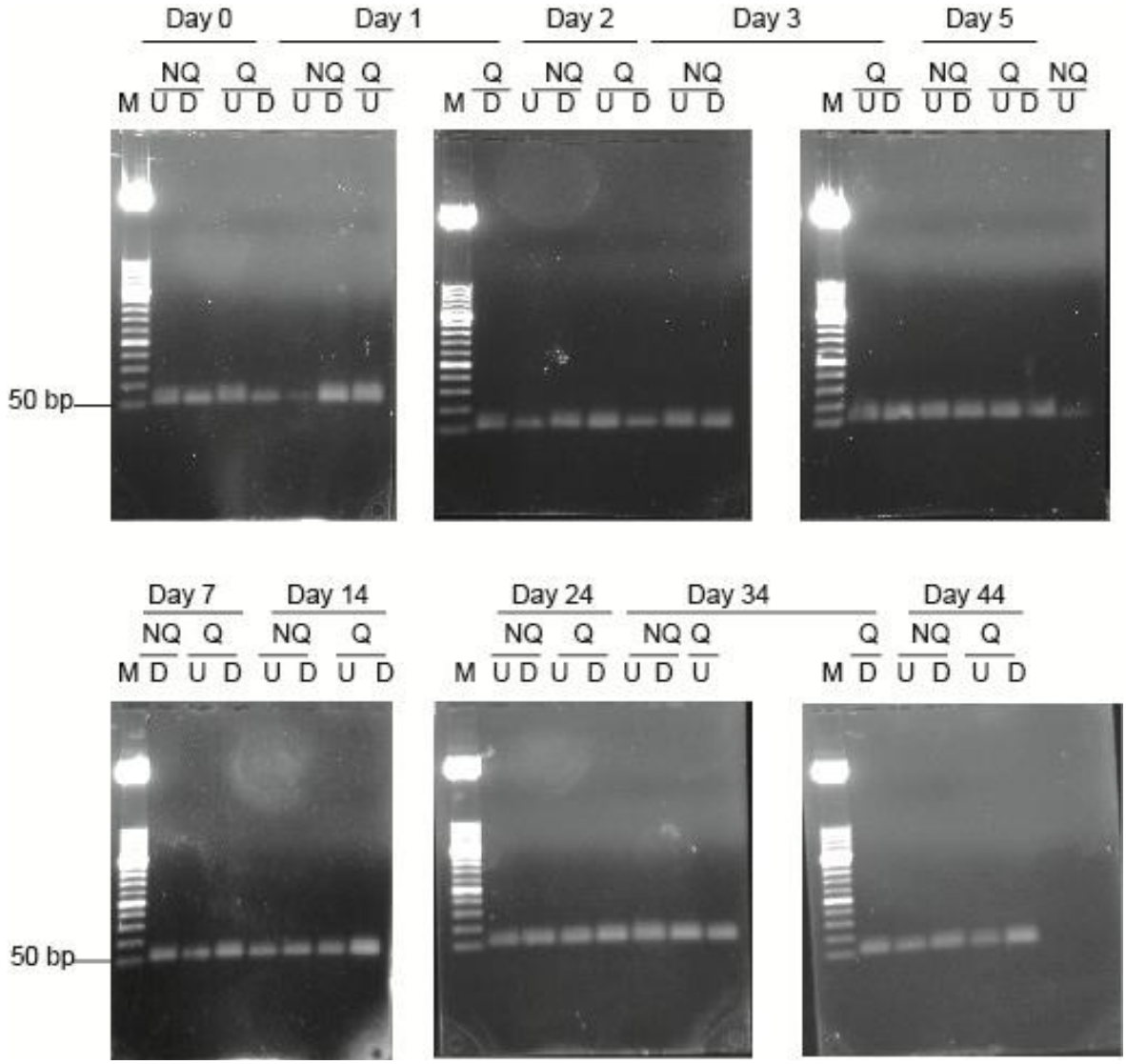


**Figure 2.3. PCR Amplification of 20 bp DNA barcodes**. The “up” (U) and “down” (D) barcodes were amplified with appropriate primer sets using the template genomic DNA isolated from non-quiescent (NQ) and quiescent (Q) sub-populations that were incubated for the culturing periods indicated above each panel. A DNA size standard is shown in lane M.

The lifespan of each histone mutant was determined by quantitating the DNA barcode levels. The basic principle is that if a specifc strain has a shortened chronological lifespan, its unique barcode level (number of sequenced barcodes) should decreasecompared to the starting level of that barcode, and possibly disappear from the population over a period of time.

Strains with extended lifespans should maintain a unique barcode at an elevated level, matching cell replication during growth to stationary phase, compared to both the starting level, andthe population average. This method of quantitating the fractional representation of a specific yeast strain and a unique barcode in a mixed population was shown to be accurate, linear, and more sensitive than microarray-based techniques (Smith et al., 2009).

**Tabe 2.1. Details of sequencing results by single-end sequencing of amplified barcode containing fragments**

| Sample | Sequences retrieved | Two matched primers | Correct length insert | Incorrect length insert | One matched primer | No primers | Barcode retrieval (%) | Barcode Ratio (U:D) | Coverage (fold) |
|---|---|---|---|---|---|---|---|---|---|
| 1 | 179953 | 153241 | 153077 | 164 | 10413 | 16296 | 85 | 1.7 | 157 |
| 2 | 227839 | 187698 | 187583 | 115 | 13842 | 26296 | 82 | 1.7 | 192 |
| 3 | 210376 | 173273 | 173180 | 93 | 12106 | 24995 | 82 | 1.3 | 177 |
| 4 | 212373 | 175067 | 174940 | 127 | 13891 | 23406 | 82 | 1.1 | 179 |
| 5 | 217886 | 181869 | 181707 | 162 | 12311 | 23700 | 83 | 1.3 | 186 |
| 6 | 201809 | 161362 | 161239 | 123 | 13624 | 26821 | 80 | 1.1 | 165 |
| 7 | 221189 | 169126 | 169000 | 126 | 15112 | 36948 | 76 | 1.1 | 173 |
| 8 | 234326 | 190063 | 189889 | 174 | 17086 | 27167 | 69 | 1.0 | 195 |
| 9 | 204927 | 169985 | 169836 | 149 | 13817 | 21112 | 83 | 1.4 | 174 |
| 10 | 234967 | 191802 | 191660 | 142 | 15145 | 28019 | 82 | 1.0 | 196 |
| 11 | 215633 | 170369 | 170218 | 151 | 15634 | 29627 | 79 | 1.2 | 174 |
| 12 | 208596 | 168107 | 167943 | 164 | 14186 | 26300 | 81 | 1.2 | 172 |
| 13 | 235078 | 192930 | 192742 | 188 | 15942 | 26201 | 82 | 1.1 | 197 |
| 14 | 224119 | 185921 | 185722 | 199 | 15341 | 22851 | 83 | 1.1 | 190 |
| 15 | 191267 | 148617 | 148488 | 129 | 12807 | 29840 | 79 | 2.1 | 152 |
| 16 | 164289 | 132724 | 132575 | 149 | 10410 | 21152 | 81 | 7.0 | 134 |
| 17 | 202549 | 166370 | 166266 | 104 | 13762 | 22417 | 82 | 1.4 | 170 |
| 18 | 434172 | 354798 | 354533 | 265 | 28210 | 51162 | 82 | 1.5 | 363 |
| 19 | 238161 | 191670 | 191494 | 176 | 16991 | 29500 | 80 | 1.5 | 196 |
| 20 | 208135 | 176602 | 176477 | 125 | 12016 | 19498 | 85 | 1.8 | 181 |

The coverage results of the barcode sequencing is shown in Table 2.1. A high number of retrieved sequences were obtained. Furthermore, low incorrect length inserts, high barcode retrieval percentage, and a high fold coverage were also obtained. Interestingly, the barcode yield displayed a bias towards the “up” DNA barcode. We used the average of the “up” and “down” barcode levels for each strain at every time point.

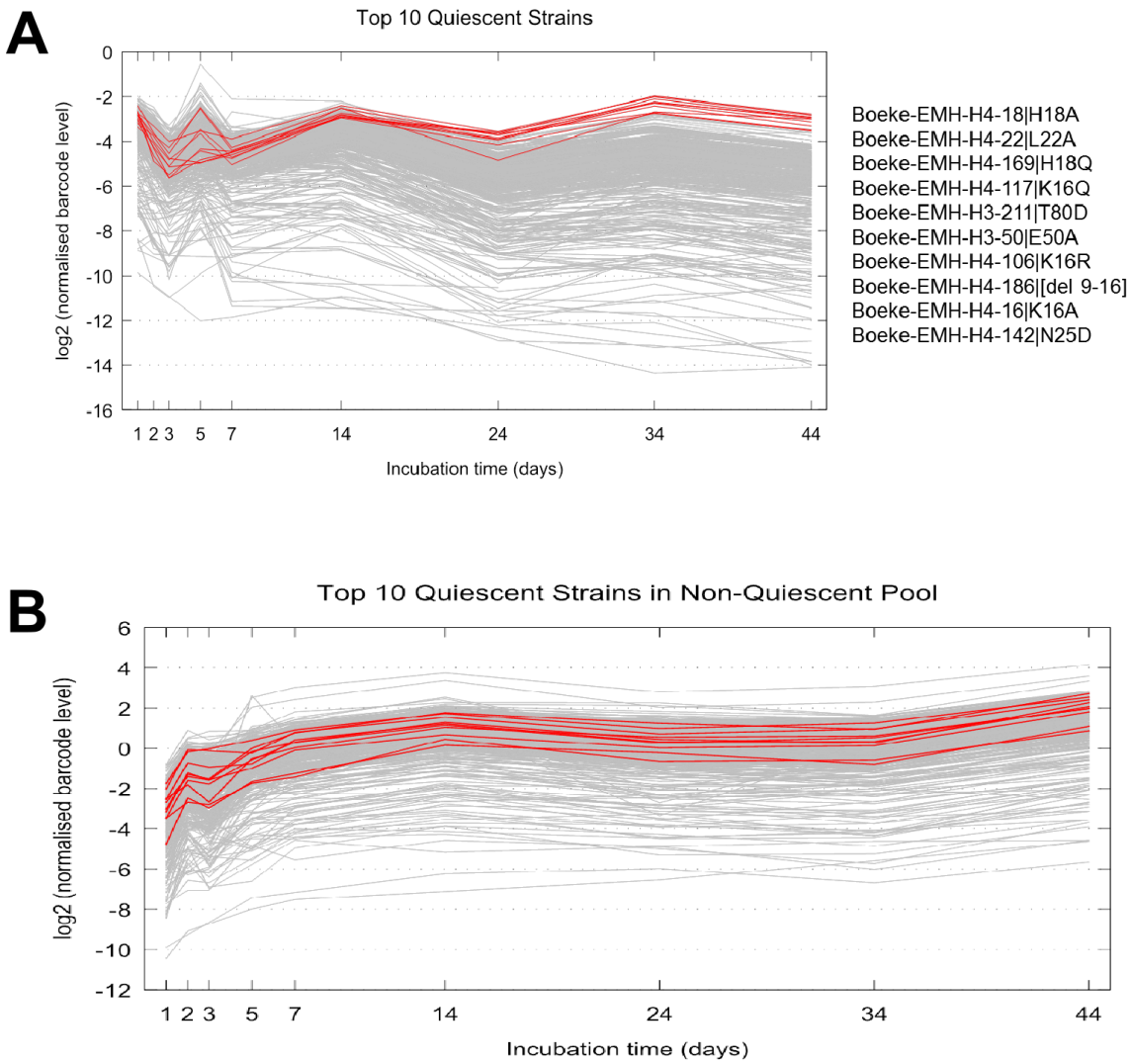


**Figure 2.4. Residues implicated in yeast lifespan extension.**
Panel A shows the quiescent DNA barcode survival curves with top 10 quiescent strains showed in red. The list of the top 10 quiescent strains is showed on the right. The histone mutant barcode levels were normalized between time points. Panel B shows the top 10 quiescent strains (showed in red) in the non-quiescent DNA barcode survival curves.

Residues such as H4K16, and H2BK123 were previously shown to effect replicative lifespan (Dang *et al*., 2009; Rhie *et al*., 2013). We were interested in identifying all residues in H3 and H4 that had an impact on chronological lifespan.Quantitation of the DNA barcodes showed that some strains decreased at a lower rate in the quiescent population (Figure 2.4 A) compared to the population average. Histone mutant H4K16Q and H4K16R strains were maintained at high

levels up to day 44 in stationary phase, compared to the population average. The location of the identified residues is shown in Figure 2.5. Strikingly, all residues implicated in lifespan extension are solvent accessible, and either on the H4 tail, involve a partial H4 tail deletion (H4Δ9-16) or are located within the Sin or Lrs sectors previously identified (Fry *et al*., 2006)

Histone mutant H4K16Q and H4K16R were previously shown to regulate replicative aging (Dai *et al*., 2008). Interestingly, any mutation of K16 (K→Q, K→R, or K→A) caused an increase in lifespan(Figure 2.4 A). This points to a requirement for H4K16 for normal lifespan. The mutations H4K16Q and H4K16R, which mimic constitutive acetylation and deacetylation respectively, may point to the requirement of a balance between the two modification states for normal growth. The silence information regulator protein Sir3, involved as a structural component in heterochromatic assemblies at silent mating loci and sub-telomeric regions, was shown to bind to the side of the nucleosome (Wang *et al*., 2013). Histone H4K16, H4H18, H4L22, H4N25, and H3T80 all interact with the Sir3 BAH domain (Armache *et al*., 2011; Wang *et al*., 2013). The only identified lifespan extension mutant that does not interact with the BAH domain is H3E50. On the nucleosome core particle, H3E50 is exposed on the lateral surface between two DNA gyres, shown in Figure 2.5 E, suggesting that H3E50 may influence yeast lifespan through a different pathway.

Figure 2.4 B shows the top 10 quiescent strains in the non-quiescent population. The figure shows that the strains that survive the longest or are implicated in lifespan extension do not necessarily constitute the minor population of non-quiescent cells. This is conceivable since the non-quiescent fraction of each

long-lived strain was suggested to provide some level of protection and nutrients to the long-lived quiescent fraction by autophagy(Aragon *et al*., 2008).

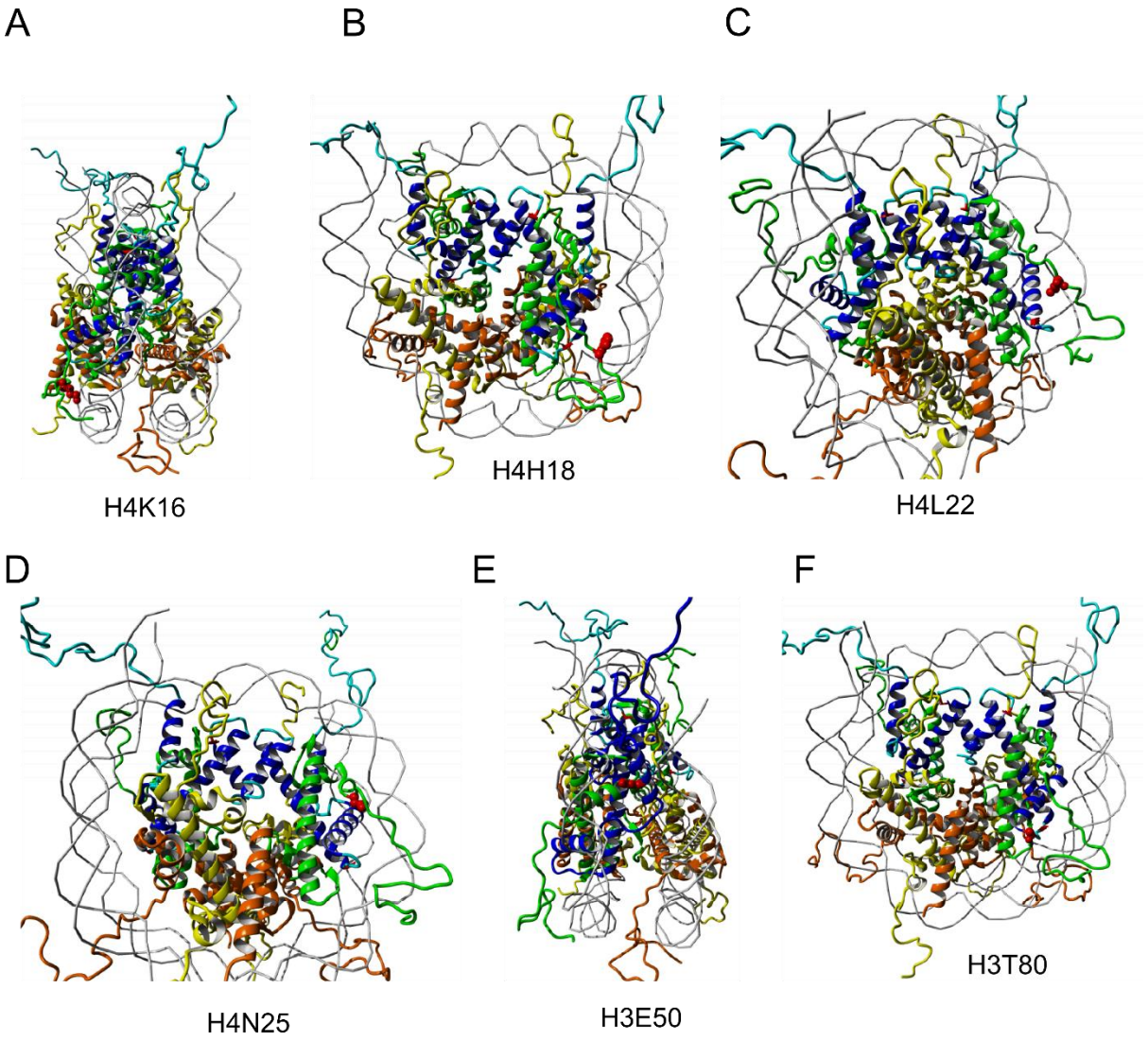


**Figure 2.5.Residues in histone H3 and H4 where substitution mutations exhibited a longer chronological lifespan.** The position of the residues (A) H4K16, (B) H4H18, (C) H4L22, (D) H4N25, (E) H3E50, and (F) H3T80 are shown in the crystal structure of the nucleosome core (PDB accession number 1KX5). The relevant residues are shown in red.

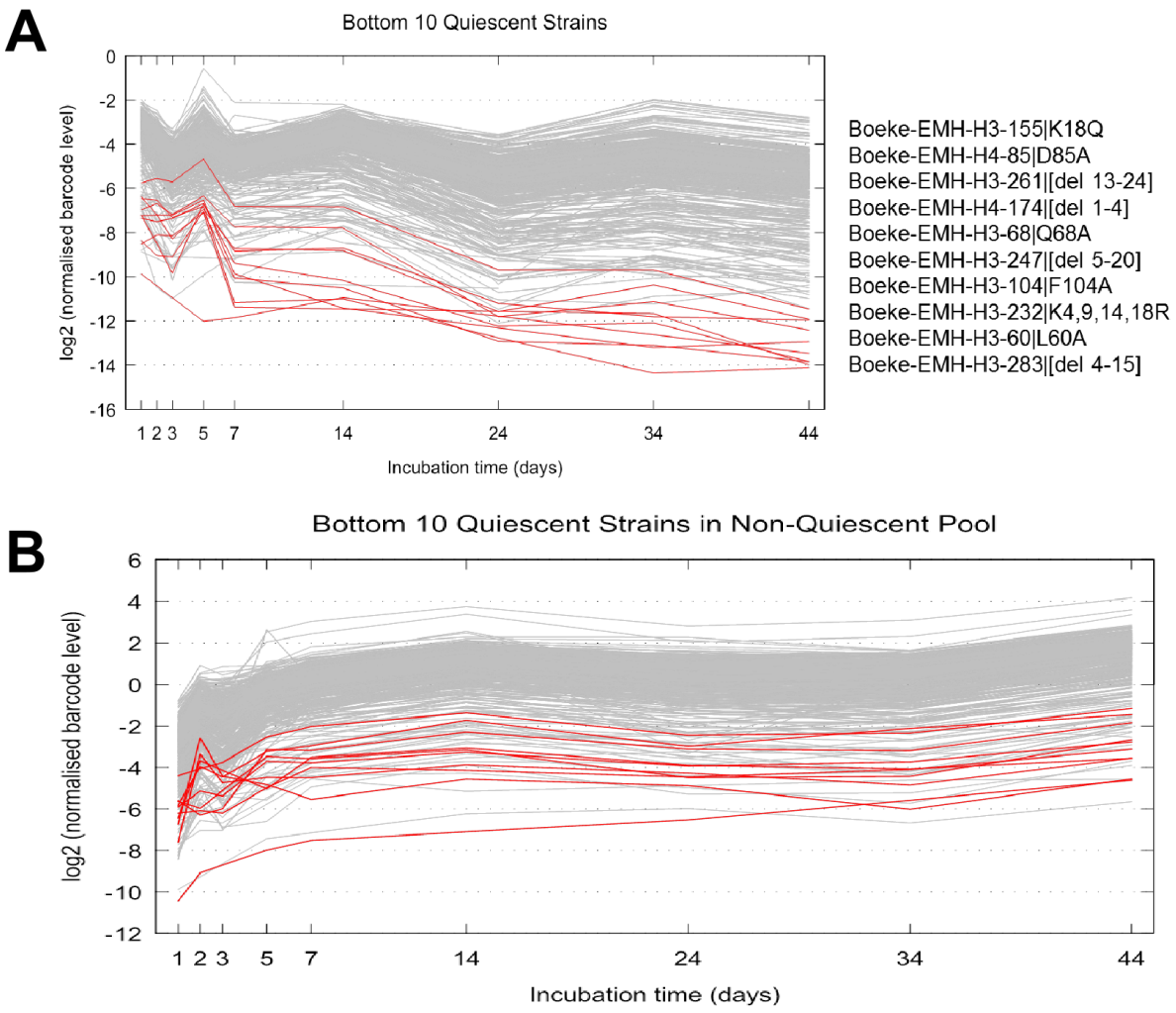


**Figure 2.6. Residues implicated in yeast lifespan reduction. Panel A shows the quiescent** DNA barcode survival curves with bottom 10 Q strains showed in red. The list of the bottom 10 Q strains is showed on the right. The histone mutant barcode levels were normalized between time points. Panel B shows non-quiescent DNA barcode survival curves with bottom 10 Q strains showed in red.

The ratio of each mutant strain, expressed as $\log_2$ ratio relative to the starting level, is shown in Figure 2.6, with the bottom 10 strains identified in Figure 2.6 A. When looking at the bottom 10 quiescent strains in the non-quiescent population, it was observed that these strains decreased in the non-quiescent pool (Figure 2.6 B), suggesting that cell that disappears from the quiescent pool appears in the non-quiescent pool.

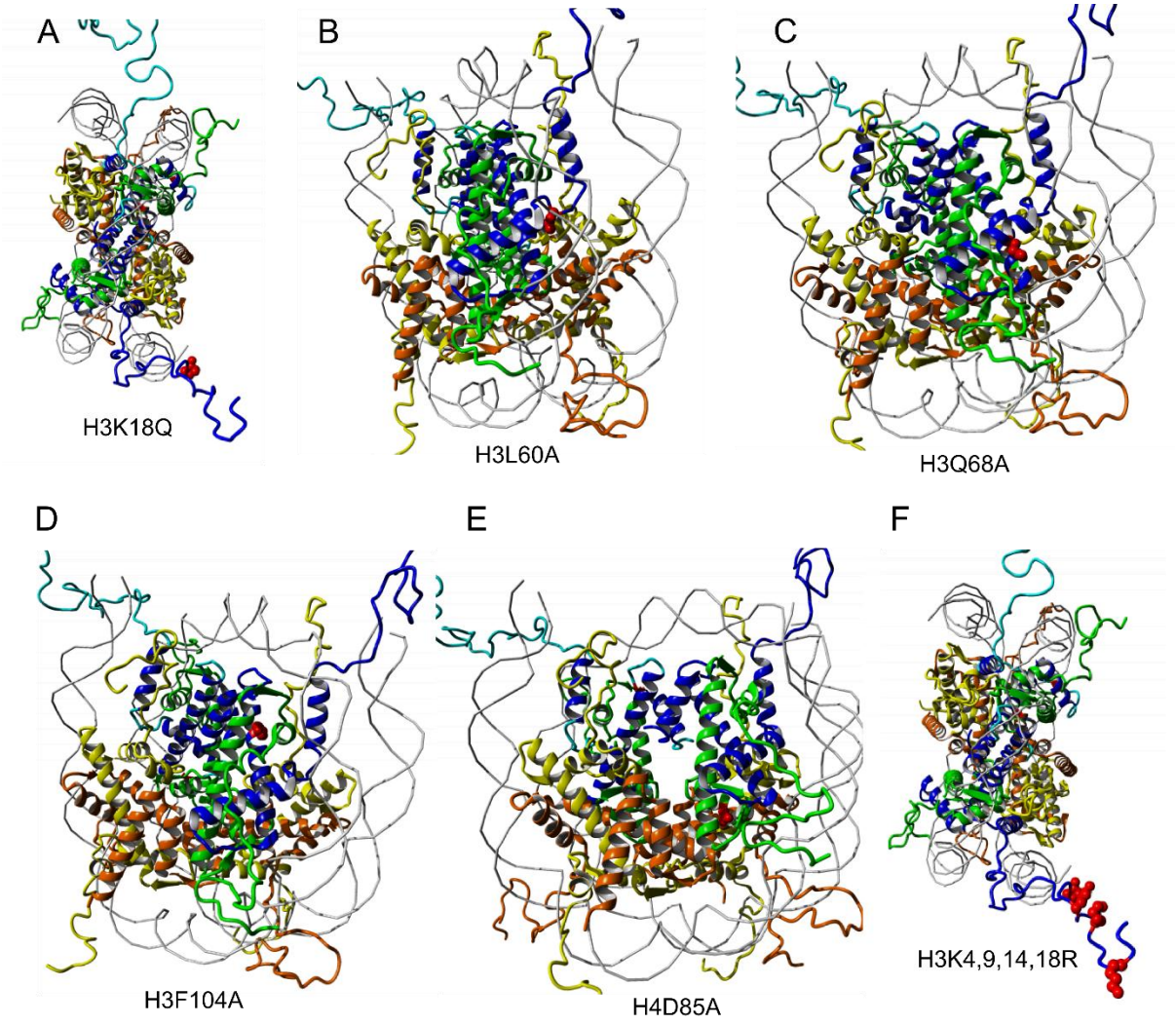


**Figure 2.7.Residues in histone H3 and H4 where substitution mutations exhibited a reduced chronological lifespan.**The position of the residues (A) H3K18Q, (B) H3L60A, (C) H3Q68A, (D) H3F104A, (E) H4D85A, and (F) H3K4,9,14,18R are shown in the crystal structure of the nucleosome core (PDB accession number 1KX5). The relevant residues are shown in red.

Histone H3 tail deletions (H3Δ13-24, H3Δ1-4, H3Δ5-20, and H3Δ4-15) strains were clearly rapidly reduced from the quiescent populations. The histone H4 tail deletion (H4Δ1-4) was also observed to disappear quickly from the quiescent pool. It is clear that a wider range of histone H3 tail deletions hada more adverse effect on lifespan compared to histone H4 tail deletions. Notably, substitution of four histone H3 tail lysine residues with arginine (H3K4, 9, 14,18R) also reduced lifespan. This suggests that mimickinghistone H3 tail lysine deacetylation decreased longevity. The

location of residues where mutations decreased lifespan is summarized in Figure 2.7. There are three histone H3 internal residues (H3Q68A, H3F104A, and H3L60A), compared to one histone H4 internal residue (H4D85A) linked to chronological lifespan reduction. All four of these mutations occur in regions that may be involved in the stabilization of the histone fold of individual core histones, or in the stabilization of histone-histone interactions in the H3-H4 tetramer and H2A-H2B binding to the H3-H4 tetramer. The histone H3K18Q mutant strain was the only histone tail residue linked with chronological lifespan reduction.

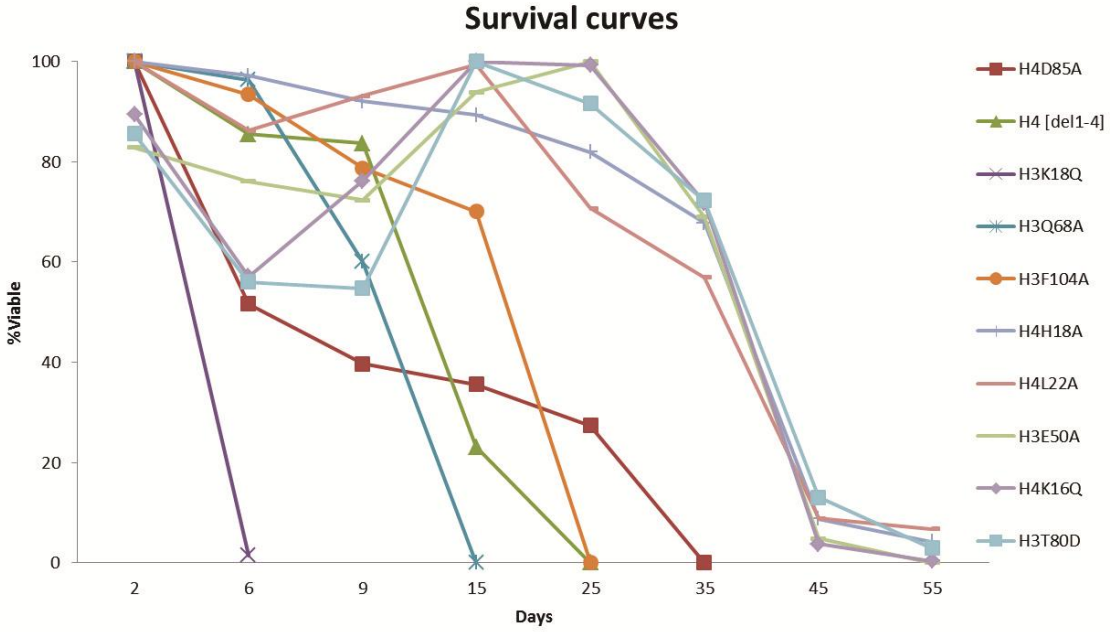


**Figure 2.8. Verification of barcode survival curves of individual strains.** Survival curves of individual strains which were implicated in lifespan extension and lifespan reduction (listed on the right) were determined for biological duplicates.

We verified the results of our barcode approach by determining the survival curves (in duplicate)for select strains implicated in lifespan regulation, above. The individual strains were maintained in batch culture for up to 55 days at 30°C. Figure 2.8 shows that the strains that were rapidly reduced in the quiescent barcode pool also exhibited a shortened chronological lifespan when tested as individual strains.

Similarly, the mutants implicated in chronological lifespan extension appear to increase notably as they enter into stationary phase. We have thus independently verified the veracity of the barcode approach to screen for mutants with reduced or extended chronological lifespans.

## 2.4. Discussion

There is increasing evidence that chromatin structure and epigenetic dynamics change during the aging process. One major mechanism for epigenetic regulation is histone modification. Histone H4K20 tri-methylation was reported to increase with age (Sarg *et al*., 2002). Histone H4K16 acetylation was observed to increase at specific sub-telomeric regions in aging cells (Dang *et al*., 2009b). Histone H3K56 deacetylation was showed to extend replicative lifespan in yeast by minimizing genome instability (Hachinohe *et al*., 2011). Santisteban and colleagues showed that histone H4K91 was located in the region of histone H4 that interacts with histone H2B, and helped to stabilize the formation of the histone octamer (Santisteban *et al*., 1997). Specific regions of the nucleosome surface are critical for the assembly of a silent chromatin structure in yeast (Park *et al*., 2002). Below, we systematically discuss the possible structural role and mechanistic impact of every residue and tail deletion mutant identified in the barcode screen above.

In the case of residues implicated in lifespan reduction, of the residues located within the histone fold domain, H3Q68 is present in $\alpha$1 of H3, and extends almost co-axially to the $\alpha$-helix axis of H3 $\alpha$2 into the space between $\alpha$1 and the DNA backbone, pointing towards the major groove at SHL°3 (Figure 2.9 A). An analysis of interactions of H3Q68 revealed no hydrogen bonding interactions.

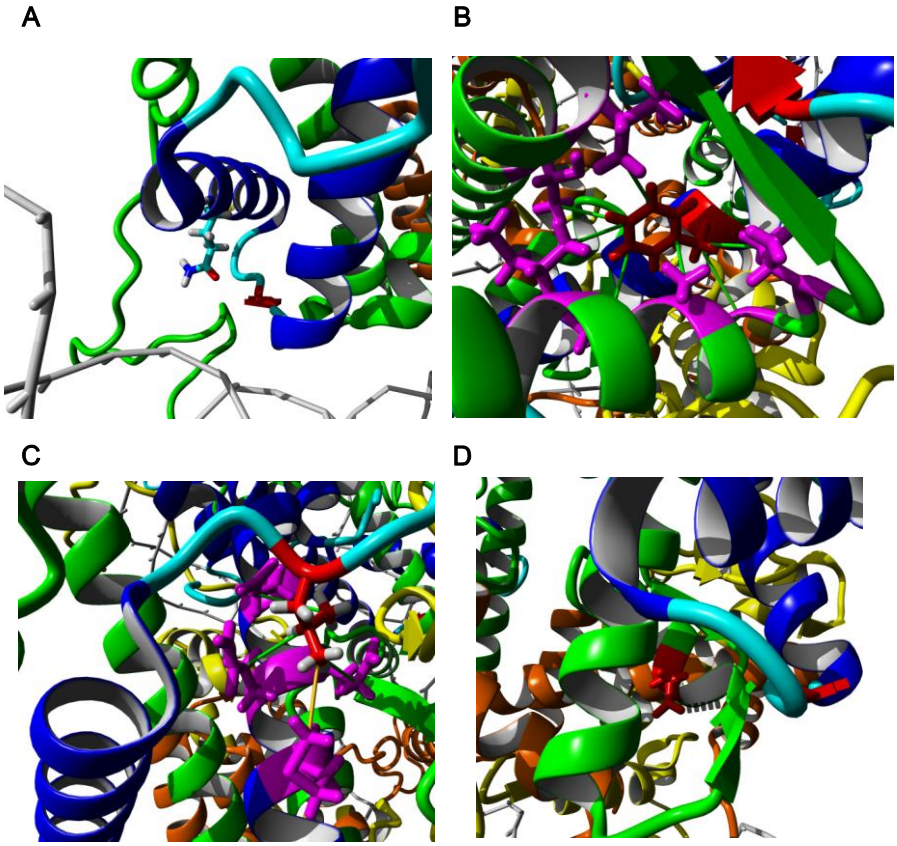


**Figure 2.9. The interactions of residues implicated in lifespan reduction.** (A) H3Q68 extends into the space between α1 and the DNA backbone. An analysis did not reveal the participation of this residue in any interactions. (B) H3F104 (red) points into the space demarcated by H4 α1-L1-α2. It is involved in extensive hydrophobic interactions (thin green lines) with I34, L37, A38, V43, G41, I50 and T54 (magenta). (C) H3L60 (red) in present on the extended α-helix preceding α1 of H3. It makes extensive hydrophobic contacts (thin green lines) with H3M90, H3Q93, H3E94 and H3E97. (D) H4D85 is located in α3 of H4, and makes a single hydrogen bond (stippled line) to the backbone hydrogen amide of V81.

H3F104 is present in α2, and extends towards the space enclosed by α1-L1-α2 of H4 (Figure 2.9 B). H3F104 makes extensive hydrophobic contact with residues in α1, L1 and α2 of histone H4. These hydrophobic interactions include I34, L37, A38 (α1), V43 and G41 (L1), and I50 and T54 (α2). These interactions are likely to contribute to the affinity and binding of H3 and H4 as part of the H3-H4 tetramer, as well as stabilizing the histone fold of H4 at α1-L1-α2 and positioning α1 to allow exit of the H4 N-terminal tail at a specific orientation from the nucleosome core.

H3L60 is present on the coiled region between the extended α-helix and α1 of H3 (Figure 2.9 C), and points towards α2 of H3, as well as the C-terminal domain of H2A. It is involved in hydrophobic interactions with H3M90 ($CH_3 \rightarrow CH_3$), H3Q93 ($CH \rightarrow CH_2$), and interactions of the leucine $CH_3$ groups with the $CH_2$ groups of H3E94 and H3E97. These interactions will stabilize the H3 histone fold, especially the orientation of the α1 helix relative to the α2 helix, and thereby contribute to the favorable binding interactions between H3 and H4.

H4D85 is located in α3, and extends into the space enclosed by α2-L2-α3. The carbonyl oxygen of D85 is involved in a single hydrogen bond to the backbone amide hydrogen that is N-terminal to V81 (Figure 2.9 D). This interaction stabilizes the histone fold in the α2-L2-α3 region of H3, and also directs the orientation of the exit angle of α3 and the short C-terminal tail into the central space. The latter orientation is expected to be crucial for optimal interaction between H4 and H2B at the four helix bundle whereby the H2A-H2B dimer is attached to the H3-H4 tetramer.

It therefore seems very likely that H3F104, H3L60 and H4D85 are involved in stabilisation of the histone fold, and the exit angles of α1 and α3 and adjacent N- and C-terminal tails. It further appears that these three residues, in particular, will play crucial roles in the association of H3 and H4 in the H3-H4 tetramer, as well as the binding of the H2A-H2B dimer to the H3-H4 tetramer in the octamer. In all three corresponding mutants that exhibited a reduced lifespan, the residues were substituted with A, which abolishes the identified hydrophobic interactions and hydrogen bonding. It would be very interesting to confirm the involvement of the three residues above in a histone binding study by measuring dissociation of the H2A-H2B dimer from the octamer, as well as dissociation of H3 and H4 in the H3-H4

dimer, at decreasing ionic strengths, where hydrophobic effects will decrease and electrostatic repulsions predominate, compared to the wild type histones.

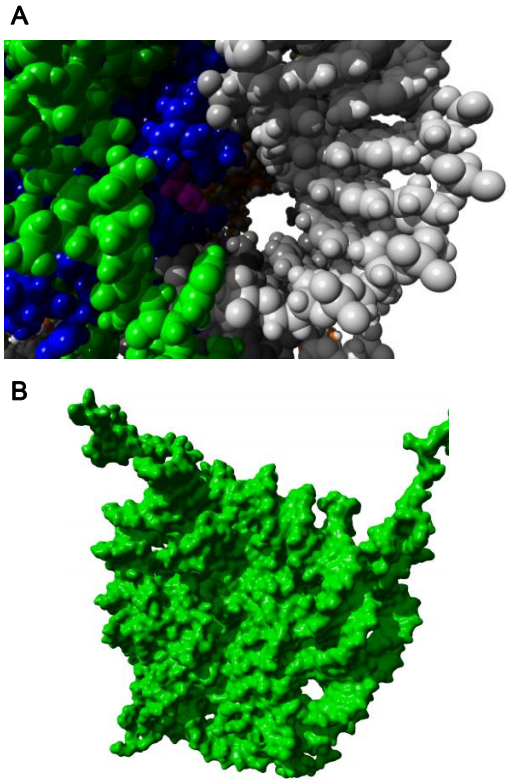


**Figure 2.10.H3Q68 interactions.**(A) The position of H3Q68 (magenta) in a space adjacent to the major groove at SHL 3 is suitable for hydrogen bonding to water molecules that may be present in the major groove of the nucleosome *in situ*. (B) The molecular surface of the nucleosome core that is solvent accessible, showing the void between H3Q68 and the DNA double helix that is part of a tunnel that extends through the core.

H3Q68 was not found to be involved in any direct interactions with residues in H3 or in other histones in the octamer, nor to the DNA backbone. Its orientation does, nonetheless, strongly suggest an interaction with the backbone. However, the residue is equidistant (approximately 8Å) from the two DNA strands, and is also some 11Å from the edge of the closest base, an adenine. We propose that H3Q68 is involved in hydrogen bonds with water molecules that would be present in the major groove at this position. It was previously shown by X-ray crystallographic analysis that a spine of water molecules were present in the minor groove, and a slightly

more disordered grouping of bridging water molecules were present in the major groove of DNA (Tereshko *et al*., 1999). Although the insertion of arginine residues into the major groove, for instance, could disrupt such associated water molecules, the crystal structure of the region between H3Q68 and the associated DNA showed a clear void that could be occupied by water molecules *in situ* (Figure 2.10 A). In fact, a trace of the molecular surface that is solvent accessible displays the clear hole in the structure that could easily accommodate an array of water molecules (Figure 2.10 B). The hydrogen bonding of H3Q68 to water molecules associated with the DNA at this position would contribute to the guiding of the DNA double helix on the correct path on the octamer surface, and would also help with the stabilization of the terminal gyre that experiences significant electrostatic repulsion from the second, adjacent DNA gyre. We therefore speculate that the structural integrity of the DNA supercoil is weakened in the H3Q68A mutant, which may translate to a structurally compromised nucleosome core. Such an unstable nucleosome core may activate the apoptotic response more quickly when the cell experiences the cellular stress associated with carbon depletion and entry into stationary phase.

Several histone readers, erases and modifiers bind to some of the residues identified in the screen above. It is possible that the effect of these mutants on longevity is imparted through many different pathways. However, previous studies on the regulation of longevity identified a modest number of signaling pathways, most notably the mTOR pathway and the protein kinase A pathway, that both, ultimately, exert an effect on the expression of stress response genes (Schmelzle and Hall, 2000; Smith *et al*., 1998). In fact, calorific restriction, previously identified by Guarente and colleagues as a common metabolic hallmark of lifespan regulation,

also feeds into cellular stress response in chronological lifespan (Lin *et al*., 2002). We were therefore inclined to think in terms of protein interactions with the nucleosome that would include all or most of the identified residues above. A search of the literature revealed one domain, the bromo-adjacent homology (BAH) domain, which was shown to bind to the side surface of the nucleosome (Armache *et al*., 2011) (Figure 2.11).

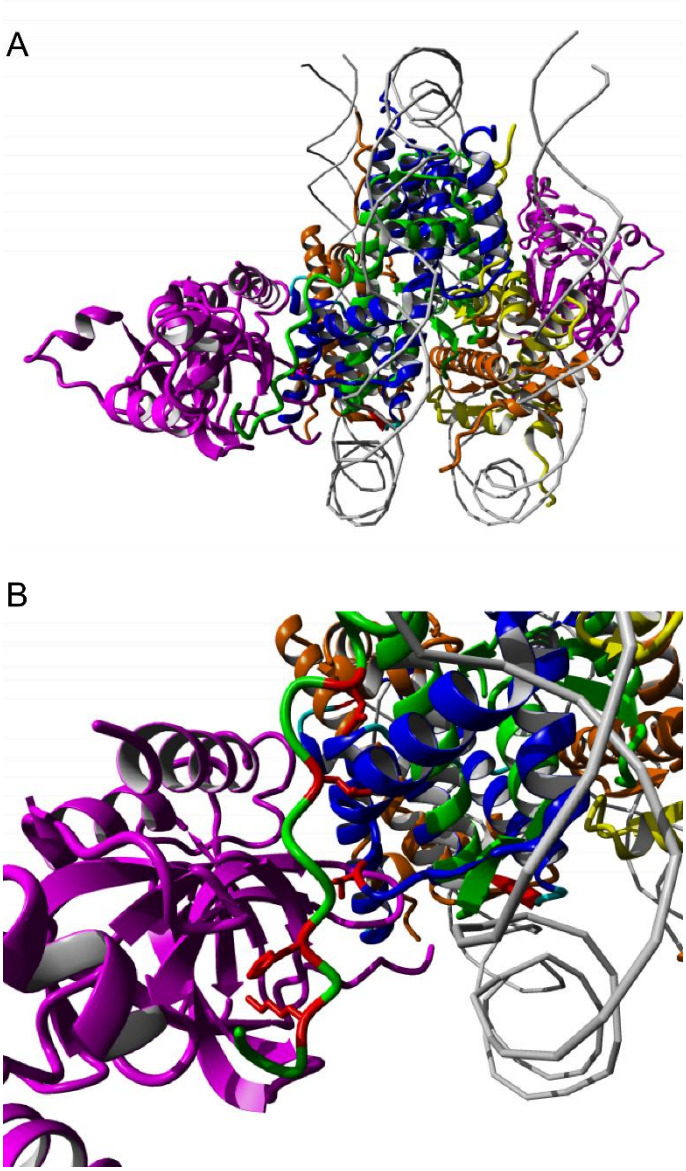


**Figure 2.11.Binding of the Sir3 BAH domain to the nucleosome core.** (A) The binding of the BAH domain of Sir3 (magenta) to the side surface of the nucleosome core is shown, based on the crystal structure (PDB accession 3TU4). (B) The residues identified in yeast mutants with extended chronological lifespans are shown in red. H4K16, H4H18 and H3T80 are at positions that should allow interaction with Sir3. The residues H4L22 and H4N25 are positioned in an orientation that suggests interaction with the adjacent H3 histone.

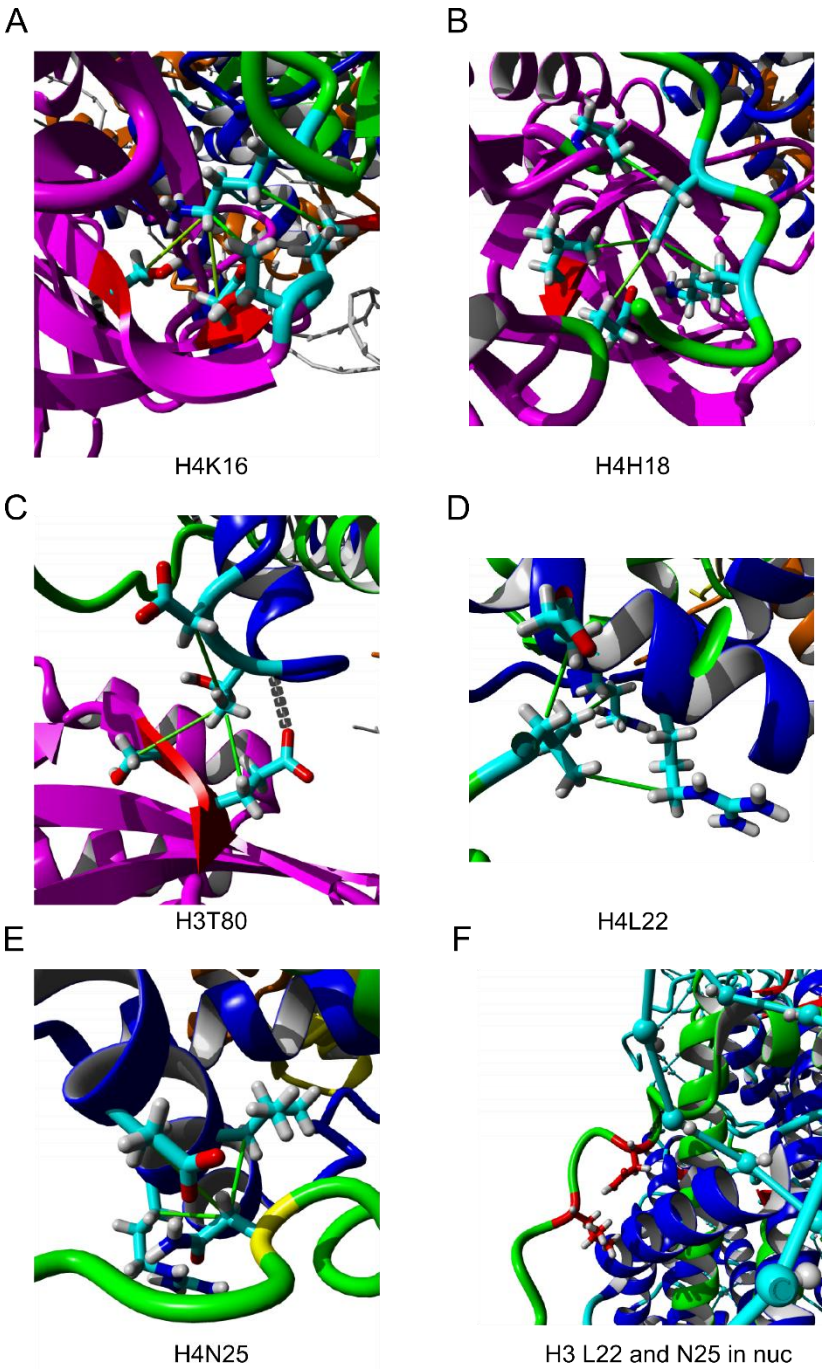


**Figure 2.12.Interactions of histone residues with the Sir3 BAH domain.** (A) Hydrophobic interactions between (A) H4K16 and the $^{2}CH_2$ of BAH D60, $^{4}CH_3$ of BAH V62, $^{4}CH_3$ of BAH T63, and $^{3}CH_2$ of BAH S67, (B) between $^{3}CH_2$ of H4H18, $^{4}CH$ of BAH L91, $^{3}CH_2$ of BAH E95, and $^{4}CH_2$ of BAH P179, and (C) between H3T80 and $^{3}CH_2$ of H3 H3D81, $^{3}CH_2$ of BAH S139, and $^{3}CH_2$ of BAH E140 is shown (thin green cylinders). (D) H4L22 interacts hydrophobically with $^{4}CH_2$ of H3R72, $^{4}CH_2$ of H3R69, and $^{3}CH_2$ of H3E73. (E) H4N25 is similarly involved in hydrophobic interactions with histone H3 via $^{3}CH_2$ of H3R69, $^{3}CH_2$ of H3E73 and $^{3}CH_2$ of H3L70. (F) In the native nucleosome core (PDB accession 1KX5) H4L22 and H4N25 are involved in identical contacts to the $\alpha$1 helix of histone H3.

The binding of the Sir3 BAH domain to a nucleosome core was solved by X-ray crystallography (Armache *et al*., 2011) and extensive contacts to H3 within the LRS domain (Fry *et al*., 2006; Norris *et al*., 2008) as well as to the H4 tail have been assigned (Armache *et al*., 2011; Norris and Boeke, 2010). In the crystal structure, H4K16 approached a "flap" in the BAH domain of Sir3, composed of two β-strands connected by a loop (see Figure 2.10). Kingston and co-workers identified a hydrogen bond between H4K16 and S67 of Sir3, but our analysis did not identify this interaction. The distance between the Sir3 BAH S67 hydroxyl oxygen and the most proximal hydrogen of the H4K16 amino group is 2.2Å, which is within hydrogen-bonding distance. However, the angle between the H4K16 N-H bond and the BAH domain S67 O is approximately 154°, which may decrease the interaction energy below the cut-off of 6.25 kJ/mol. We did, however, find extensive hydrophobic interactions between the H4K16 $CH_2$ groups and $^{2}CH_2$ of BAH D60, $^{4}CH_3$ of BAH V62, $^{4}CH_3$ of BAH T63, and $^{3}CH_2$ of BAH S67 (Figure 2.12 A). H4H18 showed hydrophobic interactions with $^{3}CH_2$ of H4H18, $^{4}CH$ of BAH L91, $^{3}CH_2$ of BAH E95, and $^{4}CH_2$ of BAH P179 (Figure 2.12 B). H3T80 displayed hydrophobic interactions to $^{3}CH_2$ of H3 H3D81, $^{3}CH_2$ of BAH S139, and $^{3}CH_2$ of BAH E140 (Figure 2.12 C). The oxygen of BAH E140 also makes a hydrogen bond to the backbone amide hydrogen N-terminal to H3T80 (Figure 2.11 C), possibly contributing to the binding affinity of the Sir3 BAH domain to the nucleosome side. The H4L22 residue orientation is such that interactions with histone H3 appears more likely compared to interactions with the Sir3 BAH domain. In fact H4L22 $^{5}CH_3$ makes hydrophobic contacts with $^{4}CH_2$ of H3R72, $^{5'}CH_3$ of H4L22 is involved with a hydrophobic interaction with $^{4}CH_2$ of H3R69, and $^{2}CH_2$ of H4L22 with $^{3}CH_2$ of H3E73 (Figure 2.12 D). H4N25 is similarly involved in hydrophobic interactions with histone H3 via $^{3}CH_3$ of H4N25 and $^{3}CH_2$ of

H3R69, $^{3}CH_2$ of H3E73 and $^{3}CH_2$ of H3L70, respectively (Figure 2.12 E). H3E50, also shown to increase chronological lifespan, was shown to be present on the lateral surface of the nucleosome, between the two DNA superhelical gyres, extending towards the major groove at SHL 1. The space between H3E50 and the edge of the nucleotide bases in the bordering major groove is in excess of 8Å, thus allowing sufficient space for a water molecule. We suggest that H3E50 is involved in hydrogen bonding to water molecules accommodated in the major groove at this location, and contributes to the guiding and stabilization of the nucleosomal DNA on the octamer surface.

The H4 tail deletion H4Δ9-16 was also shown to extend lifespan. It is likely that this tail deletion, which includes H4K16 implicated in Sir3 BAH domain binding above, reduces the ability of Sir3 to bind to the side surface of the nucleosome core, abrogating this Sir3 interaction.

The hydrophobic interaction of K4L22 and H4N25 with histone H3 is quite interesting. These interactions occur close to the start of the α1 helix at H4T30, in a region where the N-terminal tail of H4 passes over α1 of histone H3, and possibly locks the orientation of the H4 tail on the side surface of the nucleosome, and directs the exit direction of the tail where it passes close to the nucleosomal DNA at SHL 2. This interaction of K4L22 and H4N25 with the H3 α1 helix is not due to a partial displacement of the H4 tail by binding of the Sir3 BAH domain, since identical interactions are seen for H4L22 and H4N25 in the native nucleosome core structure (Figure 2.12 F).

It was previously also reported that the Rsc1 and Rsc2 sub-units of the RSC chromatin remodeling complex, as well as Orc1, a sub-unit of the ORC replication complex as well as a role player in transcriptional silencing in *S. cerevisiae*(Connelly

*et al*., 2006) possessed a BAH domain, and could bind to nucleosomes (Norris and Boeke, 2010). Rsc1 and Rsc2 are sub-units of the RSC chromatin remodeling complex, and are present in two isoforms of the complex with overlapping and with unique functions (Chambers *et al.*, 2013). Rsc1/2 is related to BAF180 in higher eukaryotes, which is part of the PBAF complex, also known as SWI/SNF-B. Interestingly, the structure of the BAH domains of the Rsc1/2 proteins and BAF180 differ from that of Sir3 and Orc1, which prompted Downs and colleagues to refer to "Rsc-like" and "Sir3-like" BAH domains. The BAH domain of Rsc1 and Rsc2 was essential for function (Cairns *et al*., 1999). In a cryo-EM structure, the nucleosome core was proposed to occupy a central cavity present in the RSC complex (Chaban *et al*., 2008). However, in the absence of docking data using high resolution X-ray structures of the complex constituents, it was not possible to derive insight into possible interactions at atomic level. Downs and colleagues reported that that Rsc2 BAH domain interacted with chromatin, assessed by ChIP assay, as well as bind to nucleosomes *in vitro*, assessed by co-IP (Chambers *et al*., 2013). Furthermore, Rsc2 BAH was shown to be able to immune-precipitate free histone H3, but not H4. It was proposed that this demonstrated a fundamental difference in the binding of the Rsc-like BAH domain to the nucleosome as compared to the Sir3-like BAH domain. However, there has been no published study to date that showed that mutants that abrogated Sir3 BAH binding to the nucleosome did not influence Rsc-like BAH domain binding. Thus, although there is a published assertion that the binding of Rsc-like BAH domains differ from that of Sir3-like BAH domains, critical control experiments remain outstanding. For this reason, we will consider the possible downstream effect of both Sir3/Orc1 and Rsc1/2 on cellular processes that could impact on longevity in yeast.

## 2. 5. Reference List


Allen, C., Büttner, S., Aragon, A.D., Thomas, J.A., Meirelles, O., Jaetao, J.E., Benn, D., Ruby, S.W., Veenhuis, M., Madeo, F., et al. (2006). Isolation of quiescent and nonquiescent cells from yeast stationary-phase cultures. J. Cell Biol. *174*, 89–100.

Aragon, A.D., Rodriguez, A.L., Meirelles, O., Roy, S., Davidson, G.S., Tapia, P.H., Allen, C., Joe, R., Benn, D., and Werner-washburne, M. (2008). Characterization of differentiated quiescent and nonquiescent cells in yeast stationary phase cultures. Mol. Biol. Cell *19*, 1271–1280.

Armache, K.-J., Garlick, J.D., Canzio, D., Narlikar, G.J., and Kingston, R.E. (2011). Structural basis of silencing: Sir3 BAH domain in complex with a nucleosome at 3.0 Å resolution. Science. *334*, 977–982.

Cairns, B.R., Schlichter, A., Erdjument-Bromage, H., Tempst, P., Kornberg, R.D., and Winston, F. (1999). Two functionally distinct forms of the RSC nucleosome-remodeling complex, containing essential AT hook, BAH, and bromodomains. Mol. Cell *4*, 715–723.

Chaban, Y., Ezeokonkwo, C., Chung, W.-H., Zhang, F., Kornberg, R.D., Maier-Davis, B., Lorch, Y., and Asturias, F.J. (2008). Structure of a RSC-nucleosome complex and insights into chromatin remodeling. Nat. Struct. Mol. Biol. *15*, 1272–1277.

Chambers, A.L., Pearl, L.H., Oliver, A.W., and Downs, J.A. (2013). The BAH domain of Rsc2 is a histone H3 binding domain. Nucleic Acids Res. *41*, 9168–9182.

Cole, H.A., Howard, B.H., and Clark, D.J. (2012). Genome-wide mapping of nucleosomes in yeast using paired-end sequencing. Methods Enzymol. *513*, 145–168.

Connelly, J.J., Yuan, P., Hsu, H., Xu, R., Sternglanz, R., and Li, Z. (2006). Structure and function of the *Saccharomyces cerevisiae* Sir3 BAH Domain. Mol. Cell. Biol. *26*, 3256–3265.

Dai, J., Hyland, E.M., Yuan, D.S., Huang, H., Bader, J.S., and Boeke, J.D. (2008). Probing nucleosome function: a highly versatile library of synthetic histone H3 and H4 Mutants. Cell *134*, 1066–1078.

Dang, W., Steffen, K.K., Perry, R., Dorsey, J.A., Johnson, F.B., Kaeberlein, M., Kennedy, B.K., and Berger, S.L. (2009). Histone H4 lysine 16 acetylation regulates cellular lifespan. Nature *459*, 802–807.

Fry, C.J., Norris, A., Cosgrove, M., Boeke, J.D., and Peterson, C.L. (2006). The LRS and SIN domains: two structurally equivalent but functionally distinct

nucleosomal surfaces required for transcriptional silencing. Mol. Cell. Biol. *26*, 9045–9059.

Greer, E.L., Maures, T.J., Hauswirth, A.G., Green, E.M., Leeman, D.S., Maro, G.S., Han, S., Banko, M.R., Gozani, O., and Brunet, A. (2010). Members of the H3K4 trimethylation complex regulate lifespan in a germline-dependent manner in C. elegans. Nature *466*, 383–387.

Hachinohe, M., Hanaoka, F., and Masumoto, H. (2011). Hst3 and Hst4 histone deacetylases regulate replicative lifespan by preventing genome instability in *Saccharomyces cerevisiae*. Genes Cells *16*, 467–477.

Jenuwein, T., and Allis, C.D. (2001). Translating the histone code. Science *293*, 1074–1080.

Lin, S.-J., Kaeberlein, M., Andalis, A.A., Sturtz, L.A., Defossez, P.-A., Culotta, V.C., Fink, G.R., and Guarente, L. (2002). Calorie restriction extends *Saccharomyces cerevisiae* lifespan by increasing respiration. Nature *418*, 344–348.

Longo, V.D. (1999). Mutations in signal transduction proteins increase stress resistance and longevity in yeast, nematodes, fruit flies, and mammalian neuronal cells. Neurobiol. Aging *20*, 479–486.

Martin, C., and Zhang, Y. (2007). Mechanisms of epigenetic inheritance. Curr. Opin. Cell Biol. *19*, 266–272.

Mersfelder, E.L., and Parthun, M.R. (2006). The tale beyond the tail: histone core domain modifications and the regulation of chromatin structure. Nucleic Acids Res. *34*, 2653–2662.

Norris, A., and Boeke, J.D. (2010). Silent information regulator 3: the Goldilocks of the silencing complex. Genes Dev. *24*, 115–122.

Norris, A., Bianchet, M.A., and Boeke, J.D. (2008). Compensatory interactions between Sir3p and the nucleosomal LRS surface imply their direct interaction. PLoS Genet. *4*, e1000301.

Park, J.-H., Cosgrove, M.S., Youngman, E., Wolberger, C., and Boeke, J.D. (2002). A core nucleosome surface crucial for transcriptional silencing. Nat. Genet. *32*, 273–279.

Rhie, B.-H., Song, Y.-H., Ryu, H.-Y., and Ahn, S.H. (2013). Cellular aging is associated with increased ubiquitylation of histone H2B in yeast telomeric heterochromatin. Biochem. Biophys. Res. Commun. *439*, 570–575.

Robinson, P.J.J., An, W., Routh, A., Martino, F., Chapman, L., Roeder, R.G., and Rhodes, D. (2008). 30 nm chromatin fibre decompaction requires both H4-K16 acetylation and linker histone eviction. J. Mol. Biol. *381*, 816–825.

Ruthenburg, A.J., Li, H., Patel, D.J., and Allis, C.D. (2007). Multivalent engagement of chromatin modifications by linked binding modules. Nat. Rev. Mol. Cell Biol. *8*, 983–994.

Santisteban, M.S., Arents, G., Moudrianakis, E.N., and Smith, M.M. (1997). Histone octamer function in vivo: mutations in the dimer-tetramer interfaces disrupt both gene activation and repression. EMBO J. *16*, 2493–2506.

Sarg, B., Koutzamani, E., Helliger, W., Rundquist, I., and Lindner, H.H. (2002). Postsynthetic trimethylation of histone H4 at lysine 20 in mammalian tissues is associated with aging. J. Biol. Chem. *277*, 39195–39201.

Schmelzle, T., and Hall, M.N. (2000). TOR, a central controller of cell growth. Cell *103*, 253–262.

Smith, A., Ward, M.P., and Garrett, S. (1998). Yeast PKA represses Msn2p/Msn4p-dependent gene expression to regulate growth, stress response and glycogen accumulation. EMBO J. *17*, 3556–3564.

Strahl, B.D., and Allis, C.D. (2000). The language of covalent histone modifications. Nature *403*, 41–45.

Tereshko, V., Minasov, G., and Egli, M. (1999). The Dickerson-Drew B-DNA dodecamer revisited at atomic resolution. J. Am. Chem. Soc. *121*, 470–471.

Wang, F., Li, G., Altaf, M., Lu, C., Currie, M. a, Johnson, A., and Moazed, D. (2013). Heterochromatin protein Sir3 induces contacts between the amino terminus of histone H4 and nucleosomal DNA. Proc. Natl. Acad. Sci. U. S. A. *110*, 8495–8500.

# CHAPTER3

## A RNA-seq Analysis of Select Histone Mutants that Cause Chronological Lifespan Extension

### 3.1. Introduction

We have identified a number of histone mutants that caused either an increase or a decrease in chronological lifespan of the yeast cell compared to both the WT parent and the population average. These residues mutated in the strains were concentrated in two regions. All residues associated with a decrease in chronological lifespan were located in the interface between histone H3 and H4. It is likely that these mutations weaken the interaction between H3 and H4, and may compromise the structural stability of the H3-H4 tetramer and the nucleosome. We speculate that such a destabilized nucleosome will facilitate the more rapid accumulation of DNA damage and accelerate cell death (see also the Discussion chapter).

The second concentration of residues were all associated with an increase in chronological lifespan, and, with the exception of H3E50 and H3T80, were all located on the solvent accessible surface of histones H3 and H4. H3E50 and H3T80 were located at positions underneath the trajectory of the DNA in the nucleosome; all other mutations were in the H4 tail (Figure 3.1). In fact, the H4 tail deletion H4$\Delta$9-16 was also associated with lifespan extension.

The location of these mutated residues is intriguing in the light of the study by Herskowitz and co-workers, who identified mutations in histones H3 and H4 that rescued the swi/snf mutant phenotype (Kruger *et al*., 1995). These mutations, called Sin mutations, were present in the conserved histone fold region of H3 and H4, often

at positions close to the path of the DNA at the site of DNA entry/exit into the nucleosome (Kruger *et al*., 1995). Grunstein and co-workers subsequently identified a number of histone H3 mutants, with mutated residues that mapped to the L1 and α1 helix, which were implicated in telomeric and HM (hidden MAT) locus silencing, as well as repression of basal transcription (Thompson *et al*., 2003).

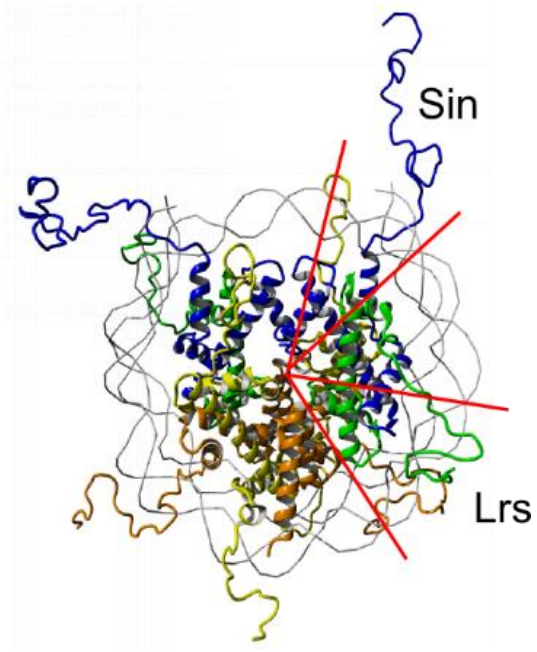


**Figure 3.1. The sectorial positions of the Sin and Lrs domains are indicated in the crystal structure (PDB accession number 1KX5, Davey et al., 2002) of the nucleosome core.** The region including H4 L1 and H3 L2 approaching the minor groove at SHL ±0.5 forms the Sin domain, and the region including H4 L2 and H3 L1 approaching the minor groove at SHL ±4.5 forms the Lrs domain.

More recently, Peterson and co-workers described two regions of the nucleosome, the Lrs (loss of rRNA silencing) domain, and the Sin domain, implicated in derepression of rRNA genes and Swi/Snf independent gene expression, respectively (Fry *et al*., 2006). The Sin domain is formed by L1 of H4 and L2 of H3 where it approaches the minor groove at SHL ±0.5.The Lrs domain is formed by L2 of H4 and L1 of H3 where it approaches the minor groove at SHL ±2.5. The position of the Lrs and Sin domains are shown in Figure 3.1.

Mutations in the Lrs domain do not cause a Sin phenotype, and *vice versa*. The Sin domain, but not the Lrs domain, is required for proper folding of chromatin (Horn *etal*., 2002). The mutations in the H3 $\alpha$1 helix and L1 loop identified by Grunstein (Thompson *et al*., 2003) overlap with the Sin and Lrs regions of the nucleosome, respectively. The locations of the Sin and Lrs domains in the nucleosome is shown in Figure 3.1, and the residues that are associated with Sin or Lrs phenotypes are listed in Table 3.1.

**Table 3.1. Residues in histones H3 and H4 previously identified as Sin or Lrs mutants.**

| Mutant | Reference |
|---|---|
| **Sin** | |
| H3E105K | Kruger *et al.*, 1995; Fry *et al.*, 2006 |
| H3R116H | Kruger *et al.*, 1995; Fry *et al.*, 2006 |
| H3T118I | Kruger *et al.*, 1995; Fry *et al.*, 2006 |
| H4V43I | Kruger *et al.*, 1995; Fry *et al.*, 2006 |
| H4R45H | Kruger *et al.*, 1995; Fry *et al.*, 2006 |
| H4R45C | Kruger *et al.*, 1995; Fry *et al.*, 2006 |
| **Lrs** | |
| H3K79E | Fry *et al.*, 2006 |
| H3K79R | Fry *et al.*, 2006 |
| H3L82S | Fry *et al.*, 2006 |
| H3R83A | Fry *et al.*, 2006 |
| H3R72G | Fry *et al.*, 2006 |
| H3A75V | Fry *et al.*, 2006 |
| H3F78L | Fry *et al.*, 2006 |
| H3E73D | Fry *et al.*, 2006 |
| H4R45C | Fry *et al.*, 2006 |
| H4R78G | Fry *et al.*, 2006 |
| H4V81A | Fry *et al.*, 2006 |
| H4K79M | Fry *et al.*, 2006 |

The structures of Sin nucleosomes, elucidated by X-ray crystallography, show that a small number of histone-DNA contacts close to the site of DNA entry/exit in the nucleosome are disrupted (Muthurajan *et al*., 2004). This may cause the dissociation of the octamer from the DNA at lower ionic strengths, and an increase in translational mobility or “sliding” (Fry *et al*., 2006). The nucleosomal DNA of the Sin nucleosome does not, however, dissociate from the octamer surface more readily, since Sin nucleosomal DNA is not more accessible to restriction enzymes (Fry *et al*., 2006). These properties were proposed to cause the independence of Sin

nucleosomes from the Swi/Snf remodelling complex (Fry *et al*., 2006), andSin mutations weaken general, basal level repression (Fry *et al*., 2006; Thompson *et al*., 2003). Both the Sin and Lrs domains are required for optimal Sir2p and Sir4p binding at both telomeric and HM loci, and in the case of the HM loci, this role is partially redundant with Sir1p function (Fry *et al*., 2006).

Fascinatingly, all of the mutated residues identified is this study that cause chronological lifespan extension are located in either the Sin and Lrs regions, but they are not all *bona vida* Sin or Lrs mutants. H3T80 is located in the Lrs domain, in L1 of H3, and approaches the DNA at SHL ±2.5. It is associated with a weak derepression of the rRNA genes (Table 3.2), and can thus be assigned as a Lrs residue.

H3E50 is located in $\alpha$1 of H3. Although this is not in H4 L1 or H3 L2, it is located in the Sin domain sector (see Figure 3.1). Also, H3E50 approaches the DNA in the vicinity of SHL ±0.5 (see Figure 3.2), which is perhaps the most important property of the Sin mutants. This residue can also tentatively be assigned as a Sin residue.

The H4K16, H4H18, H4L22 and H4N25 are all located on the N-terminal tail of H4 (Luger *et al.*, 1997). Although this tail does visually appear to be located within the Lrs sector of the nucleosome (see Figure 3.1), the location of the tail in chromatin is not yet known, and this property alone should not define the Lrs status of these residues. However, an important definition of the Lrs domain is loss of rRNA gene repression. When looking at entries for these residues in the HistoneHits database (Huang *et al*., 2009), none of these residues are associated with derepression of rRNA genes, except for H4H18, which showed a weak association (Table 3.2). In terms of this definition, H4K16, H4L22 and H4N25 are not Lrs domain residues.

H4H18 may be a Lrs domain residue due to the weak rRNA gene derepression seen for the H4H18A (but not H4H18Q) mutant.

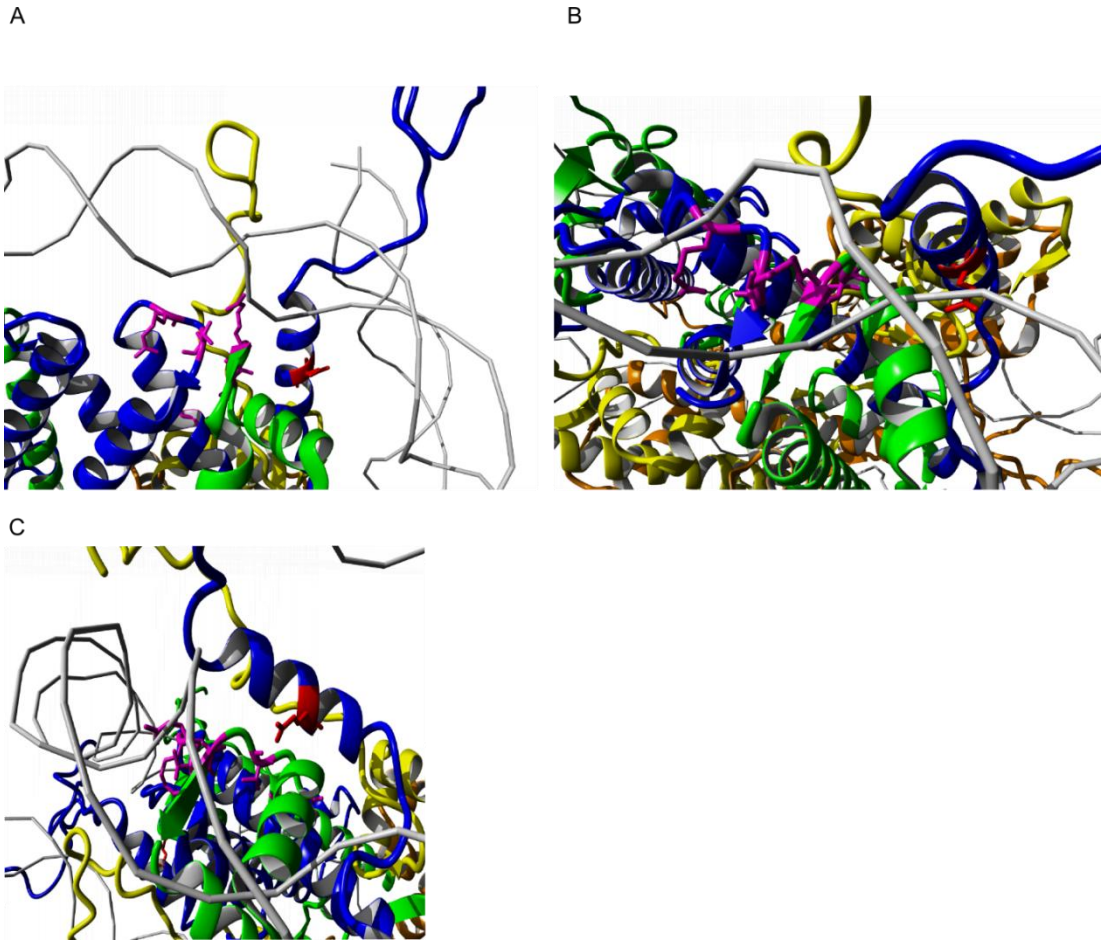


**Figure 3.2.Location of the E50A residue.A.** View of the nucleosome core approximately aligned to the superhelix axis, showing the location of residues in H4 L1 and H3 L2 previously defined as Sin mutants (Kruger et al., 1995; Fry et al., 2006) shown in purple. H3E50, located in $\alpha$1 of H1, is shown in red. **B.**The Sin residues (purple) approaches the minor groove at SHL ±0.5. This is removed the location of H3E50 (red). **C.**The H3E50 residue (red) approaches the major groove at SHL ±1.

**Table 3.2. Phenotypes of histone mutations implicated in extended chronological lifespans.**

| Number | Mutant | Domain | rRNA silencing | Telomere silencing | Mating efficiency | HM silencing |
|---|---|---|---|---|---|---|
| 1 | H4K16Q | Tail | 0 | -2 | -2 | -2 |
| 2 | H4K16A | Tail | 0 | -2 | -2 | -2 |
| 3 | H4K16R | Tail | 0 | 0 | 0 | -2 |
| 4 | H4H18A | Lrs | -1 | -2 | -2 | -2 |
| 5 | H4H18Q | Tail | 0 | -2 | 0 | -2 |
| 6 | H4N25D | Tail | 1 | -2 | 0 | -2 |
| 7 | H4L22A | Tail | 0 | -2 | -1 | -2 |
| 8 | H3T80D | Lrs | -1 | -2 | -2 | -2 |
| 9 | H3E50A | Sin | 0 | 0 | 0 | 0 |
| 10 | H4Δ9-16 | Tail | 0 | 0 | 0 | -1 |

It was therefore clear that the different mutated residues that caused an extension of chronological lifespan were associated with different phenotypic groupings, including the Sin and Lrs groups as well as a set that did not overlap with either the Sin or Lrs groups, designated as “Tail” in Table 3.2. Thus, to gain insight into the regulatory pathways that could be involved in the extension of chronological lifespan of these mutants, we undertook a RNA-seq analysis to identify gene sets that displayed significant up- or down-regulation in response to these mutations. This often allows the identification of regulatory pathways through which the mutations exert their phenotypic effect.

## 3.2. Materials and Methods

### *3.2.1. RNA-seq sample preparation*

Total RNA was isolated from 10 ml cultures of WT and histone mutant yeast strains. The RNA was purified with an RNeasy kit (Qiagen). The RNA was prepared for sequencing using the TruSeq Stranded Total RNA Sample Prep adaptor kit (Illumina). The samples were sequenced on a HiSeq 2500 instrument (Illumina) using the 100nt paired-ends sequencing protocol. Sequence files were recovered in FASTQ format. Biological replicates of each sample were independently prepared, sequenced and analyzed.

### *3.2.2. RNA-seq data analysis*

The RNA-seq data analysis was performed using the Tuxedo workflow (Trapnell *et al*., 2012). The sequence quality in the generated FASTQ files was verified with FastQC (version 0.11.2; www.bioinformatics.babraham.ac.uk/projects). The genome sequence (version 64-2-1) and associated annotation files of *S. cerevisiae* strain S288C (MATα SUC2 gal2 mal2 mel flo1 flo8-1 hap1 ho bio1 bio6) were downloaded from SGD (www.yeastgenome.org). A *bowtie2* index was built from the genome sequence file using *bowtie2-build* (bowtie-bio.sourceforge.net/bowtie2/index.shtml). The FASTQ sequences in the paired-end FASTQ sequence files were aligned to the *S. cerevisiae* genome using *tophat* (version 2.0.13; ccb.jhu.edu/software/tophat/index.shtml) and *bowtie2* (version 2.2.4; bowtie-bio.sourceforge.net/bowtie2/index.shtml). The following command line text was used:

tophat -G yeast_genome_features.gff -p 8 -o output_directory_path prefix_to_yeast_genome_index paired_end_1.fastq[,additional paired_end_1.fastq files] paired_end_2.fastq[,additional paired_end_2.fastq files]

The generated genome index and the genome annotation file in generic feature format (GFF) (Release 64-2-1; www.yeastgenome.org) were used with *tophat*.

The initial transcript files (accepted_hits.bam) generated by *tophat* were assembled using *cufflinks* (version 2.1.1; cole-trapnell-lab.github.io/cufflinks; we found that *cufflinks* version 2.2.1 terminated with a segmentation fault error, and used the older release 2.1.1 of *cufflinks*). The following command line instruction was used:

cufflinks -p 8 -g yeast_genome_features.gff -mask-file masked_transcripts_file.gff -frag-bias-correct yeast_genome.fa accepted_hits.bam

The transcript mask file consisted of non-mRNA transcripts, including all rRNA, tRNA, snoRNA and ncRNA transcripts. These transcripts were not assembled by *cufflinks*, and thus excluded from quantitation. The frag-bias-correct switch corrects for fragment bias using the genome sequence.

*Cufflink* assemblies were merged into a single assembly file with *cuffmerge*. The following command line text was used:

cuffmerge -o output_directory_path -g yeast_genome_features.gff -p 8 -s yeast_genome.fa manifest_file.txt

The manifest file contained the full path to each of the transcripts.gtf files, one entry per line, which were generated with *cufflinks*, above. Gene and transcript expression profile files were generated with *cuffquant* using the following command line:

cuffquant -p 8 -M masked_transcripts_file.gff -b yeast_genome.fa merged.gtf accepted_hits.bam

The masked_transcripts_file.gff and yeast_genome.fa files were the same files used for *cufflinks*, above. The merged.gtf file was the output file from *cuffmerge*, and the accepted_hits.bam file was the output file from *tophat*, above. The *tophat* transcript file from each sample was independently quantitated with *cuffquant*.

The differential expression of genes were analysed with *cuffdiff*. The following command line was used:

cuffdiff -L H3WT,H4WT,H4H18A,H4K16Q,H3E50A -p 8 -b yeast.fa -M mask.gff merged.gtf abundances_H3WT_1.cxb,abundances_H3WT_2.cxb abundances_H4WT_1.cxb,abundances_H4WT_2.cxb abundances_H4H18A_1.cxb,abundances_H4H18A_2.cxb abundances_H4K16Q_1.cxb,abundances_H4K16Q_2.cxb abundances_H3E50A_1.cxb

The yeast.fa and mask.gff files were the same that was used with *cufflinks*, above. The merged.gtf file was generated with *cuffmerge*, above. The abundance.cxb files were generated with *cuffquant*, above. Changing the false discovery rate (FDR command line switch) from the default 0.05 to 0.01 or using a Poisson distribution (-poisson-dispersion switch) instead of the default dispersion that is learned from each condition had no impact on the groups of genes that displayed differential expression at probability $p<0.05$.

### *3.2.3. Analysis of differential gene expression*

The text files of differentially expressed genes generated by cuffdiff were visualized with the R package cummeRbund (www.bioconductor.org/packages/release/bioc/html/cummeRbund.html) to assess

data quality. The analysis for enrichment of gene ontology terms were performed with GoEast (omicslab.genetics.ac.cn/GOEAST) (Zheng and Wang, 2008), Gorilla (cbl-gorilla.cs.technion.ac.il) (Eden *et al*., 2009) and REVIGO (revigo.irb.hr) (Supek *et al*., 2011). Semantic GO maps were generated with REVIGO were plotted in R (www.r-project.org). Gene lists were mapped to metabolic pathways using KEGG mapper (www.genome.jp).

### 3.3. Results

Total RNA was isolated from the H3WT, H4WT, H4H18A, H4K16Q and H3E50A mutant strains in late log phase, the rRNA was depleted, and 100 nt runs of the recovered RNA were sequenced by the paired-ends protocol on an IlluminaHiSeq 2500. The differential expression of genes were analysed using the "Tuxedo" workflow (Trapnell *et al*., 2012). The procedure was repeated with biological replicates for each mutant. The results from the *tophat* alignment to the *S. cerevisiae* genome is shown in Table 3.3.

**Table 3.3. Percentage of concordant alignment pairs identified with tophat in the sequence files.**

| Number | Sample | Replicate | Concordant alignment pairs (percentage) |
|---|---|---|---|
| 1 | H3WT | 1 | 64 |
| 2 | H3WT | 2 | 86 |
| 3 | H4WT | 1 | 51 |
| 4 | H4WT | 2 | 77 |
| 5 | H4K16Q | 1 | 84 |
| 6 | H4K16Q | 2 | 67 |
| 7 | H4H18A | 1 | 79 |
| 8 | H4H18A | 2 | 59 |
| 9 | H3E50A | 1 | 78 |
| 10 | H3E50A | 2 | - |

Replicate 2 of the H3E50 mutant strain did not return useable sequence information, and was excluded from subsequent analyses. The calculation of variance for this sample was based on a statistical method that considered the distribution of the data in the one sample (Trapnell *et al.*, 2012).

A plot of the dispersion for the 5 samples is shown in Figure 3.3. The level of dispersion that is seen for each of the datasets is generally small, and the trend roughly linear, suggesting that the datasets are appropriate to detect small degrees of variability between the levels of expression in different sets. When looking at the distribution of counts of the different data sets (Figure 3.4), symmetrical, overlapping distributions are seen, indicating comparable sequencing depth for the different samples.

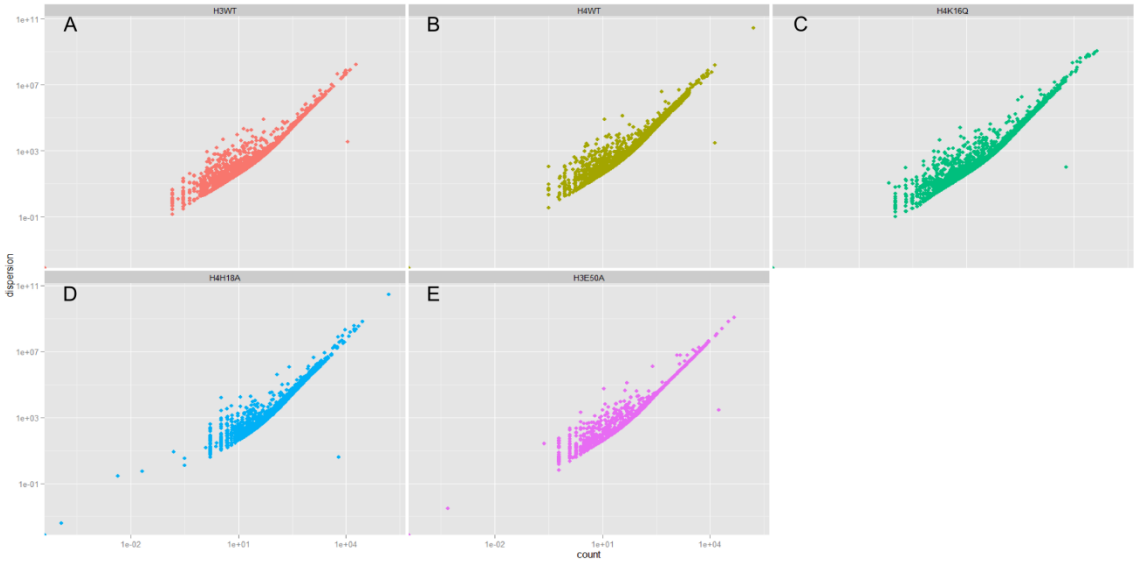


**Figure 3.3.Dispersion in RNA-seq data.** A plot of the dispersion (variance$^2$) against the counts (fragments per kilobase of sequence per million fragments mapped) is shown for the **A**, H3WT, **B**, H4WT, **C**, H4H16A, **D**, H4H18A and **E**, H3E50 data sets.

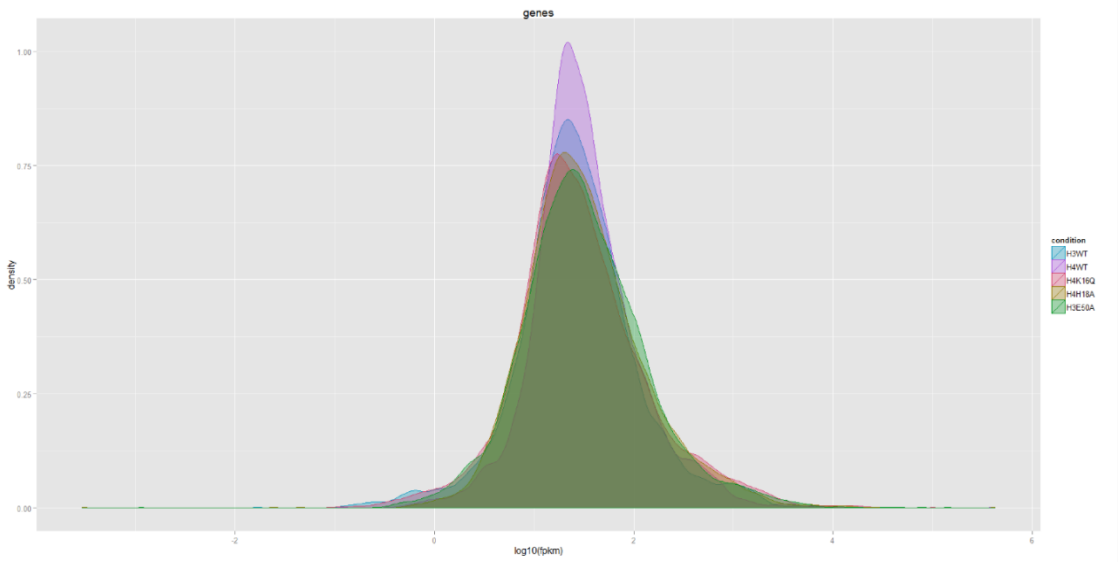


**Figure 3.4.Density distribution of mapped counts.** The density distribution as a function of fragment counts is shown for the H3WT, H4WT, H4H16A, H4H18A and H3E50 data sets, as indicated.

Genes that are differentially expressed at statistically significant ($p<0.05$) levels in the mutant relative to the corresponding parental WT strain were identified with *cuffdiff*. The numbers of such differentially expressed genes are listed in Table 3.4.

**Table 3.4.Number of genes that display statistically significant ($p<0.05$) differences in expression level between the mutant and parental WT strains.**

| Mutant | Up-regulated | Down-regulated |
|---|---|---|
| H4K16Q | 64 | 320 |
| H4H18A | 2 | 11 |
| H3E50A | 1115 | 1135 |

In order to gain insight into the regulatory paths that might be involved in the differential expression of genes within each of the three samples, we performed an analysis for enrichment of gene ontology (GO) terms. The results of the analysis for

enrichment for GO terms are shown in Table 3.5, 3.6 and 3.7 (Supplementary material).

Referring to Table 3.5, it is seen that the H4K16Q mutant displays a repressed transcriptome that is broadly associated with cellular processes involved in reproduction which includes meiosis, reciprocal recombination, chromosome organization, chromosome condensation, condensed chromosome kinetochore, microtubule organising centre and spindle pole body. A second broad section includes cellular response to stress including response to DNA damage stimulus, DNA repair, and damaged DNA binding. The third broad category is conjugation, response to pheromone, cellular response to pheromone and response to pheromone involved in conjugation with cellular fusion.

Interestingly, the response to pheromone stress is associated with down-regulation of the *STE2, BAR1, STE6, AGA2, STE5, GPA1, CSI1, STE4, SST2, AGA1, RRI1, FUS3, FAR10* and*PTC1* genes. Of these, *STE2*, *BAR1*, *STE6* and *AGA2* are known *MAT*a-specific genes with *MAT*$\alpha$2-operators identified in the promoter regions (Zhong, 1999). The observation that the *MAT*a-specific genes become repressed in the H4K16Q mutant is most likely due to the *MAT*a mating-type of the parental yeast strain. It is likely that the HML encoding *MAT*$\alpha$1 and *MAT*$\alpha$2 has become de-repressed in the H4K16Q mutant, resulting in the MAT$\alpha$2-Mcm1 facilitated repression of the *MAT*a-specific genes.

When looking at GO term enrichment for genes that are significantly up-regulated in the H4K16Q mutant, rRNA processing and maturation, rRNA export, ribosome assembly, gene expression, cytoplasmic translation and ethanol metabolic processes terms are enriched in the gene set (Figure 3.5). The cell thus appears to be growing robustly with active gene expression and protein synthesis. To gain an

insight into the major metabolic pathways that may be active under these conditions, we mapped the genes that were statistically significantly up-regulated in the H4K16Q mutant to metabolic pathways. The largest representation of genes mapped to the ribosome component map (Figure 3.6). Although there were also hits to secondary metabolite, amino acid biosynthesis and glycolysis pathways, the number of genes that mapped to these pathways were significantly less compared to the ribosome component set. This, of course, does not suggest that the latter pathways are not active. It simply means that the genes that are induced in the H4K16Q mutant are not specifically enriched for these latter pathways. No stress response genes appear to be notably up-regulated.

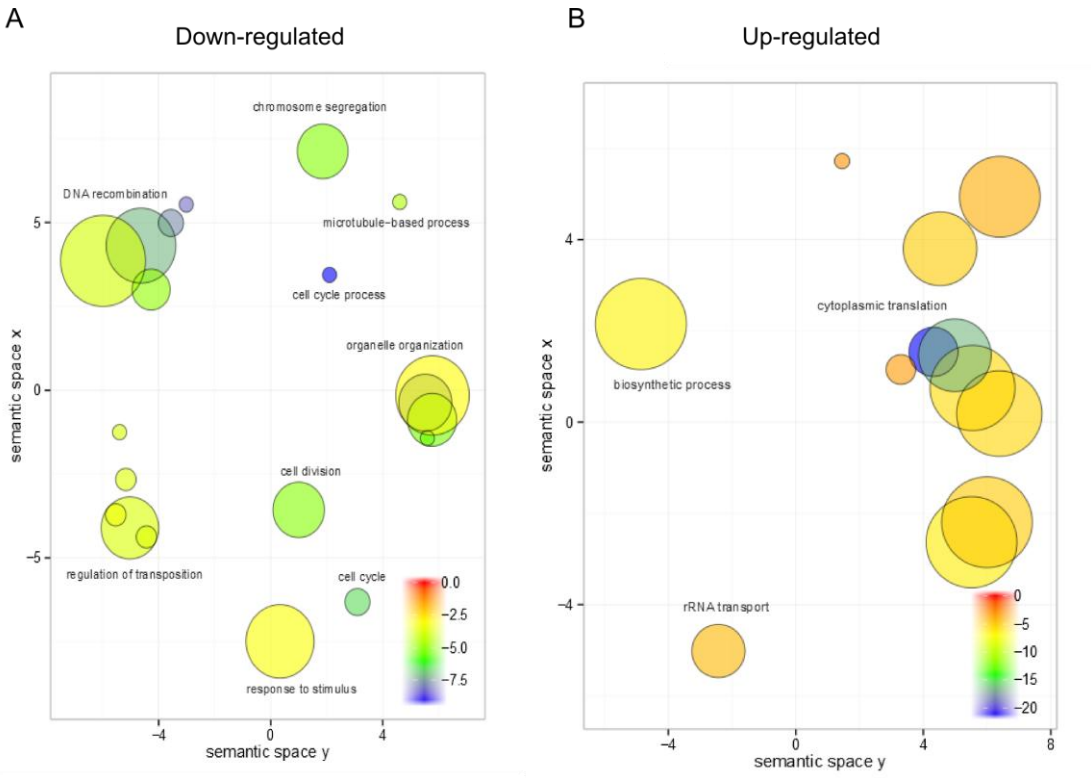


**Figure 3.5.Semantic space map of enriched GO terms.**Enrichment of GO terms for the **A.**down-regulated, and **B.** up-regulated genes in strain H4K16Q are shown. Related terms co-localize on the map. The circle sizes represent the number of genes in the grouping, and the colour indicates the p-value of the grouping according to the colour gradient key

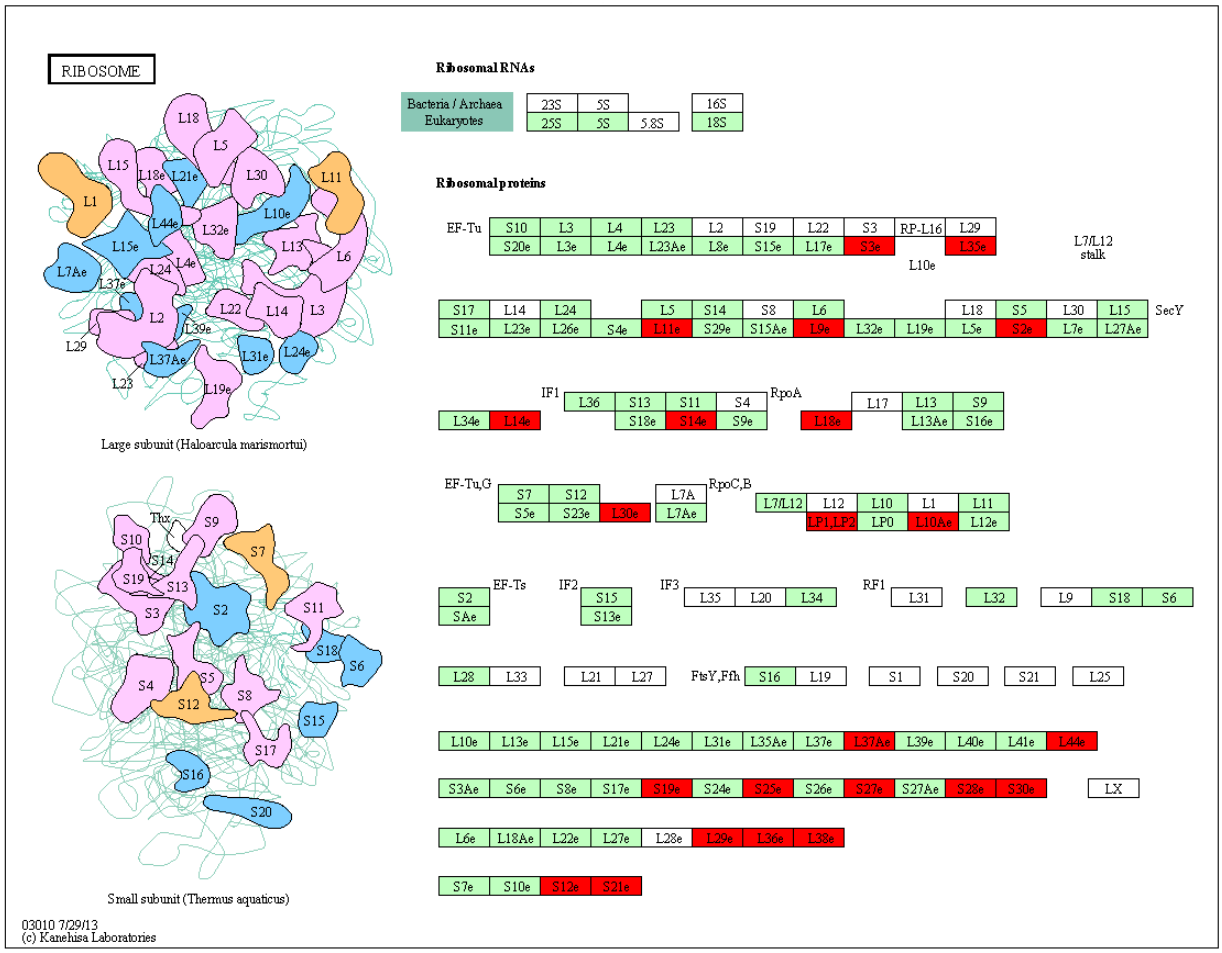


**Figure 3.6.Mapping of up-regulated genes in the H4K16Q mutant to ribosome components.** The green rectangles represent components present in *S. cerevisiae*. The red rectangles represent components encoded by genes that are significantly upregulated in the H4K16Q mutant.

Search of SPELL (spell.yeastgenome.org) that matches lists of genes to genome-wide gene expression datasets, identified chemical stimulus, heat shock, protein dephosphorylation and signalling(Düvel *et al*., 2003),cellular ion homeostasis and starvation(Barreto et al., 2012), amino acid utilization, protein phosphorylation, signalling and starvation(Chen and Powers, 2006), cell cycle regulation, DNA damage stimulus and stress(Travesa *et al*., 2012), chemical stimulus(Kitagawa *et al*., 2003), chromatin organization, heat shock, stationary phase entry and stress(Shivaswamy and Iyer, 2008), when searched with the genes upregulated by two-fold in the H4K16Q mutant. A search of the SPELL compendium with genes

repressed by at least two-fold in the H4K16Q mutant strain identified stress (Lewis *et al*., 2014) and carbon utilization, fermentation and respiration(Daran-Lapujade *et al*., 2004) as the main transcriptomic studies in which the supplied list of genes played an important role.

Looking next at the H4H18A mutant (Table 3.6), an enrichment of GO terms associated with repression: response to pheromone, response to pheromone involved in conjugation with cellular fusion and response to organic substance appear at high log odds ratios and significance. The genes associated with these GO terms are *STE2, BAR1, STE6, GPA1, STE4, AGA1*. This transcriptional response, for the reasons put forward above, most likely indicate that the HML$\alpha$ locus has become derepressed in the *MAT*a cell. Thus, it appears that both the H4K16Q and the H4H18A strain exhibit a derepression of the silent mating type loci phenotype. The semantic space map of the H4H18A mutant (Figure 3.7)

When performing a semantic space analysis of the enriched GO terms (Figure 3.7), groups representing ribosome assembly, rRNA metabolism and transport, organic molecule and small molecule metabolic processes, nitrogen compound metabolic process and cytoplasmic translation appear. We again note that no stress response genes appear highly up-regulated, and carbon metabolism genes do not appear specifically repressed.

A search of the SPELL compendium with genes upregulated at least 2-fold in the H4H18A mutant showed main overlap with the tags histone modifications, where the specific transcriptional role of H4K16 was highlighted (Dion *et al*., 2005), and chromatin organization, histone modification(Tompa and Madhani, 2007)

The two histone H4 tail mutants H4K16Q and H4H18A thus have similar, but not identical transcriptomes. The enrichment of GO terms suggests HM repression in

both strains, with active rRNA synthesis, ribosome assembly, and carbon and nitrogen metabolic processes.

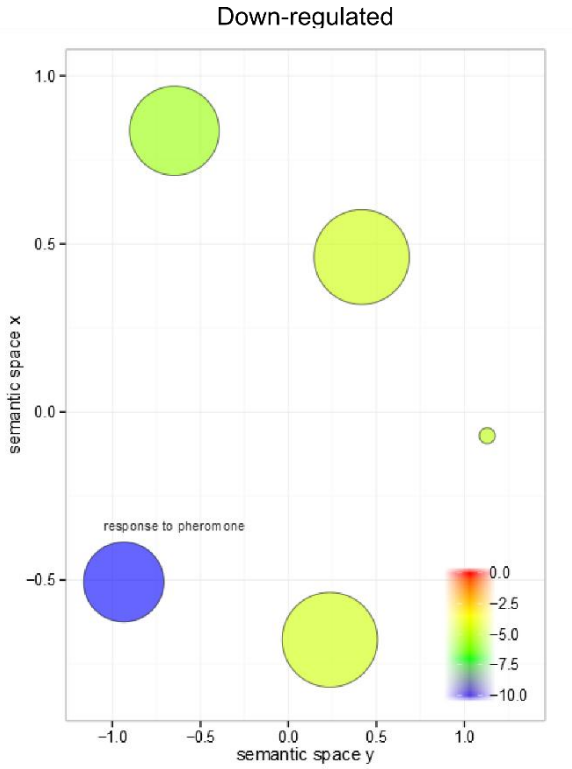


**Figure 3.7.Semantic space map of enriched GO terms for H4H18A.**Enrichment of GO terms for the down-regulated genes in the H4H18A mutant. The number of up-regulated genes in the H4H18A mutant precluded GO term analysis. Related terms co-localize on the map. The circle sizes represent the number of genes in the grouping, and the colour indicates the p-value of the grouping according to the colour gradient key

We expect a different transcriptomic profile for the H3E50A mutant, even though it also displays increased chronological lifespan. This mutated residue is likely a Sin mutant, and although an effect on Swi/Snf requirement in the H4K16Q and H4H18A mutant are not excluded, it is expected that the involvement of this chromatin remodeler in the gene expression pattern of the H3E50A mutant will generate a steady state RNA profile different from the H4 tail mutants.

Referring to Table 3.7, it is seen that ribosome biogenesis is again an enriched GO term. However, the term is now associated with genes that are

significantly down-regulated in the H3E50A mutant. This suggests that protein biosynthesis is reduced in the H3E50A mutant compared to the H3WT strain. When looking at GO terms associated with induced genes, the terms mitochondrial electron transport, tricarboxylic acid cycle, ATP synthesis coupled proton transport, oxidative phosphorylation, glutamate metabolic process, glyoxylate cycle, purine ribonucleoside triphosphate biosynthetic process appear. Significantly, the GO terms: response to hydrogen peroxide, reactive oxygen species metabolic process and response to oxidative stress appear. The upregulation of these genes may indicate that the H3E50A mutant strain is experiencing oxidative stress due to an upregulation of the oxidative phosphorylation process. When looking at the semantic map space of the H3E50A mutant (Figure 3.8), the upregulation of diverse metabolic processes in this mutant is evident. To identify the specific pathways responsible, we mapped gene lists of up-regulated genes to metabolic pathways.

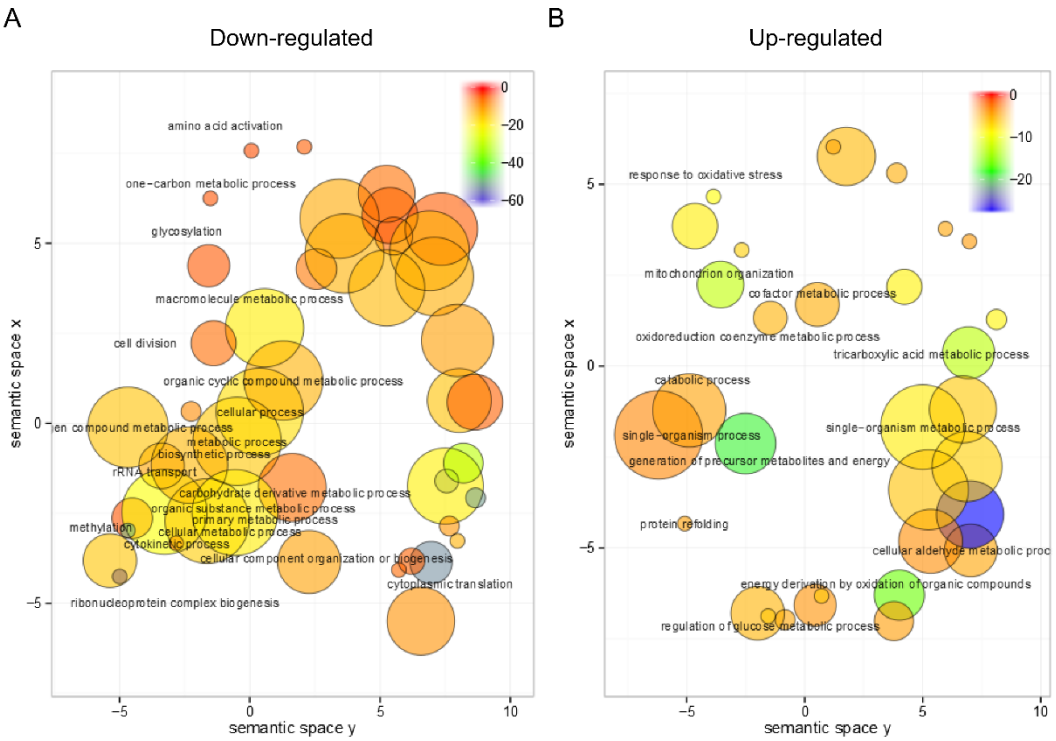


**Figure 3.8.Semantic space map of enriched GO terms.**Enrichment of GO terms for the **A.**down-regulated, and **B.** up-regulated genes in strain H3E50A are shown. Related terms co-localize on the map. The circle sizes represent the number of genes in the grouping, and the colour indicates the p-value of the grouping according to the colour gradient key

We found that the upregulated genes richly mapped to many metabolic pathways, including biosynthesis of secondary metabolites (70 genes), carbon metabolism (49 genes), oxidative phosphorylation (40 genes), TCA cycle (27 genes), pyruvate metabolism (24 genes) and peroxisome (24 genes). The superposition of the genes to the TCA cycle and oxidative phosphorylation are shown in Figures 3.9 and 3.10.

A search of the SPELL database with the genes most upregulated in the H3E50A mutant strain returned carbon utilization, fermentation, oxygen level alteration and respiration(van den Brink *et al*., 2008). The transcriptome appeared most similar to that of a culture transferred to a glucose-rich medium following glucose depletion (van den Brink et al., 2008).

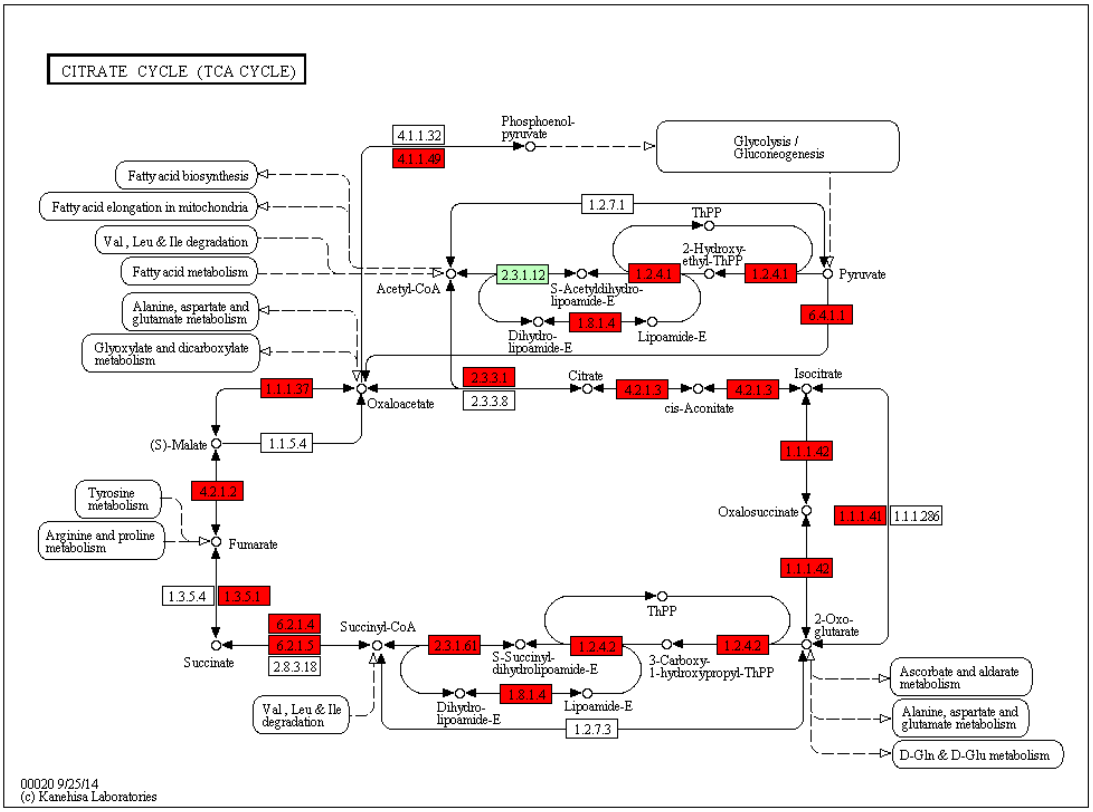


**Figure 3.9.Mapping of up-regulated genes in the H3E50A mutant to TCA cycle enzymes.** The green rectangles represent components present in *S.cerevisiae*. The red rectangles represent components encoded by genes that are significantly upregulated in the H3E50A mutant.

It appears that many metabolic processes are upregulated in the H3E50A mutant strain. The observation of enrichment of genes associated with oxidative stress response and response to hydrogen peroxide probably reflects the very active oxidative phosphorylation system in this mutant strain. Significantly, we did not observe a repression of *MAT* specific genes that indicated the derepression of the HM loci in the H3E50A strain.

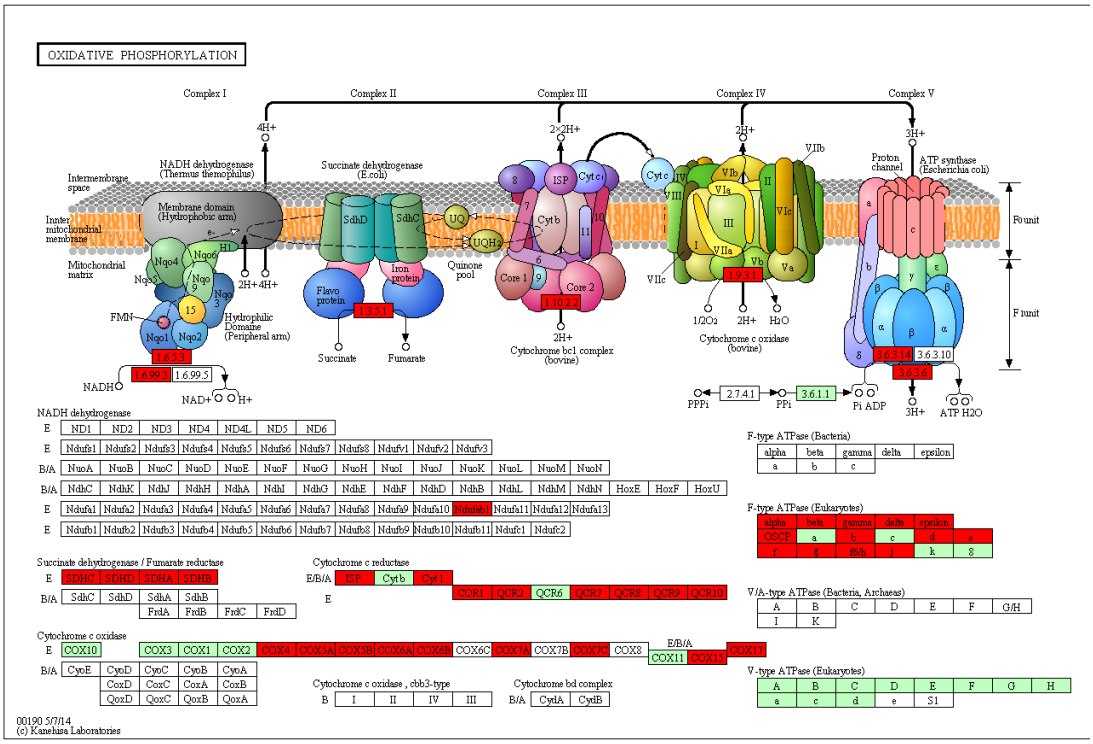


**Figure 3.10.Mapping of up-regulated genes in the H3E50A mutant to oxidative phosphorylation enzymes.** The green rectangles represent components present in *S.cerevisiae*. The red rectangles represent components encoded by genes that are significantly upregulated in the H3E50A mutant.

Therefore, although all three strains exhibited chronological lifespan extension, they differed in important regulatory processes, suggesting that the H4K16Q and H4H18A strains, on the one hand, and the H3E50 strain on the other hand, may modulate different pathways to regulate chronological lifespan. However, the transcriptomic profiles generated in late logarithmic growth phase in *S. cerevisiae* did not directly indicate what pathways were involved in lifespan extension. It is likely that we will have to look at the proteome at late stages in the chronological life of these mutants to directly identify the catalytic and regulatory agents involved in the mechanism of lifespan extension.

### 3.4. Reference List


Barreto, L., Canadell, D., Valverde-Saubí, D., Casamayor, A., and Ariño, J. (2012). The short-term response of yeast to potassium starvation. Environ. Microbiol. *14*, 3026–3042.

Van den Brink, J., Daran-Lapujade, P., Pronk, J.T., and de Winde, J.H. (2008). New insights into the *Saccharomyces cerevisiae* fermentation switch: dynamic transcriptional response to anaerobicity and glucose-excess. BMC Genomics *9*, 100.

Chen, J.C.-Y., and Powers, T. (2006). Coordinate regulation of multiple and distinct biosynthetic pathways by TOR and PKA kinases in *S. cerevisiae*. Curr. Genet. *49*, 281–293.

Daran-Lapujade, P., Jansen, M.L.A., Daran, J.-M., van Gulik, W., de Winde, J.H., and Pronk, J.T. (2004). Role of transcriptional regulation in controlling fluxes in central carbon metabolism of *Saccharomyces cerevisiae*. A chemostat culture study. J. Biol. Chem. *279*, 9125–9138.

Dion, M.F., Altschuler, S.J., Wu, L.F., and Rando, O.J. (2005). Genomic characterization reveals a simple histone H4 acetylation code. Proc. Natl. Acad. Sci. U. S. A. *102*, 5501–5506.

Düvel, K., Santhanam, A., Garrett, S., Schneper, L., and Broach, J.R. (2003). Multiple roles of Tap42 in mediating rapamycin-induced transcriptional changes in yeast. Mol. Cell *11*, 1467–1478.

Eden, E., Navon, R., Steinfeld, I., Lipson, D., and Yakhini, Z. (2009). GOrilla: a tool for discovery and visualization of enriched GO terms in ranked gene lists. BMC Bioinformatics *10*, 48.

Fry, C.J., Norris, A., Cosgrove, M., Boeke, J.D., and Peterson, C.L. (2006). The LRS and SIN domains: two structurally equivalent but functionally distinct nucleosomal surfaces required for transcriptional silencing. Mol. Cell. Biol. *26*, 9045–9059.

Horn, P.J., Crowley, K.A., Carruthers, L.M., Hansen, J.C., and Peterson, C.L. (2002). The SIN domain of the histone octamer is essential for intramolecular folding of nucleosomal arrays. Nat. Struct. Biol. *9*, 167–171.

Huang, H., Maertens, A.M., Hyland, E.M., Dai, J., Norris, A., Boeke, J.D., and Bader, J.S. (2009). HistoneHits: a database for histone mutations and their phenotypes. Genome Res. *19*, 674–681.

Kitagawa, E., Momose, Y., and Iwahashi, H. (2003). Correlation of the structures of agricultural fungicides to gene expression in *Saccharomyces cerevisiae* upon exposure to toxic doses. Environ. Sci. Technol. *37*, 2788–2793.

Kruger, W., Peterson, C.L., Sil, A., Coburn, C., Arents, G., Moudrianakis, E.N., and Herskowitz, I. (1995). Amino acid substitutions in the structured domains of histones H3 and H4 partially relieve the requirement of the yeast SWI/SNF complex for transcription. Genes Dev. *9*, 2770–2779.

Lewis, J.A., Broman, A.T., Will, J., and Gasch, A.P. (2014). Genetic architecture of ethanol-responsive transcriptome variation in *Saccharomyces cerevisiae* strains. Genetics *198*, 369–382.

Luger, K., Mäder, A.W., Richmond, R.K., Sargent, D.F., and Richmond, T.J. (1997). Crystal structure of the nucleosome core particle at 2.8 Å resolution. Nature *389*, 251–260.

Muthurajan, U.M., Bao, Y., Forsberg, L.J., Edayathumangalam, R.S., Dyer, P.N., White, C.L., and Luger, K. (2004). Crystal structures of histone Sin mutant nucleosomes reveal altered protein-DNA interactions. EMBO J. *23*, 260–271.

Shivaswamy, S., and Iyer, V.R. (2008). Stress-dependent dynamics of global chromatin remodeling in yeast: dual role for SWI/SNF in the heat shock stress response. Mol. Cell. Biol. *28*, 2221–2234.

Supek, F., Bošnjak, M., Škunca, N., and Šmuc, T. (2011). REVIGO summarizes and visualizes long lists of gene ontology terms. PLoS One *6*, e21800.

Thompson, J.S., Snow, M.L., Giles, S., McPherson, L.E., and Grunstein, M. (2003). Identification of a functional domain within the essential core of histone H3 that is required for telomeric and HM tilencing in *Saccharomyces cerevisiae.* Genetics *163*, 447–452.

Tompa, R., and Madhani, H.D. (2007). Histone H3 lysine 36 methylation antagonizes silencing in *Saccharomyces cerevisiae* independently of the Rpd3S histone deacetylase complex. Genetics *175*, 585–593.

Trapnell, C., Roberts, A., Goff, L., Pertea, G., Kim, D., Kelley, D.R., Pimentel, H., Salzberg, S.L., Rinn, J.L., and Pachter, L. (2012). Differential gene and transcript expression analysis of RNA-seq experiments with TopHat and Cufflinks. Nat. Protoc. *7*, 562–578.

Travesa, A., Kuo, D., de Bruin, R.A.M., Kalashnikova, T.I., Guaderrama, M., Thai, K., Aslanian, A., Smolka, M.B., Yates, J.R., Ideker, T., et al. (2012). DNA replication stress differentially regulates G1/S genes via Rad53-dependent inactivation of Nrm1. EMBO J. *31*, 1811–1822.

Zheng, Q., and Wang, X.-J. (2008). GOEAST: a web-based software toolkit for Gene Ontology enrichment analysis. Nucleic Acids Res. *36*, W358–W363.

Zhong, H. (1999). Identification of target sites of the alpha 2-Mcm1 repressor complex in the yeast genome. Genome Res. *9*, 1040–1047.

**Supplementary Material**

**Table 3.5. GO term enrichment for genes that are significantly (p<0.05) up-regulated or down-regulated in the H4K16Q mutant compared to the H4WT parental strain.**The biological function, cellular component and molecular function ontologies are shown separately in the table, sorted in descending order for the log odds ratio.

| -/+[a] | GOID | Ontology[b] | Term | Level[c] | Log odds ratio[d] | p[e] | Genes |
|---|---|---|---|---|---|---|---|
| - | GO:0000742 | BP | karyogamy involved in conjugation with cellular fusion | 6 | 3.27 | 1.57E-03 | FUS2, KAR3, GPA1, KAR1, SPC110, CIK1, JEM1 |
| - | GO:0007129 | BP | synapsis | 7 | 3.09 | 3.68E-03 | NDJ1, MSH5, RED1, REC8, PDS5, HFM1, ZIP1 |
| - | GO:0010525 | BP | regulation of transposition, RNA-mediated | 5 | 3.05 | 1.36E-02 | STE5, STE4, RTT103, RTT109, TEC1, FUS3 |
| - | GO:0010528 | BP | regulation of transposition | 4 | 2.95 | 1.82E-02 | STE5, STE4, RTT103, RTT109, TEC1, FUS3 |
| - | GO:0070192 | BP | chromosome organization involved in meiosis | 6 | 2.87 | 8.98E-05 | NDJ1, IPL1, MSH5, RED1, REC8, CHL4, PDS5, HFM1, ZIP1, RDH54, MMS22 |
| - | GO:0000741 | BP | karyogamy | 5 | 2.85 | 9.60E-03 | FUS2, KAR3, GPA1, KAR1, SPC110, CIK1, JEM1 |
| - | GO:0007131 | BP | reciprocal meiotic recombination | 9 | 2.55 | 1.86E-05 | MEI5, NDJ1, ECM11, MSH5, RED1, REC114, PCH2, REC8, MMS4, HFM1, RAD17, MSH3, ZIP1, RDH54, PMS1 |
| - | GO:0035825 | BP | reciprocal DNA recombination | 8 | 2.55 | 1.86E-05 | MEI5, NDJ1, ECM11, MSH5, RED1, REC114, PCH2, REC8, MMS4, HFM1, RAD17, MSH3, ZIP1, RDH54, PMS1 |
| - | GO:0007127 | BP | meiosis I | 6 | 2.12 | 3.88E-05 | MEI5, NDJ1, IPL1, ECM11, MSH5, MEI4, RED1, REC114, PCH2, REC8, MMS4, PDS5, HFM1, RAD17, MSH3, ZIP1, RDH54, DOT1, PMS1 |
| - | GO:0000747 | BP | conjugation with cellular fusion | 4 | 2.09 | 1.66E-05 | FUS2, STE2, BAR1, AGA2, KAR3, STE5, GPA1, CSI1, FUS1, STE4, KAR1, ASG7, SST2, SPC110, AGA1, CIK1, RRI1, FUS3, FAR10, PTC1, JEM1 |
| - | GO:0000746 | BP | conjugation | 3 | 2.07 | 1.84E-05 | FUS2, STE2, BAR1, AGA2, KAR3, STE5, GPA1, CSI1, FUS1, STE4, KAR1, ASG7, SST2, SPC110, |

| | | | | | | | |
|---|---|---|---|---|---|---|---|
| | | | | | | | AGA1, CIK1, RRI1, FUS3, FAR10, PTC1, JEM1 |
| - | GO:0000749 | BP | response to pheromone involved in conjugation with cellular fusion | 7 | 2.05 | 4.74E-03 | STE2, BAR1, AGA2, STE5, GPA1, CSI1, STE4, SST2, AGA1, RRI1, FUS3, FAR10, PTC1 |
| - | GO:0000819 | BP | sister chromatid segregation | 5 | 1.87 | 8.31E-03 | BRN1, KAR3, IPL1, BUB1, SCC2, CHL4, MCM21, CIK1, PDS5, ESC2, BIR1, SMC1, RDH54, MMS22 |
| - | GO:0007126 | BP | meiosis | 5 | 1.86 | 1.14E-07 | MEI5, SPS4, NDJ1, KAR3, SSP1, IPL1, ECM11, CNM67, MSH5, MEI4, RED1, DON1, REC114, PCH2, REC8, CHL4, MCM21, CIK1, MMS4, PDS5, HFM1, RAD17, NDT80, MSH3, SPO22, RMD1, SET3, ADY3, ZIP1, RDH54, DOT1, PMS1, SLK19, MMS22 |
| - | GO:0000226 | BP | microtubule cytoskeleton organization | 5 | 1.86 | 3.16E-03 | IPL1, CNM67, SPC24, CDC31, KAR1, NBP1, SPC110, BUB1, CIK1, SPC97, BIR1, MIF2, JNM1, NIP100, SPC98, SLK19 |
| - | GO:0007017 | BP | microtubule-based process | 3 | 1.81 | 1.57E-03 | KAR3, IPL1, CNM67, SPC24, CDC31, GPA1, KAR1, NBP1, SPC110, BUB1, CIK1, SPC97, BIR1, MIF2, JNM1, NIP100, SPC98, SLK19 |
| - | GO:0071444 | BP | cellular response to pheromone | 6 | 1.78 | 2.16E-02 | STE2, BAR1, AGA2, STE5, GPA1, CSI1, STE4, SST2, AGA1, RRI1, FUS3, FAR10, PTC1 |
| - | GO:0007059 | BP | chromosome segregation | 3 | 1.71 | 1.49E-04 | BRN1, KAR3, IPL1, SPC24, MSH5, RED1, BUB1, REC8, SCC2, CHL4, MCM21, CIK1, MMS4, PDS5, HDA3, ESC2, BIR1, SMC1, MIF2, SLI15, SMC6, RDH54, SLK19, MMS22 |
| - | GO:0006302 | BP | double-strand break repair | 8 | 1.71 | 9.14E-03 | MEI5, PSF1, FYV6, PSO2, YKU70, SCC2, PDS5, RTT109, ESC2, RAD17, SMC1, POL4, SMC6, LIF1, NUP120, MMS22 |
| - | GO:0019236 | BP | response to pheromone | 4 | 1.67 | 2.78E-02 | STE2, BAR1, STE6, AGA2, STE5, GPA1, CSI1, STE4, SST2, AGA1, RRI1, FUS3, FAR10, PTC1 |
| - | GO:0051656 | BP | establishment of organelle localization | 5 | 1.65 | 1.97E-02 | KAR3, NOP53, GPA1, BUB1, SEC10, CIK1, BIR1, JNM1, SEC5, NIP100, JJJ1, NUP120, MDM1, NUP82, SEC8 |
| - | GO:0009966 | BP | regulation of signal transduction | 5 | 1.6 | 1.80E-02 | FUS2, BAR1, TRS130, STE5, GPA1, CSI1, BUD5, SST2, YEL1, RRI1, BUD2, PHO80, FUS3, FAR10, PTC1, GEA1 |
| - | GO:0019953 | BP | sexual reproduction | 2 | 1.55 | 1.04E-04 | FUS2, STE2, BAR1, SPS4, AGA2, KAR3, SSP1, STE5, SPO75, DTR1, SPR3, SPO20, GPA1, CSI1, FUS1, STE4, KAR1, ASG7, SST2, SPC110, DON1, AGA1, CIK1, RRI1, ADY3, FUS3, FAR10, PTC1, JEM1 |
| - | GO:0023051 | BP | regulation of signaling | 3 | 1.54 | 2.78E-02 | FUS2, BAR1, TRS130, STE5, GPA1, CSI1, BUD5, SST2, YEL1, RRI1, BUD2, PHO80, FUS3, FAR10, PTC1, GEA1 |

| | | | | | | | |
|---|---|---|---|---|---|---|---|
| - | GO:0048610 | BP | cellular process involved in reproduction | 2 | 1.53 | 2.73E-10 | MEI5, HO, FUS2, STE2, BAR1, SPS4, NDJ1, AGA2, KAR3, SSP1, IPL1, ECM11, CNM67, MSH5, STE5, SPO75, DTR1, MEI4, SPR3, SPO20, GPA1, CSI1, FUS1, RED1, STE4, KAR1, SST2, SPC110, DON1, REC114, AGA1, PCH2, REC8, CHL4, MCM21, CIK1, MMS4, PDS5, HFM1, RAD17, RRI1, NDT80, MSH3, SPO22, RMD1, SET3, ADY3, ZIP1, FUS3, FAR10, RDH54, DOT1, PMS1, SLK19, CKA1, PTC1, MMS22, SHE3, JEM1 |
| - | GO:0010646 | BP | regulation of cell communication | 4 | 1.49 | 3.83E-02 | FUS2, BAR1, TRS130, STE5, GPA1, CSI1, BUD5, SST2, YEL1, RRI1, BUD2, PHO80, FUS3, FAR10, PTC1, GEA1 |
| - | GO:0000003 | BP | reproduction | 1 | 1.48 | 4.95E-11 | MEI5, HO, FUS2, STE2, BAR1, SPS4, NDJ1, AGA2, KAR3, SSP1, IPL1, ECM11, CNM67, AXL1, MSH5, STE5, SPO75, DTR1, MEI4, SPR3, SPO20, GPA1, CSI1, FUS1, RED1, STE4, KAR1, ASG7, BUD5, SST2, SPC110, DON1, RSR1, REC114, AGA1, PCH2, REC8, CHL4, MCM21, CIK1, MMS4, PDS5, HFM1, RAD17, GIC1, RRI1, NDT80, MSH3, SPO22, RMD1, SET3, ADY3, ATC1, BUD2, ZIP1, FUS3, FAR10, RDH54, DOT1, PMS1, SLK19, CKA1, PTC1, MMS22, SHE3, JEM1 |
| - | GO:0051640 | BP | organelle localization | 4 | 1.48 | 1.82E-02 | NDJ1, KAR3, NOP53, GPA1, BUB1, SEC10, CIK1, BIR1, ADY3, JNM1, SEC5, NIP100, JJJ1, NUP120, PTC1, MDM1, NUP82, SEC8 |
| - | GO:0044764 | BP | multi-organism cellular process | 2 | 1.44 | 9.55E-03 | FUS2, STE2, BAR1, AGA2, KAR3, STE5, GPA1, CSI1, FUS1, STE4, KAR1, ASG7, SST2, SPC110, AGA1, CIK1, RRI1, FUS3, FAR10, PTC1, JEM1 |
| - | GO:0006310 | BP | DNA recombination | 7 | 1.42 | 1.49E-03 | MEI5, HO, NDJ1, MFT1, PSF1, ECM11, MSH5, MEI4, NSE4, RED1, REC114, PCH2, REC8, YKU70, MMS4, HFM1, ESC2, RAD17, SMC1, MSH3, SMC6, LIF1, ZIP1, RDH54, DOT1, PMS1, MMS22 |
| - | GO:0051704 | BP | multi-organism process | 1 | 1.37 | 1.62E-02 | FUS2, STE2, BAR1, AGA2, KAR3, STE5, GPA1, CSI1, FUS1, STE4, KAR1, ASG7, SST2, SPC110, AGA1, CIK1, RRI1, FUS3, FAR10, PTC1, JEM1 |
| - | GO:0006281 | BP | DNA repair | 7 | 1.32 | 5.39E-04 | MEI5, PSF1, IES2, LCD1, FYV6, MSH5, NSE4, EAF7, PSO2, PCD1, YKU70, SCC2, HMI1, MMS4, PDS5, RTT109, ESC2, RAD17, SMC1, HSM3, RAD34, POL4, MSH3, SMC6, LIF1, RAD30, RDH54, DOT1, PMS1, TFB3, NUP120, RAD28, MMS22 |

| | | | | | | | |
|---|---|---|---|---|---|---|---|
| - | GO:0022402 | BP | cell cycle process | 4 | 1.23 | 1.14E-07 | MEI5, SPS4, NDJ1, BRN1, CLB6, KAR3, SSP1, IPL1, ECM11, APC4, CNM67, AXL1, LCD1, SPC24, MSH5, CDC31, MEI4, RED1, KAR1, NBP1, BUD5, DON1, RSR1, BUB1, REC114, PCH2, REC8, SCC2, CHL4, MCM21, CIK1, MMS4, PDS5, HFM1, ESC2, RAD17, BIR1, SMC1, MIF2, GIC1, NDT80, AMN1, MSH3, CDC27, SPO22, RMD1, SET3, SMC6, ADY3, ATC1, JNM1, BUD2, ZIP1, NIP100, FUS3, FAR10, SPC98, RDH54, RSC58, DOT1, PMS1, SLK19, HPC2, MMS22, SWI4 |
| - | GO:0006974 | BP | response to DNA damage stimulus | 5 | 1.19 | 1.63E-03 | MEI5, PSF1, IES2, LCD1, FYV6, MSH5, NSE4, EAF7, PSO2, PCD1, YKU70, SCC2, HMI1, MMS4, PDS5, RTT109, ESC2, RAD17, SMC1, HSM3, RAD34, POL4, MSH3, SMC6, LIF1, CTK2, RAD30, RDH54, DOT1, PMS1, CKA1, TFB3, NUP120, RAD28, MMS22 |
| - | GO:0007049 | BP | cell cycle | 3 | 1.12 | 6.54E-07 | MEI5, SPS4, NDJ1, BRN1, CLB6, KAR3, SSP1, IPL1, PSF1, ECM11, APC4, CNM67, AXL1, LCD1, SPC24, MSH5, CDC31, MEI4, SPR3, RED1, KAR1, NBP1, BUD5, DON1, RSR1, BUB1, REC114, PCH2, REC8, SCC2, CHL4, MCM21, CIK1, MMS4, PDS5, HFM1, ESC2, RAD17, BIR1, SMC1, MIF2, GIC1, NDT80, AMN1, MSH3, CDC27, SPO22, RMD1, SET3, SMC6, ADY3, ATC1, JNM1, BUD2, ZIP1, NIP100, FUS3, FAR10, SPC98, RDH54, RSC58, DOT1, PMS1, SLK19, TFB3, HPC2, MMS22, SWI4 |
| - | GO:0006259 | BP | DNA metabolic process | 6 | 1.11 | 3.11E-05 | MEI5, HO, NDJ1, BRN1, CLB6, MFT1, PSF1, ECM11, IES2, LCD1, FYV6, MSH5, MEI4, ASF1, NSE4, RED1, EAF7, PSO2, PCD1, REC114, PCH2, REC8, YKU70, SCC2, HMI1, RLF2, MMS4, PDS5, RTT109, HFM1, ESC2, RAD17, BRE2, SMC1, HSM3, ORC6, RAD34, POL4, MSH3, SMC6, LIF1, ZIP1, RAD30, RDH54, DOT1, PMS1, CKA1, TFB3, NUP120, HPC2, RAD28, MMS22, SHE3, ORC1 |
| - | GO:0051276 | BP | chromosome organization | 4 | 1.11 | 3.91E-04 | NDJ1, BRN1, KAR3, IPL1, LOH1, IES2, LCD1, MSH5, ASF1, RED1, EAF7, JHD1, CTF13, BUB1, REC8, VPS71, UBP8, YKU70, SCC2, RLF2, CHL4, MCM21, CIK1, HOS1, PDS5, RTT109, HFM1, HDA3, ESC2, BIR1, BRE2, SMC1, SIR1, SAS3, MSH3, SET3, ZIP1, RKR1, RDH54, RSC58, DOT1, NUP120, HPC2, YPL216W, MMS22 |

| | | | | | | | |
|---|---|---|---|---|---|---|---|
| - | GO:0033554 | BP | cellular response to stress | 4 | 0.79 | 2.78E-02 | MEI5, PSF1, IES2, LCD1, OXR1, ATG4, FYV6, MSH5, TRS130, ATG17, ASF1, NSE4, EAF7, PSO2, PCD1, PDR8, YKU70, SCC2, HMI1, MMS4, PDS5, RTT109, ESC2, RAD17, SMC1, HSM3, VPS15, RAD34, POL4, MSH3, VPS30, TEC1, YBP1, SMC6, LIF1, CTK2, RAD30, RDH54, DOT1, PMS1, CKA1, TFB3, NUP120, RAD28, MMS22, SWI4, GEA1 |
| - | GO:0006996 | BP | organelle organization | 3 | 0.71 | 4.37E-05 | FUS2, YMR018W, NDJ1, CBP6, MRPS17, BRN1, KAR3, IPL1, LOH1, IES2, APC4, RRG1, CNM67, COX16, LCD1, CCE1, SPC24, ATG4, MSS2, MSH5, ATG17, CDC31, GPA1, ASF1, INP1, RED1, CNL1, EAF7, KAR1, VPS41, NBP1, ILM1, JHD1, SPC110, CTF13, VPS3, BUB1, PEX27, REC8, VPS71, UBP8, YKU70, ENV11, SCC2, HMI1, RLF2, MRPS18, CHL4, MCM21, CIK1, SPC97, VPS24, HOS1, PDS5, PEP3, RTT109, HFM1, HDA3, ESC2, BIR1, BRE2, SMC1, MIF2, VPS15, SLM5, GET4, SIR1, SAS3, AMN1, MSH3, CDC27, VPS30, SET3, ADY3, JNM1, SEC5, ZIP1, VPS16, MRPL49, RKR1, NIP100, FUS3, DSL1, SPC98, RDH54, RSC58, DOT1, SLK19, NUP120, HPC2, PTC1, MRPL22, YPL216W, RSM18, MDM1, CCM1, MMS22, SHE3, SEC8, JEM1, GEA1 |
| - | GO:0051716 | BP | cellular response to stimulus | 3 | 0.69 | 1.28E-02 | MEI5, STE2, BAR1, AGA2, PSF1, IES2, LCD1, OXR1, ATG4, FYV6, MSH5, TRS130, STE5, ATG17, GPA1, ASF1, CSI1, NSE4, STE4, EAF7, BUD5, HRT3, SST2, PSO2, RSR1, PCD1, AGA1, PDR8, YKU70, SCC2, HMI1, MMS4, PDS5, RTT109, ESC2, RAD17, SMC1, HSM3, VPS15, GIC1, RRI1, RAD34, POL4, MSH3, VPS30, TEC1, YBP1, SMC6, LIF1, CTK2, BUD2, FUS3, FAR10, RAD30, RDH54, DOT1, PMS1, CKA1, TFB3, NUP120, PTC1, RAD28, MMS22, SWI4, GEA1 |
| - | GO:0090304 | BP | nucleic acid metabolic process | 5 | 0.53 | 3.68E-03 | MEI5, HO, MET32, NDJ1, CBP6, BRN1, PRP21, CLB6, MFT1, PSF1, ECM11, IES2, UPF3, LCD1, CCE1, TOA1, FYV6, MSH5, NOP53, MEI4, TAF7, ASF1, NSE4, NOP16, RED1, EAF7, TYW3, RTT103, SEN34, JHD1, PSO2, URC2, PCD1, REC114, LSM4, PXR1, PCH2, SRD1, REC8, PRP3, YAP6, UBP8, PDR8, RPC31, YKU70, SCC2, HMI1, RLF2, CGR1, LSM12, MMS4, HOS1, PDS5, RTT109, HFM1, CUS2, HDA3, ESC2, RAD17, BRE2, SMC1, HSM3, ORC6, TRI1, SLM5, SLU7, NUT1, SIR1, TAN1, RAD34, SAS3, NDT80, FYV7, POL4, MSH3, TEC1, SET3, SMC6, LIF1, CTK2, ZIP1, SRB4, RRT14, PRP4, JJJ1, RAD30, RDH54, RSC58, DOT1, YLL054C, RIC1, PMS1, |

| | | | | | | | |
|---|---|---|---|---|---|---|---|
| | | | | | | | CKA1, TFB3, NUP120, HPC2, PTC1, YPL216W, SKI7, CCM1, RAD28, MMS22, PRP9, ESC8, PET309, BUD21, SHE3, SWI4, TFC4, ORC1 |
| - | GO:0016043 | BP | cellular component organization | 2 | 0.5 | 3.38E-03 | MEI5, FUS2, STE2, YMR018W, NDJ1, CBP6, MRPS17, BRN1, KAR3, SSP1, IPL1, LOH1, IES2, APC4, RRG1, CNM67, COX16, LCD1, CCE1, TRS33, SPC24, ATG4, MSS2, TOA1, MSH5, ATG17, SPO75, DTR1, CDC31, SPO20, TAF7, GPA1, ASF1, INP1, RED1, CNL1, EAF7, KAR1, VPS41, NBP1, ILM1, JHD1, SPC110, CTF13, DON1, VPS3, BUB1, LSM4, PEX27, REC8, VPS71, UBP8, YKU70, ENV11, SCC2, HMI1, RLF2, MRPS18, CHL4, MCM21, CIK1, PAC2, SPC97, VPS24, HOS1, PDS5, PEP3, RTT109, HFM1, HDA3, ESC2, BIR1, BRE2, SMC1, HSM3, MIF2, ORC6, VPS15, SLM5, SLU7, GET4, SIR1, BPH1, SAS3, AMN1, MSH3, CDC27, VPS30, SET3, ADY3, JNM1, SEC5, ZIP1, VPS16, MRPL49, RKR1, NIP100, FUS3, JJJ1, DSL1, SPC98, RDH54, RSC58, DOT1, SLK19, NUP120, HPC2, PTC1, MRPL22, YPL216W, RSM18, MDM1, CCM1, MMS22, SHE3, SEC8, JEM1, GEA1, ORC1 |
| - | GO:0050794 | BP | regulation of cellular process | 3 | 0.49 | 2.87E-02 | FUS2, MET32, STE2, BAR1, NDJ1, CBP6, CLB6, IPL1, MFT1, IES2, TRS130, STE5, ATG17, TAF7, GPA1, ASF1, CSI1, FUS1, RED1, STE4, EAF7, YKR023W, VPS41, BUD5, RTT103, SST2, JHD1, PIG1, URC2, HAL1, RSR1, ITT1, BUB1, PXR1, PCH2, SRD1, YAP6, RFM1, UBP8, PDR8, YKU70, ROY1, MMS4, YEL1, HOS1, FYV10, PEP3, RTT109, HDA3, ESC2, BRE2, SLI15, ORC6, VPS15, TRI1, GIC1, NUT1, SIR1, RRI1, SAS3, NDT80, AMN1, SPO22, TEC1, SET3, CTK2, SPT21, AIM14, BUD2, SRB4, VPS16, RRT14, PSY4, RKR1, PHO80, FUS3, FAR10, RSC58, DOT1, YLL054C, RIC1, CKA1, TFB3, SLF1, NUP120, HPC2, PTC1, YPL216W, VAC14, SKI7, ESC8, PET309, SWI4, TFC4, GEA1, ORC1 |

| | | | | | | | |
|---|---|---|---|---|---|---|---|
| - | GO:0044763 | BP | single-organism cellular process | 2 | 0.44 | 1.27E-06 | MEI5, HO, FUS2, HXT14, STE2, BAR1, YMR018W, SPS4, STE6, ARV1, NDJ1, AGA2, CBP6, HXT7, MRPS17, SPC2, BRN1, CLB6, KAR3, SSP1, IPL1, MFT1, LOH1, PSF1, ECM11, YDL206W, IES2, APC4, RRG1, CNM67, COX16, AXL1, LCD1, CCE1, TRS33, SPC24, OXR1, ATG4, MSS2, LST7, FYV6, MSH5, TRS130, STE5, ATG17, SPO75, DTR1, CDC31, NOP53, MEI4, SPR3, SPO20, GPA1, ASF1, CSI1, NSE4, INP1, FUS1, RED1, CNL1, STE4, EAF7, KAR1, VPS41, NBP1, BUD5, HRT3, ILM1, SST2, JHD1, SPC110, PSO2, CTF13, DON1, RSR1, PCD1, VPS3, BUB1, REC114, AGA1, PXR1, PCH2, PEX27, REC8, AVL9, RCY1, ATX2, VPS71, VPS52, UBP8, PDR8, ERD2, EMP46, YKU70, ENV11, SCC2, HMI1, RLF2, MRPS18, SEC10, CHL4, MCM21, ROY1, CIK1, MMS4, YEL1, SPC97, VPS24, HOS1, PDS5, PEP3, RTT109, HFM1, HDA3, ESC2, RAD17, BIR1, BRE2, SMC1, HSM3, MIF2, SLI15, ORC6, VPS15, SLM5, GET4, GIC1, SIR1, DIA3, BPH1, RRI1, RAD34, BUG1, SAS3, NDT80, AMN1, POL4, MSH3, CDC27, VPS30, SPO22, RMD1, TEC1, SET3, YBP1, SMC6, ADY3, LIF1, ATC1, APL5, CTK2, JNM1, KCH1, SPT21, AIM14, SEC5, BUD2, ZIP1, VPS16, MRPL49, RKR1, NIP100, PHO80, FUS3, JJJ1, FAR10, DSL1, RAD30, SPC98, RDH54, RSC58, DOT1, RIC1, YKR078W, PMS1, SLK19, CKA1, TFB3, SLF1, NUP120, HPC2, PTC1, MRPL22, YPL216W, BSD2, RSM18, MDM1, CCM1, RAD28, COG8, NUP82, MMS22, ESC8, SHE3, IMH1, SWI4, KTR2, SEC8, JEM1, GEA1, ORC1 |

| | | | | | | | |
|---|---|---|---|---|---|---|---|
| - | GO:0044699 | BP | single-organism process | 1 | 0.41 | 6.89E-06 | MEI5, HO, FUS2, HXT14, STE2, BAR1, YMR018W, SPS4, STE6, ARV1, NDJ1, AGA2, CBP6, HXT7, MRPS17, SPC2, PUG1, BRN1, CLB6, KAR3, SSP1, IPL1, MFT1, LOH1, PSF1, ECM11, YDL206W, IES2, APC4, RRG1, CNM67, COX16, AXL1, LCD1, CCE1, TRS33, SPC24, OXR1, ATG4, MSS2, LST7, FYV6, MSH5, TRS130, STE5, ATG17, SPO75, DTR1, CDC31, NOP53, MEI4, SPR3, SPO20, GPA1, ASF1, CSI1, NSE4, INP1, FUS1, RED1, CNL1, STE4, EAF7, KAR1, VPS41, NBP1, BUD5, HRT3, ILM1, SST2, JHD1, SPC110, PSO2, CTF13, DON1, RSR1, PCD1, VPS3, BUB1, REC114, AGA1, PXR1, PCH2, PEX27, REC8, AVL9, RCY1, ATX2, VPS71, VPS52, UBP8, PDR8, ERD2, EMP46, YKU70, ENV11, SCC2, HMI1, RLF2, MRPS18, SEC10, CHL4, MCM21, ROY1, CIK1, MMS4, YEL1, SPC97, VPS24, HOS1, PDS5, PEP3, RTT109, HFM1, HDA3, ESC2, RAD17, BIR1, BRE2, SMC1, HSM3, MIF2, SLI15, ORC6, VPS15, SLM5, GET4, GIC1, SIR1, DIA3, BPH1, RRI1, RAD34, BUG1, SAS3, NDT80, AMN1, POL4, MSH3, CDC27, VPS30, SPO22, RMD1, TEC1, SET3, YBP1, SMC6, ADY3, LIF1, ATC1, APL5, CTK2, JNM1, KCH1, SPT21, AIM14, SEC5, BUD2, ZIP1, VPS16, MRPL49, RKR1, NIP100, PHO80, FUS3, JJJ1, FAR10, DSL1, RAD30, SPC98, RDH54, RSC58, DOT1, RIC1, YKR078W, PMS1, SLK19, CKA1, TFB3, SLF1, NUP120, HPC2, PTC1, MRPL22, YPL216W, BSD2, RSM18, MDM1, CCM1, RAD28, COG8, NUP82, MMS22, ESC8, SHE3, IMH1, SWI4, KTR2, SEC8, JEM1, GEA1, ORC1 |
| - | GO:0044450 | CC | microtubule organizing center part | 10 | 3.37 | 9.73E-04 | CNM67, CDC31, KAR1, NBP1, SPC110, SPC97, SPC98 |
| - | GO:0005875 | CC | microtubule associated complex | 9 | 2.78 | 1.25E-02 | KAR3, IPL1, CIK1, BIR1, SLI15, JNM1, NIP100 |
| - | GO:0000794 | CC | condensed nuclear chromosome | 11 | 2.16 | 3.86E-06 | MEI5, BRN1, IPL1, SPC24, MSH5, MEI4, RED1, CTF13, BUB1, REC114, REC8, KRE28, CHL4, MCM21, PDS5, RAD17, BIR1, SMC1, MIF2, SPO22, ZIP1, SLK19 |
| - | GO:0000793 | CC | condensed chromosome | 8 | 2.11 | 9.62E-07 | MEI5, BRN1, IPL1, SPC24, MSH5, MEI4, NSE4, RED1, CTF13, BUB1, REC114, REC8, KRE28, CHL4, MCM21, PDS5, RAD17, BIR1, SMC1, MIF2, SLI15, SPO22, SMC6, ZIP1, SLK19 |
| - | GO:0000778 | CC | condensed nuclear chromosome kinetochore | 13 | 2.05 | 2.85E-02 | IPL1, SPC24, CTF13, BUB1, KRE28, CHL4, MCM21, BIR1, MIF2, SLK19 |
| - | GO:0000780 | CC | condensed nuclear chromosome, | 12 | 2.02 | 1.80E-02 | IPL1, SPC24, CTF13, BUB1, REC8, KRE28, CHL4, MCM21, BIR1, MIF2, SLK19 |

| | | | | | | | |
|---|---|---|---|---|---|---|---|
| | | | centromeric region | | | | |
| - | GO:0005874 | CC | microtubule | 9 | 1.93 | 1.62E-02 | KAR3, IPL1, KAR1, CIK1, PAC2, SPC97, BIR1, SLI15, JNM1, NIP100, SPC98, SLK19 |
| - | GO:0000779 | CC | condensed chromosome, centromeric region | 10 | 1.91 | 1.80E-02 | IPL1, SPC24, CTF13, BUB1, REC8, KRE28, CHL4, MCM21, BIR1, MIF2, SLI15, SLK19 |
| - | GO:0000777 | CC | condensed chromosome kinetochore | 11 | 1.9 | 3.34E-02 | IPL1, SPC24, CTF13, BUB1, KRE28, CHL4, MCM21, BIR1, MIF2, SLI15, SLK19 |
| - | GO:0005815 | CC | microtubule organizing center | 9 | 1.89 | 7.48E-03 | KAR3, CNM67, CDC31, KAR1, NBP1, SPC110, KRE28, CIK1, SPC97, ADY3, JNM1, NIP100, SPC98, SLK19 |
| - | GO:0005816 | CC | spindle pole body | 11 | 1.89 | 7.48E-03 | KAR3, CNM67, CDC31, KAR1, NBP1, SPC110, KRE28, CIK1, SPC97, ADY3, JNM1, NIP100, SPC98, SLK19 |
| - | GO:0000775 | CC | chromosome, centromeric region | 9 | 1.88 | 4.42E-03 | IPL1, SPC24, PSH1, CTF13, BUB1, REC8, KRE28, RLF2, CHL4, MCM21, BIR1, MIF2, SLI15, SIR1, SLK19 |
| - | GO:0000922 | CC | spindle pole | 10 | 1.77 | 1.53E-02 | KAR3, CNM67, CDC31, KAR1, NBP1, SPC110, KRE28, CIK1, SPC97, ADY3, JNM1, NIP100, SPC98, SLK19 |
| - | GO:0005819 | CC | spindle | 9 | 1.73 | 4.82E-03 | KAR3, IPL1, CNM67, CDC31, KAR1, NBP1, SPC110, KRE28, CIK1, SPC97, BIR1, SLI15, ADY3, JNM1, NIP100, SPC98, SLK19 |
| - | GO:0015630 | CC | microtubule cytoskeleton | 8 | 1.56 | 1.11E-02 | KAR3, IPL1, CNM67, CDC31, KAR1, NBP1, SPC110, KRE28, CIK1, PAC2, SPC97, BIR1, SLI15, ADY3, JNM1, NIP100, SPC98, SLK19 |
| - | GO:0000228 | CC | nuclear chromosome | 10 | 1.37 | 5.67E-05 | MEI5, NDJ1, BRN1, IPL1, PSF1, LCD1, SPC24, MSH5, MEI4, RED1, RTT103, CTF13, BUB1, REC114, REC8, KRE28, VPS71, YKU70, SCC2, CHL4, MCM21, PDS5, HDA3, RAD17, BIR1, SMC1, MIF2, ORC6, NDT80, MSH3, SPO22, SET3, LIF1, ZIP1, SLK19, SWI4, ORC1 |
| - | GO:0005694 | CC | chromosome | 7 | 1.33 | 3.03E-06 | MEI5, NDJ1, LIN1, BRN1, IPL1, PSF1, LCD1, SPC24, FYV6, MSH5, MEI4, NSE4, RED1, PSH1, RTT103, CTF13, BUB1, REC114, PCH2, REC8, KRE28, VPS71, YKU70, SCC2, RLF2, CHL4, MCM21, PDS5, HDA3, RAD17, BIR1, BRE2, SMC1, MIF2, SLI15, ORC6, SIR1, NDT80, MSH3, SPO22, SET3, SMC6, LIF1, ZIP1, RAD30, SLK19, SWI4, ORC1 |
| - | GO:0044454 | CC | nuclear chromosome part | 11 | 1.23 | 4.40E-03 | NDJ1, BRN1, IPL1, PSF1, SPC24, MSH5, RED1, RTT103, CTF13, BUB1, REC8, KRE28, VPS71, YKU70, SCC2, CHL4, MCM21, PDS5, HDA3, RAD17, BIR1, SMC1, MIF2, ORC6, SET3, LIF1, ZIP1, SLK19, SWI4, ORC1 |

| | | | | | | | |
|---|---|---|---|---|---|---|---|
| - | GO:0044427 | CC | chromosomal part | 8 | 1.22 | 2.25E-04 | NDJ1, LIN1, BRN1, IPL1, PSF1, SPC24, FYV6, MSH5, NSE4, RED1, PSH1, RTT103, CTF13, BUB1, REC8, KRE28, VPS71, YKU70, SCC2, RLF2, CHL4, MCM21, PDS5, HDA3, RAD17, BIR1, BRE2, SMC1, MIF2, SLI15, ORC6, SIR1, SET3, SMC6, LIF1, ZIP1, RAD30, SLK19, SWI4, ORC1 |
| - | GO:0031981 | CC | nuclear lumen | 9 | 0.71 | 8.31E-03 | MEI5, NDJ1, BRN1, TMA23, IPL1, MFT1, PSF1, UPF3, LCD1, SPC24, TOA1, MSH5, NOP53, MEI4, TAF7, NOP16, RED1, EAF7, RTT103, CTF13, BUB1, REC114, LSM4, PXR1, PCH2, REC8, KRE28, VPS71, RFM1, UBP8, RPC31, YKU70, SCC2, CGR1, CHL4, MCM21, HOS1, PDS5, HDA3, RAD17, BIR1, BRE2, SMC1, MIF2, ORC6, TRI1, NUT1, SAS3, NDT80, FYV7, MSH3, SPO22, SET3, LIF1, CTK2, ZIP1, SRB4, RRT14, NOP8, JJJ1, SLK19, CKA1, TFB3, BUD21, SWI4, TFC4, ORC1 |
| - | GO:0043234 | CC | protein complex | 2 | 0.63 | 1.20E-04 | SPC2, BRN1, KAR3, IPL1, MFT1, PSF1, APC4, CNM67, TRS33, SPC24, LST7, TOA1, MSH5, TRS130, ATG17, CDC31, SPR3, SPO20, TAF7, GPA1, CSI1, NSE4, CNL1, STE4, EAF7, KAR1, VPS41, NBP1, HRT3, SEN34, SPC110, PIG1, CTF13, VPS3, BUB1, KRE28, VPS71, RFM1, FIG4, HUL4, VPS52, UBP8, RPC31, YKU70, SCC2, RLF2, SEC10, CHL4, MCM21, CIK1, PAC2, MMS4, SPC97, VPS24, HOS1, PDS5, FYV10, PEP3, HDA3, RAD17, BIR1, BRE2, SMC1, HSM3, MIF2, SLI15, ORC6, VPS15, GET4, NUT1, SIR1, RRI1, SAS3, MSH3, CDC27, VPS30, SET3, SMC6, ADY3, LIF1, APL5, CTK2, JNM1, SEC5, SRB4, VPS16, CUL3, NIP100, PHO80, DSL1, SPC98, RSC58, RIC1, PMS1, SLK19, CKA1, YDR306C, TFB3, NUP120, HPC2, VAC14, CAB3, SKI7, MDM1, COG8, NUP82, MMS22, SWI4, SEC8, TFC4, ORC1 |
| - | GO:0044428 | CC | nuclear part | 8 | 0.57 | 9.30E-03 | MEI5, NDJ1, LIN1, BRN1, PRP21, TMA23, IPL1, MFT1, PSF1, UPF3, APC4, LCD1, SPC24, TOA1, MSH5, CDC31, NOP53, MEI4, TAF7, CSI1, NOP16, RED1, EAF7, NBP1, RTT103, SEN34, CTF13, BUB1, REC114, LSM4, PXR1, PCH2, REC8, PRP3, KRE28, VPS71, RFM1, HUL4, UBP8, RPC31, YKU70, SCC2, CGR1, CHL4, MCM21, HOS1, PDS5, CUS2, HDA3, RAD17, BIR1, BRE2, SMC1, MIF2, ORC6, VPS15, TRI1, SLU7, NUT1, SIR1, RRI1, CAB5, SAS3, NDT80, FYV7, MSH3, CDC27, SPO22, SET3, LIF1, CTK2, ZIP1, SRB4, RRT14, PRP4, NOP8, JJJ1, RSC58, PMS1, SLK19, CKA1, TFB3, NUP120, NUP82, |

| | | | | | | | |
|---|---|---|---|---|---|---|---|
| | | | | | | | PRP9, BUD21, SWI4, JEM1, TFC4, ORC1 |
| - | GO:0043228 | CC | non-membrane-bounded organelle | 2 | 0.55 | 1.23E-02 | MEI5, NDJ1, CBP6, MRPS17, LIN1, BRN1, TMA23, KAR3, IPL1, PSF1, UPF3, CNM67, LCD1, SPC24, FYV6, MSH5, CDC31, NOP53, MEI4, SPR3, NSE4, NOP16, RED1, PSH1, KAR1, NBP1, RTT103, SPC110, CTF13, BUB1, REC114, LSM4, PXR1, PCH2, REC8, KRE28, VPS71, VPS52, YKU70, SCC2, RLF2, MRPS18, CGR1, CHL4, MCM21, CIK1, PAC2, LSM12, SPC97, PDS5, HDA3, RAD17, BIR1, BRE2, SMC1, MIF2, SLI15, ORC6, TRI1, GIC1, SIR1, NDT80, FYV7, MSH3, SPO22, SET3, SMC6, ADY3, LIF1, CTK2, YPL225W, JNM1, AIM14, ZIP1, MRPL49, RRT14, RKR1, NIP100, NOP8, JJJ1, RAD30, SPC98, YLL032C, SLK19, CKA1, MRPL22, RSM18, MDM1, INP51, BUD21, SWI4, ORC1 |
| - | GO:0043232 | CC | intracellular non-membrane-bounded organelle | 6 | 0.55 | 1.23E-02 | MEI5, NDJ1, CBP6, MRPS17, LIN1, BRN1, TMA23, KAR3, IPL1, PSF1, UPF3, CNM67, LCD1, SPC24, FYV6, MSH5, CDC31, NOP53, MEI4, SPR3, NSE4, NOP16, RED1, PSH1, KAR1, NBP1, RTT103, SPC110, CTF13, BUB1, REC114, LSM4, PXR1, PCH2, REC8, KRE28, VPS71, VPS52, YKU70, SCC2, RLF2, MRPS18, CGR1, CHL4, MCM21, CIK1, PAC2, LSM12, SPC97, PDS5, HDA3, RAD17, BIR1, BRE2, SMC1, MIF2, SLI15, ORC6, TRI1, GIC1, SIR1, NDT80, FYV7, MSH3, SPO22, SET3, SMC6, ADY3, LIF1, CTK2, YPL225W, JNM1, AIM14, ZIP1, MRPL49, RRT14, RKR1, NIP100, NOP8, JJJ1, RAD30, SPC98, YLL032C, SLK19, CKA1, MRPL22, RSM18, MDM1, INP51, BUD21, SWI4, ORC1 |
| - | GO:0043233 | CC | organelle lumen | 3 | 0.54 | 4.65E-02 | MEI5, NDJ1, CBP6, MRPS17, BRN1, TMA23, IPL1, MFT1, PSF1, UPF3, PET130, LCD1, SPC24, MSS2, TOA1, MSH5, NOP53, MEI4, TAF7, NOP16, RED1, EAF7, RTT103, CTF13, BUB1, REC114, LSM4, PXR1, PCH2, REC8, KRE28, VPS71, RFM1, UBP8, RPC31, YKU70, SCC2, HMI1, MRPS18, CGR1, CHL4, MCM21, HOS1, PDS5, HDA3, RAD17, BIR1, BRE2, SMC1, MIF2, |

| | | | | | | | |
|---|---|---|---|---|---|---|---|
| | | | | | | | ORC6, TRI1, SLM5, NUT1, SAS3, NDT80, FYV7, MSH3, SPO22, SET3, LIF1, CTK2, SAY1, ZIP1, SRB4, MRPL49, RRT14, NOP8, JJJ1, SLK19, CKA1, TFB3, MRPL22, RSM18, BUD21, SWI4, TFC4, ORC1 |
| - | GO:0070013 | CC | intracellular organelle lumen | 7 | 0.54 | 4.65E-02 | MEI5, NDJ1, CBP6, MRPS17, BRN1, TMA23, IPL1, MFT1, PSF1, UPF3, PET130, LCD1, SPC24, MSS2, TOA1, MSH5, NOP53, MEI4, TAF7, NOP16, RED1, EAF7, RTT103, CTF13, BUB1, REC114, LSM4, PXR1, PCH2, REC8, KRE28, VPS71, RFM1, UBP8, RPC31, YKU70, SCC2, HMI1, MRPS18, CGR1, CHL4, MCM21, HOS1, PDS5, HDA3, RAD17, BIR1, BRE2, SMC1, MIF2, ORC6, TRI1, SLM5, NUT1, SAS3, NDT80, FYV7, MSH3, SPO22, SET3, LIF1, CTK2, SAY1, ZIP1, SRB4, MRPL49, RRT14, NOP8, JJJ1, SLK19, CKA1, TFB3, MRPL22, RSM18, BUD21, SWI4, TFC4, ORC1 |
| - | GO:0005634 | CC | nucleus | 7 | 0.52 | 8.37E-06 | MEI5, HO, FUS2, MET32, NDJ1, LIN1, BRN1, PRP21, TMA23, CLB6, KAR3, IPL1, MFT1, PSF1, ECM11, IES2, UPF3, APC4, PES4, LCD1, SPC24, ATG4, TOA1, FYV6, MSH5, STE5, CDC31, NOP53, MEI4, TAF7, ASF1, CSI1, NSE4, NOP16, RED1, EAF7, PSH1, YKR023W, NBP1, YIG1, RTT103, SEN34, JHD1, SPC110, PSO2, CTF13, URC2, YLR271W, BUB1, REC114, LSM4, INM1, PXR1, PCH2, SRD1, REC8, PRP3, KRE28, YAP6, VPS71, RFM1, HUL4, UBP8, PDR8, RPC31, YKU70, ENV11, SCC2, RLF2, CGR1, CHL4, MCM21, ROY1, CIK1, LSM12, MMS4, SPC97, HOS1, PDS5, FYV10, RTT109, HFM1, CUS2, HDA3, ESC2, RAD17, BIR1, BRE2, SMC1, HSM3, MIF2, SLI15, ORC6, VPS15, TRI1, SLU7, GIC1, NUT1, SIR1, RRI1, YBL010C, TAN1, RAD34, CAB5, SAS3, NDT80, AMN1, FYV7, POL4, MSH3, CDC27, SPO22, TEC1, SET3, SMC6, LIF1, ATC1, CTK2, SPT21, ZIP1, SRB4, RRT14, PSY4, RKR1, PRP4, CUL3, PHO80, NOP8, FUS3, HGH1, JJJ1, DSL1, RAD30, SPC98, RDH54, RSC58, DOT1, JJJ2, YLL054C, RIC1, PMS1, SLK19, CKA1, TFB3, NUP120, HPC2, PTC1, YPL216W, RKM4, RAD28, NUP82, MMS22, PRP9, ESC8, BUD21, YOR093C, SWI4, JEM1, TFC4, ORC1 |

| | | | | | | | |
|---|---|---|---|---|---|---|---|
| - | GO:0032991 | CC | macromolecular complex | 1 | 0.4 | 1.25E-02 | CBP6, MRPS17, SPC2, LIN1, BRN1, PRP21, TMA23, KAR3, IPL1, MFT1, PSF1, UPF3, APC4, CNM67, TRS33, SPC24, LST7, TOA1, MSH5, TRS130, ATG17, CDC31, SPR3, SPO20, TAF7, GPA1, CSI1, NSE4, NOP16, CNL1, STE4, EAF7, KAR1, VPS41, NBP1, HRT3, SEN34, SPC110, PIG1, CTF13, VPS3, BUB1, LSM4, PRP3, KRE28, VPS71, RFM1, FIG4, HUL4, VPS52, UBP8, RPC31, YKU70, SCC2, RLF2, MRPS18, CGR1, SEC10, CHL4, MCM21, CIK1, PAC2, LSM12, MMS4, SPC97, VPS24, HOS1, PDS5, FYV10, PEP3, CUS2, HDA3, RAD17, BIR1, BRE2, SMC1, HSM3, MIF2, SLI15, ORC6, VPS15, SLU7, GET4, NUT1, SIR1, RRI1, SAS3, MSH3, CDC27, VPS30, SET3, SMC6, ADY3, LIF1, APL5, CTK2, YPL225W, JNM1, AIM14, SEC5, SRB4, VPS16, MRPL49, RKR1, PRP4, CUL3, NIP100, PHO80, JJJ1, DSL1, SPC98, RSC58, RIC1, PMS1, YLL032C, SLK19, CKA1, YDR306C, TFB3, SLF1, NUP120, HPC2, MRPL22, VAC14, CAB3, RSM18, SKI7, MDM1, COG8, NUP82, MMS22, PRP9, BUD21, SWI4, SEC8, TFC4, ORC1 |
| - | GO:0043231 | CC | intracellular membrane-bounded organelle | 6 | 0.2 | 3.33E-02 | MEI5, HO, FUS2, MET32, HXT14, YMR018W, STE6, ARV1, NDJ1, CBP6, HXT7, MRPS17, SPC2, LIN1, BRN1, PRP21, TMA23, CLB6, KAR3, IPL1, MFT1, PSF1, ECM11, IES2, UPF3, APC4, PES4, RRG1, PET130, COX16, LCD1, CCE1, TRS33, SPC24, OXR1, ATG4, MSS2, LST7, TOA1, FYV6, YDL211C, MSH5, TRS130, STE5, ERJ5, CDC31, NOP53, MEI4, TAF7, GPA1, ASF1, CSI1, NSE4, INP1, NOP16, RED1, EAF7, PSH1, YJR098C, YKR023W, VPS41, NBP1, YIG1, RTT103, SEN34, ILM1, JHD1, AIM22, SPC110, PSO2, CTF13, URC2, PCD1, VPS3, OMS1, YLR271W, BUB1, REC114, LSM4, INM1, PXR1, PCH2, SRD1, PEX27, REC8, PRP3, RCY1, ATX2, KRE28, YAP6, VPS71, RFM1, ECI1, FIG4, HUL4, VPS52, UBP8, PDR8, RPC31, ERD2, EMP46, YKU70, ENV11, SCC2, HMI1, RLF2, MRPS18, CGR1, CHL4, MCM21, ROY1, CIK1, LSM12, MMS4, SPC97, VPS24, HOS1, PDS5, FYV10, PEP3, RTT109, HFM1, YPL168W, CUS2, HDA3, ESC2, RAD17, BIR1, BRE2, SMC1, HSM3, MIF2, SLI15, ORC6, VPS15, TRI1, SLM5, SLU7, GIC1, NUT1, SIR1, BPH1, RRI1, YBL010C, TAN1, RAD34, YJR003C, BUG1, CAB5, SAS3, NDT80, AMN1, FYV7, POL4, MSH3, CDC27, VPS30, SPO22, TEC1, FMP32, SET3, SMC6, YBR096W, |

| | | | | | | | |
|---|---|---|---|---|---|---|---|
| | | | | | | | LIF1, ATC1, APL5, CTK2, SAY1, KCH1, SPT21, AIM14, ZIP1, SRB4, VPS16, MRPL49, RRT14, PSY4, RKR1, PRP4, CUL3, PHO80, NOP8, FUS3, HGH1, JJJ1, FAR10, DSL1, RAD30, SPC98, RDH54, PPA2, RSC58, DOT1, JJJ2, YLL054C, RIC1, PMS1, SLK19, CKA1, TFB3, NUP120, HPC2, PTC1, MRPL22, YPL216W, VAC14, RKM4, BSD2, RSM18, CCM1, RAD28, COG8, NUP82, MMS22, PRP9, ESC8, PET309, BUD21, SHE3, IMH1, YKL100C, YOR093C, SWI4, KTR2, JEM1, TFC4, GEA1, ORC1 |

| | | | | | | | |
|---|---|---|---|---|---|---|---|
| - | GO:0043227 | CC | membrane-bounded organelle | 2 | 0.2 | 3.38E-02 | MEI5, HO, FUS2, MET32, HXT14, YMR018W, STE6, ARV1, NDJ1, CBP6, HXT7, MRPS17, SPC2, LIN1, BRN1, PRP21, TMA23, CLB6, KAR3, IPL1, MFT1, PSF1, ECM11, IES2, UPF3, APC4, PES4, RRG1, PET130, COX16, LCD1, CCE1, TRS33, SPC24, OXR1, ATG4, MSS2, LST7, TOA1, FYV6, YDL211C, MSH5, TRS130, STE5, ERJ5, CDC31, NOP53, MEI4, TAF7, GPA1, ASF1, CSI1, NSE4, INP1, NOP16, RED1, EAF7, PSH1, YJR098C, YKR023W, VPS41, NBP1, YIG1, RTT103, SEN34, ILM1, JHD1, AIM22, SPC110, PSO2, CTF13, URC2, PCD1, VPS3, OMS1, YLR271W, BUB1, REC114, LSM4, INM1, PXR1, PCH2, SRD1, PEX27, REC8, PRP3, RCY1, ATX2, KRE28, YAP6, VPS71, RFM1, ECI1, FIG4, HUL4, VPS52, UBP8, PDR8, RPC31, ERD2, EMP46, YKU70, ENV11, SCC2, HMI1, RLF2, MRPS18, CGR1, CHL4, MCM21, ROY1, CIK1, LSM12, MMS4, SPC97, VPS24, HOS1, PDS5, FYV10, PEP3, RTT109, HFM1, YPL168W, CUS2, HDA3, ESC2, RAD17, BIR1, BRE2, SMC1, HSM3, MIF2, SLI15, ORC6, VPS15, TRI1, SLM5, SLU7, GIC1, NUT1, SIR1, BPH1, RRI1, YBL010C, TAN1, RAD34, YJR003C, BUG1, CAB5, SAS3, NDT80, AMN1, FYV7, POL4, MSH3, CDC27, VPS30, SPO22, TEC1, FMP32, SET3, SMC6, YBR096W, LIF1, ATC1, APL5, CTK2, SAY1, KCH1, SPT21, AIM14, ZIP1, SRB4, VPS16, MRPL49, RRT14, PSY4, RKR1, PRP4, CUL3, PHO80, NOP8, FUS3, HGH1, JJJ1, FAR10, DSL1, RAD30, SPC98, RDH54, PPA2, RSC58, DOT1, JJJ2, YLL054C, RIC1, PMS1, SLK19, CKA1, TFB3, NUP120, HPC2, PTC1, MRPL22, YPL216W, VAC14, RKM4, BSD2, RSM18, CCM1, RAD28, COG8, NUP82, MMS22, PRP9, ESC8, PET309, BUD21, SHE3, IMH1, YKL100C, YOR093C, SWI4, KTR2, JEM1, TFC4, GEA1, ORC1 |
| - | GO:0003684 | MF | damaged DNA binding | 5 | 2.73 | 2.19E-03 | LCD1, MSH5, PSO2, YKU70, RAD17, RAD34, MSH3, SMC6, RAD30 |
| | | | | | | | |
| + | GO:0002181 | BP | cytoplasmic translation | 7 | 3.87 | 9.63E-43 | RPL29, RPS30B, RPS25B, RPL1A, RPL9B, RPL38, RPS14B, RPS19B, RPL42A, RPS27B, RPL18B, RPL43B, RPS21B, RPL14B, RPL11A, RPL1B, RPS12, RPS21A, RPL35A, RPL36A, RPL30, RPP2B, RPS3, RPS28B, RPL29, RPS30B, RPS25B, RPL1A, RPL9B, RPL38, RPS14B, RPS19B, RPL42A, RPS27B, RPL18B, RPL43B, RPS21B, RPL14B, RPL11A, RPL1B, RPS12, |

| | | | | | | | |
|---|---|---|---|---|---|---|---|
| | | | | | | | RPS21A, RPL35A, RPL36A, RPL30, RPP2B, RPS3, RPS28B |
| + | GO:0006412 | BP | translation | 6 | 2.05 | 2.62E-19 | RPL29, TIF6, RPS30B, RPS25B, RPL1A, RPL9B, RPL38, RPS14B, RPS19B, RPL42A, RPS27B, RPL18B, RPL43B, RPS21B, RPL14B, RPL11A, RPL1B, RPS12, RPS21A, TEF1, RPL35A, RPS2, RPL36A, RPL30, RPP2B, RPS3, RPS28B, RPL29, TIF6, RPS30B, RPS25B, RPL1A, RPL9B, RPL38, RPS14B, RPS19B, RPL42A, RPS27B, RPL18B, RPL43B, RPS21B, RPL14B, RPL11A, RPL1B, RPS12, RPS21A, TEF1, RPL35A, RPS2, RPL36A, RPL30, RPP2B, RPS3, RPS28B |
| + | GO:0009058 | BP | biosynthetic process | 2 | 0.95 | 1.64E-09 | RPL29, TIF6, POG1, RPS30B, RPS25B, CIA2, RPL1A, RPL9B, RPL38, RPS14B, DPM1, RPS19B, RPL42A, RPS27B, RPL18B, RPL43B, RPS21B, RPL14B, RPL11A, RPL1B, RPS12, MDH2, RPS21A, TEF1, RPL35A, ILV5, RPS2, ARO4, IMD2, PDC6, RPL36A, RPL30, RPP2B, LYS1, RPS3, ADH2, RPS28B, SNZ1, RPL29, TIF6, POG1, RPS30B, RPS25B, CIA2, RPL1A, RPL9B, RPL38, RPS14B, DPM1, RPS19B, RPL42A, RPS27B, RPL18B, RPL43B, RPS21B, RPL14B, RPL11A, RPL1B, RPS12, MDH2, RPS21A, TEF1, RPL35A, ILV5, RPS2, ARO4, IMD2, PDC6, RPL36A, RPL30, RPP2B, LYS1, RPS3, ADH2, RPS28B, SNZ1 |
| + | GO:1901576 | BP | organic substance biosynthetic process | 3 | 0.93 | 8.85E-09 | RPL29, TIF6, POG1, RPS30B, RPS25B, RPL1A, RPL9B, RPL38, RPS14B, DPM1, RPS19B, RPL42A, RPS27B, RPL18B, RPL43B, RPS21B, RPL14B, RPL11A, RPL1B, RPS12, MDH2, RPS21A, TEF1, RPL35A, ILV5, RPS2, ARO4, IMD2, PDC6, RPL36A, RPL30, RPP2B, LYS1, RPS3, ADH2, RPS28B, SNZ1, RPL29, TIF6, POG1, RPS30B, RPS25B, RPL1A, RPL9B, RPL38, RPS14B, DPM1, RPS19B, RPL42A, RPS27B, RPL18B, RPL43B, RPS21B, RPL14B, RPL11A, RPL1B, RPS12, MDH2, RPS21A, TEF1, RPL35A, ILV5, RPS2, ARO4, IMD2, PDC6, RPL36A, RPL30, RPP2B, LYS1, RPS3, ADH2, RPS28B, SNZ1 |
| + | GO:0006407 | BP | rRNA export from nucleus | 10 | 4.52 | 1.10E-07 | RPS19B, RPS2, RPS3, RPS28B, RPS19B, RPS2, RPS3, RPS28B |
| + | GO:0051029 | BP | rRNA transport | 8 | 4.52 | 1.10E-07 | RPS19B, RPS2, RPS3, RPS28B, RPS19B, RPS2, RPS3, RPS28B |

| | | | | | | | |
|---|---|---|---|---|---|---|---|
| + | GO:0034645 | BP | cellular macromolecule biosynthetic process | 5 | 0.99 | 1.49E-06 | RPL29, TIF6, POG1, RPS30B, RPS25B, RPL1A, RPL9B, RPL38, RPS14B, DPM1, RPS19B, RPL42A, RPS27B, RPL18B, RPL43B, RPS21B, RPL14B, RPL11A, RPL1B, RPS12, RPS21A, TEF1, RPL35A, RPS2, RPL36A, RPL30, RPP2B, RPS3, RPS28B, RPL29, TIF6, POG1, RPS30B, RPS25B, RPL1A, RPL9B, RPL38, RPS14B, DPM1, RPS19B, RPL42A, RPS27B, RPL18B, RPL43B, RPS21B, RPL14B, RPL11A, RPL1B, RPS12, RPS21A, TEF1, RPL35A, RPS2, RPL36A, RPL30, RPP2B, RPS3, RPS28B |
| + | GO:0009059 | BP | macromolecule biosynthetic process | 4 | 0.97 | 2.56E-06 | RPL29, TIF6, POG1, RPS30B, RPS25B, RPL1A, RPL9B, RPL38, RPS14B, DPM1, RPS19B, RPL42A, RPS27B, RPL18B, RPL43B, RPS21B, RPL14B, RPL11A, RPL1B, RPS12, RPS21A, TEF1, RPL35A, RPS2, RPL36A, RPL30, RPP2B, RPS3, RPS28B, RPL29, TIF6, POG1, RPS30B, RPS25B, RPL1A, RPL9B, RPL38, RPS14B, DPM1, RPS19B, RPL42A, RPS27B, RPL18B, RPL43B, RPS21B, RPL14B, RPL11A, RPL1B, RPS12, RPS21A, TEF1, RPL35A, RPS2, RPL36A, RPL30, RPP2B, RPS3, RPS28B |
| + | GO:0044249 | BP | cellular biosynthetic process | 3 | 0.84 | 2.58E-06 | RPL29, TIF6, POG1, RPS30B, RPS25B, RPL1A, RPL9B, RPL38, RPS14B, DPM1, RPS19B, RPL42A, RPS27B, RPL18B, RPL43B, RPS21B, RPL14B, RPL11A, RPL1B, RPS12, RPS21A, TEF1, RPL35A, ILV5, RPS2, ARO4, IMD2, RPL36A, RPL30, RPP2B, LYS1, RPS3, RPS28B, SNZ1, RPL29, TIF6, POG1, RPS30B, RPS25B, RPL1A, RPL9B, RPL38, RPS14B, DPM1, RPS19B, RPL42A, RPS27B, RPL18B, RPL43B, RPS21B, RPL14B, RPL11A, RPL1B, RPS12, RPS21A, TEF1, RPL35A, ILV5, RPS2, ARO4, IMD2, RPL36A, RPL30, RPP2B, LYS1, RPS3, RPS28B, SNZ1 |
| + | GO:0044267 | BP | cellular protein metabolic process | 5 | 0.92 | 1.81E-05 | RPL29, TIF6, RPS30B, RPS25B, RPL1A, RPL9B, RPL38, RPS14B, DPM1, RPS19B, RPL42A, RPS27B, RPL18B, RPL43B, RPS21B, RPL14B, RPL11A, RPL1B, RPS12, RPS21A, TEF1, RPL35A, RPS2, RPL36A, RPL30, RPP2B, RPS3, RPS28B, RPL29, TIF6, RPS30B, RPS25B, RPL1A, RPL9B, RPL38, RPS14B, DPM1, RPS19B, RPL42A, RPS27B, RPL18B, RPL43B, RPS21B, RPL14B, RPL11A, RPL1B, RPS12, RPS21A, TEF1, RPL35A, RPS2, RPL36A, RPL30, RPP2B, RPS3, RPS28B |

| | | | | | | | |
|---|---|---|---|---|---|---|---|
| + | GO:0019538 | BP | protein metabolic process | 4 | 0.83 | 1.74E-04 | RPL29, TIF6, RPS30B, RPS25B, RPL1A, RPL9B, RPL38, RPS14B, DPM1, RPS19B, RPL42A, RPS27B, RPL18B, RPL43B, RPS21B, RPL14B, RPL11A, RPL1B, RPS12, RPS21A, TEF1, RPL35A, RPS2, RPL36A, RPL30, RPP2B, RPS3, RPS28B, RPL29, TIF6, RPS30B, RPS25B, RPL1A, RPL9B, RPL38, RPS14B, DPM1, RPS19B, RPL42A, RPS27B, RPL18B, RPL43B, RPS21B, RPL14B, RPL11A, RPL1B, RPS12, RPS21A, TEF1, RPL35A, RPS2, RPL36A, RPL30, RPP2B, RPS3, RPS28B |
| + | GO:0042254 | BP | ribosome biogenesis | 4 | 1.56 | 1.78E-04 | TIF6, RPS14B, RPS19B, RPS27B, RPS21B, RPL11A, RPS21A, RPL35A, RPS2, RPL30, RPS3, RPS28B, TIF6, RPS14B, RPS19B, RPS27B, RPS21B, RPL11A, RPS21A, RPL35A, RPS2, RPL30, RPS3, RPS28B |
| + | GO:0051168 | BP | nuclear export | 8 | 2.35 | 4.56E-04 | TIF6, RPS19B, TEF1, RPS2, RPS3, RPS28B, TIF6, RPS19B, TEF1, RPS2, RPS3, RPS28B |
| + | GO:0006405 | BP | RNA export from nucleus | 9 | 2.55 | 8.79E-04 | RPS19B, TEF1, RPS2, RPS3, RPS28B, RPS19B, TEF1, RPS2, RPS3, RPS28B |
| + | GO:0042255 | BP | ribosome assembly | 7 | 2.85 | 1.51E-03 | TIF6, RPS14B, RPS27B, RPL11A, TIF6, RPS14B, RPS27B, RPL11A |
| + | GO:0010467 | BP | gene expression | 4 | 0.71 | 2.28E-03 | RPL29, TIF6, POG1, RPS30B, RPS25B, RPL1A, RPL9B, RPL38, RPS14B, RPS19B, RPL42A, RPS27B, RPL18B, RPL43B, RPS21B, RPL14B, RPL11A, RPL1B, RPS12, RPS21A, TEF1, RPL35A, RPS2, RPL36A, RPL30, RPP2B, RPS3, RPS28B, RPL29, TIF6, POG1, RPS30B, RPS25B, RPL1A, RPL9B, RPL38, RPS14B, RPS19B, RPL42A, RPS27B, RPL18B, RPL43B, RPS21B, RPL14B, RPL11A, RPL1B, RPS12, RPS21A, TEF1, RPL35A, RPS2, RPL36A, RPL30, RPP2B, RPS3, RPS28B |
| + | GO:0022613 | BP | ribonucleoprotein complex biogenesis | 3 | 1.33 | 2.28E-03 | TIF6, RPS14B, RPS19B, RPS27B, RPS21B, RPL11A, RPS21A, RPL35A, RPS2, RPL30, RPS3, RPS28B, TIF6, RPS14B, RPS19B, RPS27B, RPS21B, RPL11A, RPS21A, RPL35A, RPS2, RPL30, RPS3, RPS28B |
| + | GO:0006116 | BP | NADH oxidation | 12 | 4.36 | 2.89E-03 | GPD2, ADH2, GPD2, ADH2 |
| + | GO:0000947 | BP | amino acid catabolic process to alcohol via Ehrlich pathway | 10 | 4.36 | 2.89E-03 | PDC6, ADH2, PDC6, ADH2 |
| + | GO:0000955 | BP | amino acid catabolic process via Ehrlich pathway | 9 | 4.23 | 4.30E-03 | PDC6, ADH2, PDC6, ADH2 |
| + | GO:0006913 | BP | nucleocytoplasmic transport | 7 | 1.94 | 6.05E-03 | TIF6, RPS19B, TEF1, RPS2, RPS3, RPS28B, TIF6, RPS19B, TEF1, RPS2, RPS3, RPS28B |

| | | | | | | | |
|---|---|---|---|---|---|---|---|
| + | GO:0051169 | BP | nuclear transport | 6 | 1.94 | 6.05E-03 | TIF6, RPS19B, TEF1, RPS2, RPS3, RPS28B, TIF6, RPS19B, TEF1, RPS2, RPS3, RPS28B |
| + | GO:0006734 | BP | NADH metabolic process | 11 | 4.1 | 6.05E-03 | GPD2, ADH2, GPD2, ADH2 |
| + | GO:0006067 | BP | ethanol metabolic process | 6 | 3.98 | 8.11E-03 | PDC6, ADH2, PDC6, ADH2 |
| + | GO:0034308 | BP | primary alcohol metabolic process | 5 | 3.98 | 8.11E-03 | PDC6, ADH2, PDC6, ADH2 |
| + | GO:0050658 | BP | RNA transport | 7 | 2.1 | 9.43E-03 | RPS19B, TEF1, RPS2, RPS3, RPS28B, RPS19B, TEF1, RPS2, RPS3, RPS28B |
| + | GO:0051236 | BP | establishment of RNA localization | 4 | 2.1 | 9.43E-03 | RPS19B, TEF1, RPS2, RPS3, RPS28B, RPS19B, TEF1, RPS2, RPS3, RPS28B |
| + | GO:0050657 | BP | nucleic acid transport | 6 | 2.08 | 1.05E-02 | RPS19B, TEF1, RPS2, RPS3, RPS28B, RPS19B, TEF1, RPS2, RPS3, RPS28B |
| + | GO:0070925 | BP | organelle assembly | 4 | 2.31 | 1.64E-02 | TIF6, RPS14B, RPS27B, RPL11A, TIF6, RPS14B, RPS27B, RPL11A |
| + | GO:0042274 | BP | ribosomal small subunit biogenesis | 5 | 2 | 1.64E-02 | RPS14B, RPS19B, RPS27B, RPS21B, RPS21A, RPS14B, RPS19B, RPS27B, RPS21B, RPS21A |
| + | GO:0000028 | BP | ribosomal small subunit assembly | 8 | 3.69 | 1.76E-02 | RPS14B, RPS27B, RPS14B, RPS27B |
| + | GO:0006403 | BP | RNA localization | 3 | 1.93 | 2.28E-02 | RPS19B, TEF1, RPS2, RPS3, RPS28B, RPS19B, TEF1, RPS2, RPS3, RPS28B |
| + | GO:0000478 | BP | endonucleolytic cleavage involved in rRNA processing | 11 | 2.66 | 2.66E-02 | RPS27B, RPS21B, RPS21A, RPS27B, RPS21B, RPS21A |
| + | GO:0000479 | BP | endonucleolytic cleavage of tricistronic rRNA transcript (SSU-rRNA, 5.8S rRNA, LSU-rRNA) | 12 | 2.66 | 2.66E-02 | RPS27B, RPS21B, RPS21A, RPS27B, RPS21B, RPS21A |
| + | GO:0090502 | BP | RNA phosphodiester bond hydrolysis, endonucleolytic | 8 | 2.63 | 2.66E-02 | RPS27B, RPS21B, RPS21A, RPS27B, RPS21B, RPS21A |
| + | GO:0006364 | BP | rRNA processing | 9 | 1.37 | 2.78E-02 | TIF6, RPS14B, RPS27B, RPS21B, RPS21A, RPL35A, RPS2, RPL30, TIF6, RPS14B, RPS27B, RPS21B, RPS21A, RPL35A, RPS2, RPL30 |
| + | GO:0015931 | BP | nucleobase-containing compound transport | 5 | 1.8 | 3.89E-02 | RPS19B, TEF1, RPS2, RPS3, RPS28B, RPS19B, TEF1, RPS2, RPS3, RPS28B |
| + | GO:0016072 | BP | rRNA metabolic process | 8 | 1.32 | 3.99E-02 | TIF6, RPS14B, RPS27B, RPS21B, RPS21A, RPL35A, RPS2, RPL30, TIF6, RPS14B, RPS27B, RPS21B, RPS21A, RPL35A, RPS2, RPL30 |
| + | GO:0000462 | BP | maturation of SSU-rRNA from tricistronic rRNA transcript (SSU-rRNA, 5.8S rRNA, LSU-rRNA) | 11 | 2.07 | 3.99E-02 | RPS14B, RPS27B, RPS21B, RPS21A, RPS14B, RPS27B, RPS21B, RPS21A |
| + | GO:0031125 | BP | rRNA 3'-end processing | 10 | 3.23 | 4.86E-02 | RPS21B, RPS21A, RPS21B, RPS21A |

| | | | | | | | |
|---|---|---|---|---|---|---|---|
| + | GO:0022626 | CC | cytosolic ribosome | 9 | 3.85 | 2.43E-44 | RPL29, RPS30B, RPS25B, RPL1A, RPL9B, RPL38, RPS14B, RPS19B, RPL42A, RPS27B, RPL18B, RPL43B, RPS21B, RPL14B, RPL11A, RPL1B, RPS12, RPS21A, RPL35A, RPS2, RPL36A, RPL30, RPP2B, RPS3, RPS28B, RPL29, RPS30B, RPS25B, RPL1A, RPL9B, RPL38, RPS14B, RPS19B, RPL42A, RPS27B, RPL18B, RPL43B, RPS21B, RPL14B, RPL11A, RPL1B, RPS12, RPS21A, RPL35A, RPS2, RPL36A, RPL30, RPP2B, RPS3, RPS28B |
| + | GO:0044445 | CC | cytosolic part | 8 | 3.42 | 3.62E-39 | RPL29, RPS30B, RPS25B, RPL1A, RPL9B, RPL38, RPS14B, RPS19B, RPL42A, RPS27B, RPL18B, ERR3, RPL43B, RPS21B, RPL14B, RPL11A, RPL1B, RPS12, RPS21A, RPL35A, RPS2, RPL36A, RPL30, RPP2B, RPS3, RPS28B, RPL29, RPS30B, RPS25B, RPL1A, RPL9B, RPL38, RPS14B, RPS19B, RPL42A, RPS27B, RPL18B, ERR3, RPL43B, RPS21B, RPL14B, RPL11A, RPL1B, RPS12, RPS21A, RPL35A, RPS2, RPL36A, RPL30, RPP2B, RPS3, RPS28B |
| + | GO:0044391 | CC | ribosomal subunit | 8 | 3.39 | 4.95E-37 | RPL29, RPS30B, RPS25B, RPL1A, RPL9B, RPL38, RPS14B, RPS19B, RPL42A, RPS27B, RPL18B, RPL43B, RPS21B, RPL14B, RPL11A, RPL1B, RPS12, RPS21A, RPL35A, RPS2, RPL36A, RPL30, RPP2B, RPS3, RPS28B, RPL29, RPS30B, RPS25B, RPL1A, RPL9B, RPL38, RPS14B, RPS19B, RPL42A, RPS27B, RPL18B, RPL43B, RPS21B, RPL14B, RPL11A, RPL1B, RPS12, RPS21A, RPL35A, RPS2, RPL36A, RPL30, RPP2B, RPS3, RPS28B |
| + | GO:0005840 | CC | ribosome | 7 | 2.96 | 2.95E-33 | RPL29, RPS30B, RPS25B, YIH1, RPL1A, RPL9B, RPL38, RPS14B, RPS19B, RPL42A, RPS27B, RPL18B, RPL43B, RPS21B, RPL14B, RPL11A, RPL1B, RPS12, RPS21A, TEF1, RPL35A, RPS2, RPL36A, RPL30, RPP2B, RPS3, RPS28B, RPL29, RPS30B, RPS25B, YIH1, RPL1A, RPL9B, RPL38, RPS14B, RPS19B, RPL42A, RPS27B, RPL18B, RPL43B, RPS21B, RPL14B, RPL11A, RPL1B, RPS12, RPS21A, TEF1, RPL35A, RPS2, RPL36A, RPL30, RPP2B, RPS3, RPS28B |
| + | GO:0022625 | CC | cytosolic large ribosomal subunit | 10 | 3.88 | 1.28E-23 | RPL29, RPL1A, RPL9B, RPL38, RPL42A, RPL18B, RPL43B, RPL14B, RPL11A, RPL1B, RPL35A, RPL36A, RPL30, RPP2B, RPL29, RPL1A, RPL9B, RPL38, RPL42A, RPL18B, RPL43B, RPL14B, RPL11A, RPL1B, RPL35A, RPL36A, RPL30, RPP2B |

| | | | | | | | |
|---|---|---|---|---|---|---|---|
| + | GO:0022627 | CC | cytosolic small ribosomal subunit | 10 | 4.14 | 3.77E-20 | RPS30B, RPS25B, RPS14B, RPS19B, RPS27B, RPS21B, RPS12, RPS21A, RPS2, RPS3, RPS28B, RPS30B, RPS25B, RPS14B, RPS19B, RPS27B, RPS21B, RPS12, RPS21A, RPS2, RPS3, RPS28B |
| + | GO:0030529 | CC | ribonucleoprotein complex | 5 | 1.95 | 9.84E-19 | RPL29, TIF6, RPS30B, RPS25B, YIH1, RPL1A, RPL9B, RPL38, RPS14B, RPS19B, RPL42A, RPS27B, RPL18B, RPL43B, RPS21B, RPL14B, RPL11A, RPL1B, RPS12, RPS21A, TEF1, RPL35A, RPS2, RPL36A, RPL30, RPP2B, RPS3, RPS28B, RPL29, TIF6, RPS30B, RPS25B, YIH1, RPL1A, RPL9B, RPL38, RPS14B, RPS19B, RPL42A, RPS27B, RPL18B, RPL43B, RPS21B, RPL14B, RPL11A, RPL1B, RPS12, RPS21A, TEF1, RPL35A, RPS2, RPL36A, RPL30, RPP2B, RPS3, RPS28B |
| + | GO:0015934 | CC | large ribosomal subunit | 9 | 3.3 | 1.65E-18 | RPL29, RPL1A, RPL9B, RPL38, RPL42A, RPL18B, RPL43B, RPL14B, RPL11A, RPL1B, RPL35A, RPL36A, RPL30, RPP2B, RPL29, RPL1A, RPL9B, RPL38, RPL42A, RPL18B, RPL43B, RPL14B, RPL11A, RPL1B, RPL35A, RPL36A, RPL30, RPP2B |
| + | GO:0005829 | CC | cytosol | 7 | 1.8 | 1.14E-16 | RPL29, RPS30B, RPS25B, GPD2, RPL1A, RPL9B, RPL38, RPS14B, RPS19B, RPL42A, RPS27B, RPL18B, ERR3, RPL43B, RPS21B, RPL14B, RPL11A, RPL1B, RPS12, MDH2, RPS21A, RPL35A, RPS2, RPL36A, RPL30, RPP2B, RPS3, RPS28B, RPL29, RPS30B, RPS25B, GPD2, RPL1A, RPL9B, RPL38, RPS14B, RPS19B, RPL42A, RPS27B, RPL18B, ERR3, RPL43B, RPS21B, RPL14B, RPL11A, RPL1B, RPS12, MDH2, RPS21A, RPL35A, RPS2, RPL36A, RPL30, RPP2B, RPS3, RPS28B |
| + | GO:0015935 | CC | small ribosomal subunit | 9 | 3.52 | 1.24E-15 | RPS30B, RPS25B, RPS14B, RPS19B, RPS27B, RPS21B, RPS12, RPS21A, RPS2, RPS3, RPS28B, RPS30B, RPS25B, RPS14B, RPS19B, RPS27B, RPS21B, RPS12, RPS21A, RPS2, RPS3, RPS28B |
| + | GO:0043228 | CC | non-membrane-bounded organelle | 2 | 1.43 | 2.63E-15 | MGM101, RPL29, TIF6, POG1, RPS30B, RPS25B, YIH1, RPL1A, HTB2, RPL9B, RPL38, RPS14B, RPS19B, RPL42A, RPS27B, RPL18B, RPL43B, RPS21B, HTA2, RPL14B, RPL11A, RPL1B, RPS12, RPS21A, TEF1, RPL35A, ILV5, RPS2, IMD2, RPL36A, RPL30, RPP2B, RPS3, RPS28B, MGM101, RPL29, TIF6, POG1, RPS30B, RPS25B, YIH1, RPL1A, HTB2, RPL9B, RPL38, RPS14B, RPS19B, RPL42A, RPS27B, RPL18B, RPL43B, RPS21B, HTA2, RPL14B, RPL11A, RPL1B, RPS12, RPS21A, TEF1, RPL35A, ILV5, RPS2, IMD2, RPL36A, RPL30, RPP2B, RPS3, RPS28B |

| | | | | | | | |
|---|---|---|---|---|---|---|---|
| + | GO:0043232 | CC | intracellular non-membrane-bounded organelle | 6 | 1.43 | 2.63E-15 | MGM101, RPL29, TIF6, POG1, RPS30B, RPS25B, YIH1, RPL1A, HTB2, RPL9B, RPL38, RPS14B, RPS19B, RPL42A, RPS27B, RPL18B, RPL43B, RPS21B, HTA2, RPL14B, RPL11A, RPL1B, RPS12, RPS21A, TEF1, RPL35A, ILV5, RPS2, IMD2, RPL36A, RPL30, RPP2B, RPS3, RPS28B, MGM101, RPL29, TIF6, POG1, RPS30B, RPS25B, YIH1, RPL1A, HTB2, RPL9B, RPL38, RPS14B, RPS19B, RPL42A, RPS27B, RPL18B, RPL43B, RPS21B, HTA2, RPL14B, RPL11A, RPL1B, RPS12, RPS21A, TEF1, RPL35A, ILV5, RPS2, IMD2, RPL36A, RPL30, RPP2B, RPS3, RPS28B |
| + | GO:0032991 | CC | macromolecular complex | 1 | 0.62 | 2.67E-03 | RPL29, TIF6, RPS30B, RPS25B, GPD2, YIH1, RPL1A, HTB2, RPL9B, RPL38, RPS14B, RPS19B, RPL42A, RPS27B, RPL18B, ERR3, RPL43B, RPS21B, HTA2, RPL14B, RPL11A, RPL1B, RPS12, RPS21A, TEF1, RPL35A, RPS2, RPL36A, RPL30, RPP2B, RPS3, RPS28B, RPL29, TIF6, RPS30B, RPS25B, GPD2, YIH1, RPL1A, HTB2, RPL9B, RPL38, RPS14B, RPS19B, RPL42A, RPS27B, RPL18B, ERR3, RPL43B, RPS21B, HTA2, RPL14B, RPL11A, RPL1B, RPS12, RPS21A, TEF1, RPL35A, RPS2, RPL36A, RPL30, RPP2B, RPS3, RPS28B |
| + | GO:0005576 | CC | extracellular region | 1 | 2.33 | 2.89E-03 | ACB1, TIR3, CWP2, PIR3, TIR1, ACB1, TIR3, CWP2, PIR3, TIR1 |
| + | GO:0031225 | CC | anchored to membrane | 4 | 2.69 | 3.13E-03 | TIR3, YDR524C-B, CWP2, TIR1, TIR3, YDR524C-B, CWP2, TIR1 |
| + | GO:0000788 | CC | nuclear nucleosome | 13 | 4.1 | 6.05E-03 | HTB2, HTA2, HTB2, HTA2 |
| + | GO:0000786 | CC | nucleosome | 10 | 3.88 | 1.05E-02 | HTB2, HTA2, HTB2, HTA2 |
| + | GO:0030684 | CC | preribosome | 6 | 1.79 | 3.99E-02 | TIF6, RPS14B, RPL35A, RPS2, RPS3, TIF6, RPS14B, RPL35A, RPS2, RPS3 |
| + | GO:0009277 | CC | fungal-type cell wall | 6 | 2.04 | 4.44E-02 | TIR3, CWP2, PIR3, TIR1, TIR3, CWP2, PIR3, TIR1 |
| + | GO:0044444 | CC | cytoplasmic part | 6 | 0.38 | 4.94E-02 | MGM101, RPL29, ATO3, RPS30B, ICY1, RPS25B, GPD2, YIH1, RPL1A, RPL9B, RPL38, RPS14B, DPM1, RPS19B, RPL42A, RPS27B, OAC1, RPL18B, ERR3, RPL43B, RPS21B, RPL14B, RPL11A, RPL1B, RPS12, MDH2, RPS21A, TEF1, RPL35A, ILV5, RPS2, YMR122W-A, RCR1, RPL36A, RPL30, RPP2B, RPS3, NCA3, RPS28B, MGM101, RPL29, ATO3, RPS30B, ICY1, RPS25B, GPD2, YIH1, RPL1A, RPL9B, RPL38, RPS14B, DPM1, RPS19B, RPL42A, RPS27B, OAC1, RPL18B, ERR3, RPL43B, RPS21B, RPL14B, RPL11A, RPL1B, RPS12, MDH2, RPS21A, TEF1, RPL35A, ILV5, RPS2, YMR122W-A, RCR1, |

| | | | | | | | |
|---|---|---|---|---|---|---|---|
| | | | | | | | RPL36A, RPL30, RPP2B, RPS3, NCA3, RPS28B |
| + | GO:0003735 | MF | structural constituent of ribosome | 2 | 3.5 | 9.08E-39 | RPL29, RPS30B, RPS25B, RPL1A, RPL9B, RPL38, RPS14B, RPS19B, RPL42A, RPS27B, RPL18B, RPL43B, RPS21B, RPL14B, RPL11A, RPL1B, RPS12, RPS21A, RPL35A, RPS2, RPL36A, RPL30, RPP2B, RPS3, RPS28B, RPL29, RPS30B, RPS25B, RPL1A, RPL9B, RPL38, RPS14B, RPS19B, RPL42A, RPS27B, RPL18B, RPL43B, RPS21B, RPL14B, RPL11A, RPL1B, RPS12, RPS21A, RPL35A, RPS2, RPL36A, RPL30, RPP2B, RPS3, RPS28B |
| + | GO:0005198 | MF | structural molecule activity | 1 | 2.95 | 1.11E-34 | RPL29, RPS30B, RPS25B, RPL1A, RPL9B, RPL38, RPS14B, RPS19B, RPL42A, RPS27B, RPL18B, RPL43B, RPS21B, RPL14B, RPL11A, RPL1B, RPS12, RPS21A, RPL35A, RPS2, RPL36A, RPL30, RPP2B, CWP2, RPS3, RPS28B, PIR3, TIR1, RPL29, RPS30B, RPS25B, RPL1A, RPL9B, RPL38, RPS14B, RPS19B, RPL42A, RPS27B, RPL18B, RPL43B, RPS21B, RPL14B, RPL11A, RPL1B, RPS12, RPS21A, RPL35A, RPS2, RPL36A, RPL30, RPP2B, CWP2, RPS3, RPS28B, PIR3, TIR1 |
| + | GO:0005199 | MF | structural constituent of cell wall | 2 | 4.36 | 3.07E-05 | CWP2, PIR3, TIR1, CWP2, PIR3, TIR1 |
| + | GO:0016616 | MF | oxidoreductase activity, acting on the CH-OH group of donors, NAD or NADP as acceptor | 4 | 2.56 | 8.11E-04 | GPD2, MDH2, ILV5, IMD2, ADH2, GPD2, MDH2, ILV5, IMD2, ADH2 |
| + | GO:0016614 | MF | oxidoreductase activity, acting on CH-OH group of donors | 3 | 2.52 | 1.05E-03 | GPD2, MDH2, ILV5, IMD2, ADH2, GPD2, MDH2, ILV5, IMD2, ADH2 |
| + | GO:0043022 | MF | ribosome binding | 3 | 3.52 | 2.66E-02 | TIF6, YIH1, TIF6, YIH1 |
| + | GO:0050662 | MF | coenzyme binding | 3 | 2.03 | 4.69E-02 | ACB1, GPD2, ILV5, PDC6, ACB1, GPD2, ILV5, PDC6 |
| a. "-" = GO terms associated with repressed genes; "+" = GO terms associated with induced genes | | | | | | | |
| b. BF = biological function; CC = cellular component; MF = molecular function | | | | | | | |

c. The number of steps to the root of GO term tree.

d. The $\log_2$ of the ratio

f. where *n* is the number of genes in the user list that falls into a given GO category, m is the total number of genes in the user list, N is total number of genes in the GO category, and M is the total number of genes in the genome.

e. Calculated from a hypergeometric distribution with a false discovery rate of 0.01.

**Table 3.6. GO term enrichment for genes that are significantly (p<0.05) down-regulated in the H4H18A mutant compared to the H4WT parental strain.** The up-regulated genes did not show any statistical significant GO term enrichment. The biological function, cellular component and molecular function ontologies are shown separately in the table, sorted in descending order for the log odds ratio.

| -/+[a] | GOID | Ontology [b] | Term | Level[c] | Log odds ratio[d] | p[e] | Genes |
|---|---|---|---|---|---|---|---|
| - | GO:0019236 | BP | response to pheromone | 4 | 5.26 | 7.11E-06 | STE2, BAR1, STE6, GPA1, STE4, AGA1 |
| - | GO:0000747 | BP | conjugation with cellular fusion | 4 | 5.09 | 7.11E-06 | STE2, BAR1, FUS2, GPA1, STE4, AGA1 |
| - | GO:0000746 | BP | conjugation | 3 | 5.08 | 7.11E-06 | STE2, BAR1, FUS2, GPA1, STE4, AGA1 |
| - | GO:0000749 | BP | response to pheromone involved in conjugation with cellular fusion | 7 | 5.48 | 3.33E-05 | STE2, BAR1, GPA1, STE4, AGA1 |
| - | GO:0071444 | BP | cellular response to pheromone | 6 | 5.22 | 5.39E-05 | STE2, BAR1, GPA1, STE4, AGA1 |
| - | GO:0044764 | BP | multi-organism cellular process | 2 | 4.44 | 5.39E-05 | STE2, BAR1, FUS2, GPA1, STE4, AGA1 |
| - | GO:0051704 | BP | multi-organism process | 1 | 4.37 | 5.39E-05 | STE2, BAR1, FUS2, GPA1, STE4, AGA1 |
| - | GO:0010033 | BP | response to organic substance | 3 | 4.33 | 5.39E-05 | STE2, BAR1, STE6, GPA1, STE4, AGA1 |
| - | GO:0000003 | BP | reproduction | 1 | 3.25 | 5.39E-05 | STE2, BAR1, FUS2, GPA1, RME1, STE4, AXL1, AGA1 |

a. "-" = GO terms associated with repressed genes; "+" = GO terms associated with induced genes

b. BF = biological function; CC = cellular component; MF = molecular function

c. The number of steps to the root of GO term tree.

d. The $\log_2$ of the ratio

where *n* is the number of genes in the user list that falls into a given GO category, m is the total number of genes in the user list, N is total number of genes in the GO category, and M is the total number of genes in the genome.

e. Calculated from a hypergeometric distribution with a false discovery rate of 0.01.

**Table 3.7. GO term enrichment for genes that are significantly (p<0.05) up-regulated or down-regulated in the H3E50A mutant compared to the H3WT parental strain.** The biological function, cellular component and molecular function ontologies are shown separately in the table, sorted in descending order for the log odds ratio.

| -/+[a] | GOID | Ontology[b] | Term | Level[c] | Log odds ratio[d] | p[e] | Genes |
|---|---|---|---|---|---|---|---|
| - | GO:0042254 | BP | ribosome biogenesis | 4 | 2.24 | 3.69E-50 | NOG1, RPL3, NOP9, UTP8, SDO1, SDA1, RPS16B, RPS2, PUF6, IMP3, RPL35B, RPS24B, RPS20, RRP12, LCP5, RPS28A, NOP12, ENP1, RPL10, RPL11B, NOC3, UTP25, DBP9, RPP0, NOP8, RRP42, RPS9A, IPI1, BRX1, RPS1A, RRB1, RPS18A, SGD1, RRP8, NOP4, URB2, RPS13, RPS6B, RPL12A, EMG1, RPS17B, DBP8, EBP2, SRM1, UTP22, NOP7, NOP16, RPS31, RPS7B, RRP14, UTP10, RPF2, SHB17, RNA1, RPS17A, ERB1, KRI1, POP5, MTR3, PRP43, UTP4, RPS14A, RPS19B, CBF5, RRP45, SYO1, TMA23, RPS19A, PWP1, RPL5, SSB1, RPS11B, RRP9, RPS11A, RPS24A, RPS10B, RPS7A, DBP2, RPL40A, FYV7, RPL12B, DIP2, RIX1, RPL25, UTP30, RPS6A, FAF1, RPS0B, UTP21, GRC3, HAS1, RAI1, RLP24, RPL6B, NOP1, MAK21, RPL6A, SAS10, NOP56, NOP58, RPL8B, RPS26B, MAK16, RPS5, FAL1, RPL8A, RPS16A, RPS18B, IPI3, NIP7, UTP9, RPL40B, LOC1, BUD22, SNU13, RPS27B, RPS1B, RPS9B, RPS10A, PXR1, GAR1 |
| - | GO:0022613 | BP | ribonucleoprotein complex biogenesis | 3 | 2.03 | 3.02E-43 | NOG1, RPL3, NOP9, UTP8, SDO1, SDA1, RPS16B, RPS2, PUF6, IMP3, RPL35B, RPS24B, RPS20, RRP12, LCP5, RPS28A, NOP12, ENP1, RPL10, RPL11B, NOC3, UTP25, DBP9, SHQ1, RPP0, NOP8, RRP42, RPS9A, IPI1, BRX1, RPS1A, RRB1, RPS18A, SGD1, RRP8, NOP4, URB2, RPS13, RPS6B, RPL12A, EMG1, RPS17B, DBP8, EBP2, SRM1, UTP22, NOP7, NOP16, RPS31, RPS7B, RRP14, UTP10, RPF2, SHB17, RNA1, RPS17A, ERB1, KRI1, POP5, MTR3, PRP43, UTP4, RPS14A, RPS19B, CBF5, RRP45, SYO1, TMA23, RPS19A, PWP1, RPL5, SSB1, RPS11B, RRP9, RPS11A, RPS24A, RPS10B, RPS7A, DBP2, RPL40A, FYV7, RPL12B, DIP2, RIX1, RPL25, UTP30, RPS6A, FAF1, RPS0B, UTP21, GRC3, HAS1, RAI1, RLP24, RPL6B, NOP1, MAK21, RPL6A, SAS10, NOP56, NOP58, RPL8B, RPS26B, MAK16, RPS5, FAL1, RPL8A, RPS16A, RPS18B, IPI3, NIP7, UTP9, RPL40B, LOC1, BUD22, SNU13, RPS27B, RPS1B, RPS9B, RPS10A, PXR1, GAR1 |
| - | GO:0051168 | BP | nuclear export | 8 | 1.51 | 0.00215 | NOG1, NOP9, UTP8, SDA1, LOS1, RPS2, RPS28A, RPS18A, SRM1, UTP22, RNA1, RPS19B, RPS19A, SSB1, RPS10B, RIX1, RPS0B, RPS26B, RPS5, RPS18B, RPS10A |
| - | GO:0006913 | BP | nucleocytoplasmic transport | 7 | 1.16 | 0.04465 | NOG1, NOP9, UTP8, SDA1, LOS1, RPS2, RPS28A, RPS18A, SRM1, UTP22, RNA1, RPS19B, RPS19A, SSB1, RPS10B, RIX1, RPS0B, RPS26B, RPS5, GPN3, RPS18B, RPS10A |
| - | GO:0051169 | BP | nuclear transport | 6 | 1.16 | 0.04465 | NOG1, NOP9, UTP8, SDA1, LOS1, RPS2, RPS28A, RPS18A, SRM1, UTP22, RNA1, RPS19B, RPS19A, SSB1, RPS10B, RIX1, RPS0B, RPS26B, RPS5, GPN3, RPS18B, RPS10A |

| | | | | | | | |
|---|---|---|---|---|---|---|---|
| - | GO:0044085 | BP | cellular component biogenesis | 2 | 1.11 | 4.37E-18 | NOG1, PMI40, RPL3, NOP9, UTP8, BUB1, SDO1, SDA1, RPS16B, RPS2, PUF6, IMP3, RPL35B, RPS24B, RPS20, RRP12, LCP5, RPS28A, NOP12, ENP1, RPL10, RPL11B, NOC3, UTP25, DBP9, SHQ1, RPP0, NOP8, PSA1, RRP42, RPS9A, IPI1, BRX1, RPS1A, CYK3, RRB1, RPS18A, SGD1, RRP8, NOP4, URB2, RPS13, RPS6B, RPL12A, EMG1, CDC3, RPS17B, DBP8, EBP2, SRM1, UTP22, NOP7, NOP16, RPS31, RPS7B, RRP14, UTP10, SPH1, RPF2, SHB17, RNA1, RPS17A, ERB1, KRI1, POP5, MTR3, PRP43, UTP4, RPS14A, RPS19B, CDC5, CDC45, CBF5, RRP45, SYO1, TMA23, RPS19A, HTB2, PWP1, RPL5, SSB1, RPS11B, RRP9, RPS11A, RPS24A, RPS10B, RPS7A, DBP2, MCM2, RPL40A, FYV7, RPL12B, DIP2, RIX1, PAC2, RPL25, UTP30, RPS6A, FAF1, RPS0B, UTP21, GRC3, HAS1, RAI1, RLP24, RPL6B, PKR1, NOP1, MAK21, RPL6A, SAS10, NOP56, NOP58, RPL8B, ASF1, RPS26B, MAK16, RPS5, FAL1, RPL8A, RPS16A, RPS18B, IPI3, NIP7, GIM3, UTP9, RPL40B, LOC1, BUD22, SNU13, RPS27B, RPS1B, RPS9B, RPS10A, PXR1, GAR1 |
| - | GO:0071840 | BP | cellular component organization or biogenesis | 1 | 0.59 | 6.72E-10 | NOG1, PMI40, RPL3, NOP9, UTP8, BUB1, GEA2, SDO1, EFR3, SDA1, LTE1, ALK2, RPS16B, RPS2, PUF6, IMP3, RIM2, RPL35B, FOB1, ETT1, RPS24B, RPS20, RRP12, SCP160, LCP5, RPS28A, CLB4, VAC17, NOP12, ENP1, RPL10, RPL11B, NOC3, UTP25, DBP9, SHQ1, TEM1, RPP0, NOP8, PSA1, RFC4, SPC97, RRP42, IRR1, RPS9A, IPI1, BRX1, RPS1A, CYK3, RRB1, RPS18A, SGD1, RRP8, BIT61, NOP4, URB2, YDR089W, RPS13, PDS5, RPS6B, RPL12A, EMG1, CDC3, RPS17B, ALK1, DBP8, EBP2, SRM1, UTP22, NOP7, NOP16, RPS31, RPS7B, RRP14, UTP10, SPH1, RPF2, SHB17, RNA1, PBP2, RPS17A, ERB1, KRI1, POP5, MTR3, PRP43, UTP4, ENV11, PRS3, RPS14A, RPS19B, DPB2, CTF8, CDC5, CDC45, CBF5, RRP45, SYO1, TMA23, RPS19A, HTB2, PWP1, KRE6, RPL5, OKP1, CLB1, SSB1, RPS11B, RRP9, YLR194C, RPS11A, RPS24A, RPS10B, RPS7A, DBP2, MCM2, RPL40A, TOF2, FYV7, DOT1, RPL12B, DIP2, RIX1, ILM1, PAC2, RPL25, UTP30, TIM17, YEF3, RPS6A, FAF1, RPS0B, UTP21, YCS4, GRC3, MCD1, HAS1, MSH2, RAI1, RLP24, CNM67, RPL6B, PKR1, SRL1, NOP1, VPS24, MAK21, RPL6A, SAS10, BRN1, CLB2, NOP56, ECM33, SPC98, NOP58, EXG2, RPL8B, ASF1, RPS26B, MAK16, CIS3, RPS5, FAL1, RPL8A, RPS16A, TPK3, CRH1, RPS18B, HXK2, TCB2, IPI3, EAF7, NIP7, GIM3, EXG1, UTP9, RPL40B, GAS1, LOC1, BUD22, SNU13, FKS1, RPS27B, RFC5, RPS1B, RPS9B, RPS10A, PCL1, PXR1, UTR2, RPA49, GAR1, MKC7 |

| | | | | | | | |
|---|---|---|---|---|---|---|---|
| - | GO:0009987 | BP | cellular process | 1 | 0.16 | 3.92E-05 | NOG1, SCJ1, PMI40, RPL3, NOP9, UTP8, BUB1, GEA2, SDO1, CHS2, EFR3, ERG2, RPL37B, SDA1, LTE1, PGM1, ALK2, SEN34, UPC2, SOP4, RPS16B, LOS1, RAD53, RPL29, RPS2, IFA38, HPM1, IMP3, RIM2, SEC63, RPL35B, GPI11, FOB1, ETT1, PIS1, TKL1, FUR1, RPA43, RPL18B, RPS24B, RPS20, URA3, RRP12, ADE6, SCP160, LCP5, RPL20B, RPS28A, CLB4, RPP2A, VAC17, YHP1, NOP12, ENP1, RPL10, RPL11B, NOC3, UTP25, MRS2, DBP9, CYS3, ERG4, TEM1, ARG1, TYS1, RPP0, PSA1, URK1, RFC4, SPC97, RRP42, IRR1, SVF1, RPS9A, IPI1, BRX1, RPL27B, RPS1A, RPL2B, RPL21B, RPS25A, MNN9, CYK3, RRB1, SAM1, PRR1, RPS18A, SGD1, WSS1, RPL31A, RPL13A, RRP8, VTS1, OAR1, BIT61, ALG5, CHS1, ESC8, DYS1, RPL26A, RPL33B, NOP4, ACO2, WRS1, TEF4, RPL20A, MCH5, URB2, YDR089W, RPS13, PDS5, SOL3, VTA1, PAN5, NSI1, RPS6B, RPL12A, EMG1, CDC3, RPS17B, ALK1, PRM7, SUR7, DBP8, EBP2, SAH1, ERP2, SRM1, UTP22, KRS1, HSL1, NOP7, RPL24B, NOP16, ASC1, RPL1B, RPS31, RPL9A, NAT5, RPS7B, RRP14, MNT2, UTP10, PLB2, SPH1, RPL26B, BUD4, RPF2, SHB17, SPC2, RNA1, MIS1, HIS1, RPP1B, PBP2, RPL32, RPS17A, ERB1, KRI1, HIS7, KCH1, POP5, RPL23A, MTR3, PRP43, UTP4, ENV11, AXL2, PRS3, IMD2, URH1, RPS14A, RPS19B, RPA135, DPB2, CTF8, DIA1, CDC5, CDC45, CBF5, RRP45, ERG6, RPL34A, TRM11, PPX1, SEC59, RPS19A, VRG4, HTB2, PWP1, RPL19B, AAH1, GCD10, KRE6, RPL5, OKP1, CLB1, SSB1, RPS11B, RRP9, YLR194C, RPS11A, SEC66, RPL18A, RPS24A, RPS10B, RTT107, RPS7A, ERG27, DBP2, RPL42A, MCM2, RPL40A, TOF2, HOM3, FYV7, RPL42B, RPL17A, DOT1, RPL12B, DIP2, RIX1, ILM1, PAC2, PFK27, FLX1, RPL25, UTP30, TIM17, GIC1, YEF3, RPS6A, FAF1, RPS0B, UTP21, YCS4, GRC3, MCD1, IMD3, ATR1, HAS1, MCD4, RPS4A, MSH2, RAI1, PHO3, RRN11, TRM10, CNM67, BIO2, RPL6B, SRP102, RPL21A, MAK3, SRL1, NOP1, VPS24, MAK21, RPL6A, RPL23B, ERP1, RPC31, SAS10, MMT1, BRN1, RPL27A, RPL2A, CLB2, TOS4, NOP56, GDT1, ECM33, SHO1, EMP70, RPS22B, SPC98, NOP58, EXG2, SER2, RPL8B, RPL24A, HPT1, IMD4, RAX2, RPL17B, ASF1, RPL14A, RPS26B, MAK16, SEC72, CIS3, RPS5, FAL1, RPL8A, EPT1, GCN3, RPS16A, GPN3, RPL16B, TPK3, RNR1, CRH1, PPT1, AAT1, RPS18B, HXT2, RPA34, HXK2, HXT1, TCB2, IPI3, EAF7, NIP7, URA7, GIM3, EXG1, PUS1, UTP9, RPL40B, GAS1, HXT4, ADE17, LOC1, BUD22, SNU13, FKS1, IRC7, RPS27B, CLN1, YMC2, BUD16, RFC5, RPS1B, CLN2, AFI1, RPS9B, RPS10A, HXT3, PCL1, SFG1, PXR1, UTR2, YJR124C, RPS22A, SCW10, YBR238C, GIC2, ARI1, RPA49, GAR1, MKC7 |
| | | | | | | | |
| + | GO:0006121 | BP | mitochondrial electron transport, succinate to ubiquinone | 9 | 3.57 | 1.04E-02 | SDH2, SDH1, SDH4, SDH3 |
| + | GO:0006099 | BP | tricarboxylic acid cycle | 7 | 3.5 | 1.55E-17 | MLS1, IDP2, YJL045W, ICL1, SDH2, CIT2, CIT1, SDH1, MDH2, KGD2, SDH4, FUM1, KGD1, SDH3, SHH4, MDH1, IDH1, ACO1, CIT3, SHH3, MDH3, IDH2 |
| + | GO:0006122 | BP | mitochondrial electron transport, ubiquinol to cytochrome c | 9 | 3.44 | 1.79E-05 | QCR10, RIP1, QCR7, CYC1, QCR2, CYT1, QCR8, QCR9 |

| | | | | | | | |
|---|---|---|---|---|---|---|---|
| + | GO:0015985 | BP | energy coupled proton transport, down electrochemical gradient | 9 | 3.39 | 1.78E-08 | ATP7, ATP16, ATP18, ATP20, ATP1, ATP4, ATP3, TIM11, ATP17, ATP2, ATP14, ATP15 |
| + | GO:0015986 | BP | ATP synthesis coupled proton transport | 12 | 3.39 | 1.78E-08 | ATP7, ATP16, ATP18, ATP20, ATP1, ATP4, ATP3, TIM11, ATP17, ATP2, ATP14, ATP15 |
| + | GO:0006119 | BP | oxidative phosphorylation | 6 | 3.36 | 1.27E-14 | SDH2, COX8, NDI1, QCR10, SDH1, COX4, RIP1, SDH4, SDH3, COX7, QCR7, CYC1, QCR2, COX6, CYT1, QCR8, COX9, GSM1, COX5A, QCR9 |
| + | GO:0006754 | BP | ATP biosynthetic process | 11 | 3.35 | 5.24E-09 | PMA2, ATP7, ATP16, ATP18, ATP20, ATP1, ATP4, ATP3, TIM11, ATP17, ATP2, ATP14, ATP15 |
| + | GO:0042773 | BP | ATP synthesis coupled electron transport | 7 | 3.34 | 1.24E-13 | SDH2, COX8, NDI1, QCR10, SDH1, COX4, RIP1, SDH4, SDH3, COX7, QCR7, CYC1, QCR2, COX6, CYT1, QCR8, COX9, COX5A, QCR9 |
| + | GO:0042775 | BP | mitochondrial ATP synthesis coupled electron transport | 8 | 3.34 | 1.24E-13 | SDH2, COX8, NDI1, QCR10, SDH1, COX4, RIP1, SDH4, SDH3, COX7, QCR7, CYC1, QCR2, COX6, CYT1, QCR8, COX9, COX5A, QCR9 |
| + | GO:0006536 | BP | glutamate metabolic process | 9 | 3.31 | 1.65E-06 | IDP2, GDH3, CIT2, CIT1, GDH2, IDH1, GAD1, PUT1, UGA2, IDH2 |
| + | GO:0022904 | BP | respiratory electron transport chain | 6 | 3.24 | 7.59E-13 | SDH2, COX8, NDI1, QCR10, SDH1, COX4, RIP1, SDH4, SDH3, COX7, QCR7, CYC1, QCR2, COX6, CYT1, QCR8, COX9, COX5A, QCR9 |
| + | GO:0006097 | BP | glyoxylate cycle | 9 | 3.22 | 7.29E-03 | MLS1, IDP2, ICL1, CIT2, MDH3 |
| + | GO:0072350 | BP | tricarboxylic acid metabolic process | 7 | 3.22 | 7.29E-03 | IDP2, CIT2, CIT1, IDH1, IDH2 |
| + | GO:0009145 | BP | purine nucleoside triphosphate biosynthetic process | 9 | 3.14 | 6.57E-08 | PMA2, ATP7, ATP16, ATP18, ATP20, ATP1, ATP4, ATP3, TIM11, ATP17, ATP2, ATP14, ATP15 |
| + | GO:0009206 | BP | purine ribonucleoside triphosphate biosynthetic | 10 | 3.14 | 6.57E-08 | PMA2, ATP7, ATP16, ATP18, ATP20, ATP1, ATP4, ATP3, TIM11, ATP17, ATP2, ATP14, ATP15 |

| | | | | | | | |
|---|---|---|---|---|---|---|---|
| | | | process | | | | |
| + | GO:0006537 | BP | glutamate biosynthetic process | 10 | 3.12 | 6.83E-04 | IDP2, GDH3, CIT2, CIT1, IDH1, PUT1, IDH2 |
| + | GO:0006123 | BP | mitochondrial electron transport, cytochrome c to oxygen | 9 | 3.12 | 6.83E-04 | COX8, COX4, COX7, CYC1, COX6, COX9, COX5A |
| + | GO:0043462 | BP | regulation of ATPase activity | 10 | 3.09 | 4.91E-02 | HSP30, STF1, INH1, AHA1 |
| + | GO:0006083 | BP | acetate metabolic process | 8 | 3.09 | 4.91E-02 | ACS1, ACH1, ALD4, ALD6 |
| + | GO:0042542 | BP | response to hydrogen peroxide | 5 | 3.09 | 4.91E-02 | CTT1, CTA1, ZWF1, CCP1 |
| + | GO:0046487 | BP | glyoxylate metabolic process | 8 | 3.05 | 1.44E-02 | MLS1, IDP2, ICL1, CIT2, MDH3 |
| + | GO:0009201 | BP | ribonucleoside triphosphate biosynthetic process | 9 | 2.89 | 9.95E-07 | PMA2, ATP7, ATP16, ATP18, ATP20, ATP1, ATP4, ATP3, TIM11, ATP17, ATP2, ATP14, ATP15 |
| + | GO:0006734 | BP | NADH metabolic process | 11 | 2.89 | 6.76E-03 | NDE2, GUT2, NDI1, GPD1, NDE1, MDH3 |
| + | GO:0006116 | BP | NADH oxidation | 12 | 2.89 | 2.55E-02 | NDE2, GUT2, NDI1, GPD1, NDE1 |
| + | GO:0009060 | BP | aerobic respiration | 6 | 2.84 | 6.00E-23 | MLS1, IDP2, YJL045W, ICL1, SDH2, MBR1, DLD1, CIT2, QCR10, CIT1, SDH1, COX4, RIP1, MDH2, KGD2, SDH4, FUM1, KGD1, SDH3, SHH4, MDH1, IDH1, QCR7, ACO1, AAC1, QCR2, COX13, CIT3, QCR8, SHH3, COR1, COX20, PET9, PET10, MDH3, QCR9, IDH2, SHY1, MAM33, ISF1, PET100 |
| + | GO:0045333 | BP | cellular respiration | 5 | 2.84 | 1.75E-27 | MLS1, IDP2, YJL045W, ICL1, SDH2, MBR1, COX8, DLD1, CIT2, NDI1, QCR10, CIT1, SDH1, COX4, RIP1, MDH2, KGD2, SDH4, FUM1, KGD1, SDH3, SHH4, MDH1, COX7, IDH1, QCR7, ACO1, AAC1, CYC1, QCR2, COX13, COX6, CYT1, CIT3, QCR8, SHH3, COX9, COR1, COX5A, COX20, PET9, PET10, MDH3, QCR9, IDH2, SHY1, MAM33, ISF1, PET100 |
| + | GO:0051346 | BP | negative regulation of hydrolase activity | 6 | 2.76 | 3.77E-02 | HSP30, TFS1, PBI2, STF1, INH1 |

| | | | | | | | |
|---|---|---|---|---|---|---|---|
| + | GO:0009142 | BP | nucleoside triphosphate biosynthetic process | 8 | 2.74 | 5.03E-06 | PMA2, ATP7, ATP16, ATP18, ATP20, ATP1, ATP4, ATP3, TIM11, ATP17, ATP2, ATP14, ATP15 |
| + | GO:0043648 | BP | dicarboxylic acid metabolic process | 7 | 2.73 | 3.45E-08 | IDP2, GDH3, CIT2, CIT1, GDH2, MDH2, KGD2, FUM1, KGD1, MDH1, IDH1, GAD1, PUT1, UGA2, MDH3, LPD1, IDH2 |
| + | GO:0019321 | BP | pentose metabolic process | 6 | 2.67 | 1.77E-02 | GND2, GCY1, SOL4, XYL2, YJR096W, ZWF1 |
| + | GO:0022900 | BP | electron transport chain | 4 | 2.67 | 4.28E-13 | YJL045W, CYB2, SDH2, COX8, NDI1, QCR10, SDH1, GRX2, COX4, RIP1, SDH4, SDH3, SHH4, COX7, QCR7, CYC1, QCR2, COX6, CYT1, QCR8, SHH3, COX9, COR1, COX5A, TRX3, FRE7, QCR9 |
| + | GO:0006740 | BP | NADPH regeneration | 11 | 2.65 | 2.27E-03 | TKL2, NQM1, GND2, SOL4, ALD4, ALD6, SOL1, ZWF1 |
| + | GO:0015980 | BP | energy derivation by oxidation of organic compounds | 4 | 2.65 | 1.44E-30 | MLS1, IDP2, ACS1, YJL045W, NDE2, ICL1, SDH2, MBR1, COX8, DLD1, CIT2, NDI1, IGD1, QCR10, CIT1, SDH1, COX4, RIP1, MDH2, KGD2, SDH4, FUM1, KGD1, SDH3, SHH4, MDH1, COX7, IDH1, QCR7, ACO1, AAC1, CYC1, QCR2, COX13, COX6, CYT1, CIT3, QCR8, SHH3, COX9, COR1, PCL7, GLC3, SGA1, COX5A, COX20, GDB1, RGI1, NDE1, PET9, PET10, MDH3, GLG2, QCR9, IDH2, SHY1, MAM33, PGM2, ISF1, PET100, GIP2 |
| + | GO:0006081 | BP | cellular aldehyde metabolic process | 3 | 2.57 | 4.74E-04 | MLS1, IDP2, ICL1, CIT2, HFD1, ALD2, MDH3, GLO1, AAD10, GLO4 |
| + | GO:0006098 | BP | pentose-phosphate shunt | 12 | 2.57 | 2.60E-02 | TKL2, NQM1, GND2, SOL4, SOL1, ZWF1 |
| + | GO:0009065 | BP | glutamine family amino acid catabolic process | 9 | 2.57 | 2.60E-02 | GDH2, GAD1, PUT1, UGA2, CAR2, CAR1 |
| + | GO:0033617 | BP | mitochondrial respiratory chain complex IV assembly | 8 | 2.53 | 1.06E-02 | COX12, COX17, COX14, COX20, SHY1, PET100, COX16 |
| + | GO:0072593 | BP | reactive oxygen species metabolic process | 3 | 2.48 | 3.45E-02 | FBP1, CTT1, SOD2, CTA1, LPD1, CCP1 |
| + | GO:0009062 | BP | fatty acid catabolic process | 9 | 2.48 | 3.45E-02 | POT1, FOX2, PDH1, CIT3, ECI1, MDH3 |
| + | GO:0006739 | BP | NADP metabolic process | 10 | 2.44 | 6.52E-03 | TKL2, NQM1, GND2, SOL4, ALD4, ALD6, SOL1, ZWF1 |

| | | | | | | | |
|---|---|---|---|---|---|---|---|
| + | GO:0042026 | BP | protein refolding | 7 | 2.39 | 4.89E-02 | HSP78, HSP104, SSE2, HSP82, HSP10, CPR6 |
| + | GO:0008535 | BP | respiratory chain complex IV assembly | 7 | 2.38 | 2.16E-02 | COX12, COX17, COX14, COX20, SHY1, PET100, COX16 |
| + | GO:0006091 | BP | generation of precursor metabolites and energy | 3 | 2.33 | 1.12E-27 | MLS1, IDP2, ACS1, YJL045W, CYB2, NDE2, ICL1, SDH2, MBR1, COX8, DLD1, CIT2, NDI1, IGD1, QCR10, CIT1, SDH1, GRX2, COX4, RIP1, MDH2, KGD2, SDH4, FUM1, KGD1, SDH3, SHH4, MDH1, COX7, IDH1, QCR7, ACO1, AAC1, CYC1, QCR2, COX13, COX6, CYT1, CIT3, QCR8, SHH3, COX9, COR1, PCL7, GSM1, GLC3, SGA1, COX5A, GLK1, COX20, GDB1, RGI1, NDE1, PET9, PET10, MDH3, TRX3, GLG2, FRE7, QCR9, IDH2, SHY1, MAM33, PGM2, ISF1, PET100, GPM2, GIP2 |
| + | GO:0009084 | BP | glutamine family amino acid biosynthetic process | 9 | 2.21 | 8.68E-03 | IDP2, GDH3, CIT2, YHR033W, CIT1, IDH1, PUT1, CAR2, IDH2 |
| + | GO:0015992 | BP | proton transport | 8 | 2.2 | 4.42E-04 | PMA2, ATP7, ATP16, ATP18, ATP20, ATP1, ATP4, ATP3, TIM11, ATP17, ATP2, ATP14, ATP15 |
| + | GO:0072329 | BP | monocarboxylic acid catabolic process | 8 | 2.19 | 2.12E-02 | POT1, FOX2, PDH1, UGA2, CIT3, ECI1, MDH3, UGA1 |
| + | GO:0043650 | BP | dicarboxylic acid biosynthetic process | 8 | 2.18 | 4.74E-02 | IDP2, GDH3, CIT2, CIT1, IDH1, PUT1, IDH2 |
| + | GO:0006818 | BP | hydrogen transport | 5 | 2.17 | 5.67E-04 | PMA2, ATP7, ATP16, ATP18, ATP20, ATP1, ATP4, ATP3, TIM11, ATP17, ATP2, ATP14, ATP15 |
| + | GO:0046496 | BP | nicotinamide nucleotide metabolic process | 9 | 2.16 | 1.33E-04 | TKL2, NDE2, NQM1, GND2, GUT2, SOL4, NDI1, ALD4, YNL200C, ALD6, SOL1, GPD1, NDE1, MDH3, ZWF1 |
| + | GO:0006112 | BP | energy reserve metabolic process | 5 | 2.16 | 1.11E-02 | IGD1, PCL7, GLC3, SGA1, GDB1, RGI1, GLG2, PGM2, GIP2 |
| + | GO:0019362 | BP | pyridine nucleotide metabolic process | 8 | 2.13 | 1.71E-04 | TKL2, NDE2, NQM1, GND2, GUT2, SOL4, NDI1, ALD4, YNL200C, ALD6, SOL1, GPD1, NDE1, MDH3, ZWF1 |
| + | GO:0046034 | BP | ATP metabolic process | 10 | 2.1 | 4.97E-05 | HEF3, PMA2, ATP7, PDR15, ATP16, ATP18, ATP20, ATP1, ATP4, PDR10, ATP3, TIM11, ATP17, ATP2, ATP14, PXA1, ATP15 |
| + | GO:0005977 | BP | glycogen metabolic process | 7 | 2.09 | 3.23E-02 | IGD1, PCL7, GLC3, SGA1, GDB1, GLG2, PGM2, GIP2 |

| | | | | | | | |
|---|---|---|---|---|---|---|---|
| + | GO:1901606 | BP | alpha-amino acid catabolic process | 9 | 2.07 | 4.28E-03 | GDH2, KGD2, GAD1, PUT1, UGA2, ALT2, CAR2, PDC6, CHA1, LPD1, CAR1 |
| + | GO:0010906 | BP | regulation of glucose metabolic process | 7 | 2.06 | 1.88E-02 | SIP4, CAT8, IGD1, PIG2, PCL7, FYV10, RMD5, YLR345W, UBC8 |
| + | GO:0033108 | BP | mitochondrial respiratory chain complex assembly | 7 | 2.02 | 2.34E-02 | COX12, QCR7, COX17, COX14, COX20, MDM35, SHY1, PET100, COX16 |
| + | GO:0055114 | BP | oxidation-reduction process | 3 | 1.98 | 9.06E-38 | MLS1, IDP2, ACS1, CTT1, YJL045W, GPX1, CYB2, TKL2, NDE2, NQM1, ICL1, SDH2, BDH2, GND2, YKL107W, GDH3, POT1, MBR1, COX8, GUT2, FOX2, DLD1, CIT2, GCY1, SOL4, NDI1, IGD1, QCR10, CIT1, SDH1, GRX2, COX4, AIM17, ALD4, MCR1, RIP1, PRX1, GDH2, MDH2, KGD2, SDH4, FUM1, KGD1, ECM4, SDH3, SHH4, MDH1, COX7, IDH1, QCR7, ACO1, AAC1, ALD6, SRX1, HFD1, PUT1, CYC1, QCR2, UGA2, COX13, COX6, CYT1, CIT3, QCR8, SHH3, HYR1, AIM33, COX9, COR1, PCL7, SOD2, YNL134C, SOL1, ALD3, GLC3, SGA1, ALD2, XYL2, COX5A, COX20, YPR127W, GDB1, IRC15, OYE3, CTA1, GPD1, AST2, RGI1, YJR096W, NDE1, YML131W, PET9, ECI1, PET10, MDH3, TRX3, AAD10, GLG2, FMP46, ZWF1, GRE2, IRC24, LPD1, FRE7, QCR9, IDH2, BDH1, CCP1, SHY1, MAM33, PGM2, ISF1, YPR172W, PET100, GIP2 |
| + | GO:0042451 | BP | purine nucleoside biosynthetic process | 8 | 1.95 | 2.43E-03 | PMA2, ATP7, ATP16, ATP18, ATP20, ATP1, ATP4, ATP3, TIM11, ATP17, ATP2, ATP14, ATP15 |
| + | GO:0046129 | BP | purine ribonucleoside biosynthetic process | 9 | 1.95 | 2.43E-03 | PMA2, ATP7, ATP16, ATP18, ATP20, ATP1, ATP4, ATP3, TIM11, ATP17, ATP2, ATP14, ATP15 |
| + | GO:0072524 | BP | pyridine-containing compound metabolic process | 4 | 1.94 | 4.42E-04 | TKL2, NDE2, NQM1, GND2, GUT2, SOL4, NDI1, ALD4, YNL200C, ALD6, SOL1, YPR127W, GPD1, NDE1, MDH3, ZWF1 |
| + | GO:0009152 | BP | purine ribonucleotide biosynthetic process | 10 | 1.92 | 2.93E-03 | PMA2, ATP7, ATP16, ATP18, ATP20, ATP1, ATP4, ATP3, TIM11, ATP17, ATP2, ATP14, ATP15 |
| + | GO:0034220 | BP | ion transmembrane transport | 6 | 1.88 | 5.54E-06 | JEN1, PUT4, PHO89, ATP7, ATP16, ATP18, ATP20, ALP1, ATP1, ATP4, AGP2, ATP3, MIR1, TIM11, DIP5, ATP17, RTC2, ATP2, ATP14, FRE7, AGP1, AVT3, ATG22, ATP15 |
| + | GO:0046365 | BP | monosaccharide | 6 | 1.84 | 2.80E-03 | TKL2, NDE2, NQM1, GND2, GCY1, SOL4, SOL1, XYL2, GLK1, YJR096W, NDE1, ZWF1, PGM2, GPM2 |

| | | | | | | | |
|---|---|---|---|---|---|---|---|
| | | | catabolic process | | | | |
| + | GO:0006164 | BP | purine nucleotide biosynthetic process | 9 | 1.84 | 5.26E-03 | PMA2, ATP7, ATP16, ATP18, ATP20, ATP1, ATP4, ATP3, TIM11, ATP17, ATP2, ATP14, ATP15 |
| + | GO:0032787 | BP | monocarboxylic acid metabolic process | 7 | 1.82 | 1.97E-06 | MLS1, IDP2, YAT1, ACS1, ACH1, CAT2, CYB2, YAT2, ICL1, CRC1, GND2, POT1, FOX2, CIT2, PDH1, ALD4, ALD6, UGA2, CIT3, AGP2, ECI1, MDH3, LAP2, GLO1, GLO4, LPD1, UGA1 |
| + | GO:0005996 | BP | monosaccharide metabolic process | 5 | 1.82 | 3.93E-05 | PCK1, FBP1, PYC1, TKL2, NDE2, NQM1, GND2, GCY1, SOL4, MDH2, AMS1, SOL1, XYL2, GLK1, YJR096W, NDE1, YLR345W, FBP26, ZWF1, GAL3, PGM2, GPM2 |
| + | GO:0006006 | BP | glucose metabolic process | 7 | 1.81 | 1.26E-03 | PCK1, FBP1, PYC1, TKL2, NDE2, NQM1, GND2, SOL4, MDH2, SOL1, GLK1, NDE1, FBP26, ZWF1, PGM2, GPM2 |
| + | GO:0006733 | BP | oxidoreduction coenzyme metabolic process | 5 | 1.8 | 2.27E-03 | TKL2, NDE2, NQM1, GND2, GUT2, SOL4, NDI1, ALD4, YNL200C, ALD6, SOL1, GPD1, NDE1, MDH3, ZWF1 |
| + | GO:0015672 | BP | monovalent inorganic cation transport | 7 | 1.78 | 2.62E-03 | ATO2, PMA2, ATP7, ADY2, ATP16, ATP18, ATP20, ATP1, ATP4, ATP3, TIM11, ATP17, ATP2, ATP14, ATP15 |
| + | GO:0042455 | BP | ribonucleoside biosynthetic process | 8 | 1.75 | 5.70E-03 | PMA2, ATP7, ATP16, ATP18, ATP20, ATP1, ATP4, ATP3, URA10, TIM11, ATP17, ATP2, ATP14, ATP15 |
| + | GO:0016054 | BP | organic acid catabolic process | 5 | 1.72 | 9.11E-04 | POT1, FOX2, PDH1, GDH2, KGD2, GAD1, PUT1, UGA2, CIT3, ALT2, CAR2, PDC6, CHA1, ECI1, MDH3, LPD1, CAR1, UGA1 |
| + | GO:0046395 | BP | carboxylic acid catabolic process | 7 | 1.72 | 9.11E-04 | POT1, FOX2, PDH1, GDH2, KGD2, GAD1, PUT1, UGA2, CIT3, ALT2, CAR2, PDC6, CHA1, ECI1, MDH3, LPD1, CAR1, UGA1 |
| + | GO:0009064 | BP | glutamine family amino acid metabolic process | 8 | 1.72 | 6.54E-03 | IDP2, GDH3, CIT2, YHR033W, CIT1, GDH2, IDH1, GAD1, PUT1, UGA2, CAR2, ARG82, CAR1, IDH2 |
| + | GO:0009163 | BP | nucleoside biosynthetic process | 7 | 1.72 | 6.54E-03 | PMA2, ATP7, ATP16, ATP18, ATP20, ATP1, ATP4, ATP3, URA10, TIM11, ATP17, ATP2, ATP14, ATP15 |
| + | GO:1901659 | BP | glycosyl compound biosynthetic process | 4 | 1.72 | 6.54E-03 | PMA2, ATP7, ATP16, ATP18, ATP20, ATP1, ATP4, ATP3, URA10, TIM11, ATP17, ATP2, ATP14, ATP15 |

| | | | | | | | |
|---|---|---|---|---|---|---|---|
| + | GO:0019318 | BP | hexose metabolic process | 6 | 1.72 | 5.97E-04 | PCK1, FBP1, PYC1, TKL2, NDE2, NQM1, GND2, SOL4, MDH2, AMS1, SOL1, GLK1, NDE1, YLR345W, FBP26, ZWF1, GAL3, PGM2, GPM2 |
| + | GO:0009260 | BP | ribonucleotide biosynthetic process | 9 | 1.7 | 7.59E-03 | PMA2, ATP7, ATP16, ATP18, ATP20, ATP1, ATP4, ATP3, URA10, TIM11, ATP17, ATP2, ATP14, ATP15 |
| + | GO:0044282 | BP | small molecule catabolic process | 4 | 1.7 | 1.55E-04 | POT1, GUT2, FOX2, PDH1, GDH2, GUT1, KGD2, GAD1, ALD6, PUT1, UGA2, CIT3, ALT2, YPR127W, CAR2, PDC6, CHA1, ECI1, MDH3, LPD1, CAR1, UGA1 |
| + | GO:0044712 | BP | single-organism catabolic process | 3 | 1.7 | 1.55E-04 | POT1, GUT2, FOX2, PDH1, GDH2, GUT1, KGD2, GAD1, ALD6, PUT1, UGA2, CIT3, ALT2, YPR127W, CAR2, PDC6, CHA1, ECI1, MDH3, LPD1, CAR1, UGA1 |
| + | GO:0019320 | BP | hexose catabolic process | 7 | 1.68 | 3.87E-02 | TKL2, NDE2, NQM1, GND2, SOL4, SOL1, GLK1, NDE1, ZWF1, PGM2, GPM2 |
| + | GO:0034599 | BP | cellular response to oxidative stress | 5 | 1.66 | 1.63E-03 | HSP12, NCE103, CTT1, GPX1, HSP104, GCY1, GRX2, MCR1, PRX1, GAD1, SRX1, UGA2, HYR1, SOD2, CTA1, YJR096W, TRX3, CCP1 |
| + | GO:0006979 | BP | response to oxidative stress | 3 | 1.63 | 1.25E-03 | HSP12, NCE103, CTT1, GPX1, HSP104, GCY1, GRX2, MCR1, PRX1, GAD1, SRX1, UGA2, HYR1, SOD2, CTA1, YJR096W, TRX3, ZWF1, CCP1 |
| + | GO:0009063 | BP | cellular amino acid catabolic process | 8 | 1.62 | 3.34E-02 | GDH2, KGD2, GAD1, PUT1, UGA2, ALT2, CAR2, PDC6, CHA1, LPD1, CAR1, UGA1 |
| + | GO:0009205 | BP | purine ribonucleoside triphosphate metabolic process | 9 | 1.59 | 7.79E-04 | HEF3, PMA2, ATP7, PDR15, ATP16, ATP18, ATP20, ATP1, ATP4, PDR10, ATP3, TIM11, GSP2, ATP17, ATP2, DNM1, ATP14, PXA1, MEF2, FZO1, ATP15 |
| + | GO:0046390 | BP | ribose phosphate biosynthetic process | 6 | 1.57 | 1.93E-02 | PMA2, ATP7, ATP16, ATP18, ATP20, ATP1, ATP4, ATP3, URA10, TIM11, ATP17, ATP2, ATP14, ATP15 |
| + | GO:0006631 | BP | fatty acid metabolic process | 8 | 1.57 | 4.47E-02 | YAT1, CAT2, YAT2, CRC1, POT1, FOX2, PDH1, CIT3, AGP2, ECI1, MDH3, LAP2 |
| + | GO:0009144 | BP | purine nucleoside triphosphate metabolic process | 8 | 1.56 | 1.02E-03 | HEF3, PMA2, ATP7, PDR15, ATP16, ATP18, ATP20, ATP1, ATP4, PDR10, ATP3, TIM11, GSP2, ATP17, ATP2, DNM1, ATP14, PXA1, MEF2, FZO1, ATP15 |
| + | GO:0016051 | BP | carbohydrate biosynthetic process | 5 | 1.55 | 2.19E-02 | PCK1, FBP1, PYC1, IGD1, MDH2, YIG1, GLC3, XYL2, GDB1, GLG2, TSL1, KNH1, PGM2, YMR085W |

| | | | | | | | |
|---|---|---|---|---|---|---|---|
| + | GO:0009199 | BP | ribonucleoside triphosphate metabolic process | 8 | 1.53 | 1.26E-03 | HEF3, PMA2, ATP7, PDR15, ATP16, ATP18, ATP20, ATP1, ATP4, PDR10, ATP3, TIM11, GSP2, ATP17, ATP2, DNM1, ATP14, PXA1, MEF2, FZO1, ATP15 |
| + | GO:0072522 | BP | purine-containing compound biosynthetic process | 5 | 1.53 | 3.67E-02 | PMA2, ATP7, ATP16, ATP18, ATP20, ATP1, ATP4, ATP3, TIM11, ATP17, ATP2, ATP14, ATP15 |
| + | GO:0044724 | BP | single-organism carbohydrate catabolic process | 5 | 1.52 | 2.27E-03 | TKL2, NDE2, NQM1, GND2, GUT2, GCY1, SOL4, GUT1, ATH1, AMS1, SOL1, SGA1, XYL2, GLK1, GDB1, YJR096W, NDE1, ZWF1, PGM2, GPM2 |
| + | GO:0044262 | BP | cellular carbohydrate metabolic process | 4 | 1.5 | 5.63E-05 | MLS1, IDP2, ICL1, GND2, GUT2, HSP104, DLD1, CIT2, IGD1, CIT1, MDH2, GUT1, YIG1, MDH1, ATH1, AMS1, CIT3, PCL7, GLC3, SGA1, GDB1, MDH3, GLG2, TSL1, KNH1, GLO4, GAL3, PGM2, GIP2 |
| + | GO:0009141 | BP | nucleoside triphosphate metabolic process | 7 | 1.43 | 3.24E-03 | HEF3, PMA2, ATP7, PDR15, ATP16, ATP18, ATP20, ATP1, ATP4, PDR10, ATP3, TIM11, GSP2, ATP17, ATP2, DNM1, ATP14, PXA1, MEF2, FZO1, ATP15 |
| + | GO:0016052 | BP | carbohydrate catabolic process | 4 | 1.42 | 5.11E-03 | TKL2, NDE2, NQM1, GND2, GUT2, GCY1, SOL4, GUT1, ATH1, AMS1, SOL1, SGA1, XYL2, GLK1, GDB1, YJR096W, NDE1, ZWF1, PGM2, GPM2 |
| + | GO:0006820 | BP | anion transport | 6 | 1.37 | 4.08E-03 | SFC1, JEN1, PUT4, PHO89, ATO2, FAT3, BTN2, ADY2, ALP1, AGP2, MIR1, PET9, POR1, DIP5, RTC2, PXA1, PIC2, LEU5, AGP1, AVT3, PHO84, ATG22 |
| + | GO:1901615 | BP | organic hydroxy compound metabolic process | 3 | 1.27 | 2.60E-02 | YAT1, CAT2, CYB2, YAT2, NDE2, GUT2, ALD4, MCR1, GUT1, YIG1, ALD6, PDC6, NDE1, GLO1, GRE2, GLO4, ARG82, BDH1, NSG2 |
| + | GO:0009117 | BP | nucleotide metabolic process | 7 | 1.27 | 3.68E-05 | TKL2, NDE2, NQM1, HEF3, GND2, GUT2, SOL4, NDI1, PHM8, ALD4, YNL200C, ALD6, PMA2, ATP7, PDR15, ATP16, ATP18, ATP20, SOL1, ATP1, ATP4, PDR10, ATP3, GPD1, URA10, NDE1, TIM11, APA2, GSP2, MDH3, ATP17, ATP2, DNM1, ATP14, ZWF1, PXA1, MEF2, FZO1, PGM2, ATP15 |
| + | GO:0006753 | BP | nucleoside phosphate metabolic process | 6 | 1.24 | 5.63E-05 | TKL2, NDE2, NQM1, HEF3, GND2, GUT2, SOL4, NDI1, PHM8, ALD4, YNL200C, ALD6, PMA2, ATP7, PDR15, ATP16, ATP18, ATP20, SOL1, ATP1, ATP4, PDR10, ATP3, GPD1, URA10, NDE1, TIM11, APA2, GSP2, MDH3, ATP17, ATP2, DNM1, ATP14, ZWF1, PXA1, MEF2, FZO1, PGM2, ATP15 |
| + | GO:0009150 | BP | purine ribonucleotide metabolic process | 9 | 1.19 | 2.68E-02 | HEF3, PMA2, ATP7, PDR15, ATP16, ATP18, ATP20, ATP1, ATP4, PDR10, ATP3, TIM11, GSP2, ATP17, ATP2, DNM1, ATP14, PXA1, MEF2, FZO1, ATP15 |
| + | GO:1901565 | BP | organonitrogen compound catabolic process | 4 | 1.17 | 5.89E-03 | HEF3, GDH2, KGD2, GAD1, PMA2, PUT1, UGA2, PDR15, ALT2, ALD3, ALD2, YPR127W, YPC1, CAR2, PDC6, PDR10, CHA1, APA2, GSP2, GUD1, DNM1, LPD1, PXA1, MEF2, CAR1, UGA1, FZO1 |

| | | | | | | | |
|---|---|---|---|---|---|---|---|
| + | GO:0044710 | BP | single-organism metabolic process | 2 | 1.16 | 1.41E-26 | MLS1, IDP2, YAT1, ACS1, ACH1, SPS100, AGX1, CTT1, CAT2, YJL045W, GPX1, CYB2, YAT2, TKL2, NDE2, NQM1, ICL1, CRC1, SDH2, HEF3, BDH2, GND2, YKL107W, GDH3, POT1, MBR1, COX8, GUT2, FOX2, DLD1, CIT2, GCY1, SOL4, NDI1, IGD1, YHR033W, QCR10, PDH1, CIT1, SDH1, PHM8, GRX2, COX4, AIM17, ALD4, MCR1, RIP1, PRX1, GDH2, MDH2, GUT1, KGD2, SHC1, SDH4, YNL200C, FUM1, YIG1, KGD1, ECM4, SDH3, SHH4, MDH1, COX7, IDH1, QCR7, ACO1, AAC1, GAD1, ALD6, PMA2, SRX1, HFD1, PUT1, CYC1, ATP7, QCR2, UGA2, COX13, COX6, PDR15, CYT1, ATP16, CIT3, QCR8, SHH3, HYR1, AIM33, COX9, COR1, PCL7, ATP18, CLD1, SOD2, ATP20, ALT2, YNL134C, SOL1, ALD3, GLC3, SGA1, ALD2, XYL2, COX5A, ATP1, COX20, YPR127W, GDB1, YPC1, IRC15, OYE3, ATP4, CAR2, PDC6, PDR10, AGP2, CTA1, ATP3, GPD1, AST2, RGI1, YGP1, URA10, YJR096W, NDE1, YML131W, PET9, TIM11, CHA1, APA2, GSP2, ECI1, PET10, MDH3, ATP17, GUD1, ATP2, TRX3, LAP2, DNM1, GPT2, GLO1, THI2, AAD10, ATP14, GLG2, FMP46, ZWF1, GRE2, GTT1, IRC24, GLO4, LPD1, PXA1, ARG82, MEF2, FRE7, QCR9, CAR1, IDH2, UGA1, BDH1, CCP1, SHY1, FZO1, MAM33, PGM2, UPS1, ISF1, YPR172W, PHO84, HPA3, PET100, NSG2, LEU4, LYS20, GIP2, ATP15 |
| + | GO:0006163 | BP | purine nucleotide metabolic process | 8 | 1.15 | 3.68E-02 | HEF3, PMA2, ATP7, PDR15, ATP16, ATP18, ATP20, ATP1, ATP4, PDR10, ATP3, TIM11, GSP2, ATP17, ATP2, DNM1, ATP14, PXA1, MEF2, FZO1, ATP15 |
| + | GO:0006811 | BP | ion transport | 5 | 1.15 | 2.81E-04 | HSP30, SFC1, JEN1, PUT4, PHO89, ATO2, FAT3, PMP3, YRO2, BTN2, PMA2, ATP7, ADY2, COX17, ATP16, ATP18, ATP20, ALP1, ATP1, ATP4, AGP2, ATP3, MIR1, PET9, POR1, TIM11, DIP5, ATP17, RTC2, ATP2, ATP14, PXA1, FRE7, PIC2, LEU5, AGP1, AVT3, PHO84, ATG22, ATP15 |
| + | GO:0009259 | BP | ribonucleotide metabolic process | 8 | 1.13 | 3.43E-02 | HEF3, PMA2, ATP7, PDR15, ATP16, ATP18, ATP20, ATP1, ATP4, PDR10, ATP3, URA10, TIM11, GSP2, ATP17, ATP2, DNM1, ATP14, PXA1, MEF2, FZO1, ATP15 |
| + | GO:0005975 | BP | carbohydrate metabolic process | 3 | 1.12 | 3.91E-05 | MLS1, PCK1, FBP1, IDP2, PYC1, TKL2, NDE2, NQM1, ICL1, GND2, CAT8, GUT2, HSP104, DLD1, CIT2, GCY1, SOL4, IGD1, CIT1, MDH2, GUT1, YIG1, MDH1, ATH1, AMS1, CIT3, PCL7, SOL1, GLC3, SGA1, XYL2, GLK1, GDB1, GPD1, YJR096W, NDE1, YLR345W, MDH3, FBP26, GLG2, TSL1, ZWF1, KNH1, GLO4, GAL3, PGM2, YMR085W, GPM2, GIP2 |
| + | GO:0019752 | BP | carboxylic acid metabolic process | 6 | 1.11 | 6.76E-06 | MLS1, IDP2, YAT1, ACS1, ACH1, SPS100, AGX1, CAT2, CYB2, YAT2, ICL1, CRC1, GND2, GDH3, POT1, FOX2, CIT2, YHR033W, PDH1, CIT1, ALD4, GDH2, MDH2, KGD2, FUM1, KGD1, ECM4, MDH1, IDH1, GAD1, ALD6, PUT1, UGA2, CIT3, ALT2, ALD3, ALD2, CAR2, PDC6, AGP2, YGP1, CHA1, ECI1, MDH3, LAP2, GLO1, GTT1, GLO4, LPD1, ARG82, CAR1, IDH2, UGA1, HPA3, LEU4, LYS20 |
| + | GO:0055086 | BP | nucleobase-containing small molecule metabolic process | 5 | 1.11 | 3.92E-04 | TKL2, NDE2, NQM1, HEF3, GND2, GUT2, SOL4, NDI1, PHM8, ALD4, YNL200C, ALD6, PMA2, ATP7, PDR15, ATP16, ATP18, ATP20, SOL1, ATP1, ATP4, PDR10, ATP3, GPD1, URA10, NDE1, TIM11, APA2, GSP2, MDH3, ATP17, GUD1, ATP2, DNM1, ATP14, ZWF1, PXA1, MEF2, FZO1, PGM2, ATP15 |
| + | GO:0043436 | BP | oxoacid metabolic process | 5 | 1.08 | 9.10E-06 | MLS1, IDP2, YAT1, ACS1, ACH1, SPS100, AGX1, CAT2, CYB2, YAT2, ICL1, CRC1, GND2, GDH3, POT1, FOX2, CIT2, YHR033W, PDH1, CIT1, ALD4, GDH2, MDH2, KGD2, FUM1, KGD1, ECM4, MDH1, IDH1, GAD1, ALD6, PUT1, UGA2, CIT3, ALT2, ALD3, ALD2, CAR2, PDC6, AGP2, YGP1, CHA1, ECI1, MDH3, LAP2, GLO1, GTT1, GLO4, LPD1, ARG82, CAR1, IDH2, UGA1, PHO84, HPA3, LEU4, LYS20 |

| | | | | | | | |
|---|---|---|---|---|---|---|---|
| + | GO:0006082 | BP | organic acid metabolic process | 4 | 1.08 | 9.55E-06 | MLS1, IDP2, YAT1, ACS1, ACH1, SPS100, AGX1, CAT2, CYB2, YAT2, ICL1, CRC1, GND2, GDH3, POT1, FOX2, CIT2, YHR033W, PDH1, CIT1, ALD4, GDH2, MDH2, KGD2, FUM1, KGD1, ECM4, MDH1, IDH1, GAD1, ALD6, PUT1, UGA2, CIT3, ALT2, ALD3, ALD2, CAR2, PDC6, AGP2, YGP1, CHA1, ECI1, MDH3, LAP2, GLO1, GTT1, GLO4, LPD1, ARG82, CAR1, IDH2, UGA1, PHO84, HPA3, LEU4, LYS20 |
| + | GO:0044723 | BP | single-organism carbohydrate metabolic process | 4 | 1.01 | 5.80E-03 | PCK1, FBP1, PYC1, TKL2, NDE2, NQM1, GND2, GUT2, HSP104, GCY1, SOL4, IGD1, MDH2, GUT1, YIG1, ATH1, AMS1, SOL1, GLC3, SGA1, XYL2, GLK1, GDB1, YJR096W, NDE1, YLR345W, FBP26, GLG2, TSL1, ZWF1, KNH1, GAL3, PGM2, YMR085W, GPM2 |
| + | GO:0055085 | BP | transmembrane transport | 5 | 1 | 3.68E-04 | SFC1, HXT5, JEN1, PUT4, HXT6, STL1, PHO89, HSP78, SSA3, ODC1, YDL199C, MDH2, SSA4, SDH3, AAC1, YJL163C, YBR241C, ATP7, ADY2, ATP16, ATP18, ATP20, ALP1, ATP1, ATP4, PDR10, AGP2, ATP3, MIR1, PET9, POR1, TIM11, DIP5, ATP17, RTC2, ATP2, HXT15, ATP14, PEX18, PXA1, FRE7, PIC2, LEU5, AGP1, AVT3, PHO84, YFR045W, ATG22, ATP15 |
| + | GO:0044281 | BP | small molecule metabolic process | 3 | 0.99 | 5.72E-10 | MLS1, IDP2, YAT1, ACS1, ACH1, SPS100, AGX1, CAT2, CYB2, YAT2, TKL2, NDE2, NQM1, ICL1, CRC1, HEF3, GND2, GDH3, POT1, GUT2, FOX2, CIT2, SOL4, NDI1, YHR033W, PDH1, CIT1, PHM8, ALD4, MCR1, GDH2, MDH2, GUT1, KGD2, YNL200C, FUM1, YIG1, KGD1, ECM4, MDH1, IDH1, GAD1, ALD6, PMA2, PUT1, ATP7, UGA2, PDR15, ATP16, CIT3, ATP18, ATP20, ALT2, SOL1, ALD3, ALD2, ATP1, YPR127W, ATP4, CAR2, PDC6, PDR10, AGP2, ATP3, GPD1, YGP1, URA10, NDE1, TIM11, CHA1, APA2, GSP2, ECI1, MDH3, ATP17, GUD1, ATP2, TRX3, LAP2, DNM1, GLO1, THI2, ATP14, ZWF1, GRE2, GTT1, GLO4, LPD1, PXA1, ARG82, MEF2, CAR1, IDH2, UGA1, BDH1, FZO1, PGM2, PHO84, HPA3, NSG2, LEU4, LYS20, ATP15 |
| + | GO:0016310 | BP | phosphorylation | 5 | 0.98 | 8.04E-03 | SDH2, COX8, NDI1, YHR033W, QCR10, SDH1, COX4, RIP1, GUT1, SDH4, SDH3, COX7, PRR2, QCR7, FMP48, CYC1, QCR2, COX6, CYT1, SIP2, QCR8, KIN82, COX9, GSM1, VHS1, COX5A, GLK1, NNK1, YLR345W, ARG82, KNS1, GAL3, QCR9, PTK1, TPK2 |
| + | GO:0006793 | BP | phosphorus metabolic process | 3 | 0.9 | 7.72E-07 | ACS1, ACH1, TKL2, NDE2, NQM1, SDH2, HEF3, GND2, COX8, GUT2, SOL4, NDI1, YHR033W, QCR10, CIT1, SDH1, PHM8, COX4, ALD4, RIP1, GUT1, KGD2, SDH4, SDP1, YNL200C, SDH3, COX7, PRR2, QCR7, ALD6, PMA2, FMP48, CYC1, ATP7, QCR2, COX6, PDR15, CYT1, SIP2, ATP16, QCR8, KIN82, COX9, ATP18, CLD1, GSM1, ATP20, VHS1, SOL1, XYL2, COX5A, ATP1, GLK1, ATP4, PDR10, ATP3, GPD1, DIA3, URA10, NDE1, NNK1, YLR345W, TIM11, APA2, GSP2, MDH3, ATP17, ATP2, DNM1, GPT2, ATP14, FBP26, ZWF1, PXA1, ARG82, KNS1, MEF2, GAL3, QCR9, FZO1, PGM2, PTK1, UPS1, YPR172W, PHO84, TPK2, GIP2, ATP15 |
| + | GO:0006796 | BP | phosphate-containing compound metabolic process | 4 | 0.86 | 6.76E-06 | TKL2, NDE2, NQM1, SDH2, HEF3, GND2, COX8, GUT2, SOL4, NDI1, YHR033W, QCR10, SDH1, PHM8, COX4, ALD4, RIP1, GUT1, SDH4, SDP1, YNL200C, SDH3, COX7, PRR2, QCR7, ALD6, PMA2, FMP48, CYC1, ATP7, QCR2, COX6, PDR15, CYT1, SIP2, ATP16, QCR8, KIN82, COX9, ATP18, CLD1, GSM1, ATP20, VHS1, SOL1, XYL2, COX5A, ATP1, GLK1, ATP4, PDR10, ATP3, GPD1, DIA3, URA10, NDE1, NNK1, YLR345W, TIM11, APA2, GSP2, MDH3, ATP17, ATP2, DNM1, GPT2, ATP14, FBP26, ZWF1, PXA1, ARG82, KNS1, MEF2, GAL3, QCR9, FZO1, PGM2, PTK1, UPS1, YPR172W, TPK2, GIP2, ATP15 |
| + | GO:0019637 | BP | organophosphate metabolic process | 4 | 0.85 | 3.29E-03 | TKL2, NDE2, NQM1, HEF3, GND2, GUT2, SOL4, NDI1, PHM8, ALD4, GUT1, YNL200C, ALD6, PMA2, ATP7, PDR15, ATP16, ATP18, CLD1, ATP20, SOL1, XYL2, ATP1, GLK1, ATP4, PDR10, ATP3, GPD1, URA10, NDE1, YLR345W, TIM11, APA2, GSP2, MDH3, ATP17, ATP2, DNM1, GPT2, ATP14, FBP26, ZWF1, PXA1, ARG82, MEF2, FZO1, PGM2, UPS1, YPR172W, ATP15 |

| | | | | | | | |
|---|---|---|---|---|---|---|---|
| + | GO:1901564 | BP | organonitrogen compound metabolic process | 3 | 0.82 | 8.87E-05 | IDP2, SPS100, AGX1, TKL2, NDE2, NQM1, HEF3, GND2, GDH3, GUT2, CIT2, SOL4, NDI1, YHR033W, CIT1, ALD4, GDH2, KGD2, SHC1, YNL200C, ECM4, IDH1, AAC1, GAD1, ALD6, PMA2, PUT1, ATP7, UGA2, PDR15, ATP16, ATP18, ATP20, ALT2, SOL1, ALD3, ALD2, ATP1, YPR127W, YPC1, ATP4, CAR2, PDC6, PDR10, ATP3, GPD1, YGP1, URA10, NDE1, TIM11, CHA1, APA2, GSP2, MDH3, ATP17, GUD1, ATP2, DNM1, GLO1, THI2, ATP14, ZWF1, GTT1, GLO4, LPD1, PXA1, ARG82, MEF2, CAR1, IDH2, UGA1, FZO1, HPA3, LEU4, LYS20, ATP15 |
| + | GO:0009056 | BP | catabolic process | 2 | 0.69 | 4.73E-04 | CTT1, TKL2, NDE2, NQM1, HEF3, GND2, POT1, ATG8, GUT2, FOX2, SUE1, GCY1, SOL4, PDH1, CIT1, PHM8, DCS2, GDH2, GUT1, KGD2, ATH1, GAD1, SAF1, YOR019W, ALD6, PMA2, PUT1, UGA2, AMS1, PDR15, ATG29, ATG34, CIT3, RNY1, ALT2, ATG36, ATG9, SOL1, ALD3, SGA1, ALD2, XYL2, GLK1, YPR127W, GDB1, YPC1, CAR2, PDC6, PDR10, CTA1, FYV10, GPD1, YJR096W, NDE1, RMD5, CHA1, APA2, GSP2, ECI1, PRB1, UBC8, MDH3, GUD1, DCS1, LAP2, DNM1, GLO1, UBX6, UBX5, ZWF1, GLO4, LPD1, PXA1, MEF2, HUL4, ATG33, CAR1, UGA1, ATG19, CCP1, FZO1, GGA1, PGM2, EDC2, ATG22, GPM2 |
| + | GO:1901575 | BP | organic substance catabolic process | 3 | 0.68 | 2.24E-03 | TKL2, NDE2, NQM1, HEF3, GND2, POT1, GUT2, FOX2, SUE1, GCY1, SOL4, PDH1, CIT1, PHM8, DCS2, GDH2, GUT1, KGD2, ATH1, GAD1, SAF1, ALD6, PMA2, PUT1, UGA2, AMS1, PDR15, CIT3, RNY1, ALT2, SOL1, ALD3, SGA1, ALD2, XYL2, GLK1, YPR127W, GDB1, YPC1, CAR2, PDC6, PDR10, FYV10, GPD1, YJR096W, NDE1, RMD5, CHA1, APA2, GSP2, ECI1, PRB1, UBC8, MDH3, GUD1, DCS1, LAP2, DNM1, GLO1, UBX6, UBX5, ZWF1, GLO4, LPD1, PXA1, MEF2, HUL4, CAR1, UGA1, ATG19, FZO1, GGA1, PGM2, EDC2, GPM2 |
| + | GO:0000275 | CC | mitochondrial proton-transporting ATP synthase complex, catalytic core F(1) | 13 | 3.89 | 3.07E-04 | ATP16, ATP1, ATP3, ATP2, ATP15 |
| + | GO:0045261 | CC | proton-transporting ATP synthase complex, catalytic core F(1) | 6 | 3.89 | 3.07E-04 | ATP16, ATP1, ATP3, ATP2, ATP15 |
| + | GO:0045273 | CC | respiratory chain complex II | 5 | 3.63 | 1.26E-03 | SDH2, SDH1, SDH4, SDH3, SHH3 |
| + | GO:0045281 | CC | succinate dehydrogenase complex | 6 | 3.63 | 1.26E-03 | SDH2, SDH1, SDH4, SDH3, SHH3 |
| + | GO:0005750 | CC | mitochondrial respiratory chain complex III | 13 | 3.57 | 6.13E-06 | QCR10, RIP1, QCR7, QCR2, CYT1, QCR8, COR1, QCR9 |

| | | | | | | | |
|---|---|---|---|---|---|---|---|
| + | GO:0045275 | CC | respiratory chain complex III | 5 | 3.57 | 6.13E-06 | QCR10, RIP1, QCR7, QCR2, CYT1, QCR8, COR1, QCR9 |
| + | GO:0005749 | CC | mitochondrial respiratory chain complex II | 13 | 3.57 | 1.04E-02 | SDH2, SDH1, SDH4, SDH3 |
| + | GO:0045257 | CC | succinate dehydrogenase complex (ubiquinone) | 7 | 3.57 | 1.04E-02 | SDH2, SDH1, SDH4, SDH3 |
| + | GO:0045283 | CC | fumarate reductase complex | 6 | 3.57 | 1.04E-02 | SDH2, SDH1, SDH4, SDH3 |
| + | GO:0005753 | CC | mitochondrial proton-transporting ATP synthase complex | 12 | 3.43 | 1.82E-09 | STF1, ATP7, ATP16, ATP18, ATP20, ATP1, ATP4, ATP3, TIM11, ATP17, ATP2, ATP14, ATP15 |
| + | GO:0045259 | CC | proton-transporting ATP synthase complex | 5 | 3.43 | 1.82E-09 | STF1, ATP7, ATP16, ATP18, ATP20, ATP1, ATP4, ATP3, TIM11, ATP17, ATP2, ATP14, ATP15 |
| + | GO:0005746 | CC | mitochondrial respiratory chain | 12 | 3.36 | 1.27E-14 | SDH2, COX12, COX8, QCR10, SDH1, COX4, RIP1, SDH4, SDH3, COX7, QCR7, QCR2, COX13, COX6, CYT1, QCR8, COX9, COR1, COX5A, QCR9 |
| + | GO:0070469 | CC | respiratory chain | 3 | 3.33 | 1.30E-16 | CYB2, SDH2, COX12, COX8, QCR10, SDH1, COX4, RIP1, SDH4, SDH3, COX7, QCR7, CYC1, QCR2, COX13, COX6, CYT1, QCR8, SHH3, COX9, COR1, COX5A, QCR9 |
| + | GO:0000276 | CC | mitochondrial proton-transporting ATP synthase complex, coupling factor F(o) | 13 | 3.12 | 6.83E-04 | ATP7, ATP18, ATP20, ATP4, TIM11, ATP17, ATP14 |
| + | GO:0045263 | CC | proton-transporting ATP synthase complex, coupling factor F(o) | 6 | 3.12 | 6.83E-04 | ATP7, ATP18, ATP20, ATP4, TIM11, ATP17, ATP14 |

| | | | | | | | |
|---|---|---|---|---|---|---|---|
| + | GO:0005751 | CC | mitochondrial respiratory chain complex IV | 13 | 3.09 | 1.97E-04 | COX12, COX8, COX4, COX7, COX13, COX6, COX9, COX5A |
| + | GO:0045277 | CC | respiratory chain complex IV | 5 | 3.09 | 1.97E-04 | COX12, COX8, COX4, COX7, COX13, COX6, COX9, COX5A |
| + | GO:0005782 | CC | peroxisomal matrix | 10 | 2.89 | 6.76E-03 | MLS1, GPX1, POT1, HYR1, CTA1, MDH3 |
| + | GO:0031907 | CC | microbody lumen | 9 | 2.89 | 6.76E-03 | MLS1, GPX1, POT1, HYR1, CTA1, MDH3 |
| + | GO:0016469 | CC | proton-transporting two-sector ATPase complex | 3 | 2.55 | 2.54E-05 | STF1, ATP7, ATP16, ATP18, ATP20, ATP1, ATP4, ATP3, TIM11, ATP17, ATP2, ATP14, ATP15 |
| + | GO:0033177 | CC | proton-transporting two-sector ATPase complex, proton-transporting domain | 4 | 2.45 | 1.55E-02 | ATP7, ATP18, ATP20, ATP4, TIM11, ATP17, ATP14 |
| + | GO:0031306 | CC | intrinsic to mitochondrial outer membrane | 12 | 2.31 | 2.68E-02 | GUT2, OM14, MCR1, OM45, HFD1, POR1, FZO1 |
| + | GO:0031307 | CC | integral to mitochondrial outer membrane | 13 | 2.31 | 2.68E-02 | GUT2, OM14, MCR1, OM45, HFD1, POR1, FZO1 |
| + | GO:0009295 | CC | nucleoid | 1 | 2.19 | 2.12E-02 | ALD4, KGD2, KGD1, IDH1, ACO1, ATP1, CHA1, LPD1 |
| + | GO:0042645 | CC | mitochondrial nucleoid | 10 | 2.19 | 2.12E-02 | ALD4, KGD2, KGD1, IDH1, ACO1, ATP1, CHA1, LPD1 |
| + | GO:0044455 | CC | mitochondrial membrane part | 11 | 2.08 | 6.35E-15 | GPX1, SDH2, COX12, COX8, GUT2, OM14, QCR10, SDH1, COX4, MCR1, RIP1, SDH4, OM45, SDH3, STF1, COX7, QCR7, HFD1, ATP7, QCR2, COX13, COX6, CYT1, ATP16, QCR8, COX9, COR1, ATP18, ATP20, COX5A, ATP1, ATP4, ATP3, MIR1, POR1, TIM11, ATP17, ATP2, ATP14, QCR9, MDM34, YME2, FZO1, UPS1, PET100, ATP15 |
| + | GO:0005743 | CC | mitochondrial inner membrane | 11 | 1.88 | 2.27E-16 | SFC1, YAT1, CAT2, YJL045W, CRC1, SDH2, COX12, COX8, GUT2, DLD1, ODC1, NDI1, QCR10, SDH1, COX4, RIP1, SDH4, SDH3, SHH4, STF1, COX7, QCR7, AAC1, ATP7, QCR2, COX13, COX6, CYT1, ATP16, QCR8, SHH3, COX9, COR1, ATP18, CYC3, ATP20, COX14, COX5A, ATP1, COX20, ATP4, ATP3, MIR1, PET9, TIM11, ATP17, ATP2, ATP14, QCR9, PIC2, YME2, SHY1, FZO1, LEU5, UPS1, YFR045W, PET100, COX16, ATP15 |

| | | | | | | | |
|---|---|---|---|---|---|---|---|
| + | GO:0005758 | CC | mitochondrial intermembrane space | 10 | 1.82 | 2.00E-03 | NCE103, CYB2, NDE2, COX12, POT1, MCR1, MPM1, CYC1, COX17, HYR1, CYC3, NDE1, MDM35, CCP1, UPS1 |
| + | GO:0019866 | CC | organelle inner membrane | 8 | 1.81 | 2.44E-15 | SFC1, YAT1, CAT2, YJL045W, CRC1, SDH2, COX12, COX8, GUT2, DLD1, ODC1, NDI1, QCR10, SDH1, COX4, RIP1, SDH4, SDH3, SHH4, STF1, COX7, QCR7, AAC1, ATP7, QCR2, COX13, COX6, CYT1, ATP16, QCR8, SHH3, COX9, COR1, ATP18, CYC3, ATP20, COX14, COX5A, ATP1, COX20, ATP4, ATP3, MIR1, PET9, TIM11, ATP17, ATP2, ATP14, QCR9, PIC2, YME2, SHY1, FZO1, LEU5, UPS1, YFR045W, PET100, COX16, ATP15 |
| + | GO:0005740 | CC | mitochondrial envelope | 9 | 1.75 | 6.81E-25 | SFC1, YAT1, NCE103, CAT2, YJL045W, GPX1, CYB2, NDE2, CRC1, SDH2, UIP4, COX12, POT1, COX8, GUT2, OM14, DLD1, SUE1, ODC1, NDI1, QCR10, PDH1, SDH1, COX4, MCR1, RIP1, MPM1, SDH4, OM45, SDH3, SHH4, STF1, COX7, BXI1, QCR7, AAC1, HFD1, CYC1, FMP33, ATP7, QCR2, COX13, COX6, COX17, CYT1, ATP16, QCR8, SHH3, HYR1, COX9, COR1, ATP18, CYC3, ATP20, COX14, COX5A, ATP1, SEN15, COX20, ATP4, ATP3, LSP1, MIR1, NDE1, PET9, POR1, JID1, TIM11, MDM35, YPR098C, ATP17, RTC2, ATP2, RDL1, DNM1, ATP14, GTT1, AIM19, QCR9, ATG33, YKR018C, MDM34, PIC2, YME2, FMP10, CCP1, SHY1, FZO1, LEU5, UPS1, FIS1, YFR045W, PET100, COX16, ATP15 |
| + | GO:0005777 | CC | peroxisome | 8 | 1.72 | 2.36E-03 | MLS1, CAT2, GPX1, POT1, FOX2, CIT2, HYR1, ATG36, CTA1, GPD1, ECI1, MDH3, DNM1, PEX18, PXA1, FIS1 |
| + | GO:0042579 | CC | microbody | 7 | 1.72 | 2.36E-03 | MLS1, CAT2, GPX1, POT1, FOX2, CIT2, HYR1, ATG36, CTA1, GPD1, ECI1, MDH3, DNM1, PEX18, PXA1, FIS1 |
| + | GO:0031966 | CC | mitochondrial membrane | 10 | 1.72 | 5.76E-21 | SFC1, YAT1, CAT2, YJL045W, GPX1, CRC1, SDH2, UIP4, COX12, COX8, GUT2, OM14, DLD1, ODC1, NDI1, QCR10, PDH1, SDH1, COX4, MCR1, RIP1, MPM1, SDH4, OM45, SDH3, SHH4, STF1, COX7, BXI1, QCR7, AAC1, HFD1, FMP33, ATP7, QCR2, COX13, COX6, CYT1, ATP16, QCR8, SHH3, COX9, COR1, ATP18, CYC3, ATP20, COX14, COX5A, ATP1, SEN15, COX20, ATP4, ATP3, LSP1, MIR1, PET9, POR1, JID1, TIM11, YPR098C, ATP17, RTC2, ATP2, RDL1, DNM1, ATP14, GTT1, AIM19, QCR9, ATG33, YKR018C, MDM34, PIC2, YME2, FMP10, SHY1, FZO1, LEU5, UPS1, FIS1, YFR045W, PET100, COX16, ATP15 |
| + | GO:0031970 | CC | organelle envelope lumen | 8 | 1.71 | 4.24E-03 | NCE103, CYB2, NDE2, COX12, POT1, MCR1, MPM1, CYC1, COX17, HYR1, CYC3, NDE1, MDM35, CCP1, UPS1 |
| + | GO:0044429 | CC | mitochondrial part | 8 | 1.55 | 5.90E-26 | SFC1, YAT1, NCE103, CAT2, YJL045W, GPX1, CYB2, NDE2, CRC1, SDH2, UIP4, COX12, POT1, COX8, GUT2, OM14, HSP78, DLD1, SUE1, ODC1, NDI1, QCR10, PDH1, CIT1, SDH1, COX4, YMR31, ALD4, MCR1, RIP1, KGD2, MPM1, SDH4, FUM1, OM45, KGD1, SDH3, SHH4, STF1, MDH1, COX7, BXI1, IDH1, QCR7, ACO1, AAC1, HFD1, PUT1, CYC1, FMP33, ATP7, QCR2, COX13, COX6, COX17, CYT1, ATP16, QCR8, SHH3, HYR1, COX9, RPM2, COR1, ATP18, CYC3, SOD2, ATP20, COX14, COX5A, ISU1, ATP1, SEN15, COX20, ATP4, CTA1, HSP10, ATP3, LSP1, MIR1, NDE1, PET9, POR1, JID1, TIM11, CHA1, MDM35, YPR098C, ATP17, RTC2, ATP2, RDL1, DNM1, ATP14, GTT1, GLO4, LPD1, AIM19, QCR9, ATG33, YKR018C, IDH2, MDM34, PIC2, YME2, FMP10, CCP1, SHY1, FZO1, LEU5, MAM33, UPS1, FIS1, RSM10, YFR045W, PET100, MRPS12, COX16, ATP15 |
| + | GO:0005741 | CC | mitochondrial outer membrane | 11 | 1.46 | 5.60E-03 | GPX1, UIP4, GUT2, OM14, PDH1, MCR1, OM45, HFD1, SEN15, LSP1, POR1, YPR098C, RDL1, DNM1, GTT1, YKR018C, MDM34, FZO1, FIS1 |

| | | | | | | | |
|---|---|---|---|---|---|---|---|
| + | GO:0031968 | CC | organelle outer membrane | 8 | 1.39 | 9.83E-03 | GPX1, UIP4, GUT2, OM14, PDH1, MCR1, OM45, HFD1, SEN15, LSP1, POR1, YPR098C, RDL1, DNM1, GTT1, YKR018C, MDM34, FZO1, FIS1 |
| + | GO:0019867 | CC | outer membrane | 2 | 1.37 | 1.07E-02 | GPX1, UIP4, GUT2, OM14, PDH1, MCR1, OM45, HFD1, SEN15, LSP1, POR1, YPR098C, RDL1, DNM1, GTT1, YKR018C, MDM34, FZO1, FIS1 |
| + | GO:0031967 | CC | organelle envelope | 7 | 1.35 | 2.81E-16 | SFC1, YAT1, NCE103, CAT2, YJL045W, GPX1, CYB2, NDE2, CRC1, SDH2, UIP4, COX12, POT1, COX8, GUT2, OM14, DLD1, SUE1, ODC1, NDI1, QCR10, PDH1, SDH1, COX4, MCR1, RIP1, MPM1, SDH4, OM45, SDH3, SHH4, STF1, COX7, BXI1, QCR7, AAC1, HFD1, CYC1, FMP33, ATP7, QCR2, COX13, COX6, COX17, CYT1, ATP16, QCR8, SHH3, HYR1, COX9, COR1, ATP18, CYC3, ATP20, COX14, COX5A, ATP1, SEN15, COX20, ATP4, ATP3, LSP1, MIR1, NDE1, PET9, POR1, JID1, TIM11, MDM35, YPR098C, GFD1, ATP17, RTC2, ATP2, RDL1, DNM1, ATP14, GTT1, POM33, AIM19, QCR9, ATG33, YKR018C, MDM34, PIC2, YME2, FMP10, CCP1, SHY1, FZO1, LEU5, UPS1, FIS1, YFR045W, PET100, COX16, ATP15 |
| + | GO:0031975 | CC | envelope | 3 | 1.35 | 2.81E-16 | SFC1, YAT1, NCE103, CAT2, YJL045W, GPX1, CYB2, NDE2, CRC1, SDH2, UIP4, COX12, POT1, COX8, GUT2, OM14, DLD1, SUE1, ODC1, NDI1, QCR10, PDH1, SDH1, COX4, MCR1, RIP1, MPM1, SDH4, OM45, SDH3, SHH4, STF1, COX7, BXI1, QCR7, AAC1, HFD1, CYC1, FMP33, ATP7, QCR2, COX13, COX6, COX17, CYT1, ATP16, QCR8, SHH3, HYR1, COX9, COR1, ATP18, CYC3, ATP20, COX14, COX5A, ATP1, SEN15, COX20, ATP4, ATP3, LSP1, MIR1, NDE1, PET9, POR1, JID1, TIM11, MDM35, YPR098C, GFD1, ATP17, RTC2, ATP2, RDL1, DNM1, ATP14, GTT1, POM33, AIM19, QCR9, ATG33, YKR018C, MDM34, PIC2, YME2, FMP10, CCP1, SHY1, FZO1, LEU5, UPS1, FIS1, YFR045W, PET100, COX16, ATP15 |
| + | GO:0005739 | CC | mitochondrion | 7 | 1.12 | 3.21E-24 | FMP16, SFC1, YNL195C, YAT1, ACS1, JEN1, ACH1, AGX1, NCE103, HXT6, FMP45, CAT2, YJL045W, GPX1, CYB2, NDE2, CRC1, SDH2, TMA10, UIP4, GDH3, COX12, POT1, MBR1, COX8, GUT2, OM14, HSP78, DLD1, MSC1, CIT2, SUE1, FMP40, ODC1, NDI1, ATO2, QCR10, PDH1, CIT1, SDH1, NCE102, GRX2, COX4, YMR31, FAT3, AIM17, ALD4, MCR1, RIP1, PRX1, GDH2, GUT1, YRO2, KGD2, MPM1, SDH4, YNL200C, FUM1, OM45, KGD1, SDH3, SHH4, STF1, MDH1, COX7, BXI1, IDH1, QCR7, ACO1, AAC1, ALD6, PMA2, FMP48, HFD1, PUT1, CYC1, FMP33, ATP7, QCR2, COX13, COX6, ADY2, COX17, CYT1, ATP16, AIM18, CIT3, QCR8, SHH3, HYR1, COX9, RPM2, COR1, ATP18, CYC3, CLD1, SOD2, ATP20, FMP23, ATG9, COX14, APJ1, INH1, COX5A, ISU1, ATP1, SEN15, COX20, GDB1, ATP4, STF2, CTA1, HSP10, ATP3, LSP1, MIR1, YDL027C, NDE1, PET9, POR1, JID1, TIM11, AIM41, CHA1, MDM35, YPR098C, ATP17, RTC2, ATP2, TRX3, DCS1, RDL1, DNM1, YNL144C, ATP14, YBL059W, FMP46, GTT1, GLO4, LPD1, AIM19, MEF2, QCR9, ATG33, YKR018C, IDH2, MDM34, PIC2, YME2, FMP10, CCP1, SHY1, FZO1, MTQ1, LEU5, MAM33, UPS1, YPL109C, FIS1, RDL2, RSM10, YFR045W, PET100, MRPS12, LEU4, COX16, LYS20, EIS1, YLR290C, YIL077C, ATP15 |
| + | GO:0031090 | CC | organelle membrane | 3 | 0.52 | 2.74E-03 | SFC1, YAT1, RTN2, AQY1, CAT2, YJL045W, GPX1, CRC1, SDH2, UIP4, COX12, ATG8, COX8, GUT2, OM14, DLD1, TFS1, ODC1, NDI1, QCR10, PDH1, SDH1, COX4, MCR1, RIP1, MPM1, SDH4, OM45, SDH3, SHH4, STF1, COX7, BXI1, QCR7, AAC1, YBR241C, HFD1, FMP33, ATP7, QCR2, COX13, AMS1, COX6, ADY2, CYT1, ATP16, QCR8, SHH3, COX9, COR1, ATP18, CYC3, ATP20, ATG9, COX14, COX5A, ATP1, SEN15, COX20, YPC1, ATP4, AGP2, ATP3, LSP1, MIR1, PET9, YET2, POR1, JID1, TIM11, DIP5, YPR098C, GFD1, ATP17, RTC2, ATP2, RHO5, SNA2, RDL1, DNM1, SNC1, ATP14, PEX18, GTT1, POM33, PXA1, AIM19, QCR9, ATG33, YKR018C, MDM34, YNL115C, PIC2, YME2, FMP10, SHY1, FZO1, LEU5, UPS1, AVT3, FIS1, YLR297W, YFR045W, ATG22, YHR140W, PET100, NSG2, COX16, EMP46, ATP15 |

| | | | | | | | |
|---|---|---|---|---|---|---|---|
| + | GO:0016021 | CC | integral to membrane | 4 | 0.5 | 1.26E-03 | HSP30, SFC1, HXT5, ACS1, YNL194C, JEN1, PUT4, PHM7, HXT6, RTN2, FMP45, AQY1, STL1, CRC1, PHO89, YKL107W, COX12, COX8, GUT2, OM14, ODC1, ATO2, QCR10, NCE102, YLR312C, COX4, FAT3, YDL199C, MCR1, PMP3, YRO2, SDH4, YKL133C, OM45, YOR152C, SDH3, SHH4, COX7, BXI1, QCR7, AAC1, YJL163C, PMA2, YBR241C, HFD1, FMP33, ATP7, QCR2, COX13, COX6, ADY2, PDR15, CYT1, ATP16, QCR8, SHH3, AIM33, COX9, COR1, ATP18, YPR010C-A, ATG9, COX14, ALP1, COX5A, ATP1, COX20, YPC1, ATP4, PDR10, AGP2, YDL218W, ATP3, MIR1, YDL027C, YML131W, PET9, YET2, POR1, JID1, TIM11, DIP5, GSP2, YPR098C, GFD1, RTC2, ATP2, HXT15, SNA2, PRM4, GPT2, SNC1, RRT6, ATP14, YBL059W, YCR061W, POM33, IRC24, PNS1, PXA1, AIM19, FRE7, QCR9, ATG33, YKR018C, MDM34, YNL115C, PIC2, YME2, FMP10, SHY1, FZO1, LEU5, YBR284W, AGP1, AVT3, FIS1, PHO84, YDR366C, YLR297W, YFR045W, ATG22, YHR140W, PET100, NSG2, COX16, EMP46, ATP15 |
| + | GO:0031224 | CC | intrinsic to membrane | 3 | 0.47 | 2.35E-03 | HSP30, SFC1, HXT5, ACS1, YNL194C, JEN1, PUT4, PHM7, HXT6, RTN2, FMP45, AQY1, STL1, CRC1, PHO89, YKL107W, COX12, COX8, GUT2, OM14, ODC1, ATO2, SPI1, QCR10, NCE102, YLR312C, COX4, FAT3, YDL199C, MCR1, PMP3, YRO2, SDH4, YKL133C, OM45, YOR152C, SDH3, SHH4, COX7, BXI1, QCR7, AAC1, YJL163C, PMA2, YBR241C, HFD1, FMP33, ATP7, QCR2, COX13, COX6, ADY2, PDR15, CYT1, ATP16, QCR8, SHH3, AIM33, COX9, COR1, ATP18, YPR010C-A, ATG9, COX14, ALP1, COX5A, TIP1, ATP1, COX20, YPC1, ATP4, PDR10, AGP2, YDL218W, ATP3, MIR1, YDL027C, YML131W, PET9, YET2, POR1, JID1, TIM11, DIP5, GSP2, YPR098C, GFD1, RTC2, ATP2, HXT15, SNA2, PRM4, GPT2, SNC1, RRT6, ATP14, YBL059W, YCR061W, POM33, IRC24, PNS1, PXA1, AIM19, FRE7, QCR9, ATG33, YPS6, YKR018C, MDM34, YNL115C, PIC2, YME2, FMP10, SHY1, FZO1, LEU5, YBR284W, AGP1, AVT3, FIS1, PHO84, YDR366C, YLR297W, YFR045W, ATG22, YHR140W, PET100, NSG2, COX16, EMP46, ATP15 |
| + | GO:0044425 | CC | membrane part | 2 | 0.42 | 2.36E-03 | HSP30, SFC1, HXT5, ACS1, YNL194C, JEN1, PUT4, PHM7, HXT6, RTN2, FMP45, AQY1, STL1, GPX1, CYB2, CRC1, PHO89, SDH2, YKL107W, UIP4, COX12, ATG8, COX8, GUT2, OM14, ODC1, ATO2, SPI1, QCR10, SDH1, NCE102, YLR312C, COX4, FAT3, YDL199C, MCR1, RIP1, PMP3, YRO2, MPM1, SDH4, YKL133C, OM45, YOR152C, SDH3, SHH4, STF1, COX7, BXI1, QCR7, AAC1, YJL163C, PMA2, YBR241C, HFD1, CYC1, FMP33, ATP7, QCR2, COX13, COX6, ADY2, PDR15, CYT1, ATP16, QCR8, SHH3, AIM33, COX9, COR1, ATP18, YPR010C-A, ATP20, ATG9, COX14, ALP1, COX5A, TIP1, ATP1, COX20, YPC1, ATP4, PDR10, AGP2, YDL218W, ATP3, RIM8, MIR1, YDL027C, YML131W, PET9, YET2, POR1, JID1, TIM11, DIP5, GSP2, YPR098C, GFD1, ATP17, RTC2, ATP2, HXT15, SNA2, PRM4, GPT2, SNC1, RRT6, ATP14, YBL059W, YCR061W, YGR130C, GTT1, POM33, IRC24, PNS1, PXA1, AIM19, FRE7, QCR9, ATG33, YPS6, YKR018C, MDM34, YNL115C, PIC2, YME2, ATG19, FMP10, SHY1, FZO1, GGA1, LEU5, YBR284W, AGP1, UPS1, AVT3, FIS1, PHO84, YDR366C, YLR297W, YFR045W, ATG22, YHR140W, PET100, NSG2, COX16, EIS1, EMP46, ATP15 |

| | | | | | | | |
|---|---|---|---|---|---|---|---|
| + | GO:0016020 | CC | membrane | 1 | 0.4 | 6.82E-04 | HSP30, SFC1, HXT5, YAT1, ACS1, YNL194C, JEN1, PUT4, HSP12, PHM7, HXT6, RTN2, FMP45, AQY1, CAT2, STL1, YJL045W, GPX1, CYB2, CRC1, PHO89, HBT1, SDH2, GND2, YKL107W, UIP4, COX12, ATG8, COX8, GUT2, OM14, DLD1, MSC1, TFS1, ODC1, NDI1, ATO2, SPI1, QCR10, PDH1, SDH1, NCE102, YLR312C, COX4, FAT3, YDL199C, MCR1, RIP1, PMP3, YRO2, MPM1, SHC1, SDH4, YKL133C, OM45, YOR152C, SDH3, SHH4, STF1, COX7, BXI1, QCR7, AAC1, YJL163C, PMA2, YBR241C, HFD1, HOR7, CYC1, FMP33, ATP7, QCR2, COX13, AMS1, COX6, ADY2, PDR15, CYT1, SIP2, ATP16, ATG34, QCR8, SHH3, AIM33, COX9, COR1, ATP18, YPR010C-A, CYC3, ATP20, ATG9, COX14, ALP1, COX5A, TIP1, ATP1, GLK1, SEN15, COX20, YPC1, ATP4, PDR10, YBL029C-A, AGP2, YDL218W, ATP3, LSP1, RIM8, MIR1, RGI1, YDL027C, YML131W, PET9, YET2, POR1, JID1, TIM11, DIP5, GSP2, PET10, YPR098C, GFD1, ATP17, RTC2, ATP2, HXT15, RHO5, SNA2, RDL1, PRM4, DNM1, GPT2, SNC1, RRT6, ATP14, YBL059W, YCR061W, PEX18, YGR130C, GTT1, POM33, IRC24, PNS1, PXA1, AIM19, FRE7, QCR9, ATG33, YPS6, YKR018C, MSC3, MDM34, YNL115C, PIC2, YME2, ATG19, FMP10, SHY1, FZO1, GGA1, LEU5, YBR284W, AGP1, UPS1, AVT3, FIS1, PHO84, YDR366C, YLR297W, YFR045W, ATG22, YHR140W, PET100, NSG2, COX16, EIS1, EMP46, ATP15 |
| + | GO:0044444 | CC | cytoplasmic part | 6 | 0.26 | 3.34E-03 | MLS1, PCK1, FBP1, FMP16, SFC1, IDP2, YNL195C, YAT1, ACS1, YNL194C, JEN1, ACH1, AGX1, HSP12, PHM7, REG2, NCE103, HXT6, RTN2, FMP45, AQY1, CAT2, PYC1, YJL045W, GPX1, CYB2, YAT2, NDE2, CRC1, SDH2, TMA10, HEF3, GND2, UIP4, GDH3, COX12, POT1, ATG8, MBR1, COX8, GUT2, HSP42, OM14, HSP78, SSA3, FOX2, HSP104, DLD1, MSC1, TFS1, CIT2, SUE1, FMP40, SOL4, ODC1, NDI1, ATO2, QCR10, PDH1, CIT1, SDH1, NCE102, GRX2, PBI2, COX4, YMR31, DCS2, FAT3, AIM17, ALD4, MCR1, RIP1, PRX1, GDH2, MDH2, GUT1, YRO2, BTN2, KGD2, MPM1, SDH4, SDP1, YNL200C, FUM1, OM45, YIG1, KGD1, SDH3, SHH4, STF1, MDH1, COX7, ATH1, BXI1, IDH1, QCR7, ACO1, AAC1, YOR019W, ALD6, PMA2, FMP48, YBR241C, HFD1, PUT1, HOR7, CYC1, FMP33, ATP7, QCR2, COX13, AMS1, COX6, ADY2, COX17, ATG29, CYT1, ATP16, AIM18, ATG34, CIT3, QCR8, SHH3, HYR1, RNY1, COX9, RPM2, COR1, ATP18, CYC3, CLD1, SOD2, ATP20, FMP23, ATG36, ATG9, COX14, APJ1, SGA1, INH1, COX5A, ISU1, ATP1, GLK1, SEN15, COX20, GDB1, YPC1, ATP4, CAR2, STF2, AGP2, CTA1, HSP10, ATP3, LSP1, GPD1, MIR1, YDL027C, NDE1, YMR114C, PET9, YET2, RMD5, SDS22, POR1, NGR1, JID1, TIM11, DIP5, AIM41, CHA1, MDM35, ECI1, PET10, YPR098C, PRB1, MDH3, ATP17, RTC2, ATP2, TRX3, DCS1, RHO5, SNA2, RDL1, DNM1, GPT2, SNC1, YNL144C, ATP14, YBL059W, FMP46, PEX18, TSL1, YDR262W, GTT1, POM33, GLO4, LPD1, PXA1, AIM19, MEF2, QCR9, ATG33, CAR1, YKR018C, IDH2, MDM34, YNL115C, PIC2, UGA1, YME2, ATG19, FMP10, CCP1, SHY1, FZO1, MTQ1, GGA1, LEU5, MAM33, PGM2, UPS1, YPL109C, AVT3, FIS1, RDL2, YGR250C, YLR297W, RSM10, YFR045W, ATG22, TMA17, YHR140W, PET100, NSG2, MRPS12, LEU4, COX16, TPK2, YNG2, LYS20, EIS1, EMP46, GIP2, YLR290C, YIL077C, ATP15 |

| | | | | | | | |
|---|---|---|---|---|---|---|---|
| + | GO:0005737 | CC | cytoplasm | 5 | 0.22 | 3.65E-05 | MLS1, PCK1, GRE1, FBP1, FMP16, SFC1, IDP2, YNL195C, YAT1, ACS1, YNL194C, JEN1, ACH1, AGX1, HSP12, HSP26, PHM7, REG2, NCE103, CTT1, RTC3, HXT6, RTN2, FMP45, AQY1, CAT2, PYC1, YJL045W, GPX1, CYB2, YAT2, TKL2, NDE2, NQM1, ICL1, CRC1, HBT1, SDH2, TMA10, HEF3, BDH2, GND2, YNR034W-A, UIP4, GDH3, COX12, CAT8, POT1, ATG8, MBR1, COX8, GUT2, HSP42, OM14, HSP78, SSA3, FOX2, HSP104, DLD1, MSC1, TFS1, CIT2, SUE1, GCY1, FMP40, SOL4, ODC1, NDI1, ATO2, MHO1, IGD1, CSR2, YJL144W, YHR033W, PIG2, QCR10, PDH1, CIT1, SDH1, NCE102, PHM8, GRX2, PBI2, SSE2, COX4, YMR31, DCS2, FAT3, AIM17, ALD4, MCR1, RIP1, PRX1, GDH2, MDH2, GUT1, YRO2, GPG1, BTN2, KGD2, MPM1, SHC1, SDH4, SDP1, YNL200C, SSA4, FUM1, OM45, YIG1, KGD1, ECM4, SDH3, SHH4, STF1, HSP82, MDH1, XBP1, COX7, ATH1, BXI1, IDH1, QCR7, ACO1, AAC1, GAD1, YOR019W, ALD6, YBR085C-A, PMA2, DBP1, FMP48, SRX1, YBR241C, HFD1, PUT1, HOR7, CYC1, FMP33, ATP7, QCR2, UGA2, COX13, AMS1, COX6, ADY2, COX17, ATG29, CYT1, SIP2, ATP16, UBI4, STI1, AIM18, ATG34, CIT3, QCR8, SHH3, HYR1, RNY1, COX9, RPM2, COR1, PCL7, ATP18, CYC3, CLD1, SOD2, ATP20, CIN5, ALT2, YNL134C, FMP23, VHS1, ATG36, ATG9, SOL1, COX14, APJ1, ALD3, GLC3, SGA1, ALD2, INH1, COX5A, ISU1, ATP1, GLK1, SEN15, COX20, YPR127W, GDB1, YPC1, IRC15, ATP4, CAR2, PDC6, STF2, AGP2, CTA1, HSP10, YDL218W, ATP3, LSP1, FYV10, GPD1, MIR1, AST2, RGI1, URA10, YJR096W, YDL027C, NDE1, NNK1, YMR114C, YML131W, PET9, YET2, AHA1, RMD5, YLR345W, SDS22, POR1, CPR6, NGR1, JID1, TIM11, DIP5, YPL247C, AIM41, CHA1, APA2, MDM35, ECI1, PET10, YPR098C, PRB1, GFD1, UBC8, MDH3, ATP17, RTC2, GUD1, ATP2, TRX3, YER079W, DCS1, RHO5, LAP2, SNA2, RDL1, DNM1, GPT2, SNC1, GLO1, YNL144C, ATP14, UBX5, SIP5, FBP26, GLG2, YBL059W, YCR061W, FMP46, PEX18, TSL1, ZWF1, CIA2, YGR130C, GRE2, YDR262W, GTT1, POM33, IRC24, GLO4, SDS24, LPD1, PXA1, KNS1, AIM19, MEF2, GAL3, QCR9, ATG33, CAR1, YKR018C, RCN2, AHC1, IDH2, MDM34, YNL115C, PIC2, UGA1, YME2, BDH1, ATG19, FMP10, CCP1, SHY1, FZO1, MTQ1, GGA1, LEU5, MAM33, PGM2, BOP3, UPS1, YPL109C, EDC2, AVT3, MRP8, FIS1, RDL2, YPR172W, WTM1, YGR250C, YLR297W, RSM10, YFR045W, ATG22, TMA17, YMR085W, YHR140W, HPA3, PET100, NSG2, MRPS12, LEU4, GPM2, COX16, TPK2, YNG2, LYS20, EIS1, EMP46, GIP2, YLR290C, YIL077C, SDS23, ATP15 |
| + | GO:0008177 | MF | succinate dehydrogenase (ubiquinone) activity | 5 | 3.63 | 1.26E-03 | YJL045W, SDH2, SDH1, SDH4, SDH3 |
| + | GO:0004029 | MF | aldehyde dehydrogenase (NAD) activity | 5 | 3.63 | 1.26E-03 | ALD4, ALD6, HFD1, ALD3, ALD2 |
| + | GO:0004030 | MF | aldehyde dehydrogenase [NAD(P)+] activity | 5 | 3.63 | 1.26E-03 | ALD4, ALD6, HFD1, ALD3, ALD2 |
| + | GO:0005315 | MF | inorganic phosphate | 5 | 3.57 | 1.04E-02 | PHO89, MIR1, PIC2, PHO84 |

| | | | | | | | |
|---|---|---|---|---|---|---|---|
| | | | transmembrane transporter activity | | | | |
| + | GO:0008121 | MF | ubiquinol-cytochrome-c reductase activity | 9 | 3.53 | 5.27E-05 | QCR10, RIP1, QCR7, QCR2, QCR8, COR1, QCR9 |
| + | GO:0016679 | MF | oxidoreductase activity, acting on diphenols and related substances as donors | 3 | 3.53 | 5.27E-05 | QCR10, RIP1, QCR7, QCR2, QCR8, COR1, QCR9 |
| + | GO:0016681 | MF | oxidoreductase activity, acting on diphenols and related substances as donors, cytochrome as acceptor | 4 | 3.53 | 5.27E-05 | QCR10, RIP1, QCR7, QCR2, QCR8, COR1, QCR9 |
| + | GO:0016635 | MF | oxidoreductase activity, acting on the CH-CH group of donors, quinone or related compound as acceptor | 4 | 3.41 | 3.34E-03 | YJL045W, SDH2, SDH1, SDH4, SDH3 |
| + | GO:0000104 | MF | succinate dehydrogenase activity | 4 | 3.31 | 1.13E-03 | YJL045W, SDH2, SDH1, SDH4, SDH3, SHH3 |
| + | GO:0046933 | MF | proton-transporting ATP synthase activity, rotational mechanism | 13 | 3.26 | 1.31E-05 | ATP7, ATP16, ATP18, ATP1, ATP3, ATP17, ATP2, ATP14, ATP15 |

| | | | | | | | |
|---|---|---|---|---|---|---|---|
| + | GO:0004602 | MF | glutathione peroxidase activity | 5 | 3.09 | 4.91E-02 | GPX1, GRX2, HYR1, GTT1 |
| + | GO:0046912 | MF | transferase activity, transferring acyl groups, acyl groups converted into alkyl on transfer | 4 | 3.02 | 4.02E-03 | MLS1, CIT2, CIT1, CIT3, LEU4, LYS20 |
| + | GO:0004601 | MF | peroxidase activity | 4 | 2.81 | 1.02E-03 | CTT1, GPX1, GRX2, PRX1, HYR1, CTA1, GTT1, CCP1 |
| + | GO:0016684 | MF | oxidoreductase activity, acting on peroxide as acceptor | 3 | 2.81 | 1.02E-03 | CTT1, GPX1, GRX2, PRX1, HYR1, CTA1, GTT1, CCP1 |
| + | GO:0004129 | MF | cytochrome-c oxidase activity | 9 | 2.65 | 2.27E-03 | COX12, COX8, COX4, COX7, COX13, COX6, COX9, COX5A |
| + | GO:0015002 | MF | heme-copper terminal oxidase activity | 3 | 2.65 | 2.27E-03 | COX12, COX8, COX4, COX7, COX13, COX6, COX9, COX5A |
| + | GO:0016675 | MF | oxidoreductase activity, acting on a heme group of donors | 3 | 2.65 | 2.27E-03 | COX12, COX8, COX4, COX7, COX13, COX6, COX9, COX5A |
| + | GO:0016676 | MF | oxidoreductase activity, acting on a heme group of donors, oxygen as acceptor | 4 | 2.65 | 2.27E-03 | COX12, COX8, COX4, COX7, COX13, COX6, COX9, COX5A |
| + | GO:0046961 | MF | proton-transporting ATPase activity, rotational mechanism | 13 | 2.62 | 3.93E-05 | ATP7, ATP16, ATP18, ATP20, ATP1, ATP4, ATP3, TIM11, ATP17, ATP2, ATP14, ATP15 |

| | | | | | | | |
|---|---|---|---|---|---|---|---|
| + | GO:0015078 | MF | hydrogen ion transmembrane transporter activity | 8 | 2.59 | 6.50E-13 | COX12, COX8, QCR10, COX4, RIP1, COX7, QCR7, PMA2, ATP7, QCR2, COX13, COX6, ATP16, QCR8, COX9, COR1, ATP18, ATP20, COX5A, ATP1, ATP4, ATP3, TIM11, ATP17, ATP2, ATP14, QCR9, ATP15 |
| + | GO:0044769 | MF | ATPase activity, coupled to transmembrane movement of ions, rotational mechanism | 12 | 2.57 | 5.63E-05 | ATP7, ATP16, ATP18, ATP20, ATP1, ATP4, ATP3, TIM11, ATP17, ATP2, ATP14, ATP15 |
| + | GO:0015077 | MF | monovalent inorganic cation transmembrane transporter activity | 7 | 2.41 | 9.20E-12 | PHO89, COX12, COX8, QCR10, COX4, RIP1, COX7, QCR7, PMA2, ATP7, QCR2, COX13, COX6, ATP16, QCR8, COX9, COR1, ATP18, ATP20, COX5A, ATP1, ATP4, ATP3, TIM11, ATP17, ATP2, ATP14, QCR9, ATP15 |
| + | GO:0016209 | MF | antioxidant activity | 1 | 2.35 | 7.67E-04 | CTT1, GPX1, GRX2, PRX1, ECM4, SRX1, HYR1, SOD2, CTA1, GTT1, CCP1 |
| + | GO:0016903 | MF | oxidoreductase activity, acting on the aldehyde or oxo group of donors | 3 | 2.19 | 2.12E-02 | ALD4, KGD1, ALD6, HFD1, UGA2, ALD3, ALD2, LPD1 |
| + | GO:0050660 | MF | flavin adenine dinucleotide binding | 5 | 2.09 | 3.23E-02 | YJL045W, NDE2, DLD1, NDI1, SDH1, IRC15, NDE1, LPD1 |
| + | GO:0019829 | MF | cation-transporting ATPase activity | 12 | 2.07 | 1.13E-03 | PMA2, ATP7, ATP16, ATP18, ATP20, ATP1, ATP4, ATP3, TIM11, ATP17, ATP2, ATP14, ATP15 |
| + | GO:0042625 | MF | ATPase activity, coupled to transmembrane movement of ions | 11 | 2.01 | 1.71E-03 | PMA2, ATP7, ATP16, ATP18, ATP20, ATP1, ATP4, ATP3, TIM11, ATP17, ATP2, ATP14, ATP15 |
| + | GO:0022890 | MF | inorganic cation transmembrane transporter activity | 6 | 1.92 | 1.28E-08 | PHO89, COX12, COX8, ATO2, QCR10, COX4, RIP1, COX7, QCR7, PMA2, ATP7, QCR2, COX13, COX6, ADY2, ATP16, QCR8, COX9, COR1, ATP18, ATP20, COX5A, ATP1, ATP4, ATP3, TIM11, ATP17, ATP2, ATP14, QCR9, PHO84, ATP15 |
| + | GO:0016614 | MF | oxidoreductase activity, acting on | 3 | 1.86 | 2.27E-05 | IDP2, CYB2, BDH2, GND2, GUT2, FOX2, DLD1, GCY1, MDH2, MDH1, IDH1, YNL134C, XYL2, YPR127W, GPD1, YJR096W, MDH3, AAD10, ZWF1, GRE2, IDH2, BDH1 |

| | | | | | | | |
|---|---|---|---|---|---|---|---|
| | | | CH-OH group of donors | | | | |
| + | GO:0016491 | MF | oxidoreductase activity | 2 | 1.83 | 8.60E-23 | IDP2, CTT1, YJL045W, GPX1, CYB2, NDE2, SDH2, BDH2, GND2, YKL107W, GDH3, COX12, COX8, GUT2, FOX2, DLD1, GCY1, NDI1, QCR10, SDH1, GRX2, COX4, AIM17, ALD4, MCR1, RIP1, PRX1, GDH2, MDH2, SDH4, KGD1, ECM4, SDH3, MDH1, COX7, IDH1, QCR7, ALD6, SRX1, HFD1, PUT1, QCR2, UGA2, COX13, COX6, QCR8, SHH3, HYR1, AIM33, COX9, COR1, SOD2, YNL134C, ALD3, ALD2, XYL2, COX5A, YPR127W, IRC15, OYE3, CTA1, GPD1, AST2, YJR096W, NDE1, YML131W, MDH3, TRX3, PRM4, AAD10, FMP46, ZWF1, GRE2, GTT1, IRC24, LPD1, FRE7, QCR9, IDH2, BDH1, CCP1, YPR172W |
| + | GO:0016616 | MF | oxidoreductase activity, acting on the CH-OH group of donors, NAD or NADP as acceptor | 4 | 1.77 | 1.97E-04 | IDP2, BDH2, GND2, FOX2, DLD1, GCY1, MDH2, MDH1, IDH1, YNL134C, XYL2, YPR127W, GPD1, YJR096W, MDH3, AAD10, ZWF1, GRE2, IDH2, BDH1 |
| + | GO:0016820 | MF | hydrolase activity, acting on acid anhydrides, catalyzing transmembrane movement of substances | 4 | 1.74 | 2.14E-03 | PMA2, ATP7, PDR15, ATP16, ATP18, ATP20, ATP1, ATP4, PDR10, ATP3, TIM11, ATP17, ATP2, ATP14, PXA1, ATP15 |
| + | GO:0042626 | MF | ATPase activity, coupled to transmembrane movement of substances | 10 | 1.74 | 2.14E-03 | PMA2, ATP7, PDR15, ATP16, ATP18, ATP20, ATP1, ATP4, PDR10, ATP3, TIM11, ATP17, ATP2, ATP14, PXA1, ATP15 |
| + | GO:0008324 | MF | cation transmembrane transporter activity | 5 | 1.74 | 1.41E-09 | JEN1, PUT4, STL1, PHO89, COX12, COX8, ATO2, QCR10, COX4, RIP1, COX7, QCR7, PMA2, ATP7, QCR2, COX13, COX6, ADY2, ATP16, QCR8, COX9, COR1, ATP18, ATP20, COX5A, ATP1, ATP4, AGP2, ATP3, TIM11, ATP17, RTC2, ATP2, ATP14, PNS1, QCR9, YKL091C, AGP1, AVT3, PHO84, ATP15 |
| + | GO:0043492 | MF | ATPase activity, coupled to movement of substances | 9 | 1.67 | 3.70E-03 | PMA2, ATP7, PDR15, ATP16, ATP18, ATP20, ATP1, ATP4, PDR10, ATP3, TIM11, ATP17, ATP2, ATP14, PXA1, ATP15 |
| + | GO:0050662 | MF | coenzyme binding | 3 | 1.63 | 5.22E-04 | IDP2, YJL045W, CYB2, NDE2, GND2, DLD1, NDI1, SDH1, KGD1, IDH1, YLL056C, IRC15, OYE3, PDC6, GPD1, NDE1, ZWF1, GRE2, LPD1, IDH2, YPR172W |

| | | | | | | | |
|---|---|---|---|---|---|---|---|
| + | GO:0015399 | MF | primary active transmembrane transporter activity | 4 | 1.61 | 5.77E-03 | PMA2, ATP7, PDR15, ATP16, ATP18, ATP20, ATP1, ATP4, PDR10, ATP3, TIM11, ATP17, ATP2, ATP14, PXA1, ATP15 |
| + | GO:0015405 | MF | P-P-bond-hydrolysis-driven transmembrane transporter activity | 5 | 1.61 | 5.77E-03 | PMA2, ATP7, PDR15, ATP16, ATP18, ATP20, ATP1, ATP4, PDR10, ATP3, TIM11, ATP17, ATP2, ATP14, PXA1, ATP15 |
| + | GO:0048037 | MF | cofactor binding | 2 | 1.57 | 9.10E-06 | IDP2, AGX1, YJL045W, CYB2, NDE2, GND2, DLD1, NDI1, SDH1, SDH4, KGD1, SDH3, IDH1, GAD1, YLL056C, SHH3, ALT2, IRC15, OYE3, CAR2, PDC6, GPD1, NDE1, CHA1, ZWF1, GRE2, LPD1, IDH2, UGA1, YPR172W, PPZ2 |
| + | GO:0015075 | MF | ion transmembrane transporter activity | 4 | 1.57 | 1.28E-09 | HSP30, SFC1, JEN1, PUT4, STL1, PHO89, COX12, COX8, ODC1, ATO2, QCR10, COX4, RIP1, YRO2, COX7, QCR7, PMA2, ATP7, QCR2, COX13, COX6, ADY2, ATP16, QCR8, COX9, COR1, ATP18, ATP20, ALP1, COX5A, ATP1, ATP4, AGP2, ATP3, POR1, TIM11, DIP5, ATP17, RTC2, ATP2, ATP14, PNS1, QCR9, YKL091C, LEU5, AGP1, AVT3, PHO84, ATP15 |
| + | GO:0022804 | MF | active transmembrane transporter activity | 3 | 1.5 | 2.40E-04 | SFC1, JEN1, STL1, CRC1, PHO89, AAC1, PMA2, ATP7, PDR15, ATP16, ATP18, ATP20, ATP1, ATP4, PDR10, ATP3, MIR1, PET9, TIM11, ATP17, ATP2, ATP14, PXA1, PIC2, PHO84, ATP15 |
| + | GO:0051082 | MF | unfolded protein binding | 3 | 1.42 | 4.91E-02 | HSP26, HSP42, SSA3, HSP104, SSA4, HSP82, HSP31, APJ1, COX20, HSP10, CPR6, SHY1, PET100, NSG2 |
| + | GO:0022857 | MF | transmembrane transporter activity | 2 | 1.36 | 5.74E-10 | HSP30, SFC1, HXT5, JEN1, PUT4, HXT6, AQY1, STL1, CRC1, PHO89, COX12, COX8, ODC1, ATO2, QCR10, COX4, YDL199C, RIP1, YRO2, COX7, QCR7, AAC1, PMA2, YBR241C, ATP7, QCR2, COX13, COX6, ADY2, PDR15, ATP16, QCR8, COX9, COR1, ATP18, ATP20, ALP1, COX5A, ATP1, ATP4, PDR10, AGP2, ATP3, MIR1, PET9, POR1, TIM11, DIP5, ATP17, RTC2, ATP2, HXT15, ATP14, PNS1, PXA1, QCR9, PIC2, YKL091C, LEU5, AGP1, AVT3, PHO84, ATP15 |
| + | GO:0022891 | MF | substrate-specific transmembrane transporter activity | 3 | 1.31 | 5.78E-08 | HSP30, SFC1, HXT5, JEN1, PUT4, HXT6, AQY1, STL1, PHO89, COX12, COX8, ODC1, ATO2, QCR10, COX4, YDL199C, RIP1, YRO2, COX7, QCR7, PMA2, YBR241C, ATP7, QCR2, COX13, COX6, ADY2, ATP16, QCR8, COX9, COR1, ATP18, ATP20, ALP1, COX5A, ATP1, ATP4, AGP2, ATP3, POR1, TIM11, DIP5, ATP17, RTC2, ATP2, HXT15, ATP14, PNS1, QCR9, YKL091C, LEU5, AGP1, AVT3, PHO84, ATP15 |
| + | GO:0022892 | MF | substrate-specific transporter activity | 2 | 1.09 | 9.10E-06 | HSP30, SFC1, HXT5, JEN1, PUT4, HXT6, AQY1, STL1, PHO89, COX12, COX8, ODC1, ATO2, QCR10, COX4, YDL199C, RIP1, YRO2, COX7, QCR7, PMA2, YBR241C, ATP7, QCR2, COX13, COX6, ADY2, ATP16, QCR8, COX9, COR1, ATP18, ATP20, ALP1, COX5A, ATP1, ATP4, AGP2, ATP3, POR1, TIM11, DIP5, ATP17, RTC2, ATP2, HXT15, ATP14, PNS1, QCR9, YKL091C, LEU5, AGP1, UPS1, AVT3, PHO84, ATP15 |
| + | GO:0005215 | MF | transporter activity | 1 | 1.09 | 9.20E-07 | HSP30, SFC1, HXT5, JEN1, PUT4, HXT6, AQY1, STL1, CRC1, PHO89, COX12, COX8, ODC1, ATO2, QCR10, COX4, YDL199C, RIP1, YRO2, COX7, QCR7, AAC1, PMA2, YBR241C, ATP7, QCR2, COX13, COX6, ADY2, PDR15, ATP16, QCR8, COX9, COR1, ATP18, ATP20, ALP1, COX5A, ATP1, ATP4, PDR10, AGP2, ATP3, MIR1, PET9, POR1, TIM11, DIP5, ATP17, RTC2, ATP2, HXT15, ATP14, PNS1, PXA1, QCR9, PIC2, YKL091C, LEU5, AGP1, UPS1, AVT3, PHO84, YFR045W, ATP15 |

| | | | | | | | |
|---|---|---|---|---|---|---|---|
| + | GO:0003824 | MF | catalytic activity | 1 | 0.41 | 1.39E-05 | MLS1, PCK1, FBP1, IDP2, YAT1, ACS1, ACH1, AGX1, NCE103, CTT1, CAT2, PYC1, YJL045W, GPX1, CYB2, YAT2, TKL2, NDE2, NQM1, ICL1, SDH2, HEF3, BDH2, GND2, YKL107W, GDH3, COX12, POT1, COX8, GUT2, HSP78, SSA3, FOX2, HSP104, DLD1, CIT2, GCY1, SOL4, NDI1, YHR033W, QCR10, PDH1, CIT1, SDH1, PHM8, GRX2, PBI2, COX4, DCS2, AIM17, ALD4, MCR1, RIP1, PRX1, GDH2, MDH2, GUT1, KGD2, SDH4, SDP1, YNL200C, SSA4, FUM1, KGD1, ECM4, SDH3, HSP82, MDH1, COX7, ATH1, PRR2, IDH1, QCR7, ACO1, GAD1, SAF1, ALD6, PMA2, DBP1, FMP48, SRX1, HFD1, PUT1, ATP7, QCR2, UGA2, COX13, AMS1, COX6, PDR15, YLL056C, SIP2, ATP16, AIM18, CIT3, HSP31, QCR8, KIN82, SHH3, HYR1, AIM33, RNY1, COX9, RPM2, COR1, ATP18, CYC3, CLD1, SOD2, ATP20, ALT2, YNL134C, VHS1, SOL1, ALD3, GLC3, SGA1, ALD2, XYL2, COX5A, TIP1, ATP1, GLK1, SEN15, YPR127W, GDB1, YPC1, IRC15, OYE3, ATP4, CAR2, PDC6, PDR10, CTA1, ATP3, FYV10, GPD1, AST2, DIA3, URA10, YJR096W, NDE1, NNK1, YML131W, RMD5, YLR345W, CPR6, TIM11, AIM41, CHA1, APA2, GSP2, ECI1, PRB1, UBC8, MDH3, ATP17, GUD1, ATP2, TRX3, DCS1, RHO5, LAP2, RDL1, PRM4, DNM1, GPT2, GLO1, AAD10, ATP14, FBP26, GLG2, FMP46, TSL1, ZWF1, GRE2, GTT1, IRC24, GLO4, LPD1, PXA1, ARG82, KNS1, MEF2, FRE7, HUL4, GAL3, QCR9, CAR1, YPS6, AHC1, IDH2, UGA1, BDH1, CCP1, FZO1, MTQ1, YBR284W, PGM2, PTK1, MGT1, YPL109C, RDL2, YPR172W, YMR085W, HPA3, LEU4, GPM2, TPK2, YNG2, LYS20, PPZ2, ATP15 |

a. "-" = GO terms associated with repressed genes; "+" = GO terms associated with induced genes

b. BF = biological function; CC = cellular component; MF = molecular function

c. The number of steps to the root of GO term tree.

d. The $\log_2$ of the ratio

where *n* is the number of genes in the user list that falls into a given GO category, m is the total number of genes in the user list, N is tota number of genes in the genome.

e. Calculated from a hypergeometric distribution with a false discovery rate of 0.01.

# CHAPTER 4

## Quantitative Proteomics of Chronologically Aging WT Yeast

### 4.1. Introduction

Aging is a complex process of accumulation of molecular, cellular, and organ damage in mammals, leading to disease and death (Blasco, 2005). The chronological lifespan of *S. cerevisiae* is measured, typically in stationary phase, by monitoring the time non-dividing cells remain viable in culture. Yeast chronological aging models aging of post-mitotic mammalian cells (Longo *et al*., 1996). Stationary phase cultures of yeast include both quiescent and non-quiescent cells (Werner-Washburne *et al*., 2002). Non-quiescent cells are less dense, budded and unbudded cells. Non-quiescent cells are also composed of replicatively older cells that rapidly lose the ability to reproduce (Davidson *et al*., 2011). However, the quiescent cells are dense, unbudded daughter cells formed after glucose exhaustion (Allen *et al*., 2006). Quiescent cells are long lived, stress resistant, and can re-enter mitotic cell cycle(Davidson *et al*., 2011). Stationary phase cultures showed characteristics associated with quiescence, including a thick cell wall, decreased metabolic rate and accumulation of a variety of storage molecules such as trehalose and glycogen (Werner-Washburne *et al*., 1996). In addition to increased stress resistance, quiescent cells showed decreased transcription and translation (Werner-Washburne *et al*., 1996). Differences in mRNA levels between exponential and stationary phase cultures, and non-quiescent and quiescent cells are known, but little is known about changes in the total protein of a chronologically aging yeast. To date the only protein analysis of stationary phase yeast cells was performed using two-dimensional

polyacrylamide gel electrophoresis (2D-PAGE) over a 28 day period (Fuge *et al*., 1994).

We used isobaric tag for relative and absolute quantification (iTRAQ), a multiplexed protein strategy that utilized multiplex isobaric amine specific tags to provide relative and absolute measurements of proteins in a mixture. The 8-plex iTRAQ reagent kit was used to label all peptides from different samples harvested from non-quiescent and quiescent populations at different time points. The samples were then pooled and fractionated by 2D chromatography, and analysed by tandem mass spectrometry (MS/MS).

## 4.2. Materials and Methods

### *4.2.1. Yeast Strains and Media*

Wild type strain, JDY86 {*MATa, his3Δ200, leu2Δ0, K2Δ0, trp1Δ63, ura3Δ0*, *met15Δ0, can1::MFA1pr-HIS3*}. All chemicals were of biochemical analysis or of molecular biology purity.

### *4.2.2. Yeast Protein Extraction*

Non-quiescent and quiescent cells were harvested at different time points as previously described. Cell pellets were resuspended in pre-warmed, 1.13 ml cracking buffer [6 M guanidine hydrochloride, 1% (w/v) octylglucopyranoside, 0.1% (w/v) Rapigest, 40 mM MOPS pH6.8, 0.1% (w/v) EDTA, 2 µl of 0.5 M Tris(2-carboxyethyl)phosphine hydrochloride (TCEP), 70 µl protease inhibitor cocktail, 50 µl of 100X PMSF]. The cell suspensions were transferred to a micro-centrifuge tube containing 80 µl of glass beads per 7.5 $OD_{600}$units of cells. The samples were heated at 70°C for 10 min, and vortexed vigorously for 1 min. The cell debri and unbroken cells were centrifuged in a micro-centrifuge at 20 817 x g for 5 min at 4°C. Supernatant was transferred to a fresh micro-centrifuge tube, and place on ice. The pellets containing cell debris and unbroken cells were then placed in 100°C boiling water bath for 3-5 min, and vortexed vigorously for 1 min. The pellets were then centrifuged in a micro-centrifuge at 20 817 x g for 5 min at 4°C. Each supernatant was combined. The supernatant was precipitated using 5 volumes of cold acetone, and trichloroacetic acid (TCA) to a final concentration of 20% (w/v). Total protein was collected by centrifugation at 17 418 x g for 5 min at 4°C.

### *4.2.3. In-Solution Protein digestion*

A 5 µl of total protein (~100µg) samples was aliquoted into 1.5 ml centrifuge tubes, the samples were diluted to 10 µl with 50 mM triethylammonium bicarbonate (TEAB), 1 µl of 100 mM TCEP prepared in 50 mM TEAB was added, and the samples were incubated at 60°C for 1h. The total protein samples were allowed to cool down to room temperature, 1 µl of 100 mM methyl methanethiosulfonate prepared in 2-propanol was added, and the samples were incubated at room temperature for 15 min. The total protein samples were further diluted to 45 µl with 50 mM TEAB, digested by adding 5 µg of trypsin. The enzymatic digestion was then allowed at 37°C for 18h.

### *4.2.4. Labelling with iTRAQ 8-Plex Reagent(s)*

The pH of the digestion reaction was increased to over by adding 10 µl of 1 M TEAB. The vials of the iTRAQ reagents were allowed to reach room temperature and 70 µl of 2-propanol was added. Freshly prepared iTRAQ solution was transferred to each digested protein sample tube and incubated at room temperature for 2h. The peptide samples were desalted using $C_{18}$ micro-SPE columns (SiliCycle).

### *4.2.5. First Dimension Chromatography*

Hydrophilic Interaction Liquid Chromatography (HILIC) was used for first dimension separation of peptides. HILIC was performed using a quaternary amine anion exchange resin and eluted step wise with sodium perchlorate. Fractions were collected and desalted at high pH using a $C_{18}$ micro-SPE columns (SiliCycle).

### *4.2.6. Second Dimension Chromatography*

Second dimension chromatography was performed on Dionex-Ultimate 3000 nano-UHPLC (Thermo Scientific) equipped with a heated column compartment and chilled autosampler. Chromatography was performed at 50°C using a 50cm in-house manufactured column (75 µm ID x 15 cm $C_{18}$). Peptides were eluted in a step wise gradient: A, 2% acetonitrile; 0.1% formic acid and B, 100% acetonitrile; 0.1% formic acid. Flow rate was set to 300 nl/min.

### *4.2.7. Mass Spectromery*

Mass spectrometry was performed using Q Exactive hybrid quadrupole-orbitrap mass spectrometer (Thermo Scientific). Analysis was set to internal calibration and acquisition parameters, and adjusted as required. All fractions were analysed at least once.The data were acquired using a data-dependent data acquisition mode in which, for each cycle, the 15 most abundant multiply charged precursor ions (+2 to +4) with an m/z between 400 and 1800 were selected for HCD fragmentation (MS/MS) with the 15 sec dynamic exclusion setting.

### *4.2.8. Data Analysis and Interpretation*

For iTRAQ protein identification, the raw mass data were processed with Proteome Discoverer 1.3 (Thermo Scientific) and searched with in-house Mascot software (Matrix Science) against a UniProt *S.cerevisiae* database. In the database search, full tryptic specificity was required with tolerance set at one missed cleavage.iTRAQ 8-plex modification of the N terminus and K were set as fixed modifications. Deamination of the N terminus, and oxidation of methionine were set as variable modifications. The initial precursor mass tolerance was set to 10 ppm, and the fragment ion level was set to 0.02 Da. The data files generated by Mascot

were processed using Scaffold Q+ (Proteome Software).The fragmentation of the attached multiplex tag generated a reporter ion that was used to relatively quantify the peptides and the proteins from which they originate. The analysis for enrichment of gene ontology terms were performed with GOEAST (omicslab.genetics.ac.cn/GOEAST) (Zheng and Wang, 2008).

#### *4.2.9. Mitochondrial Protein Staining*

Non-quiescent and quiescent cells were collected at day 6 as previously described. Cell pellets were resuspended in 10 mM HEPES buffer pH7.4, containing 5% glucose. MitoTracker GreenFM (Molecular Probes) was added to a final concentration of 100 nM. Cells were incubated at room temperature for 15-30 min, and visualized at 490 nm excitation wavelength by fluorescent microscopy.

### 4.3. Results

The proteome of aging of the WT strain of the histone H3 and H4 mutant library was determined in order to compare with the proteome of the selected mutants (Chapter 5). A survival curve of the WT strain was constructed by growing yeast cultures into stationary phase for up to 66 days in shaking flasks, and the number of colony forming units were calculated (Figure 4.1). At specific times fractions were collected and separated into quiescent and non-quiescent populations using Percoll gradients as described previously. Total protein was isolated from the two populations and iTRAQ tagged. Each sample was further separated by HILIC chromatography and quantitated on a Q Exactive mass spectrometer.

Approximately 1000 proteins in each sample were identified using Mascot and Tandem search engines. False positive cut off was set at 99% protein confidence with a minimum of two unique peptides at 95% confidence. A 1.5 fold change was

used to distinguish significant change in the abundance of differentially expressed proteins. Out of the approximately 1000 proteins identified in the quiescent population, 32 proteins were up-regulated with more than 1.5 fold changes ($p \leq 0.05$) in at least one time point (Table 4.1). The quiescent population showed significant up-regulation of stress response proteins (in green) (Table 4.1). The up-regulated stress response proteins contained proteins such as Sis1, which is required for mis-folded protein transport (Park *et al*., 2013). The oxidative stress response proteins such as superoxide dismutase and peroxisomal catalase A, and heat shock proteins such as HspSSA3 and Hsp26 were also up-regulated.

In addition, chemical response protein, S-formylglutathione hydrolase, was also up-regulated which is involved in detoxification of formaldehyde (Degrassi *et al*., 1999).

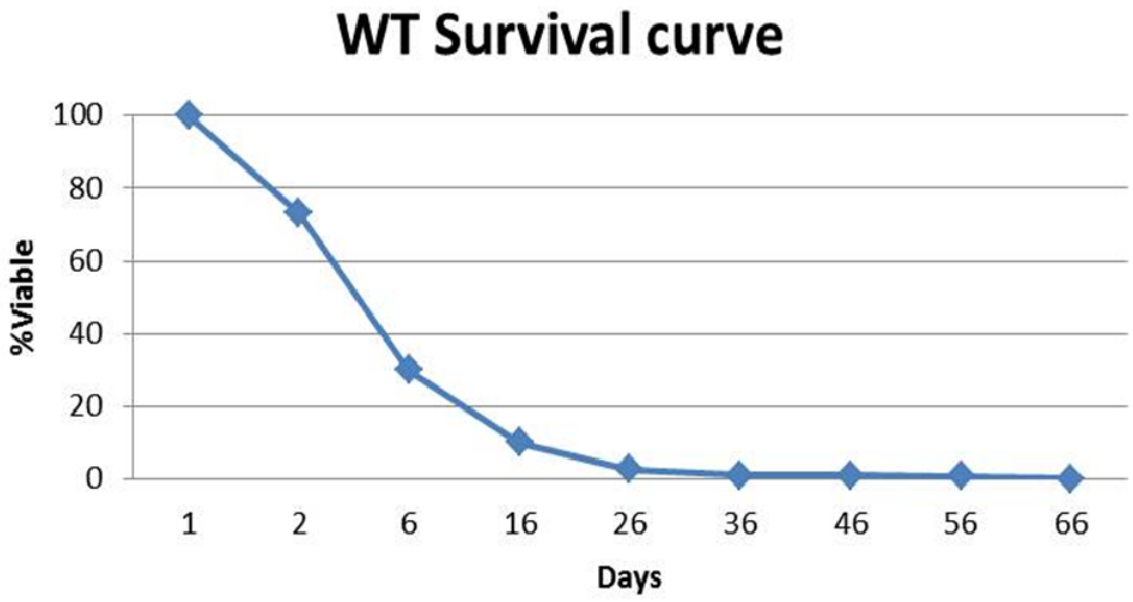


**Figure 4.1.Chronological lifespan of JDY86 WT strain.**
Two biologically independent cultures were used to construct the survival curve. Serial dilutions were plated onto YPD plates and colony forming units per ml were calculated over 60 days.

When looking at Table 4.1, we observed different protein up-regulation patterns over time. Some protein expression patterns increased linearly over 66 days, some increased for a short period, and others increased and remained constant. There were 45% of protein expression profiles that increased linearly, suggesting that the majority of the up-regulated proteins in quiescent cells are required in gradually increasing levels to maintain cell viabilityunder glucose depletion.

We report that 27% of the protein expression profiles in quiescent cells increased for a short period, it is possible that these proteins may require a significant amount of energy to synthesise and are degraded by proteolysis to be used for nutrient recycling (Werner-Washburne *et al*., 1993).

In addition, we also noted 27% of the protein expression profiles increased and remained constant, suggesting that these proteins are tightly regulated in stationary phase growth.

**Table 4.1. List of up-regulated proteins of chronologically aging quiescent cells**

| Protein Name | Day1 | Day2 | Day6 | Day16 | Day46 | Day66 | P-Value |
|---|---|---|---|---|---|---|---|
| Potassium-activated aldehyde dehydrogenase, mitochondrial | 0 | 0.3629 | 0.2317 | 1.6362 | 2.0306 | 1.9221 | <0.0001 |
| Alcohol dehydrogenase 2 | 0 | 0.0564 | 0.1279 | 1.4617 | 1.8469 | 1.5731 | 0.005 |
| Protein SIS1 | 0 | 0.4972 | 0.3867 | 0.6295 | 0.7407 | 1.4314 | <0.0001 |
| Citrate synthase, mitochondrial | 0 | 0.3681 | 0.3015 | 1.1632 | 1.0935 | 1.2005 | <0.0001 |
| Acetyl-CoA hydrolase | 0 | 0.575 | 0.6919 | 1.0607 | 1.3854 | 1.2799 | <0.0001 |
| ATP synthase subunit gamma, mitochondrial | 0 | 0.4523 | 0.5643 | 1.275 | 1.1732 | 1.1278 | <0.0001 |
| Superoxide dismutase, mitochondrial | 0 | 0.2598 | 0.054 | 0.5934 | 1.3678 | 1.8062 | <0.0001 |
| ATP synthase subunit f, mitochondrial | 0 | 0.0454 | 0.2165 | 0.6389 | 1.1062 | 1.2927 | 0.041 |
| Cytochrome b-c1 complex subunit 7 | 0 | 0.4299 | 0.4601 | 1.358 | 1.1657 | 1.3345 | <0.0001 |
| Mitochondrial outer membrane protein | 0 | 0.738 | 0.5987 | 1.4598 | 1.4023 | 0.6733 | <0.0001 |
| Cytochrome c oxidase subunit 6, mitochondrial | 0 | 0.4764 | 0.624 | 1.3054 | 1.2024 | 1.0526 | <0.0001 |
| Heat shock protein SSA3 | 0 | 0.5095 | 0.2731 | 0.8977 | 1.3387 | 0.8747 | <0.0001 |
| Protease A inhibitor 3 | 0 | 0.2202 | 0.5604 | 1.7517 | 1.1721 | 0.1004 | 0.00055 |
| External NADH-ubiquinone oxidoreductase 1, mitochondrial | 0 | 0.3776 | 0.3034 | 1.1946 | 1.4391 | 1.364 | <0.0001 |
| Malate synthase 1, glyoxysomal | 0 | 1.0936 | 0.5398 | 1.9099 | 1.5545 | 1.4629 | <0.0001 |
| Succinate dehydrogenase assembly factor 1 homolog, mitochondrial | 0 | 0.4142 | -0.008 | 1.3202 | 1.6212 | 1.0902 | 0.039 |
| Peroxisomal catalase A | 0 | 1.9361 | 2.0236 | 3.5075 | 3.0565 | 2.9821 | 0.038 |
| Protein FMP16, mitochondrial | 0 | 0.462 | 1.1046 | 2.311 | 1.3721 | -0.3633 | 0.05 |
| Malate dehydrogenase, mitochondrial | 0 | 0.9641 | 0.7547 | 1.5261 | 1.1378 | 1.0759 | <0.0001 |
| Dihydrolipoyllysine-residue succinyltransferase | 0 | 0.3862 | 0.4612 | 1.1817 | 1.3289 | 1.2447 | <0.0001 |
| ATP synthase subunit alpha, mitochondrial | 0 | 0.5331 | 0.4896 | 1.0433 | 1.4174 | 1.2481 | <0.0001 |
| Dihydrolipoyl dehydrogenase, mitochondrial | 0 | 0.3781 | 0.1328 | 0.7619 | 0.8375 | 1.2337 | <0.0001 |
| Acetyl-coenzyme A synthetase 1 | 0 | 1.0968 | 0.7651 | 1.6797 | 1.662 | 1.494 | <0.0001 |
| Isocitrate dehydrogenase, cytoplasmic | 0 | 0.4355 | 0.3353 | 1.3095 | 1.2905 | 1.3503 | <0.0001 |
| Rotenone-insensitive NADH-ubiquinone oxidoreductase, mitochondrial | 0 | 0.0336 | 0.4961 | 0.8649 | 1.0277 | 1.5729 | <0.0001 |
| Heat shock protein 26 | 0 | 0.7538 | 1.0485 | 1.0485 | 2.2274 | 1.9326 | <0.0001 |
| S-formylglutathione hydrolase | 0 | 0.1267 | 0.3807 | 0.8917 | 1.3682 | 1.1012 | 0.005 |
| Transcriptional modulator | 0 | 0.3 | 0.3131 | 0.4376 | 0.9714 | 1.684 | <0.0001 |
| Cytochrome b-c1 complex subunit 1, mitochondrial | 0 | 0.4138 | 0.243 | 0.8925 | 1.2157 | 1.6388 | <0.0001 |
| ATP synthase subunit beta, mitochondrial | 0 | 0.1722 | 0.1537 | 0.8508 | 1.2909 | 1.1061 | <0.0001 |
| Uncharacterized protein YOR020W-A | 0 | 0.7259 | 0.8654 | 1.8589 | 1.2076 | 0.302 | 0.04 |
| ATP synthase subunit d | 0 | 0.7243 | 0.5145 | 1.4333 | 1.6122 | 2.0522 | <0.0001 |

On the other hand, there were 21 down-regulated proteins in the quiescent population with more than 1.5 fold changes ($p \leq 0.05$) in protein expression in at least one time point (Table 4.2). The majority of the down-regulated proteins were ribosome associated proteins (in red), and few translation associated proteins (in orange) (Table 4.2), supporting the observed shutdown of protein synthesis during aging (Motizuki and Tsurugi, 1992).

**Table 4. 2. List of down-regulated proteins of chronologically aging quiescent cells**

| Protein Name | Day1 | Day2 | Day6 | Day16 | Day46 | Day66 | P-Value |
|---|---|---|---|---|---|---|---|
| 60S ribosomal protein L31-A | 0 | -0.823 | -0.4481 | -1.0083 | -1.2917 | -1.6571 | <0.0001 |
| 10 kDa heat shock protein, mitochondrial | 0 | 0.1442 | 0.5365 | 0.6285 | -0.1484 | -1.1324 | <.0001 |
| 60S ribosomal protein L32 | 0 | -0.6992 | -0.2038 | -0.8137 | -1.0474 | -1.0882 | <0.0001 |
| 40S ribosomal protein S27-B | 0 | -0.7023 | -0.4818 | -0.6638 | -1.6936 | -2.0933 | <0.0001 |
| Ribosome-associated complex subunit SSZ1 | 0 | -0.2475 | -0.5888 | -0.7194 | -1.1773 | -1.1901 | <0.0001 |
| Nuclear segregation protein | 0 | 0.1337 | -0.1667 | -0.2165 | -0.971 | -1.0398 | <0.0001 |
| 60S ribosomal protein L36-B | 0 | -0.4748 | -0.1008 | -0.8902 | -1.1796 | -1.9389 | 0.001 |
| Aromatic/aminoadipate aminotransferase 1 | 0 | -0.2292 | -0.2322 | -0.7916 | -1.1182 | -1.3094 | <0.0001 |
| Alanine--tRNA ligase, mitochondrial | 0 | -0.4765 | -0.6952 | -0.8825 | -1.2343 | -1.1086 | <0.0001 |
| 60S ribosomal protein L37-A | 0 | -0.4514 | -0.0394 | -0.5789 | -1.1572 | -1.7621 | <0.0001 |
| (DL)-glycerol-3-phosphatase 1 | 0 | -0.1219 | -0.7377 | -1.3316 | -0.9954 | -1.1798 | <0.0001 |
| Translation machinery-associated protein 10 | 0 | -1.0061 | -0.8822 | -0.8524 | -1.9751 | -2.1282 | <0.0001 |
| 3,4-dihydroxy-2-butanone 4-phosphate synthase | 0 | -0.3349 | -0.7062 | -0.6138 | -1.334 | -1.4686 | <0.0001 |
| Pyruvate kinase 1 | 0 | -0.6949 | -0.4094 | -1.1028 | -0.9805 | -1.0188 | <0.0001 |
| Elongation factor 2 | 0 | -0.2924 | -0.481 | -0.815 | -1.0977 | -1.3072 | <0.0001 |
| Translation machinery-associated protein 7 | 0 | -0.729 | -0.2218 | -0.4869 | -1.4664 | -1.7633 | 0.00032 |
| 60S ribosomal protein L36-A | 0 | -0.4625 | -0.0749 | -0.8224 | -0.9184 | -1.5377 | 0.004 |
| 6-phosphogluconolactonase 3 | 0 | -0.5279 | -1.3344 | -1.4472 | -1.5793 | -1.3959 | <0.0001 |
| 60S ribosomal protein L26-A | 0 | -0.6431 | -0.0913 | -0.6309 | -1.3272 | -1.2537 | 0.049 |
| Very-long-chain enoyl-CoA reductase | 0 | 0.4131 | -0.3192 | -0.2636 | -1.2631 | -1.8 | 0.033 |
| 60S ribosomal protein L14-A | 0 | -1.0012 | -0.6046 | -1.2675 | -1.3409 | -1.198 | 0.003 |

In addition, out of the approximately 1000 proteins identified in the non-quiescent population, 43 proteins were up-regulated with more than 1.5 fold changes ($p \leq 0.05$) in protein expression in at least one time point (Table 4.3). Most up-regulated proteins in the non-quiescent population were mitochondrial structural proteins (in green) and stress response proteins (in orange) (Table 4.3). Among the up-regulated stress response proteins, NADH-cytochrome b5 reductase 2 was showed to be involved in cellular response to oxidative stress (Lee *et al*., 2001). Prohibitin 1 was showed to respond to improper protein folding (Nijtmans *et al*., 2000). GTP-binding protein YPT52 was showed to be involved in endoplasm-to-vacuole targeting (Nickerson *et al*., 2012). In addition, oxidative stress response protein, peroxisomal catalase A, autophagy related protein 27, and Hsp70 nucleotide exchange factor FES1 were among the up-regulated stress response proteins.

Interestingly, cytochrome c1, heme protein (asterisk) was also up-regulated in non-quiescent population.

**Table 4.3. List of up-regulated proteins of chronologically aging non-quiescent cells**

| Protein Name | Day1 | Day2 | Day6 | Day16 | Day46 | Day66 | P-Value |
|---|---|---|---|---|---|---|---|
| Potassium-activated aldehyde dehydrogenase, mitochondrial | 0 | -0.0761 | 0.3377 | 0.8653 | 2.3283 | 2.0038 | <.0001 |
| Mitochondrial outer membrane protein porin 1 | 0 | 0 | 0.2304 | 0.1971 | 1.2773 | 1.7516 | <.0001 |
| Cytochrome b-c1 complex subunit 2, mitochondrial | 0 | 0.0263 | 0.1985 | 0.4156 | 1.5655 | 2.0723 | <.0001 |
| Alcohol dehydrogenase 2 | 0 | -0.1481 | 0.2108 | 0.4996 | 1.1864 | 1.6071 | <.0001 |
| Cytochrome b-c1 complex subunit 1 | 0 | 0.0417 | 0.1037 | 0.3161 | 1.7583 | 2.6124 | <.0001 |
| Glucan 1,3-beta-glucosidase | 0 | 0.0269 | 0.0821 | 0.4756 | 1.3174 | 1.9547 | <.0001 |
| Acetyl-CoA hydrolase | 0 | 0.3475 | 1.0425 | 0.9342 | 1.4234 | 1.0765 | <.0001 |
| Citrate synthase, mitochondrial | 0 | -0.0577 | 0.4052 | 0.6791 | 1.4467 | 1.1206 | <.0001 |
| Phosphoenolpyruvate carboxykinase [ATP] | 0 | 0.7482 | 1.408 | 1.4275 | 1.3741 | 1.551 | <.0001 |
| 2-oxoglutarate dehydrogenase, mitochondrial | 0 | 0.1616 | 0.6063 | 0.7488 | 1.4446 | 1.1785 | <.0001 |
| Protein BMH2 | 0 | -0.0784 | 0.355 | 0.2617 | 1.0334 | 1.2397 | 0.009 |
| Dihydrolipoyllysine-residue succinyltransferase | 0 | -0.0532 | 0.539 | 0.5528 | 1.5822 | 1.1912 | <.0001 |
| Malate synthase 1 | 0 | 0.1431 | 0.3526 | 0.7335 | 1.0091 | 1.0943 | <.0001 |
| NADH-cytochrome b5 reductase 2 | 0 | 0.0073 | 0.6018 | 0.726 | 1.1015 | 1.0037 | <.0001 |
| Peroxisomal hydratase-dehydrogenase-epimerase | 0 | 0.1029 | 0.1833 | 0.5343 | 1.0851 | 1.1006 | <.0001 |
| Rotenone-insensitive NADH-ubiquinone oxidoreductase, mitochondrial | 0 | 0.0908 | 0.081 | 0.3454 | 1.4809 | 1.9668 | <.0001 |
| Isocitrate dehydrogenase, cytoplasmic | 0 | 0.1667 | 0.4949 | 0.7398 | 1.3955 | 1.6044 | <.0001 |
| Cytochrome b-c1 complex subunit Rieske, mitochondrial | 0 | 0.132 | 0.1513 | 0.4821 | 1.5846 | 1.8706 | <.0001 |
| Acetyl-coenzyme A synthetase 1 | 0 | 0.6651 | 1.0704 | 1.3409 | 1.2719 | 1.2869 | <.0001 |
| Protein YGP1 | 0 | -0.2018 | 0.1032 | 0.3536 | 0.7653 | 1.2842 | 0.0002 |
| Mitochondrial phosphate carrier protein | 0 | -0.0799 | 0.1034 | 0.3338 | 1.3019 | 1.1159 | 0.0006 |
| ATP synthase subunit d, mitochondrial | 0 | 0.0435 | 0.6332 | 0.6372 | 1.4118 | 0.9957 | <.0001 |
| Isocitrate dehydrogenase [NAD] subunit 2, mitochondrial | 0 | 0.2373 | 0.4556 | 0.7225 | 1.5364 | 1.2331 | <.0001 |
| Cytochrome c1, heme protein, mitochondrial * | 0 | 0.0156 | 0.069 | 0.295 | 1.1556 | 1.5557 | <.0001 |
| Mitochondrial outer membrane protein OM45 | 0 | 0.4562 | 1.1918 | 1.1847 | 1.149 | 0.3438 | <.0001 |
| Cytochrome b-c1 complex subunit 7 | 0 | 0.3092 | 0.4832 | 0.907 | 1.7917 | 2.1953 | 0.001 |
| Respiratory growth induced protein 2 | 0 | -0.246 | 0.3777 | 0.9738 | 1.4163 | 1.4746 | <.0001 |
| Prohibitin-1 | 0 | -0.1534 | 0.0889 | 0.1127 | 1.1796 | 1.0007 | 0.00032 |
| Mitochondrial peculiar membrane protein 1 | 0 | -0.1642 | 0.5964 | 0.8048 | 1.6681 | 1.6082 | 0.012 |
| Succinate dehydrogenase [ubiquinone] iron-sulfur subunit, mitochondrial | 0 | 0.0211 | 0.32 | 0.6654 | 1.5097 | 1.3157 | <.0001 |
| Cytochrome b2, mitochondrial | 0 | 0.0343 | 0.1024 | 0.4454 | 1.1025 | 0.9906 | <.0001 |
| ATP synthase subunit 4, mitochondrial | 0 | 0.1504 | 0.2193 | 0.4033 | 2.0706 | 1.0524 | <.0001 |
| Altered inheritance of mitochondria protein 24, mitochondrial | 0 | -0.1799 | 0.0934 | 0.3088 | 1.0719 | 1.0315 | <.0001 |
| Peroxisomal catalase A | 0 | -0.0034 | 0.2844 | 0.6071 | 0.9631 | 1.0641 | 0.003 |
| Inactive diphosphatase DCS2 | 0 | 0.1909 | 0.1206 | 0.631 | 0.9517 | 1.2037 | <.0001 |
| Invertase 2 | 0 | 0.254 | 0.5655 | 1.0358 | 1.126 | 1.3857 | <.0001 |
| Cytochrome b-c1 complex subunit 10 | 0 | -0.1038 | 0.292 | 0.7545 | 1.9729 | 2.2896 | 0.009 |
| GTP-binding protein YPT52 | 0 | 0.5892 | 0.5692 | 0.7571 | 1.0194 | 1.1438 | <.0001 |
| Putative mitochondrial carnitine O-acetyltransferase | 0 | 0.5936 | 0.7269 | 0.6498 | 1.2375 | 1.0898 | <.0001 |
| Mitochondrial organizing structure protein 1 | 0 | 0.3974 | 0.4061 | 0.8531 | 1.6137 | 1.4409 | 0.00092 |
| Autophagy-related protein 27 | 0 | 0.0617 | 0.304 | 0.2781 | 0.9154 | 1.3304 | 0.045 |
| 54S ribosomal protein L8, mitochondrial | 0 | 0.2146 | -0.1096 | 0.7442 | 1.8347 | 1.5893 | 0.044 |
| Hsp70 nucleotide exchange factor FES1 | 0 | -0.4092 | 1.2102 | 1.8284 | 2.5067 | 2.806 | 0.038 |

To verify whether the up-regulation of mitochondrial structural proteins and stress response protein in the wild type, non-quiescent population was due to cell function or leakage of mitochondria due to lysis, the quiescent and non-quiescent

populations were stained with a yeast mitochondrial stain, MitoTracker GreenFM, which accumulates in functioning mitochondria by reacting with accessible peptides and proteins to form a green fluorescent conjugate. Mitochondrial staining, surprisingly, showed no statistically significant difference between wild type, quiescent and non-quiescent populations (Figure 4.2).

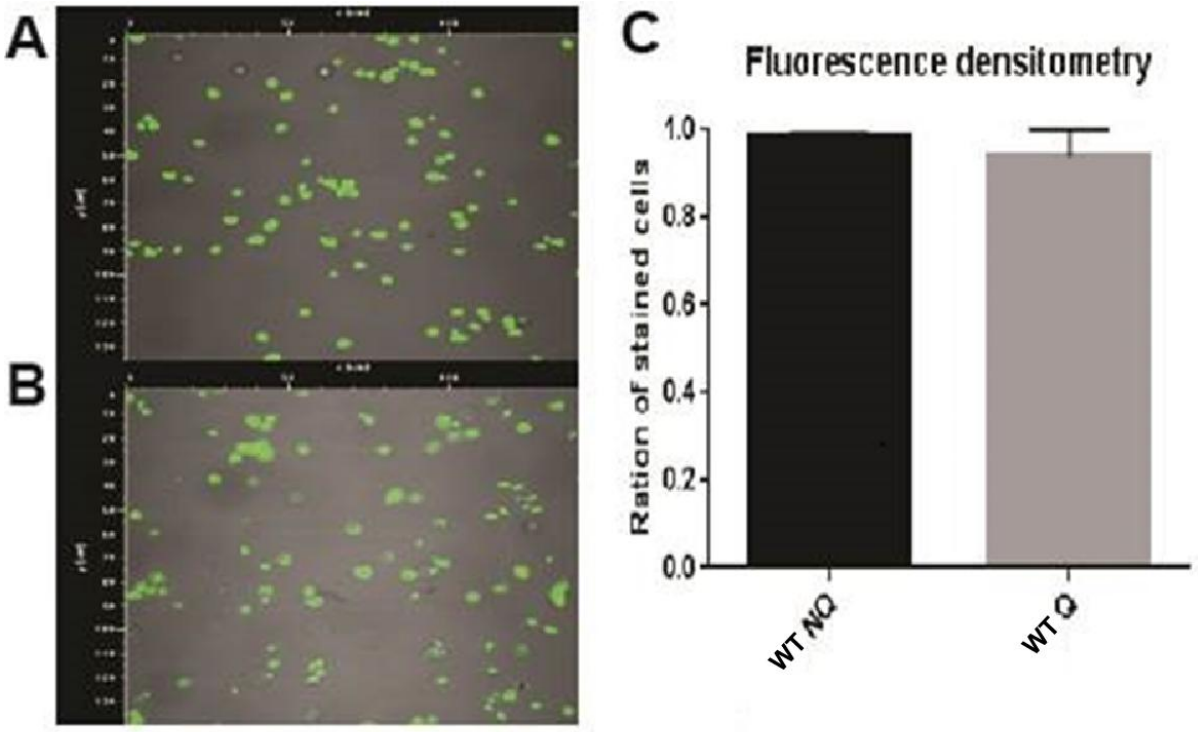


**Figure 4.2.Mitochondrial staining of wild type quiescent and non-quiescent populations.**Laser scanningconfocal microscopy images of cells stained by MitoTracker GreenFM probe. Merged green and light fields of wild type quiescent (panel A) and non-quiescent (panel B) populations. The ration of stained green cells over the total number of cells is showed in panel C. Standard deviation bars represent four technical replicates.

To characterise the biological processes that are significantly enriched, functional analysis was performed on the identified quiescent and non-quiescent total proteins using GOEAST software. Each protein identified was statistically analysed to evaluate, and ascribed its GO term. The most significantly enriched GO terms of the quiescent and non-quiescent population are listed in Table 4.4 and Table 4.5 respectively. GO analysis revealed that differentially expressed proteins

during chronological aging participated in several biological processes. The most significant biological processes in the quiescent population were oxidation-reduction process, energy derivation by oxidation of organic compounds, and single-organism metabolic process (Table 4.4), implying that chronologically aging WT cells are viable even though they are not dividing, and require energy for minimal metabolic activities. Interestingly, purine nucleoside triphosphate biosynthetic process (in green) which is involved in DNA synthesis was also significantly enriched, chronological aging terms (in green) and age-dependent response to oxidative stress (in green) were also significantly enriched.

**Table 4. 4. Gene Ontology (GO) functional analysis of chronologically aging quiescent pool proteins**

| GOID | Ontology | Term | P-Value |
|---|---|---|---|
| GO:0055114 | biological_process | oxidation-reduction process | 4.31E-08 |
| GO:0015980 | biological_process | energy derivation by oxidation of organic compounds | 5.04E-08 |
| GO:0044710 | biological_process | single-organism metabolic process | 2.12E-07 |
| GO:0045333 | biological_process | cellular respiration | 5.53E-07 |
| GO:0006091 | biological_process | generation of precursor metabolites and energy | 7.42E-07 |
| GO:0009145 | biological_process | purine nucleoside triphosphate biosynthetic process | 0.00047 |
| GO:0001300 | biological_process | chronological cell aging | 0.00092 |
| GO:0072593 | biological_process | reactive oxygen species metabolic process | 0.00402 |
| GO:0009152 | biological_process | purine ribonucleotide biosynthetic process | 0.0059 |
| GO:0001306 | biological_process | age-dependent response to oxidative stress | 0.0244 |

Similarly, in the non-quiescent population the most significantly enriched biological processes were oxidation-reduction process, energy derivation by oxidation of organic compounds and single-organism metabolic process.

**Table 4.5.Gene Ontology (GO) functional analysis of chronologically aging non-quiescent pool proteins**

| GOID | Ontology | Term | P-Value |
|---|---|---|---|
| GO:0055114 | biological_process | oxidation-reduction process | 5.41E-09 |
| GO:0015980 | biological_process | energy derivation by oxidation of organic compounds | 3.44E-08 |
| GO:0044710 | biological_process | single-organism metabolic process | 4.83E-08 |
| GO:0042775 | biological_process | mitochondrial ATP synthesis coupled electron transport | 1.22E-07 |
| GO:0006119 | biological_process | oxidative phosphorylation | 1.32E-07 |

## 4.4. Discussion

Aging is the result of a balance between damage and repair. The rate of aging and the appearance of age-related phenotype are regulated by stress response and repair pathways (Kourtis and Tavernarakis, 2011). In Table 4.1, proteome quantitative analysis of the quiescent population showed the up-regulation of protein classes associated with stress response, including superoxide dismutase, and heat shock proteins.

The up-regulation of oxidative stress response proteins in quiescent population is consistent with the showed low reactive oxygen species in quiescent cells (Allen *et al*., 2006). Superoxide is one of the most abundant reactive products of oxygen generated through oxidative phosphorylation in the mitochondria. ROS can damage cellular macromolecules and high levels of oxidative damage products are strongly linked with aging (Hekimi and Guarente, 2003). Lifespan extension in yeast, worms, flies and mice can be increased up to several fold by mutations in genes that increase protection against superoxide and other stresses (Longo and Finch, 2003). We noted that superoxide dismutase was up-regulated in the chronologically aging,WT quiescent cells (Table 4.1), which was showed to catalyze the breakdown of superoxide into hydrogen peroxide and water, suggesting their integral role in ROS regulation (Fridovich, 1995). It was showed that the death of

yeast population is regulated in part by superoxide generated in mitochondria and was delayed by high expression levels of superoxide dismutases or human antiapoptotic protein Bcl-2 (Fabrizio *et al*., 2004).

The high abundance of heat shock proteins we observed is in agreement with the involvement of heat shock protein genes in aging. It was noted that heat shock proteins were induced in different stressful conditions, and the efficiency of heat shock response was noted to decline with age (Sőti and Csermely, 2000; Werner-Washburne *et al*., 1989). It is suggested that intracellular protein denaturation caused by metabolic stresses during aging may signal the activation of the heat shock genes (Ananthan *et al*., 1986). In fruit fly it was showed that the expression of heat shock genes was transient at temperatures below 37°C, suggesting a self-regulating mechanism (Lindquist, 1980). The rate-limiting step in the deactivation of heat shock genes is the degradation of large quantities of abnormal proteins caused by metabolic insults. The abnormal proteins include conformationally altered and inactive enzymes, and proteins that are oxidatively damaged (Gershon and Gershon, 1970; Stadtman and Levine, 2003). Heat shock proteins ensure survival under stressful conditions that yeast cells face in stationary phase. Heat shock proteins have important roles in the synthesis, transport and folding of proteins (Gething and Sambrook, 1992). The up-regulation of heat shock proteins we observed during aging may enhance proper protein folding under starvation and conditions that encourages protein aggregates.

We observed a striking down-regulation in the quiescent population for ribosome associated proteins,supporting the observed shutdown of protein synthesis during aging (Motizuki and Tsurugi, 1992). The primary functions of TOR, Sch9 and PKA is to regulate protein translation in response to environmental conditions

(Jorgensen *et al*., 2004; Powers and Walter, 1999). Under conditions of glucose exhaustion or nitrogen starvation, or upon inhibition of TOR with rapamycin, ribosomal protein transcription is strikingly reduced and translation is largely impaired (Jorgensen *et al*., 2004; Powers and Walter, 1999). Ribosome synthesis requires significant mass and energy, therefore, it is possible that mRNA levels of ribosomal protein genes are notably reduced under stressful conditions (Gasch *et al*., 2000). In addition, rDNA is down-regulated in response to a number of stresses, and ribosomal protein genes are among the tightly co-regulated genes in the yeast genome (Nierras and Warner, 1999). We noted a drastic down-regulation of the 60S ribosomal proteins in Table 4.2., which is in agreement with the increased yeast lifespan upon deletion of genes encoding 60S subunit proteins(Steffen *et al*., 2008).

Table 4.3 showed that mitochondrial structural and stress response proteins were up-regulated in chronologically aging non-quiescent cells. The up-regulation of mitochondrial structural and stress response proteins was suggested to be a response mechanism to mitochondrial damage, and was linked to Huntington's disease and Alzheimer's disease in humans (Manczak *et al*., 2011; Shirendeb *et al*., 2011). Mitochondrial structural proteins play an important role in the organisation and assembly of the electron transport chain (Green and Hechter, 1965). We showed an increase in mitochondrial outer membrane protein porin, Por1p, in Table 4.3.The involvement of Por1p either to cytochrome c release or to cell survival has been contradictory (Harris *et al*., 2000; Priault *et al*., 1999). The deletion of *POR1* gene was showed to enhance apoptosis, suggesting that Por1p protects against apoptosis. It maybe that cells need to increase Por1p levels to protect directly against apoptosis, which further points to the advanced damaged state of non-quiescent cells.

Among the stress response protein up-regulated in non-quiescent population, Protein BMH2 was up-regulated which is involved in DNA damage checkpoint and is linked to protection against stress-induced apoptosis (Clapp *et al*., 2012; Lottersberger *et al*., 2003). *BMH2*is one of two genes in yeast that show strong similarity to the ubiquitous and highly conserved 14-3-3 gene family (Gelperin *et al*., 1995). The function of 14-3-3 protein is not well understood, but it may play a role insignal transduction(Burbelo and Hall, 1995).

The up-regulation of mitochondrial structural proteins, stress response protein, and the putative cytochrome c1, heme protein (Table 4.3) is consistent with apoptotic conditions (Madeo, 1997).Cytochrome c1, is one of the catalytic subunits of the cytochrome bc1 complex and is essential for electron transfer within the complex and forrespiratory growth(Hunte *et al*., 2003). Apoptotic phenotypes such as translocation of cytochrome c and the production of ROS occur prior to cell death(Kluck, 1997). The translocation of cytochrome c from mitochondria to the cytosol initiates the mitochondrial apoptosome complex that activates caspases (Adrain and Martin, 2001). Cytochrome c is loosely bound to the outer face of the inner mitochondrial membrane, and its translocation to the cytosol disrupts the electron flow at complex III, a site of the respiratory chain, and may redirect the electron transfer to the generation of ROS (Cai *et al*., 1998). Aging cultures were demonstrated to accumulate ROS, which is typically a precursor to age-induced apoptosis (Herker *et al*., 2004).

We next looked at autophagy-related protein 27 in Table 4.3, which is a type I membrane protein involved in autophagy and the cytoplasm to vacuole targeting (Cvt) pathway; and is suggested to be involved in membrane delivery to the phagophore assembly site (Wurmser and Emr, 2002). Autophagy is tightly regulated

because degradation of bulk of cytoplasm can be lethal. In yeast, induction of autophagy is repressed by the Tor pathway (via TORC1) through dephosphorylation of Atg13p and complex formation between Atg13p-Atg17p-Atg1p (Suzuki *et al*., 2004). It was reported that Atg27 is another transmembrane protein required for Atg9 cycling (Yen *et al*., 2007). Atg9 localizes to mitochondria, and cycles between this compartment and the pre-autophagosomal structure, the site of organization for Cvt vesicle and autophagosome formation (Tucker *et al*., 2003). It was showed that under nitrogen starvation deletion of *ATG27* leads to reduced autophagy (Yen *et al*., 2007). In yeast, autophagy is defined as a single cell's adaptation to starvation. Under starvation conditions, autophagy is required to maintain adequate amino acid levels which are needed for protein synthesis, especially proteins that are up-regulated by starvation, and decrease in protein synthesis is the result of autophagy deficiency (Onodera and Ohsumi, 2005; Suzuki *et al*., 2011). The up-regulation of Atg27 in WT non-quiescent cells may contribute to the stress resistance of quiescent cells by providing nutrients and energy, and also suggest the damaged state of non-quiescent cells.

## 4.5 Reference List


Adrain, C., and Martin, S.J. (2001). The mitochondrial apoptosome: a killer unleashed by the cytochrome seas. Trends Biochem. Sci. *26*, 390–397.

Allen, C., Büttner, S., Aragon, A.D., Thomas, J.A., Meirelles, O., Jaetao, J.E., Benn, D., Ruby, S.W., Veenhuis, M., Madeo, F., et al. (2006). Isolation of quiescent and nonquiescent cells from yeast stationary-phase cultures. J. Cell Biol. *174*, 89–100.

Ananthan, J., Goldberg, A., and Voellmy, R. (1986). Abnormal proteins serve as eukaryotic stress signals and trigger the activation of heat shock genes. Science (80-. ). *232*, 522–524.

Blasco, M.A. (2005). Telomeres and human disease: ageing, cancer and beyond. Nat. Rev. Genet. *6*, 611–622.

Burbelo, P.D., and Hall, A. (1995). 14-3-3 Proteins: Hot numbers in signal transduction. Curr. Biol. *5*, 95–96.

Cai, J., Yang, J., and Jones, D. (1998). Mitochondrial control of apoptosis: the role of cytochrome c. Biochim. Biophys. Acta - Bioenerg. *1366*, 139–149.

Clapp, C., Portt, L., Khoury, C., Sheibani, S., Norman, G., Ebner, P., Eid, R., Vali, H., Mandato, C.A., Madeo, F., et al. (2012). 14-3-3 protects against stress-induced apoptosis. Cell Death Dis. *3*, e348.

Davidson, G.S., Joe, R.M., Roy, S., Meirelles, O., Allen, C.P., Wilson, M.R., Tapia, P.H., Manzanilla, E.E., Dodson, A.E., Chakraborty, S., et al. (2011). The proteomics of quiescent and nonquiescent cell differentiation in yeast stationary-phase cultures. Mol. Biol. Cell *22*, 988–998.

Degrassi, G., Uotila, L., Klima, R., and Venturi, V. (1999). Purification and properties of an esterase from the yeast *Saccharomyces cerevisae* and Identification of the Encoding Gene. Appl. Envir. Microbiol. *65*, 3470–3472.

Fabrizio, P., Battistella, L., Vardavas, R., Gattazzo, C., Liou, L.-L., Diaspro, A., Dossen, J.W., Gralla, E.B., and Longo, V.D. (2004). Superoxide is a mediator of an altruistic aging program in *Saccharomyces cerevisae*. J. Cell Biol. *166*, 1055–1067.

Fridovich, I. (1995). Superoxide radical and superoxide dismutases. Annu. Rev. Biochem. *64*, 97–112.

Fuge, E.K., Braun, E.L., and Werner-Washburne, M. (1994). Protein synthesis in long-term stationary-phase cultures of *Saccharomyces cerevisae*. J. Bacteriol. *176*, 5802–5813.

Gasch, A.P., Spellman, P.T., Kao, C.M., Carmel-Harel, O., Eisen, M.B., Storz, G., Botstein, D., and Brown, P.O. (2000). Genomic expression programs in the response of yeast cells to environmental changes. Mol. Biol. Cell *11*, 4241–4257.

Gelperin, D., Weigle, J., Nelson, K., Roseboom, P., Irie, K., Matsumoto, K., and Lemmon, S. (1995). 14-3-3 proteins: potential roles in vesicular transport and Ras signaling in *Saccharomyces cerevisae*. Proc. Natl. Acad. Sci. *92*, 11539–11543.

Gershon, H., and Gershon, D. (1970). Detection of inactive enzyme molecules in ageing organisms. Nature *227*, 1214–1217.

Gething, M.J., and Sambrook, J. (1992). Protein folding in the cell. Nature *355*, 33–45.

Green, D.E., and Hechter, O. (1965). Assembly of membrane subunits. Proc. Natl. Acad. Sci. U. S. A. *53*, 318–325.

Harris, M.H., Vander Heiden, M.G., Kron, S.J., and Thompson, C.B. (2000). Role of oxidative phosphorylation in Bax toxicity. Mol. Cell. Biol. *20*, 3590–3596.

Hekimi, S., and Guarente, L. (2003). Genetics and the specificity of the aging process. Science *299*, 1351–1354.

Herker, E., Jungwirth, H., Lehmann, K.A., Maldener, C., Fröhlich, K.-U., Wissing, S., Büttner, S., Fehr, M., Sigrist, S., and Madeo, F. (2004). Chronological aging leads to apoptosis in yeast. J. Cell Biol. *164*, 501–507.

Hunte, C., Palsdottir, H., and Trumpower, B.L. (2003). Protonmotive pathways and mechanisms in the cytochrome bc1 complex. FEBS Lett. *545*, 39–46.

Jorgensen, P., Rupes, I., Sharom, J.R., Schneper, L., Broach, J.R., and Tyers, M. (2004). A dynamic transcriptional network communicates growth potential to ribosome synthesis and critical cell size. Genes Dev. *18*, 2491–2505.

Kluck, R.M. (1997). The release of Cytochrome c from mitochondria: a primary site for Bcl-2 regulation of apoptosis. Science (80-. ). *275*, 1132–1136.

Kourtis, N., and Tavernarakis, N. (2011). Cellular stress response pathways and ageing: intricate molecular relationships. EMBO J. *30*, 2520–2531.

Lee, J.-S., Huh, W.-K., Lee, B.-H., Baek, Y.-U., Hwang, C.-S., Kim, S.-T., Kim, Y.-R., and Kang, S.-O. (2001). Mitochondrial NADH-cytochrome b5 reductase plays a crucial role in the reduction of d-erythroascorbyl free radical in *Saccharomyces cerevisae*. Biochim. Biophys. Acta - Gen. Subj. *1527*, 31–38.

Lindquist, S. (1980). Translational efficiency of heat-induced messages in *Drosophila melanogaster* cells. J. Mol. Biol. *137*, 151–158.

Longo, V.D., and Finch, C.E. (2003). Evolutionary medicine: from dwarf model systems to healthy centenarians? Science *299*, 1342–1346.

Longo, V.D., Gralla, E.B., and Valentine, J.S. (1996). Superoxide dismutase activity is essential for stationary phase survival in *Saccharomyces cerevisae*: mitochodnrial production of toxic oxygen species *in vivo*. J. Biol. Chem. *271*, 12275–12280.

Lottersberger, F., Rubert, F., Baldo, V., Lucchini, G., and Longhese, M.P. (2003). Functions of *Saccharomyces cerevisae* 14-3-3 proteins in response to DNA damage and to DNA replication stress. Genetics *165*, 1717–1732.

Madeo, F. (1997). A yeast mutant showing diagnostic markers of Early and Late Apoptosis. J. Cell Biol. *139*, 729–734.

Manczak, M., Calkins, M.J., and Reddy, P.H. (2011). Impaired mitochondrial dynamics and abnormal interaction of amyloid beta with mitochondrial protein Drp1 in neurons from patients with Alzheimer's disease: implications for neuronal damage. Hum. Mol. Genet. *20*, 2495–2509.

Motizuki, M., and Tsurugi, K. (1992). The effect of aging on protein synthesis in the yeast *Saccharomyces cerevisae*. Mech. Ageing Dev. *64*, 235–245.

Nickerson, D.P., Russell, M.R.G., Lo, S.-Y., Chapin, H.C., Milnes, J.M., and Merz, A.J. (2012). Termination of isoform-selective Vps21/Rab5 signaling at endolysosomal organelles by Msb3/Gyp3. Traffic *13*, 1411–1428.

Nierras, C.R., and Warner, J.R. (1999). Protein kinase C enables the regulatory circuit that connects membrane synthesis to ribosome synthesis in *Saccharomyces cerevisae*. J. Biol. Chem. *274*, 13235–13241.

Nijtmans, L.G., de Jong, L., Artal Sanz, M., Coates, P.J., Berden, J.A., Back, J.W., Muijsers, A.O., van der Spek, H., and Grivell, L.A. (2000). Prohibitins act as a membrane-bound chaperone for the stabilization of mitochondrial proteins. EMBO J. *19*, 2444–2451.

Onodera, J., and Ohsumi, Y. (2005). Autophagy is required for maintenance of amino acid levels and protein synthesis under nitrogen starvation. J. Biol. Chem. *280*, 31582–31586.

Park, S.-H., Kukushkin, Y., Gupta, R., Chen, T., Konagai, A., Hipp, M.S., Hayer-Hartl, M., and Hartl, F.U. (2013). PolyQ proteins interfere with nuclear degradation of cytosolic proteins by sequestering the Sis1p chaperone. Cell *154*, 134–145.

Powers, T., and Walter, P. (1999). Regulation of ribosome biogenesis by the rapamycin-sensitive TOR-signaling pathway in *Saccharomyces cerevisae*. Mol. Biol. Cell *10*, 987–1000.

Priault, M., Chaudhuri, B., Clow, A., Camougrand, N., and Manon, S. (1999). Investigation of Bax-induced release of cytochrome c from yeast mitochondria . Permeability of mitochondrial membranes, role of VDAC and ATP requirement. Eur. J. Biochem. *260*, 684–691.

Shirendeb, U., Reddy, A.P., Manczak, M., Calkins, M.J., Mao, P., Tagle, D.A., and Reddy, P.H. (2011). Abnormal mitochondrial dynamics, mitochondrial loss and mutant huntingtin oligomers in Huntington's disease: implications for selective neuronal damage. Hum. Mol. Genet. *20*, 1438–1455.

Sőti, C., and Csermely, P. (2000). Molecular chaperones and the aging process. Biogerontology *1*, 225–233.

Stadtman, E.R., and Levine, R.L. (2003). Free radical-mediated oxidation of free amino acids and amino acid residues in proteins. Amino Acids *25*, 207–218.

Steffen, K.K., MacKay, V.L., Kerr, E.O., Tsuchiya, M., Hu, D., Fox, L.A., Dang, N., Johnston, E.D., Oakes, J.A., Tchao, B.N., et al. (2008). Yeast life span extension by depletion of 60s ribosomal subunits is mediated by Gcn4. Cell *133*, 292–302.

Suzuki, K., Noda, T., and Ohsumi, Y. (2004). Interrelationships among Atg proteins during autophagy in *Saccharomyces cerevisae*. Yeast *21*, 1057–1065.

Suzuki, S.W., Onodera, J., and Ohsumi, Y. (2011). Starvation induced cell death in autophagy-defective yeast mutants is caused by mitochondria dysfunction. PLoS One *6*, e17412.

Tucker, K.A., Reggiori, F., Dunn, W.A., and Klionsky, D.J. (2003). Atg23 is essential for the cytoplasm to vacuole targeting pathway and efficient autophagy but not pexophagy. J. Biol. Chem. *278*, 48445–48452.

Werner-Washburne, M., Becker, J., Kosic-Smithers, J., and Craig, E.A. (1989). Yeast Hsp70 RNA levels vary in response to the physiological status of the cell. J. Bacteriol. *171*, 2680–2688.

Werner-Washburne, M., Braun, E., Johnston, G.C., and Singer, R.A. (1993). Stationary phase in the yeast *Saccharomyces cerevisae*. Microbiol. Mol. Biol. Rev. *57*, 383–401.

Werner-Washburne, M., Braun, E.L., Crawford, M.E., and Peck, V.M. (1996). Stationary phase in *Saccharomyces cerevisae*. Mol. Microbiol. *19*, 1159–1166.

Werner-Washburne, M., Wylie, B., Boyack, K., Fuge, E., Galbraith, J., Weber, J., and Davidson, G. (2002). Comparative analysis of multiple genome-scale data sets. Genome Res. *12*, 1564–1573.

Wurmser, A.E., and Emr, S.D. (2002). Novel PtdIns(3)P-binding protein Etf1 functions as an effector of the Vps34 PtdIns 3-kinase in autophagy. J. Cell Biol. *158*, 761–772.

Yen, W.-L., Legakis, J.E., Nair, U., and Klionsky, D.J. (2007). Atg27 is required for autophagy-dependent cycling of Atg9. Mol. Biol. Cell *18*, 581–593.

Zheng, Q., and Wang, X.-J. (2008). GOEAST: a web-based software toolkit for Gene Ontology enrichment analysis. Nucleic Acids Res. *36*, W358–W363.

# CHAPTER5

## AStudy of the Proteomes of Histone Mutant Yeast Strains that Exhibit Extended Chronological Lifespans

### 5.1. Introduction

In previous Chapters we have identified specific histone H3 and H4 mutants that exhibited extended chronological lifespans relative to the population average. We have investigated the transcriptomes of these mutants, and have shown that the transcriptomic profiles of the H4K16A and H4H18A mutants were similar, and both showed HM derepression, with active rRNA synthesis, ribosome assembly, and carbon and nitrogen metabolic processes. The H3E50 mutant strain genes associated with mitochondrial electron transport, tricarboxylic acid cycle, ATP synthesis coupled proton transport, oxidative phosphorylation, glutamate metabolic process, glyoxylate cycle, and purine ribonucleoside triphosphate biosynthetic processes were upregulated, painting the picture of a cell that is very actively utilising nutrients. Importantly, we didn't see upregulation of stress response genes in the H4K16Q and H4H18A strains. Genes associated with response to hydrogen peroxide, reactive oxygen species metabolic process and response to oxidative stress appeared in the H3E50A mutant. We suggested that upregulataion of these genes may be tied to the very high metabolic activity of the H3E50A mutant strain. We could not identify a common set of genes that were highly expressed or highly repressed that was mechanistically linked with extension of chronological lifespan. For this reason we decided to investigate the proteome of the aged histone mutant strains. Since we previously saw, when investigating the proteome of an aging yeast cell (Chapter 4) that proteins that were highly upregulated at day 45 and day 60

during extended incubation in stationary phase, were already significantly upregulated by day 14, we decided to incubate the histone mutant strains for up to 14 days in the expectation that any important changes in the proteome should be visible by that time. We discuss the results of this proteomic study below.

## 5.2. Materials and Methods

### *5.2.2. Yeast Protein Extraction*

The quiescent cells of selected histone yeast mutant strains were harvested at different time points as previously described. Cell pellets were resuspended in pre-warmed, 1.13 ml cracking buffer [6 M guanidine hydrochloride, 1% (w/v) octylglucopyranoside, 0.1% (w/v) Rapigest, 40 mM MOPS pH6.8, 0.1% (w/v) EDTA, 2 µl of 0.5 M Tris(2-carboxyethyl)phosphine hydrochloride (TCEP), 70 µl protease inhibitor cocktail, 50 µl of 100X PMSF]. The cell suspensions were transferred to a micro-centrifuge tube containing 80 µl of glass beads per 7.5 $OD_{600}$ units of cells. The samples were heated at 70°C for 10 min, and vortexed vigorously for 1 min. The cell debris and unbroken cells were centrifuged in a micro-centrifuge at 20 817 x g for 5 min at 4°C. The supernatant was transferred to a fresh micro-centrifuge tube, and placed on ice. The pellets containing cell debris and unbroken cells were placed in 100°C boiling water bath for 3-5 min, and vortexed vigorously for 1 min. The pellets were then centrifuged in a micro-centrifuge at 20 817 x g for 5 min at 4°C. Each supernatant was combined. The supernatant was precipitated using 5 volumes of cold acetone, and trichloroacetic acid (TCA) to a final concentration of 20% (w/v). Total protein was collected by centrifugation at 17 418 x g for 5 min at 4°C. Following air drying at room temperature the pellet was dissolved in 100 mM diluted

triethylammonium bicarbonate (TEAB) containing 4 M guanidine-HCl and 1% octylgluco-mano-pyranoside.

### *5.2.3. In-Solution Protein digestion*

The protein solution was reduced for 30 minutes at 37°C by adding 50 mM triscarboxyethyl phosphine (TCEP; Fluka) in 100 mM TEAB. Following reduction, cysteine residues were modified to methylthio using 200 mM methane methylthiosulphonate (MMTS; Sigma) in 100 mM TEAB for 30 minutes. The protein solution was then diluted to 98 µl with 100 mM TEAB, digested with 10 µl of 1 µg/µl trypsin (Promega) solution and incubating at 37 °C overnight. The peptide solution was dried down and resuspended in 20 µl 500 mM TEAB, pH8.

### *5.2.4. Labelling with iTRAQ 8-Plex Reagent(s)*

The iTRAQ 8-plex tags were dissolved in 70 µl 2-propanol as per manufacturer's instructions and added to the respective peptide solution tubes. The labelling reactions were allowed to proceed for two hours and a 2 µl aliquot was removed from each sample for quality control analysis, 200 µl of sterile water was added to each peptide labelling solution and the tags were hydrolysed for two hours. The sample volumes were subsequently reduced and the individual samples combined.

### *5.2.5. Desalting*

Residual digestion reagents were removed using an in-house manufactured $C_{18}$ stage tip (Empore Octadecyl $C_{18}$ extraction discs; Supelco). The sample was loaded onto the stage tip following activation of the $C_{18}$ membrane with 30 µl methanol (Sigma) and equilibrated with 30µl of 2% (v/v) acetonitrile: 0.05% (v/v)

TFA. The bound sample was washed with 30 μl of 2% (v/v) acetonitrile: (v/v) 0.05% TFA and eluted with 30 μl 50% (v/v) acetonitrile: (v/v) 0.05% TFA. The eluate was evaporated to dryness. The dried peptides were dissolved in 2% (v/v) acetonitrile: 0.1% (v/v) FA for LC-MS analysis.

### *5.2.6. Liquid Chromatography*

Liquid chromatography was performed on a Thermo Scientific Ultimate 3000 RSLC equipped with a 2 cm x 100 μm $C_{18}$ trap column and a 50 cm x 75 μm in-house manufactured $C_{18}$ column (Luna $C_{18}$, 5 μm; Phenomenex) analytical column. The solvent system employed was: Solvent A, 2% (v/v) acetonitrile: 0.1% (v/v) FA and Solvent B, 100% (v/v) acetonitrile. The sample was loaded onto the $C_{18}$ trap column at a flow rate of 5 μl/min from a temperature controlled autosampler set at 7°C. Loading was performed for 10 min before the sample was eluted onto the analytical column. Flow rate was set to 300 nl/min and the gradient generated using Chromeleon non-linear gradient 7 (Dionex) as follows: 2.0% A for 6 min; 2%-35% B from 6-140 min, 35-50% B from 140-150 min and 50%-80% B from 150-160 minutes. The column was washed for 10 min with 80% B followed by equilibration. Chromatography was performed at 50°C and the outflow delivered to the mass spectrometer through a stainless steel nano-bore emitter.

### *5.2.7. Mass spectrometry*

Mass spectrometry was performed using a Thermo Scientific Orbitrap Fusion Tribid mass spectrometer equipped with a Nanospray Flex ionization source. The sample was introduced through a stainless steel nano-bore emitter. Data was collected in positive mode with spray voltage set to 1.9 kV and ion transfer capillary set to 275°C. Spectra were internally calibrated using polysiloxane ions at m/z =

445.12003 and 371.10024. MS1 scans were performed using the orbitrap detector set at 12 000 resolution over the scan range 350-1650 Da with automatic gain control (AGC) target at 2 E5 and maximum injection time of 50 msec. Data was acquired in profile mode.

MS2 acquisitions were performed using monoisotopic precursor selection for ion with charges (+2 to +7) with error tolerance set to +/- 10ppm. Precursor ions were excluded from fragmentation once for a period of 45 sec. Precursor ions were selected for fragmentation in HCD mode using the quadrupole mass analyzer with HCD energy set to 35%. Fragment ions were detected in the ion trap mass analyzer using rapid scan rate. The AGC target was set to 5E4 and the maximum injection time to 50 msec. The data was acquired in centroid mode. Quantitative data was acquired in MS3 using synchronous precursor selection (SPS). The MS2 precursors were selected with an isolation window of *m/z*=200 and detection following HCD fragmentation in the orbitrap mass analyser at 60 000 resolution over the scan range *m/z*=100-500.

### *5.2.8. Data Analysis*

The raw files were generated by the mass spectrometer were imported into Proteome Discoverer v1.4 (Thermo Scientific) and processed using the Mascot algorithm (Matrix Science) and SequestHT algorithm, included in Proteome Discoverer workflow. Dynamic modifications were set as acetyl (N-term), deamidation (NQ), oxidation (M), and iTRAQ 8-plex (Y). Static modifications were set as methylthio (C), and iTRAQ 8-plex (N-term). Peptide validation was performed using the percolator node set to search against a decoy database with strict FDR 1%. Additional analysis was performed using the Adromeda (included with Maxquant 1.5.0.0and the X! Tandem Sledgehammer (2013/09/01.1) algorithms. Dynamic and

static modifications were set as before. Database interrogation was performed against the UniProt *S. cerevisiae* database (2014 edition) with trypsin cleavage allowing for 2 missed cleavages. A total of six output files were generated using the above mentioned algorithms. The output files were combined for statistical analysis and quantitation using Scaffold software version 4.4.1.1 (Proteomesoftware). Quantitation were set to spectral counting with normalization and regulation reported as fold change per category (fold change times p<=0.0002). Protein filter settings were FDR at 5% with minimum of 3 peptides per protein. Gene ontology assignment was also performed using gene association GO database.

## 5.3. Results

Many mechanisms have been proposed to explain the phenomenon of lifespan extension. Most of the suggested mechanisms ultimately involve expression of stress response genes. It is generally thought that the expression of stress response genes and stress response proteins protect the cell against possible damage that stress can cause, i.e., diminish the impact that the stress may have on cellular processes. There are many different types of stress, including temperature, ionic, pH, nutrient and oxidative stress. The latter stress has received much attention in the longevity research field due to the reduction in this stress with calorie restriction, a state of low nutrition that was shown by the Guarente group to be involved in longevity in several different model organisms (Lin *et al*., 2002)

To gain insight into the mechanism(s) that underlie the extension of chronological lifespan in the H3 and H4 histone mutant strains that we have identified, we investigated the proteomes of these strains at day 2 and day 14 post-inoculation. The day 2 strain will be past diauxic shift, but will not have entered stationary phase, and the day 14 culture will be in stationary phase. We observed in a previous proteomic study that major proteome differences visible at day 45 and day 60 of incubation were already clearly visible at day 14, hence the decision to incubate the strains for only 14 days. Total proteins were extracted, trypsin digested, and labelled with isotopically coded iTRAQ reagents, and quantitated on the Fusion orbitrap (Thermo Scientific) mass spectrometer. We firstly normalized the 14 day protein levels to the day 2 protein levels of the same strain.

The proteins that exhibited a significant up or down-regulation at day 14 relative to day 2 of H4K16Q mutant strain are shown in Table 5.1. An analysis of GO term enrichment for the upregulated proteins showed no enrichment, meaning that

there is no single specific class or process that is particularly active in terms of the number of protein members of that class that are up-regulated. However, a perusal of the list of up-regulated proteins will identify many interesting proteins.

Snz1 is involved in vitamin B6 biosynthesis, and is associated with organophosphate metabolic processes. It is regulated by, among others, Fkh1,Gcn4, Pho4, and Rap1 (Rodríguez-Navarro *et al*., 2002). Although Fkh1, a member of the forkhead family of transcriptional regulators, was shown to activate genes in response to temperature stress, and is involved in HM silencing, it is not biologically clear why induction of Snz1 should be associated with long lifespan (Venters *et al*., 2011). Jhd2 induction is interesting because it is a JmjC domain family histone demethylase involved in global demethylation of H3K4, a histone mark added by Set1 and associated with active transcription (Boa *et al*.). Jhd2 ( alias Kdm5) is involved in the regulated shutdown of transcription during gametogenesis, and is also implicated in condensation and silencing of the rRNA loci (Ryu and Ahn, 2014). Jhd2 is negatively regulated by H3K14 acetylation (Maltby *et al*., 2012).

Egd2 is associated with ribosomes in the cytoplasm, and is the $\alpha$-subunit of the nascent polypeptide-associated complex (NAC) which is involved in protein sorting and translocation. It is not clear what the biological reason is behind upregulation of this protein involved in processing synthesized proteins. Met6 is involved in methionine biosynthesis for two glutamines. Mam33 is a mitochondrial matrix protein, involved in oxidative phosphorylation. Gcy1 is a member of the aldo-keto reductase (AKR) family and is a glycerol dehydrogenase, and was shown to increases in response to DNA replication stress(Tkach *et al*., 2012). Cdc37 and Hsp42 are heat-shock proteins involved in protein folding. Ysa1 is a Nudix family hydrolase, shown to metabolize O-acetyl-ADP-ribose to AMP and acetylated ribose-

5'-phosphate (Rafty *et al*., 2002). The transfer of lysine acetyl group to NAD+ by Sir2forms nicotinamide and O-acetyl-ADP-ribose. The appearance of a metabolic product of Sir2, an enzyme implicated in lifespan extension, and the up-regulation of an enzyme involved in the breakdown of the metabolite, is quite fascinating. It was previously shown that Sir2 was inhibited by nicotinamide (Bitterman *et al*., 2002), and that O-acetyl-ADP-ribose blocked or delayed oocyte maturation and cell division in embryo blastomeres (Borra *et al*., 2002). Is the level of O-acetyl-ADP-ribose high in the H4K16Q mutant, hence the increase in the level of Ysa1? And, can this high level of O-acetyl-ADP-ribose be due to Sir2 deacetylase activity? We will discuss these questions in more detail in subsequent Chapters.

The two enzymes associated with resistance to oxidative damage and extended lifespan, Sod1 and Sod2, are both detectable, but not significantly up-regulated relative to the 2 day culture.

**Table 5.1. Differentially regulated proteins in the H4K16Q mutant strain**.Proteins that showed statistically significant differences in quantitated levels in day 14 *versus* day 2 cultures are listed. The ratios of day 14 to day 2 levels are shown.

| ID | Gene | Ratio | Description | Stress |
|---|---|---|---|---|
| YMR096W | **SNZ1** | **25.6** | **Protein involved in vitamin B6 biosynthesis** | |
| YJR119C | **JHD2** | **14.9** | **JmjC domain family histone demethylase** | |
| YHR193C | **EGD2** | **7.9** | **Alpha subunit of the nascent polypeptide-associated complex (NAC)** | |
| YER091C | **MET6** | **7.5** | **Cobalamin-independent methionine synthase** | |
| YIL070C | **MAM33** | **7.1** | **Acidic protein of the mitochondrial matrix** | |
| YOR120W | **GCY1** | **5.7** | **Glycerol dehydrogenase** | **1** |
| YEL020W-A | **TIM9** | **5.6** | **Essential protein of the mitochondrial intermembrane space** | |
| YGR020C | **VMA7** | **5.5** | **Subunit F of the V1 peripheral membrane domain of V-ATPase** | |
| YNR032C-A | **HUB1** | **4.8** | **Ubiquitin-like protein modifier** | |
| YER067W | **RGI1** | **4.3** | **Protein of unknown function** | **1** |
| YDR168W | **CDC37** | **4.1** | **Essential Hsp90p co-chaperone** | **3** |
| YDL181W | **INH1** | **3.5** | **Protein that inhibits ATP hydrolysis by the F1F0-ATP synthase** | |
| YDR171W | **HSP42** | **3.5** | **Small heat shock protein (sHSP) with chaperone activity** | **3** |
| YBR111C | **YSA1** | **3.3** | **Nudix hydrolase family member with ADP-ribose pyrophosphatase activity** | |
| YHR089C | **GAR1** | **3.3** | **Protein component of the H/ACA snoRNP pseudouridylase complex** | |
| YOL109W | **ZEO1** | **3.2** | **Peripheral membrane protein of the plasma membrane** | |
| YHR008C | **SOD2** | **1** | **Mitochondrial manganese superoxide dismutase** | **2** |
| YJR104C | **SOD1** | **1** | **Cytosolic copper-zinc superoxide dismutase** | **2** |
| YOR063W | **RPL3** | **0.5** | **Ribosomal 60S subunit protein L3** | |
| YML100W | **TSL1** | **0.5** | **Large subunit of trehalose 6-phosphate synthase/phosphatase complex** | |
| YDR335W | **MSN5** | **0.4** | **Karyopherin** | |
| 1=Replicate stress, 2=Oxidative stress, 3=Heat-shock, protein folding stress, 4=PKA related, | | | | |

Turning our attention next to the H4H18A mutant strain, it was found that an analysis of enriched GO terms associated with up-regulated proteins identify the processes of lysine biosynthesis via aminoadipic acid, organophosphate metabolism and carbohydrate derivative metabolism (Figure 5.1). Looking at individual proteins that are upregulated, Snz1, Jhd2, Gcy1, Hub1, and Ysa1 are again seen. Thus 33% identical proteins are up-regulated in the H4K16Q and H4H18A mutant strains, reflecting the similar transcriptomic profiles of these two strains in exponential phase. Proteins that are seen in H4H18A that were not seen in the H4K16Q strain include

Rnr2, a subunit of a ribonucleotide-diphosphate reductase that is involved in dNTP synthesis, and is regulated by DNA replication and DNA damage, Sah1, a S-adenosyl-L-homocysteine hydrolase which breaks down S-adenosyl-L-homocysteine, the product left after donation of an activated methyl group from S-adenosyl-L-methionine (SAM). The latter compound, of course, is the source of methyl groups transferred by methyltransferases such as Set1 and Set2. Thus, at face value, and assuming that the enzyme level matches an up-regulation in metabolite level, methylation of proteins using SAM as co-factor appears to be very active. This is not a contradiction in the observed up-regulation of Jmd2, since the latter enzyme demethylates specifically H3K4, whereas SAM is involved in the methylation of many other lysine and arginine residues, some of them representing epigenetic marks for transcriptional down-regulation, a transcriptional adjustment that is observed in stationary phase in *S. cerevisiae*(Werner-Washburne *et al*., 1996).

Hyr1 was also up-regulated in the H4H18A mutant. Hyr1 is a thiol peroxidase that is sensitive to intracellular levels of hydrogen peroxide. Under conditions of elevated oxidative stress, Hyr1 forms a disulfide bond with Yap1, inhibiting the nuclear export of the latter factor, and facilitating the transcriptional function of Yap1 of other stress response genes (Delaunay *et al*., 2002).

Atg7 is a protein involved in the formation of the pre-autophagosomal structure. Autophagy is the process whereby large portions of the cytoplasm are fused with the vacuole, allowing breakdown of compounds for recycling. It was shown that methionine restriction extended chronological lifespan, and that this phenomenon was dependent on proteins involved in autophagy, including Atg7 (Ruckenstuhl *et al*., 2014). It was also previously shown that spermidine mediated

induction of autophagy was associated with lifespan extension in numerous model organisms (Eisenberg *et al*., 2009).

Hnt1 is a adenosine 5'-monophosphoramidase, a protein that was shown to increase in response to DNA replication stress (Tkach *et al*., 2012). Replicative stress was suggested to be a major influence on genome stability, DNA damage and the regulation of chronological lifespan (Burhans and Weinberger, 2007). Ccp1 is a mitochondrial cytochrome-c peroxidase involved in the cellular response to oxidative stress (Charizanis *et al*., 1999).

As with the H4K16Q mutant, the Sod1 and Sod2 levels were also not significantly up-regulated in the H4H18A histone mutant strain.

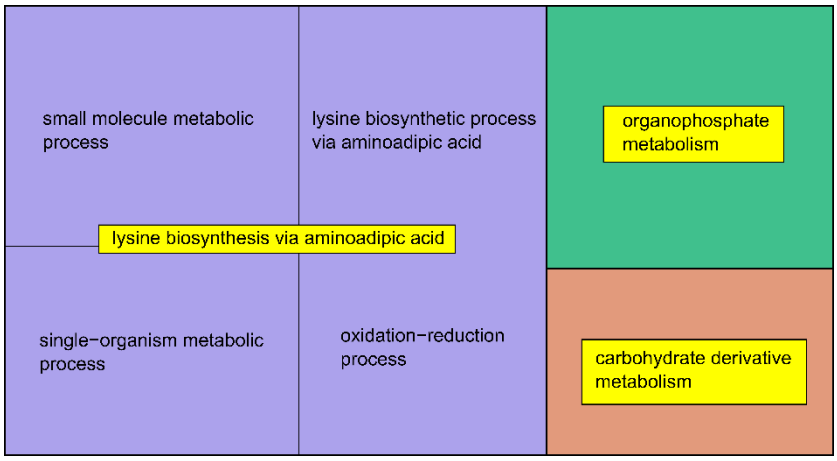


**Figure 5.1. Treemap representation of enriched GO terms for proteins that are up-regulated at day 14 in the H4H18A mutant strain.**

**Table 5.2. Differentially regulated proteins in the H4H18A mutant strain**.Proteins that showed statistically significant differences in quantitated levels in day 14 *versus* day 2 cultures are listed. The ratio of day 14 to day 2 levels are listed.

| ID | Name | Ratio | Description | Stress |
|---|---|---|---|---|
| YMR096W | SNZ1 | 10.3 | Protein involved in vitamin B6 biosynthesis | |
| YJR119C | JHD2 | 9.8 | JmjC domain family histone demethylase | |
| YJL026W | RNR2 | 8.2 | Ribonucleotide-diphosphate reductase (RNR), small subunit | 6 |
| YER043C | SAH1 | 6.2 | S-adenosyl-L-homocysteine hydrolase | |
| YIR037W | HYR1 | 5.8 | Thiol peroxidase | 2 |
| YOR120W | GCY1 | 5 | Glycerol dehydrogenase | 1 |
| YNR032C-A | HUB1 | 4.9 | Ubiquitin-like protein modifier | |
| YIL094C | LYS12 | 4.6 | Homo-isocitrate dehydrogenase | |
| YBR111C | YSA1 | 4.5 | Nudix hydrolase family member with ADP-ribose pyrophosphatase activity | |
| YHR171W | ATG7 | 4.3 | Autophagy-related protein and dual specificity member of the E1 family | 4 |
| YDL182W | LYS20 | 4.2 | Homocitrate synthase isozyme and functions in DNA repair | |
| YDL125C | HNT1 | 4.1 | Adenosine 5'-monophosphoramidase | 1 |
| YKR066C | CCP1 | 4.1 | Mitochondrial cytochrome-c peroxidase | 2 |
| YLR249W | YEF3 | 3.8 | Translation elongation factor 3 | |
| YGR240C | PFK1 | 3.7 | Alpha subunit of heterooctameric phosphofructokinase | |
| YJR104C | SOD1 | 1.1 | Cytosolic copper-zinc superoxide dismutase | 2 |
| YHR008C | SOD2 | 1 | Mitochondrial manganese superoxide dismutase | 2 |
| YHR089C | GAR1 | 0.4 | Protein component of the H/ACA snoRNP pseudouridylase complex | |
| YML100W | TSL1 | 0.4 | Large subunit of trehalose 6-phosphate synthase/phosphatase complex | |
| YBR243C | ALG7 | 0.3 | UDP-N-acetyl-glucosamine-1-P transferase | |
| YDL195W | SEC31 | 0.2 | Component of the Sec13p-Sec31p complex of the COPII vesicle coat | |
| 1=Replicate stress, 2=Oxidative stress, 4=PKA related, 6=Damage response | | | | |

Looking next at the H3T80D mutant strain, no enrichment of GO terms were seen for differentially expressed proteins. Looking at the list of up- and down-regulated proteins (Table 5.3) the up-regulation of the Gln4 tRNA synthetase is unexpected, and the biological reason for this is unclear.Rsr1 is a GTP-binding protein of the Ras/protein kinase A (PKA) pathway previously implicated in chronological lifespan extension in yeast (Longo, 2003). Spg1 is a small (95 residue) protein encoded by the nuclear genome, but detected in mitochondria, that is required for high temperature survival during stationary phase (Reinders *et al.*, 2006). In contrast, the protein Csf1 is required for fermentation, but only at low (5°C) temperatures (Tokai *et al*., 2000). The precise functional role of Csf1 is

currentlyunknown. Ynk1 is a nucleoside diphosphate kinase, involved in transferring the γ-phosphate from ATP to a nucleoside diphosphate, and is up-regulated in response to DNA replication stress (Tkach *et al*., 2012).

**Table 5.3. Differentially regulated proteins in the H3T80D mutant strain.**Proteins that showed statistically significant differences in quantitated levels in day 14 *versus* day 2 cultures are listed. The ratio of day 14 to day 2 levels are listed.

| ID | Name | Ratio | Description | Stress |
|---|---|---|---|---|
| YOR168W | **GLN4** | **9.1** | **Glutamine tRNA synthetase** | |
| YGR152C | **RSR1** | **7.7** | **GTP-binding protein of the Ras superfamily** | **4** |
| YHL035C | **VMR1** | **7.1** | **Vacuolar membrane protein** | **5** |
| YGR240C | **PFK1** | **6.0** | **Alpha subunit of heterooctameric phosphofructokinase** | |
| YOR120W | **GCY1** | **5.9** | **Glycerol dehydrogenase** | **1** |
| YDR168W | **CDC37** | **4.8** | **Essential Hsp90p co-chaperone** | **3** |
| YJL066C | **MPM1** | **4.1** | **Mitochondrial intermembrane space protein of unknown function** | |
| YML103C | **NUP188** | **4.1** | **Subunit of the inner ring of the nuclear pore complex (NPC)** | |
| YDR014W-A | **HED1** | **4.0** | **Meiosis-specific protein** | |
| YPL170W | **DAP1** | **3.8** | **Heme-binding protein** | **6** |
| YMR107W | **SPG4** | **3.1** | **Protein required for high temperature survival during stationary phase** | **3** |
| YLR087C | **CSF1** | **3.0** | **Protein required for fermentation at low temperature** | **3** |
| YKL067W | **YNK1** | **3.0** | **Nucleoside diphosphate kinase** | **1** |
| YLR061W | **RPL22A** | **2.9** | **Ribosomal 60S subunit protein L22A** | |
| YJR104C | **SOD1** | **1.0** | **Cytosolic copper-zinc superoxide dismutase** | **2** |
| YHR008C | **SOD2** | **1.0** | **Mitochondrial manganese superoxide dismutase** | **2** |
| YDL061C | **RPS29B** | **0.7** | **Protein component of the small (40S) ribosomal subunit** | |
| YML073C | **RPL6A** | **0.6** | **Ribosomal 60S subunit protein L6A** | |
| YJL153C | **INO1** | **0.4** | **Inositol-3-phosphate synthase** | |
| YBR035C | **PDX3** | **0.3** | **Pyridoxine (pyridoxamine) phosphate oxidase** | |
| 1=Replicate stress, 2=Oxidative stress, 3=Heat-shock, protein folding stress, 4=PKA related, 5=Chemical stress, 6=Damage response | | | | |

Many of the proteins that display elevated levels in the histone mutant strain in day 14 compared to day 2 have annotations that link them to a DNA replication stress, oxidative stress, heat-shock, protein folding stress, PKA related, chemical stress, and damage response stress, including DNA damage response (Tables 5.1, 5.2 and 5.3).

**Table 5.4. Differentially regulated proteins in the H3E50A mutant strain**. Proteins that showed statistically significant differences in quantitated levels in day 14 versus day 14 H3WT cultures are listed. The ratio of day 14 to day 14 levels are listed.

| ID | Name | Ratio | Description | Stress |
|---|---|---|---|---|
| YNL069C | **RPL16B** | **25.0** | **Ribosomal 60S subunit protein L16B** | |
| YER120W | **SCS2** | **10.8** | **Integral ER membrane protein, regulates phospholipid metabolism** | **1** |
| YNL052W | **COX5A** | **10.4** | **Subunit Va of cytochrome c oxidase** | |
| YOR168W | **GLN4** | **8.4** | **Glutamine tRNA synthetase** | **4** |
| YLR087C | **CSF1** | **8.1** | **Protein required for fermentation at low temperature** | **3** |
| YJR105W | **ADO1** | **5.7** | **Adenosine kinase** | |
| YLR178C | **TFS1** | **5.3** | **Inhibitor of carboxypeptidase Y (Prc1p), and Ras GAP (Ira2p)** | |
| YCL043C | **PDI1** | **5.2** | **Protein disulfide isomerase** | **3** |
| YJL190C | **RPS22A** | **4.9** | **Protein component of the small (40S) ribosomal subunit** | |
| YNL071W | **LAT1** | **4.5** | **Dihydrolipoamide acetyltransferase component (E2) of the PDC** | |
| YLL041C | **SDH2** | **4.3** | **Iron-sulfur protein subunit of succinate dehydrogenase** | |
| YLR304C | **ACO1** | **4.3** | **Aconitase** | |
| YDR353W | **TRR1** | **4.3** | **Cytoplasmic thioredoxin reductase** | |
| YGL147C | **RPL9A** | **4.0** | **Ribosomal 60S subunit protein L9A** | |
| YHR008C | **SOD2** | **1.5** | **Mitochondrial manganese superoxide dismutase** | |
| YJR104C | **SOD1** | **1.5** | **Cytosolic copper-zinc superoxide dismutase** | |
| YGR240C | **PFK1** | **1.0** | **Alpha subunit of heterooctameric phosphofructokinase** | |
| YGR193C | **PDX1** | **0.9** | **E3-binding protein of the mitochondrial pyruvate dehydrogenase complex** | |
| YGR097W | **ASK10** | **0.4** | **Component of RNA polymerase II holoenzyme** | |
| YLR147C | **SMD3** | **0.4** | **Core Sm protein Sm D3** | |
| YDR450W | **RPS18A** | **0.2** | **Protein component of the small (40S) ribosomal subunit** | |
| 1=Replicate stress, 2=Oxidative stress, 3=Heat-shock, protein folding stress, 4=PKA related, 5=Chemical stress, 6=Damage response | | | | |

However, it is possible that any change in the proteome that allows extension of lifespan occurs early, and has already occurred by day 2, in which case the analysis above would miss the differentially expressed protein. For this reason we also looked at the differential expression in the histone mutant strain at day 14 normalised to the wildtype, parental strain, also at day 14.

Looking at the upregulated proteome of the H3E50A mutant at day 14 (Table 5.4), RPL16B, a 60S ribosomal subunit protein, is seen upregulated 25-fold. It is not immediately clear why a ribosomal protein should be upregulated in deep stationary

phase in the histone mutant compared to the parental wild type strain. Interestingly, RPL16B, like most ribosomal protein, is regulated by Rap1. We will be discussing the possible role of Rap1 in a subsequent Chapter. Scs2 is involved in phospholipid metabolism, and interacts with FFAT motifs with VAMP-associated protein, affectingtransportation to the endoplasmic reticulum. However, it was also shown that Scs2 over-expression rescued telomeric shortening and de-repression in a strain over-expressing Mec1, a cell-cycle checkpoint protein. Scs2 deletion caused telomeric de-repression. A Scs2 mutant increased cellular senescence associated with a *mec1tel1* double knock-out (Craven and Petes, 2001). Cox5A is a member of the mitochondrial electron transport chain.Ado1 is an adenosine kinase and is required for the utilization of SAM. Tfs1 is an inhibitor of carboxypeptidase Y, and was also shown to regulate the PKA signalling pathway by binding and inactivating Ira2, a negative regulator of RAS function (Chautard *et al*., 2004). Pdi1 is a Protein disulfide isomerase involved in unfolded protein pathways. Rps22A is a ribosomal protein in the 40S sub-unit. Trr1 is a cytoplasmic thioredoxin reductase involved in sensing the state of the thioredoxin system. Trr1 is responsible for maintaining Trx1p and Trx2p in a reduced state (Tkach *et al*., 2012). Trx1/2, in turn, provides reducing equivalents to Rnr2, found to be upregulated in day14 in the H4H18A mutant strain (see Table 5.2). Trr1 is induced by Yap1. Interestingly, as mentioned above, Yap1 is activated by, among others, Hyr1, which was also found to be upregulated in the H4H18A strain (Table 5.2). The superoxide dismutases 1 and 2 were both found to be slightly up-regulated (1.5-fold) in the mutant *versus* WT strain. The ribosomal protein RPS18A was present at a 5-fold lower level in the mutant strain, showing that Rap1 responsive ribosomal proteins are not up-regulated as a general rule.

We have previously encountered the up-regulation of Vmr1, Rpl16B, Rsr1, Scs2, Cox5A, Gln4, Hsp82, Mpm1, Lat11, Tfs1, Dap1, Sod1 and Sod2. The up-regulation of histone H3 is a new observation (Table 5.5). As was previously mentioned, apart from its role as part of heterochromatin at telomeres, Rap1 is also involved in the activation of many genes, including glycolytic and ribosomal protein genes. In a telomerase *tlc1*Δ strain, exhibiting telomere shortening and Rap1 redistribution, Rap1 binds at many new sites that it does not occupy in a WT cell. These sites, which total approximately 500, are generally located upstream in the promoter region of genes, and are called new Rap1 targets at senescence (NRTS).

**Table 5.5. Differentially regulated proteins in the H3T80D mutant strain.** Proteins that showed statistically significant differences in quantitated levels in day 14 *versus* day 14 H3WT cultures are listed. The ratio of day 14 to day 14 levels are listed.

| ID | Name | Ratio | Description | Stress |
|---|---|---|---|---|
| YHL035C | VMR1 | 96.0 | Vacuolar membrane protein | |
| YNL069C | RPL16B | 29.6 | Ribosomal 60S subunit protein L16B | |
| YGR152C | RSR1 | 24.7 | GTP-binding protein of the Ras superfamily | 4 |
| YER120W | SCS2 | 10.5 | Integral ER membrane protein, regulates phospholipid metabolism | |
| YNL052W | COX5A | 9.9 | Subunit Va of cytochrome c oxidase | |
| YPL028W | ERG10 | 8.4 | Acetyl-CoA C-acetyltransferase (acetoacetyl-CoA thiolase) | |
| YBR010W | HHT1 | 7.7 | Histone H3 | |
| YOR168W | GLN4 | 7.5 | Glutamine tRNA synthetase | |
| YPL240C | HSP82 | 7.2 | Hsp90 chaperone | 3 |
| YNL121C | TOM70 | 7.1 | Component of the TOM (translocase of outer membrane) complex | |
| YJL066C | MPM1 | 5.6 | Mitochondrial intermembrane space protein of unknown function | |
| YNL071W | LAT1 | 4.9 | Dihydrolipoamide acetyltransferase component (E2) of the PDC | |
| YLR178C | TFS1 | 4.8 | Inhibitor of carboxypeptidase Y (Prc1p), and Ras GAP (Ira2p) | 4 |
| YPL170W | DAP1 | 4.7 | Heme-binding protein | 6 |
| YJR104C | SOD1 | 1.4 | Cytosolic copper-zinc superoxide dismutase | |
| YHR008C | SOD2 | 1.4 | Mitochondrial manganese superoxide dismutase | |
| YGR097W | ASK10 | 0.9 | Component of RNA polymerase II holoenzyme | |
| YFR053C | HXK1 | 0.9 | Hexokinase isoenzyme 1 | |
| YLR147C | SMD3 | 0.4 | Core Sm protein Sm D3 | |
| YDR450W | RPS18A | 0.1 | Protein component of the small (40S) ribosomal subunit | |

Relocation of Rap1 to NRTSs is not driven simply by mass-action, but requires the DNA damage checkpoint protein Mec1 (Platt *et al*., 2013). The histone genes are also repressed by the Mec1 dependent action of Rap1. Thus, the detection of the Hht1 protein (no other up-regulated histones were detected), suggests that the cell is not becoming senescent, and may also point to some underlying chromatin fragmentation and histone release.

Tom70 is a mitochondrial translocase involved in importing proteins destined for the mitochondrion. Mpm1 is a mitochondrial intermembrane space protein, currently of unknown function (Inadome *et al*., 2001).

Vmr1 is a vacuolar transport protein involved in multidrug resistance. Rpl16B is a 60S ribosomal sub-unit protein, transcriptionally regulated by Rap1and is involved in protecting the cell from oxidative or reductive stress, and was also shown to respond to DNA replicative stress.*TFS1* encodes an anionicphospholipid bindingprotein with roles in regulation of theprotein kinase A (PKA) signalling pathwayas well as inhibition of the vacuolar protease CPY. *TSF1* suppression was found to be mediated through interaction with and inhibition of the GTPase-activating proteinIra2p, a negative regulator of RAS function. Scs2 interacts with FFAT motifs in Opi1p, Swh1p, Osh2p, and Osh3p; involved in telomeric silencing; N-terminally acetylated, binds 5.8 S rRNA; transcriptionally regulated by Rap1p a change that would render the up-regulated protein below the differential cut-off.

## 5.4. Reference List


Bitterman, K.J., Anderson, R.M., Cohen, H.Y., Latorre-Esteves, M., and Sinclair, D.A. (2002). Inhibition of silencing and accelerated aging by nicotinamide, a putative negative regulator of yeast sir2 and human SIRT1. J. Biol. Chem. *277*, 45099–45107.

Boa, S., Coert, C., and Patterton, H.G. *Saccharomyces cerevisiae* Set1p is a methyltransferase specific for lysine 4 of histone H3 and is required for efficient gene expression. Yeast *20*, 827–835.

Borra, M.T., O'Neill, F.J., Jackson, M.D., Marshall, B., Verdin, E., Foltz, K.R., and Denu, J.M. (2002). Conserved enzymatic production and biological effect of O-acetyl-ADP-ribose by silent information regulator 2-like NAD+-dependent deacetylases. J. Biol. Chem. *277*, 12632–12641.

Burhans, W.C., and Weinberger, M. (2007). DNA replication stress, genome instability and aging. Nucleic Acids Res. *35*, 7545–7556.

Charizanis, C., Juhnke, H., Krems, B., and Entian, K.-D. (1999). The mitochondrial cytochrome c peroxidase Ccp1 of *Saccharomyces cerevisiae* is involved in conveying an oxidative stress signal to the transcription factor Pos9 (Skn7). Mol. Gen. Genet. MGG *262*, 437–447.

Chautard, H., Jacquet, M., Schoentgen, F., Bureaud, N., and Benedetti, H. (2004). Tfs1p, a member of the PEBP family, inhibits the Ira2p but not the Ira1p Ras GTPase-activating protein in *Saccharomyces cerevisiae*. Eukaryot. Cell *3*, 459–470.

Craven, R.J., and Petes, T.D. (2001). The *Saccharomyces cerevisiae* suppressor of choline sensitivity (SCS2) gene is a multicopy Suppressor of mec1 telomeric silencing defects. Genetics *158*, 145–154.

Delaunay, A., Pflieger, D., Barrault, M.B., Vinh, J., and Toledano, M.B. (2002). A thiol peroxidase is an $H_2O_2$ receptor and redox-transducer in gene activation. Cell *111*, 471–481.

Eisenberg, T., Knauer, H., Schauer, A., Buttner, S., Ruckenstuhl, C., Carmona-Gutierrez, D., Ring, J., Schroeder, S., Magnes, C., Antonacci, L., *et al*. (2009). Induction of autophagy by spermidine promotes longevity. Nat Cell Biol *11*, 1305–1314.

Lin, S.-J., Kaeberlein, M., Andalis, A.A., Sturtz, L.A., Defossez, P.-A., Culotta, V.C., Fink, G.R., and Guarente, L. (2002). Calorie restriction extends *Saccharomyces cerevisiae* lifespan by increasing respiration. Nature *418*, 344–348.

Longo, V.D. (2003). The Ras and Sch9 pathways regulate stress resistance and longevity. Exp. Gerontol. *38*, 807–811.

Maltby, V.E., Martin, B.J.E., Brind'Amour, J., Chruscicki, A.T., McBurney, K.L., Schulze, J.M., Johnson, I.J., Hills, M., Hentrich, T., Kobor, M.S., *et al*. (2012). Histone H3K4 demethylation is negatively regulated by histone H3 acetylation in *Saccharomyces cerevisiae*. Proc. Natl. Acad. Sci. U. S. A. *109*, 18505–18510.

Platt, J.M., Ryvkin, P., Wanat, J.J., Donahue, G., Ricketts, M.D., Barrett, S.P., Waters, H.J., Song, S., Chavez, A., Abdallah, K.O., *et al*. (2013). Rap1 relocalization contributes to the chromatin-mediated gene expression profile and pace of cell senescence. Genes Dev. *27*, 1406–1420.

Rafty, L.A., Schmidt, M.T., Perraud, A.-L., Scharenberg, A.M., and Denu, J.M. (2002). Analysis of O-acetyl-ADP-ribose as a target for Nudix ADP-ribose hydrolases. J. Biol. Chem. *277*, 47114–47122.

Reinders, J., Zahedi, R.P., Pfanner, N., Meisinger, C., and Sickmann, A. (2006). Toward the complete yeast mitochondrial proteome: multidimensional separation techniques for mitochondrial proteomics. J. Proteome Res. *5*, 1543–1554.

Rodríguez-Navarro, S., Llorente, B., Rodríguez-Manzaneque, M.T., Ramne, A., Uber, G., Marchesan, D., Dujon, B., Herrero, E., Sunnerhagen, P., and Pérez-Ortín, J.E. (2002). Functional analysis of yeast gene families involved in metabolism of vitamins B1 and B6. Yeast *19*, 1261–1276.

Ruckenstuhl, C., Netzberger, C., Entfellner, I., Carmona-Gutierrez, D., Kickenweiz, T., Stekovic, S., Gleixner, C., Schmid, C., Klug, L., Sorgo, A.G., *et al*. (2014). Lifespan extension by methionine restriction requires autophagy-dependent vacuolar acidification. PLoS Genet. *10*, e1004347.

Ryu, H.-Y., and Ahn, S. (2014). Yeast histone H3 lysine 4 demethylase Jhd2 regulates mitotic rDNA condensation. BMC Biol. *12*, 75.

Tkach, J.M., Yimit, A., Lee, A.Y., Riffle, M., Costanzo, M., Jaschob, D., Hendry, J.A., Ou, J., Moffat, J., Boone, C., *et al*. (2012). Dissecting DNA damage response pathways by analyzing protein localization and abundance changes during DNA replication stress. Nat. Cell Biol. *14*, 966–976.

Tokai, M., Kawasaki, H., Kikuchi, Y., and Ouchi, K. (2000). Cloning and characterization of the CSF1 gene of *Saccharomyces cerevisiae*, which is required for nutrient uptake at low temperature. J. Bacteriol. *182*, 2865–2868.

Venters, B.J., Wachi, S., Mavrich, T.N., Andersen, B.E., Jena, P., Sinnamon, A.J., Jain, P., Rolleri, N.S., Jiang, C., Hemeryck-Walsh, C., *et al*. (2011). A comprehensive genomic binding map of gene and chromatin regulatory proteins in Saccharomyces. Mol. Cell *41*, 480–492.

Werner-Washburne, M., Braun, E.L., Crawford, M.E., and Peck, V.M. (1996). Stationary phase in *Saccharomyces cerevisiae*. Mol. Microbiol. *19*, 1159–1166.

# CHAPTER 6

# Discussion

## 6.1. Chronological Lifespan

The regulation of lifespan is controlled by a complex, inter-twined, cross-talking network involving many signalling pathways and processes. It is not simply the deferment of induction of apoptosis. It was proposed as early as 1956 that free radicals caused oxidative damage to macromolecules which disrupted cellular processes, leading to aging and senescence (Harman, 1956, 1972). The “free radical theory of aging” posits that reactive oxygen species cause oxidative damage to macromolecules, including nucleic acids, proteins and lipids, and that accumulation of damage beyond a threshold renders the chemistry of the cell dysfunctional, resulting in the inability to maintain cellular chemistry in a high energy state of disequilibrium, resulting in eventual cell death.

The reactive oxygen species are generated by respiration in the mitochondrion (Figure 6.1). Leakage of electrons from the transport chain complexes to molecular oxygen results in the formation of the superoxide anion, $O_2^-$. The $O_2^-$, in itself, is not highly oxidative, but the sequential conversion to $H_2O_2$ by a dismutase enzyme, and subsequent reduction to $OH^-$ by a reduced metal, forms one of the strongest oxidizing agents in nature (Figure 6.1). The $OH^-$can also be converted to the equally powerful oxidant, peroxinitrile, by reacting with $NO^-$. These compounds, $O_2^-$, $H_2O_2$, $OH^-$ and peroxinitrile, are collectively known as reactive oxygen species (ROS) (Turrens, 2003).

The mitochondrion contains many enzymes tasked with limiting oxidative damage by converting ROS to less reactive compounds. A copper-zinc superoxide

dismutase (CuZnSod) and manganese superoxide dismutase (MnSod), represented in *S.cerevisiae* by Sod1, which is constrained to the cytoplasm and mitochondrial intermembrane space, and by Sod2, which is located in the mitochondrial matrix, respectively, is responsible for converting $O_2^-$ to both $H_2O_2$ or $O_2$. Cytochrome *c* is also found in the intermembrane space of the mitochondrion, and scavenges $O_2^-$.

A substitution mutation in the mitochondrial targeting sequence of MnSod has been associated with Parkinson's disease in humans. Similarly, 10% of the cases of the neurodegenerative familial amyotrophic lateral sclerosis (ALS) is linked to a mutation in the human CuZnSod gene (Turrens, 2003). It is therefore clear that efficient clearance of $O_2^-$is crucial to limit the occurrence of diseases of aging in humans. It was also shown in *S. cerevisiae* that deletion of either Sod1 or Sod2 caused a significant reduction in RLS (Unlu and Koc, 2007), and increase in oxidative DNA damage, assessed by a comet assay (Muid *et al*., 2014). Is was further shown that a Sod1 deletion mutant exhibited a shortened CLS (Feser *et al*., 2010). Over-expression of Sod1, in conjunction with increased copper levels and Lys7, its dedicated Cu-loading chaperone, increased CLS (Harris *et al*., 2005). Similarly, deletion of Sod2 decreased CLS (Laschober *et al*., 2010; Weinberger *et al*., 2010), and over-expression of Sod2 extended CLS (Fabrizio *et al*., 2003). The cytoplasmic catalase, Ctt1, involved with the conversion of $H_2O_2$ to $H_2O$, is also required to limited oxidative stress (Ribeiro *et al*., 2014). $H_2O_2$ is transported to the peroxisome, where Cta1, converts it to $H_2O$, or where $H_2O_2$ is used in oxidative, metabolic processes (Figure 6.1). Thus, there is a significant body of evidence linking CLS to the generation of ROSs and the requirement for scavenging and transformation of the oxidative compounds. It is therefore evident that limiting oxidative damage is a crucial process in extending CLS. It is therefore not surprising

that many studies elucidating pathways involved in CLS extension, converge on limiting general and oxidative stress (Longo and Fabrizio, 2012). We briefly discuss the TOR/Sch9 and Ras/Cyr1/PKA pathways below, that terminate in the expression of stress response proteins.

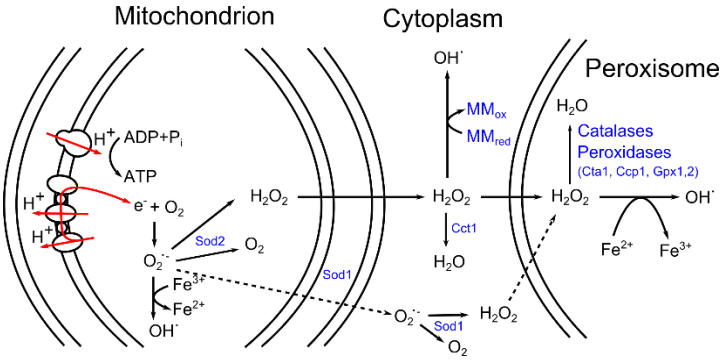


**Figure 6.1.The generation and inactivation of ROS in the cell.**The formation of $O_2^-$ by leakage of electrons to $O_2$in the mitochondrion is shown. The $O_2^-$ is converted by Sod2 to $H_2O_2$ and $O_2$. $H_2O_2$ appearing in the cytoplasm is converted to $H_2O$ by Cct1. Oxidation of macromolecules (MM) by $H_2O_2$ generates highly reactive $OH^•$. $O_2^-$ that appears in the cytoplasm is converted to $O_2$ and $H_2O_2$ by Sod1. In the peroxisome $H_2O_2$ is converted to $H_2O$ by Cta1, Ccp1, Gpx1 and Gpx2. Oxidation of metal ions in the peroxisome will generate $OH^•$.

## 6.2. The TOR/Sch9 Pathway

One of the earliest identified regulators of lifespan is calorie restriction (CR), caused by the depletion of the carbon or nitrogen source, or both. A link between CR and lifespan has been shown in a range of organisms spanning from unicellular organisms such as *S. cerevisiae*(Lin *et al*., 2002), to the mammalian rhesus monkeys (Colman *et al*., 2014). Calorie restriction is generally associated with the induction of stress response genes, which decreases the stress experienced by the yeast cell, allowing an extended lifespan. The causative link between decreased impact of stress and lifespan is quite tenuous in the literature. The link is usually

based on the growth of yeast on a non-fermentable carbon source at non-restrictive levels, the ensuing up-regulation of respiration processes, and subsequent extension of CLS (Smith *et al*., 2007). Respiration above a threshold in both exponential phase as well as in stationary phase was needed to extend CLS in response to CR (Ocampo *et al*., 2012). A screen of long-lived strains in *S. cerevisiae* showed that mutants that inhibited the TOR pathway, a signalling pathway sensitive to nutrient levels, mimicked a CR response, including the expression of stress response genes, and displayed an extended CLS (Powers *et al*., 2006).

The TOR pathway, mediated by the TORC complexes, regulates cell growth as a function of nutrient state, amino acid levels, energy status, and oxygen and cell stress. There are two TORC complexes in *S. cerevisiae*. TORC1 consists of the Tor1 or the Tor2 serine/threonine protein kinase, and Kog1, Lst8, and Tco89. Tor1 arose from Tor2 through whole-genome duplication in *S. cerevisiae*. TORC1 is sensitive to the antibiotic rapamycin, which binds to Fpr1, which then associates in its liganded state with the Tor1 protein, inhibiting the function of the complex. TORC2, which is rapamycin insensitive, consists of Tor2 and Avo1, Avo2, Tsc11, Lst8, Bit61, Slm1, and Slm2.

TORC1 is involved in a plethora of processes including: protein synthesis, ribosome biogenesis, autophagy and transcriptional activation. Under conditions where nutrients are readily available, TORC1 inhibits activators that stimulate expression of genes involved in nitrogen catabolite repression, the retrograde response, and stress response. Genes involved in ribosome biosynthesis (Ribi genes) are simultaneously activated. The Ribi regulon consists of many hundreds of ribosomal protein and non-ribosomal protein genes, and is rapidly induced in response to sudden nutrient availability. The Ribi regulon genes contain PAC

(Polymerase A and C) and RRPE (ribosomal RNA-processing element) sites, and are targets of both the TOR and PKA pathways (Lippman and Broach, 2009).

The transcription factor activation typically occurs through the action of TORC1 on downstream effectors, Sit4 phosphatase and Yak1 kinase, which alter the phosphorylation pattern of transcriptional activators, modulating its binding to a cytoplasmic anchor protein and thus regulating its transfer to the nucleus. Under nutrient-rich conditions, TORC1 stimulated cell growth and biosynthesis by phosphorylation of Sch9, an AGC family kinase, which in turn phosphorylates Tod6, Dot6 and Stb3, which bind to the upstream PAC sites and activates Ribi genes (Huber *et al*., 2011; Lippman and Broach, 2009). When the TOR pathway is repressed, Sch9 is not phosphorylated, and the un-phosphorylated Tod6, Dot6 and Stb3 proteins, bound to the PAC sites, now recruit the Rpd3L deactylase complex, thus inhibiting expression of Ribi genes.

Pharmacological inhibition of the TOR pathway extends CLS (Powers *et al*., 2006) and deletion of*SCH9* or *TOR1* extends chronological lifespan in *S. cerevisiae*(Longo, 2003). Mutations in Sch9 was shown to extend CLS in *S. cerevisiae* by up to three-fold, an effect that required the activators Msn2/Msn4 and protein kinase Rim15 (Fabrizio *et al*., 2001). TORC maintains Rim15 in a phosphorylated state, which anchors the protein in the cytoplasm,

Bmh1, homologous to the highly conserved 14-3-3 protein family, was also implicated as a player in the TOR signalling pathway. Bmh1 was phosphorylated at S238 with chronological aging, and this modification was delayed by calorie restriction or inhibition of the TOR pathway. A *Δbmh1* strain displayed extended lifespan, and caused a decrease in the generation of reactive oxygen species, and

activated HSE gene transcription. These effects required Msn2/4 and Rim5 (Wang *et al*., 2009).

### 6.3. PKA Pathway

The carbon sensitive Protein kinase A (PKA) pathway is mediated by the PKA complex, composed of a heterotetramer that is formed by two copies of the cAMP-responsive Bcy1, and two kinase sub-units encoded by *TPK1/2/3*. The G-protein Ras2 activates PKA via adenylyl cyclase (Cyr1) in response to glucose availability. Deletion of RAS2, which functions upstream of CYR1, increases CLS in a Msn2/Msn4 and Rim15 dependent manner (Fabrizio *et al*., 2003). The PKA complex is involved in disrupting binding of Dot6 to the PCA element, thus activating genes involved in ribosome biosynthesis and cell growth (Lippman and Broach, 2009). In glucose rich media, PKA phosphorylates Msn2/4, which blocks its nuclear transfer, keeping it from activating stress response genes (Morano *et al*., 2012).

### 6.4. Oxidative Damage

TORC1 deficient yeast strains have a higher level of oxidative phosphorylation enzymes per mitochondrion, increased respiratory coupling, and produce higher levels of ROS, which was proposed to represent a signalling pathway that extends chronological lifespan (Pan *et al*., 2011).Chronological lifespan extension is often explained in terms of protection of the cell from oxidative damage. It was shown that CR or elevation of intra-cellular $H_2O_2$ or exposure to $H_2O_2$ induced the cytoplasmic and mitochondrial Sod1 and Sod2 enzymes, which decreased superoxide anions, and extended chronological lifespan (Mesquita *et al*., 2010). Guarente and colleagues showed that CR depleted cellular levels of NADH, a competitive inhibitor of Sir2, suggesting that replicative lifespan extension by CR was

due to the lifting of Sir2 inhibition (Lin *et al*., 2004). Smith and co-workers, however, showed that extension of chronological lifespan was Sir2 (and homologs Hst1, Hst2, Hst3 and Hst4) independent (Smith *et al*., 2007). Very importantly, this group further showed that low temperature and high osmolarity enhanced the lifespan extension effect of CR, suggesting that there are more than one pathway, and that the lifespan extension effects are additive (Smith *et al*., 2007). Over-expression of both Sod1 and Sod2 extended CLS, by delaying modification of aconitase, a mitochondrial superoxide-sensing protein (Fabrizio *et al*., 2003).

### 6.5. Stress Response Gene Regulation

Heat Shock Factor 1 (Hsf1) activates a wide range of genes, including chaperones (Hsp26, Hsp30, Hsp82, etc), cell wall and cytoskeleton genes, small molecule transport genes, energy generation genes (PKG1, TDH3, etc.), defense against oxidative stress genes (CUP1, GTT1, etc.), signal transduction genes, carbohydrate metabolism genes, vesicular transport genes, and ubiquitination and proteolysis genes in response to starvation (Hahn *et al*., 2004). Hsf1 binds to the heat shock element (HSE) upstream of many target genes, which is composed of three NGAAN inverted repeats, which can be arranged in direct, gapped, or spaced arrangements. The different arrangements of the monomeric sequence unit appear to define classes of stress response genes that are activated by Hsf1 by slightly different mechanisms. Activation of many stress responsive genes require the remodeler Swi/Snf (Shivaswamy and Iyer, 2008).

Apart from the HSE, there are also distinct STRE elements. Msn2 and Msn4 are also environmental stress response transcription factors, like Hsf1. The Rpd3L deacetylase complex is required for activation of Msn2/4 dependent genes (Ruiz-

Roig *et al*., 2010). Msn2/4 contain a C-terminal zinc-finger that binds to the CCCCT stress response elements (STREs) present upstream of approximately 200 different stress response genes. It was shown that nucleosome occlusion of the Msn2 binding site influenced the ability of the transcription factor to bind and induce gene expression (Elfving *et al*., 2014). Msn2 was also shown to influence local nucleosome structure with binding. It is perhaps not surprising that Msn2 binding depends on Swi/Snf (Erkina *et al*., 2008). SWI/SNF was required for activation as well as repression of genes during heat shock (Shivaswamy and Iyer, 2008). Snf2 was recruited to ribosomal protein genes and Hsf1 target genes during heat shock (Shivaswamy and Iyer, 2008). When the Msn2 zinc-finger is unphosphorylated, Msn2/4 are cytoplasmic, anchored to the Bmh2 protein (Beck and Hall, 1999). Yak1 phosphorylates and activates stress response factors Msn2/4 and Hsf1 under low-glucose conditions (Morano *et al*., 2012). When Msn2/4 becomes hyperphosphorylated, it translocates to the nucleus to activate stress response genes (Jacquet *et al*., 2003).

Sod1 is a Cu-Zn superoxide dismutase predominantly found in the cytoplasm as well as in the mitochondrial inter-membrane space. Unlike higher eukaryotes, *S. cerevisiae* expresses a second dismutase, the Mn specific Sod2, which is mitochondrial. Both enzymes catalyse the conversion of superoxide anions to molecular oxygen and hydrogen peroxide. In addition to its catalytic role, Sod1 is also rapidly relocated to the nucleus in response to elevated ROS levels, including $H_2O_2$, as part of an oxidative signalling pathway. The Sod1 relocation is regulated by Mec1/ATM and its downstream effector Dun1/Cds1 kinase, which phosphorylates Sod1 at S60 and S99. Phosphorylated, nuclear Sod1 binds to the promoters of oxidative resistance and repair genes (Tsang *et al*., 2014).

Yap1 is a basic leucine zipper protein from the AP-1 superfamily. It contains a nuclear localization signal as well as a nuclear export signal, and a N-terminal and a C-terminal cysteine residue cluster. Normally Yap1 is transported to the nucleus at basal rates, where it binds to and is exported by the exporting Crm1. In the presence of an oxidizing reagent such as diamine, the cysteine residue becomes modified and the interaction with Crm1 abolished, resulting in the nuclear concentration of Yap1 where it can activate oxidative stress response genes. In the presence of $H_2O_2$, Yap1 is folded by chaperones Ybp1 and Gpx3 in a manner where cysteine residues from the N-terminal and C-terminal cysteine clusters are linked. This conformation also allows nuclear accumulation, and activation of peroxide responsive genes (Morano *et al*., 2012). Yap1 and the functionally related Skn7 ultimately activate the two superoxide dismutases (*SOD1* and *SOD2*), a peroxiredoxin (TSA1), and an alkyl hydroperoxide reductase (AHP1), among other stress response genes. Sod1. Sod2, Tsa1 and Ahp1, along with other catalases, peroxiredoxins, glutathione peroxidases and thioredoxins contribute to maintain the oxidative homeostasis of the cell, protecting the DNA and proteins from oxidative damage that could result in cell death. In the presence of oxidative stress, Hyr1 catalyses the formation of a disulphide bridge in the C-terminal region of Yap1. This masks the exportin signal, allowing nuclear accumulation of Yap1.

In the nucleus the protein binds upstream of oxidative response genes such as *TRR1*, *TRX2*, *GSH1*, and *GLR1*. Trr1 and Trx2 are negative regulators of Yap1 (Tkach *et al*., 2012). Similar to Yap1, Skn7 is also involved in expression of stress response genes. Interestingly, the Tup1-Ssn6 complex is recruited to stress response genes by Skn7 (Hanlon *et al*., 2011). Tup1-Ssn6 is a general transcriptional repressor that is recruited to numerous loci by DNA-binding Tup1-

recruiters, such as the Mat$\alpha$2 repressor. Grunstein and colleagues showed that Tup1 recruited Hda1, causing deactylation of the surrounding chromatin, and concomitant gene repression (Wu *et al*., 2001). Pennings and co-workers also showed that Ssn6-Tup recruited Hda1 and Rpd3, causing hypoacetylation of nucleosomes in the sub-telomerically located FLO1 promoter, and transcriptional repression (Fleming *et al*., 2014). Tup1 was previously shown to preferentially interact with deacetylated histone H3 and H4 N-termini *in vitro*(Edmondson *et al*., 1996). In fact, it was shown that the H3$\Delta$1-28, H4$\Delta$4-14, H4$\Delta$4-19 and H4K12Q,K16Q histone mutants individually exhibited a weakened interaction with a truncated Tup1 protein *in vitro*, and caused derepression of a Tup1 repressible reporter gene in *S. cerevisiaein vivo*(Edmondson *et al*., 1996). It was previously shown that Sir3 interacted with H4H18, H4K16 and H3T80 as well as other residues on the side surface of the nucleosome (Armache *et al*., 2011). This therefore suggests that Sir3 and Tup1 at least partially share an interaction surface on the nucleosome some. We note that the H4$\Delta$9-16 and H4K16Q mutants caused the extension of CLS. This suggests that both Ssn6-Tup1 binding as well as Sir3 binding may be compromised in some of the extended CLS mutant strains. Pennings and colleagues also showed that a H4S47C Sin mutant strain exhibited derepression of the *FLO1* gene, in a Snf2 dependent manner (Fleming and Pennings, 2001). Interestingly, the *FLO1* gene was derepressed in the *ssn6*$^{-}$*snf2*$^{-}$ double mutant, showing that the expression was independent of Swi/Snf due to the Sin mutation in histone H4 (Fleming and Pennings, 2001).

The Struhl lab showed that Ssn6-Tup1 was not simply a repressor. The phosphorylation of Sko1 by Hog1 MAP kinase caused Ssn6-Tup1 to recruit SAGA and Swi/Snf, activating hyperosmotic stress response genes (Proft and Struhl, 2002). In a follow-up study it was shown that acetylation of H3 occurred at Tup1

repressible promoters in a *hda1*$^{-}$ strain, but that this did not cause transcriptional derepression, suggesting that deactylation of chromatin is not a prerequisite for expression of the tested stress response genes (Wong and Struhl, 2011). The authors further suggested that Tup1 repressed transcription by blocking the recruitment of Gcn5, the catalytic sub-unit of the SAGA acetyltransferase complex (Wong and Struhl, 2011).

Brown and colleagues showed that a set of about 900 genes in *S. cerevisiae* responded to a variety of stress conditions including heat shock, oxidative shock, osmotic shock and nutrient depletion (Gasch *et al*., 2000). The transcription factors Yak1, Msn2 and Msn4 were shown to play a significant role in the activation of most of these stress response genes (Gasch *et al*., 2000). Tup1-Ssn6 was shown to be involved in the repression of many stress response genes. Transcriptional activators that antagonized Tup1-Ssn6 included the DNA damage response Crt1, the hypoxia stress response Rox1,

Presumably an activating modification of Skn7 abolishes interaction with Tup1-Ssn6, allowing activation of the stress response gene. In a screen for transcriptional factors that recruited Tup1-Ssn6, Cin5, Skn7, Phd1, and Yap6 was identified (Hanlon *et al*., 2011). All five transcription factors are involved with the regulation of stress response genes (Hanlon *et al*., 2011).

The following yeast gene were found to be critical for CLS: *KGD1*, *SOD2*, *RPL31A*, *NCR1*, *LYS9*, *SHM1*, *GCN5*, *HAP3*, *PIM1*, *PRY1*, *ATG18*, *CYC1*, *RPL13B*, *MSW1*, *RAD27*, *YDC1* and*TIF3*(Laschober *et al*., 2010). In our proteomic analysis of proteins that were upregulated or down-regulated in strains with extended CLS, we identified Sod1, and Sod2.Smerdon and colleagues (Nag *et al.*, 2008) reported that the Sin mutant H4R45H displayed an enhanced rate of nucleotide excision repair

(NER) at the silent HML$\alpha$, repressed *GAL10* and RPB2 loci.However, neither HML$\alpha$ nor *GAL10* was derepressed, and the increased nuclease accessibility of the H4R45H Sin nucleosomes were suggested to reflect a chromatin structure more amenable to effective NER. An analysis of microarray data of the H4R45H mutant (GEO accession GSE11282; www.ncbi.nlm.nih.gov/geo/) showed 517 genes that were down-regulated by 2-fold or more (adjusted $p<0.05$) and 44 genes up-regulated by 2-fold or more (adjusted $p < 0.05$). Mapping these gene lists to GO terms showed that up-regulated genes were associated with iron homeostasis, and down-regulated genes with carbohydrate metabolic processes and ascospore wall assembly. There was no indication of up-regulation of electron transport processes or the TCA cycle, as was seen for the H3E50A mutant, showing that up-regulation of oxidative phosphorylation was not a transcriptomic characteristic of Sin mutants.

### 6.6. Alternative Pathways for Extension of CLS and Future Work

Rap1 (Repressor-activator protein 1) is associated with repression of silent mating type loci and telomere maintenance and repression, as well as activation of ribosomal protein (Moehle and Hinnebusch, 1991) and glycolytic genes (Drazinic *et al*., 1996). Rap1 contains an N-terminal BRCT domain, important in signalling in the DNA damage response, and possesses a phosphate binding pocket that can bind to DNA or a phosphopeptide (Sheng *et al*., 2011). Rap1 further contains a central Myb-like domain that assumes a three helix bundle fold, of which the last two helices adopt a helix-turn-helix fold, and binds with high affinity to the telomere repeat sequence $TG_{2–3}$-$(TG)_{1–6}$(Wahlin and Cohn, 2000), and was also implicated in non-sequence specific, low affinity binding to DNA (Feldmann and Galletto, 2014). A Rap1 specific C-terminal (RCT) domain is also present that was shown to be a

protein-protein interaction domain, facilitating binding to the human telomere repeat sequence binding protein hTrf2, recruiting hRap1 to telomeres, which represses non-homologous end-joining (Chen *et al*., 2011). In *S. cerevisiae*, Rap1 binds directly to telomere repeat sequences, recruiting Sir3 to the telomeres via interaction with the RCT domain (Chen *et al*., 2011). Thus, Sir3 can bind to both the side surface of nucleosomes (Armache *et al*., 2011; Connelly *et al*., 2006) as well as to the RCT domain of Rap1 (Chen *et al*., 2011). It is not clear whether the binding of Sir3 to Rap1 or to the nucleosome is the major interaction at the telomeres and at the HM loci. It seems fair that the initial recruitment to the telomeres and the HM loci may occur by binding to Rap1, and propagation of the heterochromatin complex by binding of Sir3 to the side of the nucleosome, where Sir2 has deacetylated H4K16.

Rap1 was also shown to interact with Gcr1, where activation of glycolytic genes involves stabilization of DNA binding of Gcr1 by Rap1 at an UAS at glycolytic gene promoters (Drazinic *et al*., 1996). The exact Rap1 domain involved in the interaction between Gcr1 and Rap1 is not yet known (Lopez *et al*., 1998). It was previously shown that Rap1 also activated ribonucleotide reductase genes in response to DNA damage (Tomar *et al*., 2008). The RNR genes are also involved in telomere length maintenance (Tomar *et al*., 2008). It is known that telomere length remains approximately constant with replicative aging in *S. cerevisiae*(D'Mello and Jazwinski, 1991). We could not locate any published study that addressed telomere length as a function of incubation period in stationary phase. However, in the absence of DNA replication and a subsequent need for telomere repair, it seems reasonable to assume that telomere length will be fairly constant during extended stationary phase incubation, except if there is exonucleotylic damage and no repair. However, the heterochromatic nature of telomeres should limit gratuitous,

exonucleolytic degradation. Since there is a direct relationship between telomere length and the number of Rap1 molecules associated at the telomere (Marcand *et al*., 1997), an increase in Rap1 level in extended stationary phase in the absence of telomere shortening suggests that the increased concentration is not due to re-mobilisation of telomeric Rap1, but rather due to active synthesis of the protein. However, in the absence of direct evidence, it remains possible that the increase in Rap1 may be due to re-distribution due to degradation of telomeres, or due to apoptosis of a sub-population of cells in the quiescent fraction, contributing to a higher level of soluble Rap1 which may also be experimentally more extractable. However, the resolution of these points and the many consequential ideas require targeted experiments.Future work will have to first test using gel shift assays the lack of binding of Sir3 on the nucleosomes of the histone mutant strains that are implicated in longevity. Since Sir3 cannot be recruited to the telomeres by Rap1, does Rap1 relocate to other regions of the genome in order to rescue telomere shortening and damage? ChIP-seq experiments would be ideal to address this question.

A genetic screen for proteins that disrupted telomere silencing identified a number of proteins, then of unknown function, designated Disruptor of Telomeric silencing protein (Singer *et al*., 1998). Dot5 is a nuclear thiol peroxidase; and acts as an alkyl-hydroperoxide reductase in post-diauxic growth phase. Dot5 was shown to be upregulated more than 30-fold under continuous oxidative stress (Belli *et al*., 2004).

Dot6, a SANT domain containing sub-unit of the Rpd3L complex, distributes to the nucleus following replicative stress (phosphorylated by Yak1 kinase?), binding

to PAC, and is involved in rRNA and ribosome biosynthesis. Dot1 is a H3K79 specific methyltransferase, and is required for telomeric silencing.

Components of the Swi/Snf complex rapidly move from the nucleus to the cytosol during induced hypoxia, showing that compartementalisation of Swi./Snf may be sensitive to oxygen stress (Dastidar *et al*., 2012), although the direction of the partitioning is opposite to that expected.

## 6.7. Reference List


Armache, K.-J., Garlick, J.D., Canzio, D., Narlikar, G.J., and Kingston, R.E. (2011). Structural basis of silencing: Sir3 BAH domain in complex with a nucleosome at 3.0 A resolution. Science *334*, 977–982.

Chen, Y., Rai, R., Zhou, Z.-R., Kanoh, J., Ribeyre, C., Yang, Y., Zheng, H., Damay, P., Wang, F., Tsujii, H., *et al*. (2011). A conserved motif within RAP1 has diversified roles in telomere protection and regulation in different organisms. Nat. Struct. Mol. Biol. *18*, 213–221.

Colman, R.J., Beasley, T.M., Kemnitz, J.W., Johnson, S.C., Weindruch, R., and Anderson, R.M. (2014). Caloric restriction reduces age-related and all-cause mortality in rhesus monkeys. Nat Commun *5*.

Connelly, J.J., Yuan, P., Hsu, H.-C., Li, Z., Xu, R.-M., and Sternglanz, R. (2006). Structure and function of the *Saccharomyces cerevisiae* Sir3 BAH domain. Mol. Cell. Biol. *26*, 3256–3265.

D'Mello, N.P., and Jazwinski, S.M. (1991). Telomere length constancy during aging of *Saccharomyces cerevisiae*. J. Bacteriol. *173*, 6709–6713.

Drazinic, C.M., Smerage, J.B., Lopez, M.C., and Baker, H. V (1996). Activation mechanism of the multifunctional transcription factor repressor-activator protein 1 (Rap1p). Mol. Cell. Biol. *16*, 3187–3196.

Edmondson, D.G., Smith, M.M., and Roth, S.Y. (1996). Repression domain of the yeast global repressor Tup1 interacts directly with histones H3 and H4. Genes Dev. *10*, 1247–1259.

Elfving, N., Chereji, R. V, Bharatula, V., Bjorklund, S., Morozov, A. V, and Broach, J.R. (2014). A dynamic interplay of nucleosome and Msn2 binding regulates kinetics of gene activation and repression following stress. Nucleic Acids Res. *42*, 5468–5482.

Erkina, T.Y., Tschetter, P.A., and Erkine, A.M. (2008). Different requirements of the SWI/SNF complex for robust nucleosome displacement at promoters of heat shock factor and Msn2- and Msn4-regulated heat shock genes. Mol. Cell. Biol. *28*, 1207–1217.

Fabrizio, P., Pozza, F., Pletcher, S.D., Gendron, C.M., and Longo, V.D. (2001). Regulation of longevity and stress resistance by Sch9 in yeast. Science *292*, 288–290.

Fabrizio, P., Liou, L.-L., Moy, V.N., Diaspro, A., Valentine, J.S., Gralla, E.B., and Longo, V.D. (2003). SOD2 functions downstream of Sch9 to extend longevity in yeast. Genetics *163*, 35–46.

Feldmann, E.A., and Galletto, R. (2014). The DNA-binding domain of yeast Rap1 interacts with double-stranded DNA in multiple binding modes. Biochemistry *53*, 7471–7483.

Feser, J., Truong, D., Das, C., Carson, J.J., Kieft, J., Harkness, T., and Tyler, J.K. (2010). Elevated histone expression promotes life span extension. Mol. Cell *39*, 724–735.

Fleming, A.B., and Pennings, S. (2001). Antagonistic remodelling by Swi-Snf and Tup1-Ssn6 of an extensive chromatin region forms the background for FLO1 gene regulation. EMBO J. *20*, 5219–5231.

Fleming, A.B., Beggs, S., Church, M., Tsukihashi, Y., and Pennings, S. (2014). The yeast Cyc8-Tup1 complex cooperates with Hda1p and Rpd3p histone deacetylases to robustly repress transcription of the subtelomeric FLO1 gene. Biochim. Biophys. Acta *1839*, 1242–1255.

Gasch, A.P., Spellman, P.T., Kao, C.M., Carmel-Harel, O., Eisen, M.B., Storz, G., Botstein, D., and Brown, P.O. (2000). Genomic Expression Programs in the Response of Yeast Cells to Environmental Changes. Mol. Biol. Cell *11*, 4241–4257.

Hanlon, S.E., Rizzo, J.M., Tatomer, D.C., Lieb, J.D., and Buck, M.J. (2011). The stress response factors Yap6, Cin5, Phd1, and Skn7 direct targeting of the conserved co-repressor Tup1-Ssn6 in *S. cerevisiae*. PLoS One *6*, e19060.

Harman, D. (1956). Aging: a theory based on free radical and radiation chemistry. J. Gerontol. *11*, 298–300.

Harman, D. (1972). The biologic clock: the mitochondria? J. Am. Geriatr. Soc. *20*, 145–147.

Harris, N., Bachler, M., Costa, V., Mollapour, M., Moradas-Ferreira, P., and Piper, P.W. (2005). Overexpressed Sod1p acts either to reduce or to increase the lifespans and stress resistance of yeast, depending on whether it is Cu(2+)-deficient or an active Cu,Zn-superoxide dismutase. Aging Cell *4*, 41–52.

Huber, A., French, S.L., Tekotte, H., Yerlikaya, S., Stahl, M., Perepelkina, M.P., Tyers, M., Rougemont, J., Beyer, A.L., and Loewith, R. (2011). Sch9 regulates ribosome biogenesis via Stb3, Dot6 and Tod6 and the histone deacetylase complex RPD3L. EMBO J. *30*, 3052–3064.

Laschober, G.T., Ruli, D., Hofer, E., Muck, C., Carmona-Gutierrez, D., Ring, J., Hutter, E., Ruckenstuhl, C., Micutkova, L., Brunauer, R., *et al*. (2010). Identification of evolutionarily conserved genetic regulators of cellular aging. Aging Cell *9*, 1084–1097.

Lin, S.-J., Kaeberlein, M., Andalis, A.A., Sturtz, L.A., Defossez, P.-A., Culotta, V.C., Fink, G.R., and Guarente, L. (2002). Calorie restriction extends *Saccharomyces cerevisiae* lifespan by increasing respiration. Nature *418*, 344–348.

Lin, S.-J., Ford, E., Haigis, M., Liszt, G., and Guarente, L. (2004). Calorie restriction extends yeast life span by lowering the level of NADH. Genes Dev. *18*, 12–16.

Lippman, S.I., and Broach, J.R. (2009). Protein kinase A and TORC1 activate genes for ribosomal biogenesis by inactivating repressors encoded by Dot6 and its homolog Tod6. Proc. Natl. Acad. Sci. *106*, 19928–19933.

Longo, V.D. (2003). The Ras and Sch9 pathways regulate stress resistance and longevity. Exp. Gerontol. *38*, 807–811.

Longo, V.D., and Fabrizio, P. (2012). Chronological aging in *Saccharomyces cerevisiae*. Subcell. Biochem. *57*, 101–121.

Lopez, M.C., Smerage, J.B., and Baker, H. V (1998). Multiple domains of repressor activator protein 1 contribute to facilitated binding of glycolysis regulatory protein 1. Proc. Natl. Acad. Sci. U. S. A. *95*, 14112–14117.

Marcand, S., Gilson, E., and Shore, D. (1997). A protein-counting mechanism for telomere length regulation in yeast. Science *275*, 986–990.

Mesquita, A., Weinberger, M., Silva, A., Sampaio-Marques, B., Almeida, B., Leao, C., Costa, V., Rodrigues, F., Burhans, W.C., and Ludovico, P. (2010). Caloric restriction or catalase inactivation extends yeast chronological lifespan by inducing $H_2O_2$ and superoxide dismutase activity. Proc. Natl. Acad. Sci. U. S. A. *107*, 15123–15128.

Moehle, C.M., and Hinnebusch, A.G. (1991). Association of RAP1 binding sites with stringent control of ribosomal protein gene transcription in *Saccharomyces cerevisiae*. Mol. Cell. Biol. *11*, 2723–2735.

Muid, K.A., Karakaya, H.C., and Koc, A. (2014). Absence of superoxide dismutase activity causes nuclear DNA fragmentation during the aging process. Biochem. Biophys. Res. Commun. *444*, 260–263.

Ocampo, A., Liu, J., Schroeder, E.A., Shadel, G.S., and Barrientos, A. (2012). Mitochondrial respiratory thresholds regulate yeast chronological life span and its extension by caloric restriction. Cell Metab. *16*, 55–67.

Pan, Y., Schroeder, E.A., Ocampo, A., Barrientos, A., and Shadel, G.S. (2011). Regulation of yeast chronological life span by TORC1 via adaptive mitochondrial ROS signaling. Cell Metab. *13*, 668–678.

Powers, R.W. 3rd, Kaeberlein, M., Caldwell, S.D., Kennedy, B.K., and Fields, S. (2006). Extension of chronological life span in yeast by decreased TOR pathway signaling. Genes Dev. *20*, 174–184.

Proft, M., and Struhl, K. (2002). Hog1 kinase converts the Sko1-Cyc8-Tup1 repressor complex into an activator that recruits SAGA and SWI/SNF in response to osmotic stress. Mol. Cell *9*, 1307–1317.

Ribeiro, T.P., Fernandes, C., Melo, K. V, Ferreira, S.S., Lessa, J.A., Franco, R.W.A., Schenk, G., Pereira, M.D., and Horn, A.J. (2014). Iron, copper, and manganese complexes with *in vitro* superoxide dismutase and/or catalase activities that keep *Saccharomyces cerevisiae* cells alive under severe oxidative stress. Free Radic. Biol. Med. *80C*, 67–76.

Ruiz-Roig, C., Vieitez, C., Posas, F., and de Nadal, E. (2010). The Rpd3L HDAC complex is essential for the heat stress response in yeast. Mol. Microbiol. *76*, 1049–1062.

Sheng, Z.-Z., Zhao, Y.-Q., and Huang, J.-F. (2011). Functional evolution of BRCT domains from binding DNA to protein. Evol. Bioinform. Online *7*, 87–97.

Smith, D.L.J., McClure, J.M., Matecic, M., and Smith, J.S. (2007). Calorie restriction extends the chronological lifespan of *Saccharomyces cerevisiae* independently of the Sirtuins. Aging Cell *6*, 649–662.

Tkach, J.M., Yimit, A., Lee, A.Y., Riffle, M., Costanzo, M., Jaschob, D., Hendry, J.A., Ou, J., Moffat, J., Boone, C., *et al*. (2012). Dissecting DNA damage response pathways by analyzing protein localization and abundance changes during DNA replication stress. Nat. Cell Biol. *14*, 966–976.

Tomar, R.S., Zheng, S., Brunke-Reese, D., Wolcott, H.N., and Reese, J.C. (2008). Yeast Rap1 contributes to genomic integrity by activating DNA damage repair genes. EMBO J. *27*, 1575–1584.

Tsang, C.K., Liu, Y., Thomas, J., Zhang, Y., and Zheng, X.F.S. (2014). Superoxide dismutase 1 acts as a nuclear transcription factor to regulate oxidative stress resistance. Nat. Commun. *5*, 3446.

Turrens, J.F. (2003). Mitochondrial formation of reactive oxygen species. J. Physiol. *552*, 335–344.

Unlu, E.S., and Koc, A. (2007). Effects of deleting mitochondrial antioxidant genes on life span. Ann. N. Y. Acad. Sci. *1100*, 505–509.

Wahlin, J., and Cohn, M. (2000). *Saccharomyces cerevisiae* RAP1 binds to telomeric sequences with spatial flexibility. Nucleic Acids Res. *28*, 2292–2301.

Weinberger, M., Mesquita, A., Caroll, T., Marks, L., Yang, H., Zhang, Z., Ludovico, P., and Burhans, W.C. (2010). Growth signaling promotes chronological aging in budding yeast by inducing superoxide anions that inhibit quiescence. Aging (Albany. NY). *2*, 709–726.

Wong, K.H., and Struhl, K. (2011). The Cyc8-Tup1 complex inhibits transcription primarily by masking the activation domain of the recruiting protein. Genes Dev. *25*, 2525–2539.

Wu, J., Suka, N., Carlson, M., and Grunstein, M. (2001). TUP1 utilizes histone H3/H2B-specific HDA1 deacetylase to repress gene activity in yeast. Mol.Cell *7*, 117–126.

## SUMMARY

In this study we maintained histone mutant strains in a batch culture. We observed that some strains significantly decreased at a lower rate in the quiescent population.Some strains disappeared from quiescent population more rapidly, surprisingly, these strains did not increase in the non-quiescent population, suggesting that they may lyse and die.Residues that are implicated in lifespan extension are mostly histone tail residues and residues that are located in the solvent accessible region, suggesting that these residues may be bound by another protein(s) such as the silent information regulator, Sir3, via a BAH domain.All residues that are implicated in lifespan reduction are localised internally on the nucleosome core except for H3K18, suggesting their role in destabilising the nucleosome structure. This may allow elevated levels of DNA damage, and induce apoptosis.

The gene expression studies of cells at late log phaseshowed that although all selected strains exhibited chronological lifespan extension, they had two distinct regulatory processes, suggesting that the H4K16Q and H4H18A strains, on the one hand, and the H3E50 strain on the other hand, may modulate different pathways to regulate chronological lifespan.The GO term enrichment for genes that are significantly up-regulated in the H4K16Q and H4H18A mutants, include rRNA processing and maturation, rRNA export, ribosome assembly, gene expression, cytoplasmic translation and ethanol metabolic processes. On the other hand, the GO term enrichment for induced genes in H3E50A mutant, include, mitochondrial electron transport, tricarboxylic acid cycle, ATP synthesis coupled proton transport, oxidative phosphorylation, glutamate metabolic process, glyoxylate cycle, and purine

ribonucleoside triphosphate biosynthetic process. In addition, response to hydrogen peroxide, reactive oxygen species metabolic process, and response to oxidative stress appeared. It appears that many metabolic processes are upregulated in the H3E50A mutant strain. It is likely that the increased metabolism leads to storage of energy to be used in long starvation periods.

The proteome studies of H4K16Q and H4H18A mutants at late stages of growth showed similar profiles. Snz1 is involved in vitamin B6 biosynthesis. It is regulated by, among others, Rap1. Jhd2 induction is interesting because it is a histone demethylase involved in global demethylation of H3K4, a histone mark added by Set1 and associated with active transcription. Gcy1 is a glycerol dehydrogenase, and was shown to increase in response to DNA replication stress. In H3E50A mutant, ribosomal protein, RPL16B, which is regulated by Rap1 was upregulated. Scs2 is involved in phospholipid metabolism, it was also shown that Scs2 over-expression rescued telomeric shortening and was de-repressed in a strain over-expressing Mec1. Tfs1 is an inhibitor of carboxypeptidase Y, and was also shown to regulate the PKA signalling pathway.

We propose that Sir3, which is recruited to the silent chromatin by Rap1, cannot bind to the telomere nucleosomes, therefore, Rap1 redistributes to other regions of the genome of histone mutants. The regions, which Rap1 may relocate to, include stress response, DNA replication and damage stress response, and telomere maintenance genes.

**Keywords:***Saccharomyces cerevisiae***,** histone mutants, longevity, chronological lifespan, cellular stress response, chromatin, epigenetics, aging.